Optimisation of dynamic heterogeneous rainfall sensor networks in the context of citizen observatories

Chacon Hurtado, Juan

Publication date
2019

Document Version
Final published version

Citation (APA)
Chacon Hurtado, J. (2019). *Optimisation of dynamic heterogeneous rainfall sensor networks in the context of citizen observatories*. [Dissertation (TU Delft), Delft University of Technology]. CRC Press / Balkema - Taylor & Francis Group.

Precipitation drives the dynamics of flows and storages in water systems, making its monitoring essential for water management. Conventionally, precipitation is monitored using in-situ and remote sensors. In-situ sensors are arranged in networks, which are usually sparse, providing continuous observations for long periods at fixed points in space, and due to the high costs of such networks, they are often sub-optimal. To increase the efficiency of the monitoring networks, we explore the use of sensors that can relocate as rainfall events develop (dynamic sensors), as well as increasing the number of sensors involving volunteers (citizens). This research focusses on the development of an approach for merging heterogeneous observations in non-stationary precipitation fields, exploring the interactions between different definitions of optimality for the design of sensor networks, as well as development of algorithms for the optimal scheduling of dynamic sensors. This study was carried out in three different case studies, including Bacchiglione River (Italy), Don River (U.K.) and Brue Catchment (U.K.) The results of this study indicate that optimal use of dynamic sensors may be useful for monitoring precipitation to support water management and flow forecasting.

ISBN 978-0-367-41706-2

CRC Press
Taylor & Francis Group
A BALKEMA BOOK

This book is printed on paper from sustainably managed forests and controlled sources

an informa business

Optimisation of Dynamic Heterogeneous Rainfall Sensor Networks in the Context of Citizen Observatories | Juan Carlos Chacon-Hurtado

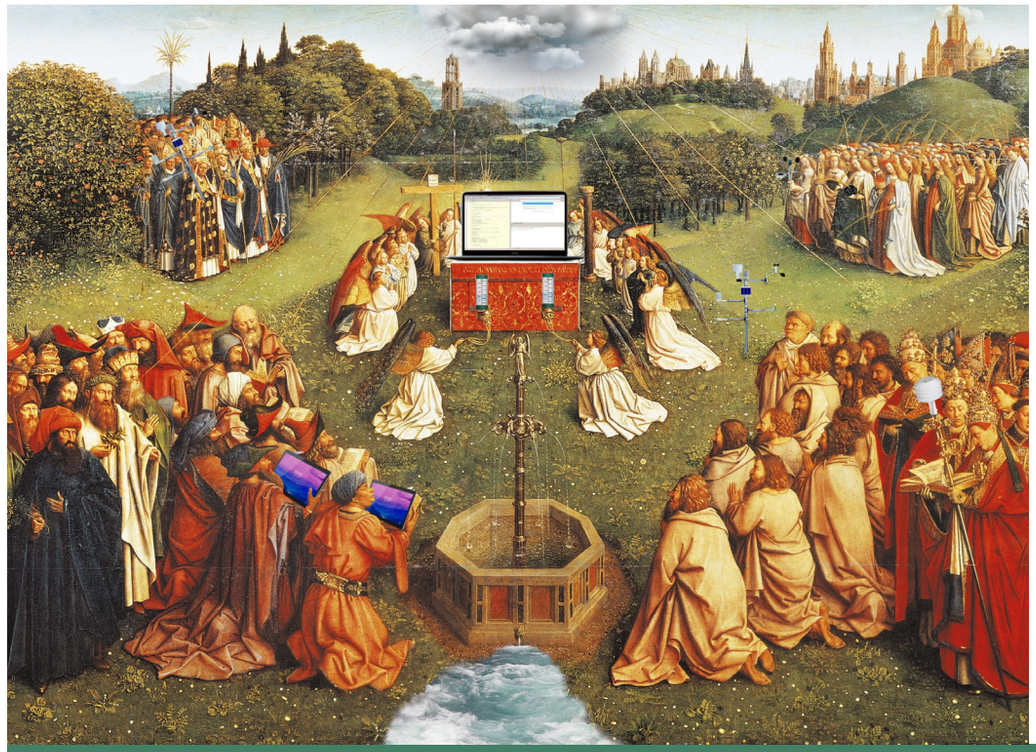

Optimisation of Dynamic Heterogeneous Rainfall Sensor Networks in the Context of Citizen Observatories

Juan Carlos Chacon-Hurtado

OPTIMISATION OF DYNAMIC HETEROGENEOUS RAINFALL SENSOR NETWORKS IN THE CONTEXT OF CITIZEN OBSERVATORIES

Juan Carlos CHACON-HURTADO

OPTIMISATION OF DYNAMIC HETEROGENEOUS RAINFALL SENSOR NETWORKS IN THE CONTEXT OF CITIZEN OBSERVATORIES

DISSERTATION

Submitted in fulfillment of the requirements of
the Board for Doctorates of Delft University of Technology
and
of the Academic Board of the IHE Delft
Institute for Water Education
for
the Degree of DOCTOR
to be defended in public on
Tuesday, 24 September 2019, at 15:00 hours
in Delft, the Netherlands

by

Juan Carlos CHACON-HURTADO
Master of Science in Water Engineering, UNESCO-IHE
born in Cali, Colombia

This dissertation has been approved by the
promotor: Prof. dr. D. P. Solomatine and
copromotor: Dr. J. L. Alfonso

Composition of the doctoral committee:

Rector Magnificus TU Delft	Chairman
Rector IHE Delft	Vice-Chairman
Prof. dr. D. P. Solomatine	IHE Delft / TU Delft, promotor
Dr. J. L. Alfonso	IHE Delft, copromotor

Independent members:

Prof.dr.ir. N.C. van de Giesen	TU Delft
Prof.dr.ir. N. E. C. Verhoest	Ghent University, Belgium
Prof.dr. A. Bárdossy	University of Stuttgart, Germany
Prof.dr.ir. R. Uijlenhoet	Wageningen University
Prof.dr.ir. A.W. Heemink	TU Delft, reserve member

CRC Press/Balkema is an imprint of the Taylor & Francis Group, an informa business

Published by:
CRC Press/Balkema
Schipholweg 107C, 2316 XC, Leiden, the Netherlands
Pub.NL@taylorandfrancis.com
www.crcpress.com – www.taylorandfrancis.com
ISBN 978-0-367-41706-2

Acknowledgments

This is it. This is a testament of what part of my life has been in these years. However, it is also the beginning (of this document), and what it will be from now on. This has been a long, hard, challenging, rewarding and amazing experience that lead not only to a PhD thesis, but also to innumerous experiences that make part of what I am. What I am today, would have not been possible without all of the people that gave me so much during this time, and whom I will always be grateful.

First of all, I would like to thank my promotor, Prof. Dimitri Solomatine and my supervisor, Dr. Leonardo Alfonso who trusted me with this task, and whose support and care made this possible. Thank you both for believing in me. Thank you for the long discussions, for the late hours, for the always constructive criticism, for bearing with my stubbornness, and for the pressure when it was needed. Thank you for helping me grow and find my way through these years. I will always remember the kindness and trust you gave me.

Mauri (aka. Dr. Mazzoleni), my project buddy who became a beloved friend. Thanks for all that happened during these years, for helping me going through the hard times, and for being with me celebrating in the good ones. I owe you many, and we will always have Krakow to remember.

Also, I would like to thank the European Commission and its Framework Programme (FP7). Without it, the WeSenseIt project would have not been possible, and consequently this thesis. Also to the Dutch government and SurfSara, for providing the computational resources that were required in order to complete the experimental work of a lifetime, in the span of a PhD. To all of the collaboration communities (GitHub, Wikimedia, Stack Exchange, GEOSS), for the unlimited support, the possibility of active participation, and for pushing the boundaries of what is possible when individuals collaborate. Thanks to Prof. Ezio Todini, when his words had the answer for a critical point in this research. In addition, thanks to Job van der Werf, for translating the summary of this thesis.

I would like to take this time to thank my parents and family, that have made so much to let me be where, and who, I am. Gracias mama y gracias papa por todo, nada de esto hubiera sido posible sin ustedes. Andrés, sin saber que se podía hacer con un computador, probablemente estaría haciendo otra cosa en este momento! Also, I know that my friends from forever will always stay with me, even when we are not around; Gracias mis peces, Alberto, Ernesto, Fernando y Rubén.

In addition, I would like to thank the people who made possible that I started this adventure in academia. Fabio and Maria Alejandra, thank you for showing me this road, and for helping me draft this living dream, from an age in which I believed this was beyond reality. Thank you

(prof.) András Szollosi-Nagy for challenging me with tasks that filled me with enthusiasm about research, philosophy, Kalman Filters and many other topics, and Dr. Dirk Schwanenberg for making me grow as a researcher in the field of hydrology.

My friends from these years, you have been my support during this times, making it impossible to be writing these lines without you. Neiler, thanks for it all! It has been amazing to find you and for supporting me through it all. Elena, thank you for all we have shared, and for helping me to find the strength to finalise this. Laura, for always being so unconditional, so close, so honest, so true. Also thanks to my closest friends whom I had the opportunity to share so much for so many years, Yared, Angelica, Gonzalo, Thaine, Anika, Alida, Fer, Natalia, Juancho, Kun, Alex (Kaune and Kerensky), Arlex, Pan, Patricia, Zaki, Juliette, Alessandro, Fernanda (Achete and Braga), Mohaned, Sara, Vero, Mark, Jessica, Mario, Stefan Aki, Benno, Lydia, Mohan, Jaka, Diego, Pablo, and Miguel.

To my friends who I found during the latter years of this process, but with whom I learned to value so much, Irene, Kelly, Ana, Milk, Joanne, Adele, Wuwu, Andres, Mauricio, Can, Thymen, Adriana, Maribel, Claudia, Katherin, Pin, Omar, Berend, Patricia, Bernadete, Victor, Bianca, Oscar, Vitali, Micah, Shahnoor, Lucia, Carlo, Paulina, Sandra, Mary, Silas, Elisa, Erika, Peter, Jeffrey, Camila, Janice, and anyone who I may have missing, as you have all being part of my life during these years in IHE. My hommies, that taught me so much about what is going on in this place Alena, Lianne, Kalle, Karel, Yelle, Damien, Wietse, Flore, Femke, Jeffrey, David, Florence, Xinyu, Dominic, Tom, Djurre, Stijn, Jilles, and Jurek, thank you for sharing it with me.

I want to also take the opportunity to thank my lecturers, who later became my colleagues, from the Hydroinformatics group: Gerald, Andreja, Ioana, Biswa and Schalk-Jan for being amazing people to work with, and for giving me the chance of sharing so many things; I could not ask for better colleagues than you. To all of the staff at IHE that made me feel at home: Mario, Arthur, Zoran, Miro, Michael, Hans, Uta, Jolanda, Anique, and the Sodexo Crew, Luz, Seema, John and Esther.

Finally, I would like to thank one of the key elements in this research. Whose bitterness was always there to wake me, shake me, push me through the day, or just simply help me contemplate what was around me. Sometimes simultaneously. The object of many comments, the starter of many conversations, the excuse for not working all the time as well. A love-hate relationship, but love at the end, thank you IHE coffee machine.

Summary

Precipitation drives the dynamics of flows and storages in the water system, and therefore its monitoring is essential for efficient water management. The understanding of the dynamics of the water system have wide social impacts, as water is a central element in many areas that range from agricultural productivity, hydropower and risk management. By understanding the dynamics of the water system, it is possible to design politics regarding the use (allocation) of water resources, flood and drought protection, and the development of water safety plans, among other activities.

Precipitation is conventionally monitored using (in-situ) and remote sensors. In-situ sensors are (usually) sparsely located in the catchment, providing point observations for long periods of time. In contrast, remote sensors provide spatial estimations of precipitation at the cost of accuracy. As consequence, these two observation methods are seemed as complementary and in practice, merging both information sources have proven a positive synergy. However, the reach of operational remote sensors (such as radar and microwave links) is limited, as its implementation costs are often high.

Leaving out remote sensors, the alternatives to improve the precipitation monitoring can come by either increasing the number of in-situ sensors or by using alternative techniques for monitoring. Focusing in the former, the best possible scenario includes the availability of an infinite amount of in-situ sensors, which is fundamentally sub-optimal as precipitation events have both temporal and spatial structure. Considering the latter, it is envisioned that the continuous relocation of "in-situ" sensors (dynamic), may be a more efficient way to monitor precipitation than static in-situ sensors, as it can actively exploit its spatio-temporal structure.

To increase the efficiency of the conventional monitoring networks, this work explores the use of sensors that can travel to different locations as rainfall events develop (dynamic sensors), as well as scaling the number of sensors with the help of volunteers (citizens). To this end, several challenges, identified and addressed in this thesis, need to be addressed first, such as 1) how to estimate precipitation fields using heterogeneous observations? 2) how to optimally design static sensor networks? and 3) how to schedule the position of dynamic sensors (when and where they have to be located)?

This research focus on the development of a method for merging heterogeneous observations in non-stationary precipitation fields, exploring the interactions between different definitions of optimality for the design of static sensor networks, and the development of algorithms for the optimal scheduling of dynamic sensors. In addition, a generic framework for monitoring network design is proposed, as a step forward in the integration and consensus of existing methods.

The results of this study indicate that using dynamic sensors are useful for monitoring precipitation, under some conditions. First, using dynamic sensors do not always yield positive results (but never negative) in the precipitation measurement, as the uncertainty in the precipitation in a given time interval grows exponentially with respect to the time that the dynamic sensor remains in the target position (hence displacement). Second, the availability of in-situ sensors should be enough to detect the precipitation events as they occur, so it is possible to signal the dynamic sensors to engage. Third, the dynamic sensors should respond as requested by the scheduling algorithm, indicating that the areas of interest can be reached in the prescribed time frame.

Samenvatting

Neerslag drijft de dynamiek van stromingen en opslag binnen het water systeem, en het monitoren daarvan is daarom essentieel voor efficiënt waterbeleid. Het begrijpen van de dynamiek van een water systeem heeft wijde sociale gevolgen, omdat water een centraal element is in verschillende gebieden, bijvoorbeeld agrarische productiviteit, waterkracht en risicomanagement. Door de dynamiek van een watersysteem te begrijpen is het mogelijk om beleid in te richten met betrekking tot, onder andere, gebruik (toewijzing) van watervoorraden, bescherming tegen overstromingen en droogte, en de ontwikkeling van waterveiligheidsplannen.

Neerslag is conventioneel gemonitord met behulp van in-situ- en afstandssensoren. In-situ sensoren zijn (gewoonlijk) schaars gelegen in een stroomgebied, en verstrekken punt observaties over langere periodes. Tegenstellend, afstandssensoren geven ruimtelijke schattingen van neerslag ten koste van de nauwkeurigheid. Deze twee observatie methodes lijken complementair en uit de praktijk blijkt dat het samenvoegen van beide informatie bronnen synergetisch kan zijn. Maar het bereik van operationele afstandssensoren (zoals radar en straalverbindingen) is gelimiteerd omdat de implementatie kosten vaak hoog zijn.

Zonder de afstandssensoren zijn de alternatieven voor het verbeteren van het monitoren van neerslag ofwel het aantal in-situ sensoren verhogen of door gebruik te maken van alternatieven technieken. Het beste scenario voor de eerst genoemde methode is de beschikbaarheid van een oneindige hoeveelheid in-site sensors. Dit is fundamenteel suboptimaal omdat neerslag gebeurtenissen zowel een temporale als een ruimtelijke structuur hebben. Voor het laatstsgenoemde alternatief, een continue verplaatsing van de ‘in-situ’ sensoren (dynamisch) een efficiëntere manier van neerslag monitoren kan zijn, vergeleken met statische sensoren, omdat deze techniek actief de spatiotemporele structuur kan benutten.

Om de efficiëntie van conventionele meetnetwerken te verbeteren onderzoekt dit werk het gebruik van sensoren die zich kunnen verplaatsen naar verschillende locaties terwijl een regenbui zich ontwikkeld (dynamische sensoren) en het opschalen van het aantal sensoren met behulp van vrijwilligers (burgers). Hiervoor zijn een aantal uitdagingen geïdentificeerd en aangepakt in deze thesis, waaronder 1) hoe kunnen neerslag velden ingeschat worden met behulp van heterogene observaties? 2) hoe kan een statisch meetnetwerk optimaal ontworpen worden en 3) hoe kan de positie van dynamische sensoren gepland worden (waar moeten ze wanneer zijn geplaatst)?

Dit onderzoek legt de nadruk op het ontwikkelen van een methode voor het samenvoegen van heterogene observaties in niet-stationaire neerslag velden, het onderzoeken van de interacties tussen verschillende definities van optimaliteit voor het ontwerp van statische meetnetwerken, en het ontwikkelen van algoritmes voor het optimaal plannen van dynamische sensoren. Een

generiek kader voor het ontwerp van een meetnetwerk is voorgesteld, als een stap voorwaarts richting integratie en consensus over bestaande methodes.

De resultaten geven aan dat het gebruik van dynamische sensoren kan werken voor het monitoren van neerslag, onder bepaalde condities. Eerst, het gebruik van dynamische sensoren levert niet altijd positieve (maar nooit negatieve) resultaten op, omdat de onzekerheid in de neerslag over een gegeven tijdspan exponentieel groeit met de tijd dat een dynamische sensor in de beoogde positie blijft. Ten tweede, de beschikbaarheid van in-situ sensoren zou genoeg moeten zijn om neerslag gebeurtenissen te detecteren, dus is het mogelijk om een waarschuwing te sturen voor de dynamische sensoren om deel te nemen. Ten derde, de dynamische sensoren zouden moeten reageren zoals gevraagd door het planning algoritme, aangevend dat het interessegebied kan worden bereikt in de aangegeven tijdsspanne.

Table of contents

1. Introduction

1.1 Background

Optimal design of sensor networks is a key procedure for improved water management in a wide sense, as it provides information about the states of any water system. For example, in relation to the river basin or catchment scale, design of sensor networks is (and has been) a relevant topic since the beginning of the International Hydrological decade between 1965 and 1974 (TNO 1986), until today (Pham and Tsai 2016, Chacon-Hurtado et al. 2017). During this period, the scientific community has not yet arrived to an agreement about a unified methodology for sensor network design due to the diversity of cases, criteria, assumptions, and limitations. This is evident from the range of existing reviews on hydrometric network design, such as those presented by WMO (1972, 2008), TNO (1986), Nemec and Askew (1986), Knapp and Marcus (2003), Pryce (2004), NRC (2004), Mishra and Coulibaly (2009), and Chacon-Hurtado et al. (2017).

The design of rainfall and streamflow sensor networks depends to a large extent on the scale of the processes to be monitored and the objectives to address (TNO 1986, Loucks et al. 2005, Loucks and van Beek 2017). Therefore, the temporal and spatial resolution of measurements are driven by the measurement objectives. For example, information for long-term planning does not require the same level of temporal resolution as for operational hydrology (WMO 2009, Dent 2012). On the global and country scale, sensor networks are commonly used for climate studies and trend detection (Cihlar et al. 2000, WMO 2009, Environment Canada 2010, Marsh 2010, Whitfield et al. 2012, Grabs and Thomas 2001) and denoted as National Climate Reference Networks (WMO 2009). On a regional or catchment-scale, applications require careful selection of monitoring stations, since water resources planning and management decisions, such as operational hydrology and water allocation, require high temporal and spatial resolution data (Dent 2012).

1.2 Motivation

Most of the greatest devastating natural phenomena are water-related. This considers floods, landslides, storms and tsunamis. This situation have been compiled by several studies, including Barredo (2009), Di Baldassarre et al. (2010) and Jonkman (2005), which shows that especially flood events have been increasing consistently during the last years, reason why this problem is more acute than ever.

"Between 1998 and 2009, Europe suffered over 213 major damaging floods, including the catastrophic floods along the Danube and Elbe rivers in summer 2002. Severe floods in 2005

further reinforced the need for concerted action. Between 1998 and 2009, floods in Europe have caused some 1126 deaths, the displacement of about half a million people and at least €52 billion in insured economic losses" (EU Commission 2012)

To confront this situation, various governmental agencies have tried to implement mechanisms to provide a framework that allows the mitigation of this kind of events. In Europe, the E.U. has implemented several regulations in order to minimise the impact that these events might have, including the Directive 2007/60/EC on the assessment and management of flood risks. *This Directive now requires Member States to assess if all water courses and coast lines are at risk from flooding, to map the flood extent and assets and humans at risk in these areas and to take adequate and coordinated measures to reduce this flood risk. With this Directive also reinforces the rights of the public to access this information and to have a say in the planning process* (EU Commission 2012).

As a product of this initiative, projects such as FLOODsite and CRUE ERA-NET provided methodological approaches to direct and promote the integration at a technical and scientific level among all the member states. Several other projects also follow these general action lines, such as KULTURisk, FloodProbe, UrbanFlood, and WeSenseIt, among others.

In these projects, the use of monitoring and information systems is seen as one of the key elements to cope with the difficulties related to flood management. The main approach is centred on model-based operational hydrological forecasting systems, which use monitoring systems as a starting point. These monitoring systems are usually composed by remote sensing observations and hydrometric sensor networks. The former consists of indirect observations coming mainly from Earth observation satellites and weather radar. The latter encompasses all the in-situ observations such as rain gauges, soil moisture probes and streamflow gauges.

Hydrometric sensor networks provide data about hydrological variables of interest for a specific purpose. Traditionally, these networks consist of sensors that remain fixed in selected locations during long time periods. These sensor networks are conventionally expensive to install and maintain, therefore, they are generally sparse and insufficient (Mishra and Coulibaly 2009). To complement these data sources, alternatives such as remote sensors and citizen observatories have been developed in the recent years.

Remote sensors have become relevant as information sources for many hydrological systems (WMO 2008). However, these remote observations are not yet able to replace in-situ measurements due to the relatively high error, and the need for ground verification to correct its estimations (Yilmaz et al. 2005, Espinosa et al. 2015). Additionally, not all of the variables of interest in the hydrological cycle can be measured accurately enough by remote sensors. Due to these reasons, the use of in-situ sensor networks is still necessary.

Alternatively, citizen observatories are an emerging option for the monitoring of environmental variables, which is characterised by the collection of data by the general public. By including citizens in the data collection process, the communication between modellers and citizens

change from a one-directional channel, into a two-directional interaction (Wehn et al. 2015). One of the ways to allow this interaction, consists in letting the citizens making measurements using relatively low-cost, and usually portable sensors (Lanfranchi et al. 2014, Alfonso et al. 2015, Huwald et al. 2016). Citizen-based monitoring, with the help of inexpensive personal sensors, still does not play a significant role despite of the potential benefits that they might bring in terms of coverage and public engagement. It is envisioned that the synergies between these two monitoring paradigms may be of use in the near future.

This portable (dynamic) sensors are characterised by the fact that they do not remain in the same position over long time periods. Including dynamic sensors to complement the established hydrological monitoring networks may be seen as an attractive cost-effective alternative to extend the capabilities of a sensor networks. These sensors support adaptive strategies of data collection, providing flexibility which enables the network to accommodate to different precipitation events and diverse measurement objectives.

The data coming from citizens can be collected in the three different temporal frames: as pre-event, post-event or in real-time data. Pre-event data consists in the use of information coming from citizens of variables that may influence hydrological processes such as blockages in rivers, or characterisation of land use cover (Tserstou et al. 2017). Post-event data refers to information which is gathered after an event occur (McDougall and Temple-Watts 2012). Real-time data consists in data which is directly transmitted once it is collected (Huwald et al. 2016).

The use of dynamic precipitation sensors that transmit real-time data may be of interest in the context of operational hydrology (Terakawa 2003). The use of real-time data has been essential in flood management, early warning systems, hydropower production and water management during the last decades (NOAA 1998, de Haij and Wauben 2010). It has also been shown that there are potential benefits in using dynamic sensors for activities such as precipitation monitoring for flood forecasting (Chacon-Hurtado et al. 2016).

Some of the limitations of using dynamic sensors for monitoring precipitation are related to the difficulties using the acquired information, reliability of the measurements, and absence of conceptual development for integration. Data coming from dynamic sources may lead to an increase in uncertainty, with respect to data coming from conventional sensors, and it is difficult to quantify it, as this type of sensors are relatively new and usually do not operate over controlled conditions. Additionally, the systematic framework to integrate observations from dynamic sensors into conventional data streams is lacking. There are some experiences documented related to integration of dynamic sensors for different applications, as described in Ballari et al. (2012), Dantu et al. (2005) and Haberlandt and Sester (2010). However such studies and applications are still quite limited.

One of the benefits of using dynamic sensors for precipitation monitoring is the expected increase in network efficiency which will help reducing the large costs associated with the operation and maintenance of sensor networks. Costs of deployment and maintenance of hydrometric sensor networks constitute the single most expensive part in an operational

hydrologic system, usually associated with the cost of equipment, maintenance and replacement in case of malfunction, among others. Due to this, reduction of monitoring networks is not a new subject, and generally follows economic limitations, as can be demonstrated on an example of the New Zealand's monitoring network (Pearson 1998), and the Canadian hydrometric network (Environment Canada 2010).

Yet another benefits of using dynamic sensors is the possibility of reconfigure the network for different precipitation events under different management objectives. In this direction, the sensor networks can adjust to a given precipitation event as it develops, but the deployment strategy follows its final objective. For example, flood management requires sensor networks that are suitable to capture the magnitude of the precipitation events in detail, while water allocation activities may require sensor networks which are adequate to obtain spatially accurate information. In other words, networks serve a purpose, and depending on it, the design of the optimal sensor network has to be chosen or adopted accordingly.

In this direction, the design of monitoring networks is an inductive-reasoning problem (from particular observations to general assessments), as data is usually limited to few locations, and therefore, the problem of optimal design naturally is ill-posed. As a consequence, a large number of candidate solutions, which are close to each other in terms of quality are generated (objective space). From a practical point of view, one might argue that the best measurements are those that make predictions closer to the observable truth, which suggests a *fit to the purpose* approach (*I*-optimality). This situation might seem ideal, but uncertainties in the chain from data to decisions, lead to a high number of optimal (or close-to-optimal) solutions in the objective space, which do not necessarily converge to similar network configurations (decision space).

Moreover, uncertainty in measurements and models makes the definition of optimality quite a complex issue, especially in dynamic and non-stationary fields. This situation suggests that optimal location of sensors in these conditions cannot be unique or static (i.e. found once and for all). In other words, optimal observations can only be achieved by using dynamic sensors in dynamic environments. This is a recognised issue, and the reason why adaptive modelling arises as one of the research directives in the Hydroinformatics Chair at IHE Delft (Solomatine 2012).

1.3 Innovation

To make use of these new potential sources of information, the WeSenseIt project worked on the development of citizen observatories of water, which had among its objectives to enhance environmental monitoring and forecasting. This was tackled by changing the information flow paradigm, "from sensors to citizens", to a two-way communication stream, enabling the active participation of these subjects in the modelling process. This participation, even if it is not massive, provides additional valuable information which cannot be captured by the established monitoring networks, leading to more reliable estimates of the environmental variables.

Two of the most important objectives of the WeSenseIt project were to develop low-cost sensors to effectively measure and retrieve information about different hydrological variables, and to provide a platform in which the observations coming from observing citizens become available. This research work, as a particular part of the WeSenseIt project, addresses the optimal location (when and where) of dynamic sensors for precipitation monitoring to improve the state of knowledge of the water system.

From the perspective of the natural process, the optimal sensor location in dynamic, noisy, and heterogeneously observed environments, is a challenge due to a number of aspects: the definition of optimality, assumptions in modelling tools, limited displacement capabilities of the sensors, and the intermittency of data streams (random location at a random time) coming from citizen observations.

In this respect, this thesis innovates in the modelling of precipitation fields and the design of static and dynamic sensor networks. First, methodologies for the merging of heterogeneous data into common data streams for modelling of non-stationary precipitation fields are developed. By doing so, the basis for using the citizen data in precipitation is established. Second, features and techniques for the design of static sensor networks are presented, offering a wide and comprehensive view on these topics. Finally, we propose and test methodologies for the design of dynamic sensor networks for monitoring precipitation, aiming to exploit the development and use of citizens' observations.

1.4 Objectives

1.4.1 Main Objective

Develop and improve methods for optimal design of dynamic rainfall sensor networks with varying physical topology, in heterogeneous data environments for operational hydrological systems.

1.4.2 Specific Objectives

1. Formulate a generic framework for the design of precipitation sensor networks.
2. Improve geostatistical methods for interpolation of precipitation fields, allowing for intermittent heterogeneous measurements under non-stationary conditions.
3. Enhance methods for the efficient design of static precipitation sensor networks for streamflow simulation.
4. Develop a methodological approach for optimal scheduling of dynamic sensor networks, which include data from dynamic physical sensors with varying uncertainty, and from citizen observatories.

1.5 Layout of this thesis

This thesis explores several aspects of the design of precipitation monitoring networks with dynamic sensors as shown in Figure 1.1. First, a literature review on sensor network design is carried out, and a generic framework for design is suggested, as presented in Chapter 2. Second, the case studies are introduced in Chapter 3. Next, a set of developed tools for incorporating heterogeneous observations, coming from citizens and dynamic gauges in non-stationary fields, are presented in Chapter 4. Following, several aspects of the static sensor networks design are explored in Chapter 5, such as the effect of the coordinate systems in posing the optimisation problem, the relationship among objective functions, the solutions of the optimisation problem, and evaluation of the solutions' robustness, using model-based and model-free approaches. Finally, three strategies for scheduling of dynamic sensor for monitoring, which are rooted in the methods developed in Chapter 4, and the lessons learned of Chapter 5, are presented in Chapter 6, and applied in all the case studies. The topical structure of this thesis is presented in Figure 1.2.

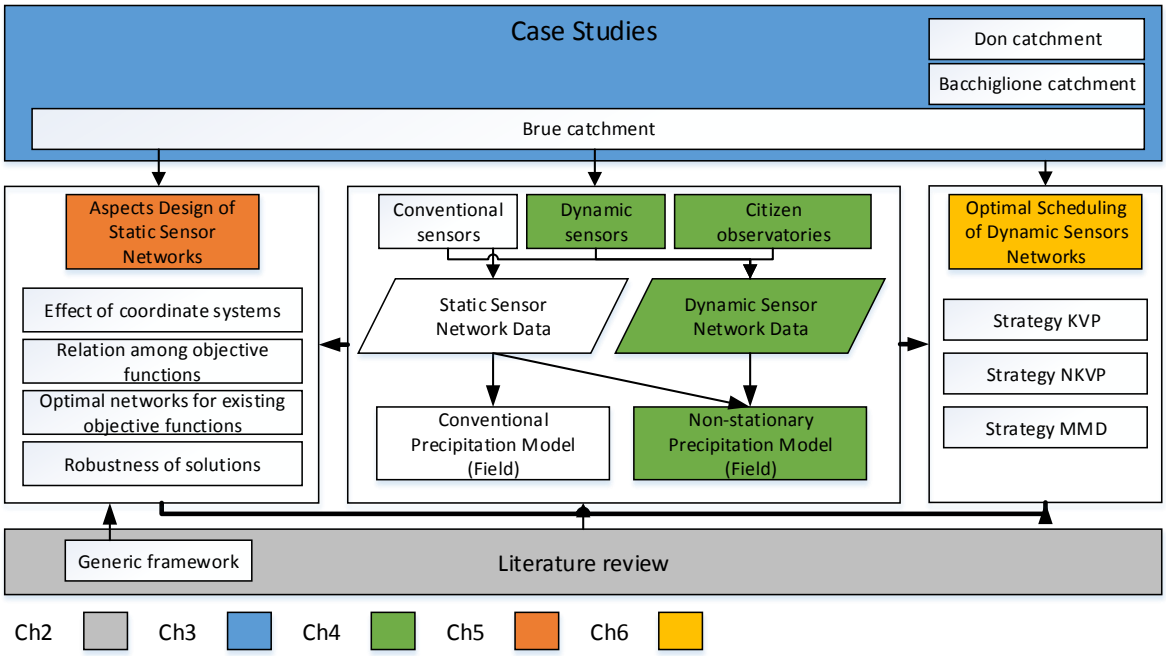

Figure 1.1 Methodology of this dissertation

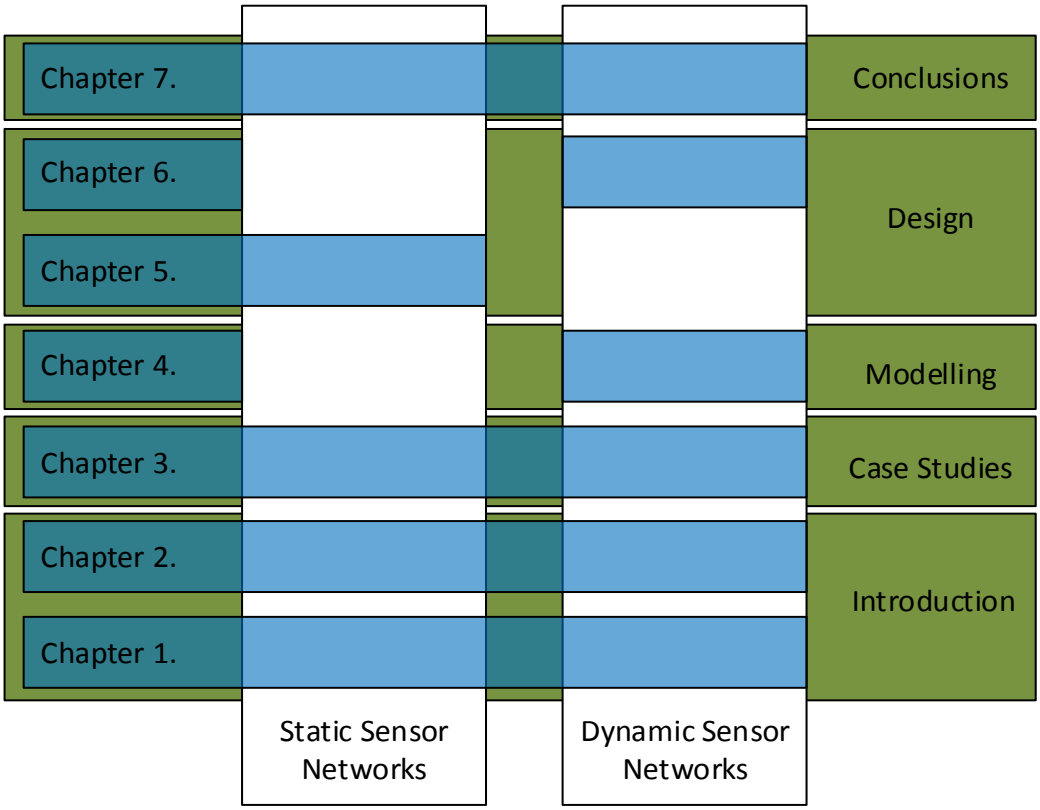

Figure 1.2 Layout of the this dissertation

1.6 Highlights

In this thesis we may highlight the following points:

- A generic framework for sensor network design is proposed.
- Methods for the integration of observations coming from heterogeneous sources (dynamic and citizen observations) are developed.
- Geostatistical methods for the interpolation of non-stationary fields are developed and tested.
- Comparison of methods for the design of static precipitation sensor networks is carried out.
- Diverse deployment strategies, for scheduling the position of dynamic precipitation sensor networks that complement conventional networks are developed and tested.

2. Literature review and proposed framework

2.1 Introduction

The main objective of this thesis requires establishing a generic, literature-based framework to optimally design rainfall sensor networks and to identify current knowledge gaps. In particular, different challenging aspects emerge from the addition of dynamic components (such as the citizen observatories) to the network design, data heterogeneity and quality.

The review includes current techniques for the measurement of precipitation, including in-situ, remote, and social sensors. Then, it introduces the concepts of modelling spatially distributed variables in order to establish the geostatistical models used in the simulation of precipitation fields and identifying their limitations. Subsequently, the chapter expands with concepts of hydrological modelling, specifically lumped conceptual models used in the simulation of discharge estimates. After, the chapter explores the current approaches for designing sensor networks and proposes a classification and a generic framework.

2.2 Sensors and sensor networks

A sensor is defined as *a device that responds to a physical stimulus (as heat, light, sound, pressure, magnetism, or a particular motion) and transmits a resulting impulse (as for measurement or operating a control)* (Merriam-Webster's 2013). This definition establishes that the use of a sensor allows gathering information from the surrounding environment, abstracting it into a certain impulse. Examples of sensors are precipitation gauges, level gauges, flow meters, sight, smell, etc.

Sensors provide data about a certain variable of interest, and in most of cases, only a spectrum of it, due to the limitations on each sensing technique (Hart and Martinez 2006). These limited sensing capabilities are justified by the expected utility of the measurements, accuracy, information processing capabilities and scale of the process that is to be addressed. As an example, the human visible spectrum goes from wavelengths of approximately 390 nm to 720 nm (Schubert 2006), even though electromagnetic radiation wavelengths can be significantly higher or lower in regular conditions, as UV rays or heat among many others types. This example of the human eye represents the sensing element as a tool for a given purpose (in this case, survival), while in the cases of other species the visual spectrum is different, adapting the sensor to other conditions to fulfil the same purpose, improve survival chances.

In the case of environmental monitoring, the purpose of sensors is to abstract numerical information of certain variables in order to be used by models to produce information about the current states of the hydrological system, or to forecasts other variables of interest. Different types of sensors are used for the measurement of the same variable, advocating desirable properties with regards to its coverage, resolution, uncertainty and reliability, among others (Khalleghi et al. 2013).

In the case of environmental variables, sensors are characterised by being deployed into a specific site, where they remain for long time periods. To compensate for the lack of spatial representativeness of the measurements, the sensors are deployed into networks which carry out coordinated measurements, increasing the spatial coverage of the observations. As consequence, sensor networks provide a more complete picture of spatially distributed processes such as precipitation and temperature.

Sensors (and therefore sensor networks) require to transmit the recorded data (measurements) to be used by, and then transformed into decisions. The transmission encompasses all the activities regarding with information retrieval from the sensor, to a data centre. The capacity recording information will vary within different sensor classes, and will affect the frequency, resolution and availability of the measurements, which are directly related with the measurement principle of the sensor. The data transmission can be as simple as manual readings (WMO 2008), or as elaborate as automatic data collection in real-time, being justified for the type of decisions to be made.

Manual reading is based in an operator performing an observation of a gauge, which reading is going to be stored in an analogue format (paper) or digital media (SMS, picture, database entry, etc.). Afterwards, this information has to be transmitted to a central information centre where will be accessed by the user. These measurements are generally used to monitor large scale hydrological processes and large scale irrigation control (van Overloop et al. 2013).

Automatic data collection is a powerful tool that provides continuous real-time data about environmental variables, and at the same time it removes human-induced errors in the measurement chain. The benefits include a more systematic assessment of the measurement quality, and error traceability. The features of automatic data collection are of great value in situations where the response time between actions and benefits are immediate, such as hydropower operation, small scale irrigation, and flood emergency management. The conditions for automatic data collection require autonomous sensors which can be located in isolated areas which, in some cases, may be far from electrical and communications grids.

The installation of different data collection systems is subject to the available budget, the information use and the type of decision to make. This includes not only the selection of the technology, but also the operation and maintenance of the equipment. Additionally, the characteristics of the sensors have to correspond to the level of certainty which is expected from the measurements, so the measurements can be carried out in a cost-effective manner (Singh et al. 1986).

2.2.1 **Conventional precipitation measurements**

Conventional precipitation measurements are carried out in in-situ by gauges similar to the described in the WMO in the guide for metrological practices (WMO 2008). This guide also provides guidelines for installation conditions and the reading procedures to ensure a common background for data sharing of standard meteorological observations. However, these guidelines only cover standard meteorological observations, and the use of different methods, procedures or variables is not supported by these recommendations. In this direction, the WMO (2008) have standardised most of the sensor design and installation requirements.

According to WMO (2008), the instruments for rainfall measurement consists in a device that captures the precipitation droplets. Storage, weighing, floating and tipping-bucket type of gauges calculate the total volume of collected precipitation in a given time interval, while disdrometers and acoustic-type gauges characterise the droplets, not only providing measurements of precipitation, but also a drop size distribution.

2.2.2 **Dynamic sensors**

The use of dynamic gauges is currently in active development in applications such as airborne radar measurements, robotic vision and surveillance. The purpose of a mobile sensor is to overcome limitations of limited observability a sensor in a fixed location (Liu et al. 2005), especially in dynamic environments, or with dynamic targets. Additionally, the development of unmanned aircrafts (Witayangkurn et al. 2011) pose an interesting opportunity in data acquisition using dynamic sensors, and its integration is an important research focus in the future development of monitoring systems.

The integration of dynamic sensors in operational meteorology is limited due to the difficulties in its deployment, and lack of the theory to support its use. This situation leads to only a few examples in the literature, where only conceptual approaches and small tests have been conducted. Haberdlandt and Sester (2010) and Veas et al. (2012) agreed that the potential benefits of moving sensors in environmental applications are a promising field, but it requires to mature in the upcoming years.

2.2.3 **Citizen observatories**

A less explored information source in hydrology is the concept of citizen observatories (Wehn and Evers 2015, Ferri et al. 2016). Citizen observatories use the information provided by citizens, ranging from simple observations to measurements with standard equipment, into the data stream of conventional instruments. In its simplest form, observations come from a judgement of a variable (such as high or low water level in a canal, or heavy or light precipitation). This approach is mostly valuable when models or measurements are significantly expensive (Cooke 1991). The participation of the citizen in the observatories can consider that these subjects as experts or no, leading to elitist assessments on one side, and crowd observations (Kamel Boulos et al. 2011), in the other end.

Experts are those observers whose judgement can be inaccurate, but are systematically consistent with its observations, reducing the randomness of in the error of its observations. This systematic error permits to integrate observations using constrained errors between different events. Dealing with expert judgements, Cooke (1991) considers the so-called *classical model* (structured expert judgement). It establishes the best estimate of certain parameter as a linear function of experts' estimates, which must be calibrated by the measurement of the same (or other) variable(s) in the test cases. This can be seen as calibration of the expert knowledge base. Applications of this method can be found in Cooke and Goosens (2008).

In spite of the selected approach, many of these observations are only partially true, especially in complex scenarios such as hydrological processes. This occurs due to the incompleteness in observations and the inherent simplifications associated with the conceptualisation of the processes. This lack of knowledge cannot be reflected into uncertainty estimations, which leads to the possibilistic framework (Dubois and Prade 1993, Loquin and Dubois 2010). The possibilistic framework considers that the reasoning yield from inductive knowledge might be better represented by belief functions, instead of probability distributions. In other words, accounting for the uncertainty not only to the lack of certainty about the processes, but also for the lack of understanding. This thesis will not explore this concept or its application in citizen observatories, but understand its relevance and importance in this topic.

The participation of citizens in the observatories can be split into 5 main groups (Figure 2.1). Due to this, there will be different approaches in order to evaluate the information coming from these sources, as well as the methods to acquire the sensed information. It is foreseen that crowdsourcing techniques can be used to address the information present in social media, but not particularly directed to the authorities (involvement level 2). The establishment of a web-based platforms, SMS or mobile Apps, encourage participation of individuals (involvement level 3) by giving the opportunity to directly communicate the sensed information (observations or gauge readings). In current citizen observatories projects, experiments with small groups of citizens (engaged users, involvement level 4) with physical sensors are carried out with promising results. On top of the sensing pyramid are those users who own, maintain and transmit measurements using their own sensors (involvement level 5).

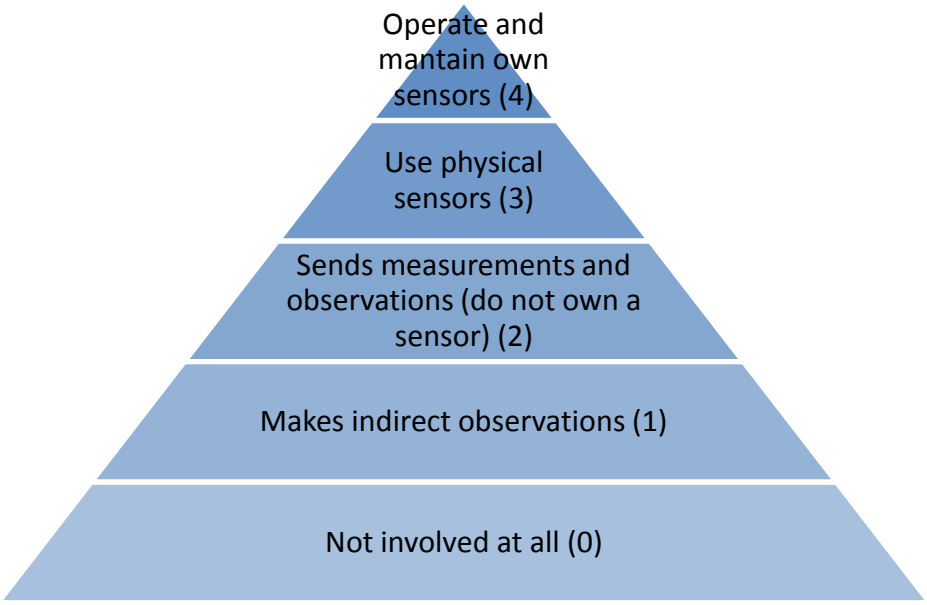

Figure 2.1 Expected participation in different involvement levels

The community participates in all the levels, being the more challenging the 1 and 2, due to the nature of the given information. This is because one of the main characteristics is the uncertainty around the estimates made by individuals who might not be trained for this purpose, as well as the use of channels whose information content can be very noisy.

2.2.4 **Sensor network design**

Sensors are commonly arranged in networks to fulfil requirements of representativeness, accuracy and uncertainty (Sorooshian et al. 2011, Morrissey et al. 1995) in the observation of physical processes. The definition of a sensor network includes in itself the concept of topology, which represents the way in which the network is arranged. These arrangements might vary depending on the physical constraints (physical topology) of sensor location and the description of information flows (logical topology) (Gallo and Hancock 2002). Considering this, two apparently identical sensor networks can be significantly different.

From the most theoretical point of view, the design of a sensor network use the same concepts as experimental design (Fisher 1974). The design of a sensor network should ensure representativeness of the measurements, at the time that can be used to derive the conclusions that drive the measurements (EU Commission 2000, EPA 2002). In the context of rainfall-runoff hydrological modelling, sensor networks should provide the sufficient data for accurate the simulation and forecasting of discharge and water levels, at stations of interest.

The objectives of the sensor network design have been categorised into two groups, the optimality alphabet (Herzberg et al. 1972, Box 1982, Kiefer and Wolfowitz 1985, Fedorov and Hackl 1997, Pukelsheim 2006, Montgomery 2012) which uses different letters to name different design criteria, and the Bayesian framework (Chaloner and Verdinelli 1995, DasGupta 1996). The alphabetic design is based on the linearization of models, optimising particular criteria of the information matrix (Fedorov and Hackl 1997, Guestrin et al. 2005, Chakraborty and Deglon

2008). Bayesian methods are centred on principles of decision making under uncertainty, in which it seeks to maximise the gain in information (Shannon 1948) between the prior and posterior distributions of parameters, inputs or outputs (Lindley 1956, Chaloner and Verdinelli 1995). Among the most used alphabetic objectives are the D-optimal, which minimises the area of the uncertainty ellipsoids around the model parameters; and G-optimal, which minimises the variance of the predicted variable, which can also be used as objective functions in the Bayesian design.

These objectives are indirectly addressed in the literature, by using several functional alternatives in the form of model-based and model-free approaches for sensor network design. These categorisation will be later discussed in depth. One of the main limitations in the application of sensor network design, using the experimental design is the lack of block experimental design (Kirk 2009), as is impossible to replicate initial conditions in a non-controlled environment, such as natural processes.

On the practical end, the design of a sensor network should start with the institutional setup, purposes, objectives and priorities of the network (Loucks et al. 2005, WMO 2008). From the technical point of view, an optimal measurement strategy requires the identification of the process, for which data is required (Casman et al. 1988, Ali and Narasimhan 1993, Guestrin et al. 2005, Dent 2012). Considering that neither the information objectives are unique and consistent, nor the characterisation of the processes is complete, the re-evaluation of the sensor network design should occur regularly. This re-evaluation should be considered when either the studied process, information needs, information use, or the modelling objectives change. Consequently, regulations regarding monitoring activities are not often strict in terms of station density, but in the suitability of data to provide information about the status of the water system (EU Commission 2000, EPA 2002).

The design of meteorological and hydrometric sensor networks should consider at least three aspects. First, it should meet various objectives that are sometimes conflicting (Loucks et al. 2005, Kollat and Reed 2006, Kollat et al. 2011). Second, it should be robust under the events of failure of one or more measurement stations (Kotecha et al. 2008). Third, it must take into account different purposes and users with different temporal and spatial scales (Singh et al. 1986). Therefore, the design of an optimal sensor network is a multi-objective problem (Alfonso 2010, Volkmann et al. 2010).

The sensor network design can also be seen from an economic perspective (Loucks et al. 2005). In most cases, the main limitation in the deployment of sensor networks is related to costs, being sometimes the main driver of decisions related to reduction of the monitoring networks. The valuation between the costs of the sensor networks and the cost of having insufficient information is not usually considered, because the assessment of the consequences of decisions is made a-posteriori (Loucks et al. 2005, Alfonso et al. 2016). In most studies, it is seen that the improvement of information content metrics (e.g., entropy, uncertainty reduction, among others) is marginal as the number of extra sensors increases (Pardo-Igúzquiza 1998, Dong et al. 2005, Ridolfi et al. 2011), and thus the selection of the adequate number of sensors can be based

on a threshold in the rate of increment in the objective function. However, in many practical applications the number of available sensors may be defined by budget limitations. Therefore, the optimal number of sensors in a network is strictly case-specific (WMO 2008).

2.2.5 Scenarios for sensor network design: augmentation, relocation and reduction

Scenarios for designing of sensor networks may be categorised into three groups: augmentation, relocation and reduction (NRC 2004, Mishra and Coulibaly 2009, Barca et al. 2015). *Augmentation* refers to the deployment of at least one additional sensor in the network, whereas *Reduction* refers to the opposite case, where at least one sensor is removed from the original network. *Relocation* is about repositioning the existing network nodes.

The lack of data usually drives the sensor network augmentation, whereas economic limitations usually push for reduction. These costs of the sensor network usually relate to the deployment of physical sensors in the field, transmission, maintenance and continuous validation of data (WMO 2008).

Augmentation and relocation problems are fundamentally similar, as they require estimation of the measured variable at ungauged locations. For this purpose, statistical models of the measured variable are often employed. For example, Rodriguez-Iturbe and Mejia (1974) described rainfall regarding its correlation structure in time and space; Pardo-Igúzquiza (1998) expressed areal averages of rainfall events with ordinary Kriging estimation; Chacón-Hurtado et al. (2009) represented rainfall fields using block Kriging. In contrast, for network reduction, the analysis is driven by what-if scenarios, as the measurements become available. Dong et al. (Dong et al. 2005) employ this approach to re-evaluate the efficiency of a river basin network based on the results of hydrological modelling.

In principle, augmentation and relocation aim to increase the performance of the network (Pardo-Igúzquiza 1998, Nowak et al. 2010). In reduction, on the contrary, network performance is usually decreased. The driver for these decisions is usually related to factors such as operation and maintenance costs (Moss et al. 1982, Dong et al. 2005).

2.3 Models of precipitation for rainfall-runoff simulation

2.3.1 From sensor measurements to fields and areal average

Precipitation is measured using a variety of techniques, which spans from field gauges to earth-observation systems. Rain gauges are the primal information source, and can be classified as recording or no-recording, which alters the temporal resolution of the measurements, as observations are made either manually by an operator, or continuously recoded on time (WMO 2008a). On catchment and regional scale, weather radars have gained momentum due to its ability to cover vast areas at a relatively high temporal and spatial resolution (Buswell et al. 1954, Sauvageot 1994, Wagner et al. 2009, Abo-Monasar and Al-Zahrani 2014), and with

different resolutions depending on the frequency bands (Thorndahl et al. 2017). On the continental and global scale, earth observations systems provides precipitation data at a relatively coarse temporal and spatial resolutions, with the advantage of being ubiquitous (Michaelides et al. 2009).

Hydrological models for rainfall-runoff modelling usually make use of different type of precipitation data, depending on how the spatial variability of the model is represented. The most common categories for describing the spatial variability, are the distributed, semi-distributed and lumped models. The distributed models make use of the precipitation fields, as the hydrological processes are modelled as points in a grid such as the SHE model (Abbott et al. 1986), VIC (Liang et al. 1994), SWAT (Arnold et al. 1993), TOPMODEL (Beven and Kirkby 1979), among others. In the case of semi-distributed and lumped models, average precipitation is calculated over the catchment or sub-catchment (Sugawara 1961, Lindström et al. 1997, Solomatine and Wagener 2011), simplifying the heterogeneity of the precipitation fields.

Considering this, precipitation data is usually required either in form of fields or as average over the catchment For the simulation of precipitation fields, several techniques have been employed (Sluiter 2009, Li and Heap 2011), mapping from point observations to fields such as Thiessen polygons (Chow et al. 1988), Kriging (Journel and Huijbregts 1978, Cressie 1993, Deutsch and Journel 1998, Holawe and Dutter 1999, Bostan et al. 2012), Copula (Bardossy and Pegram 2013, Bardossy and Li 2008), Splines (Hutchinson 1995, Tait et al. 2006), IDW (Garcia et al. 2008, Soenario and Sluiter 2010), or Machine Learning (Kanesvski et al. 2009), among others. For estimating areal average precipitation, an alternative is to directly integrate the precipitation fields over the catchment, or estimates under the assumption of homogeneous networks.

One example of the latter uses a best linear unbiased estimator (BLUE) for estimating the average precipitation. The average precipitation $\overline{P}$ is a linear combination of the measurements. The set of weights is such that minimises the variance of the estimation of the precipitation error, using a Best Linear Unbiased Estimator (BLUE, Equation 2.1). This method is widely used in meteorological applications (Daley 1991), as in hydrological modelling applications (Lindström et al. 1997).

$$\bar{P} = \sum_{\alpha=1}^{S} w_\alpha P_\alpha \qquad \textit{Equation 2.1}$$

$$w_\alpha = \left[\sum_{\alpha=1}^{S} cov(P_\alpha, P_j) cov\left(O_\alpha, O_j\right)\right]^{-1} cov(P', P_\alpha) \qquad \textit{Equation 2.2}$$

Where $\bar{P}$ is the average precipitation over the catchment calculated from S stations, w is the weight to each station, P_α is the recorded precipitation at station α, O is the observation error and P' is a first estimate of the precipitation at each station.

2.3.2 **Stationarity assumptions**

A random field can be defined as a collection of random variables (i.e. precipitation intensity at a specific point in space). Spatially distributed variables can be modelled as random fields to exploit the spatial dependency among the measurements. The dependence (or covariance structure) among measurements can be fixed in time and space, being the field stationary. On the contrary, if the dependence among the measurements varies in either time or space, the variable is considered as non-stationary.

A random field can be temporal, spatial or directionally stationary (Fuentes 2005). Temporal stationarity means that there is no change in the moments of the distribution in time. Spatial stationarity ensures that there are no changes in the moments of the distribution at different locations in the domain. Directional stationarity means that the covariance structure is isotropic, and thus, there is no difference in the direction in which the covariance between a pair of points is taken.

Temporal stationarity assumptions are tested using methods such as PSR (Priestley and Subba-Rao 1969), Dickey-Fuller (Dickey and Fuller 1979), Augmented Dickey-Fuller (Said and Dickey 1984), KPSS (Kwiatkowski et al. 1992) and Leybourne-McCabe (Leybourne and McCabe 1994, 1999). There are also methods which rely on the representation of the data series in the frequency domain, via Fourier or wavelet transforms (Bose and Steinhardt 1996, Fuentes 2005).

Methods based on covariance structure analysis, and spatial spectral analysis, are commonly used to evaluate the spatial stationarity. Bose and Steinhardt (1996) proposed the evaluation of stationarity via centrosymmetry of the spatial covariance structure. Ephaty et al. (2001) and Fuentes (2005) presented a methodology to evaluate stationarity and isotropy, testing the homogeneity of the spatial spectra at different locations. These methods are suited for large quantities of spatial data, such as the ones provided by remote sensing, and its use may be limited in scattered observations (Velasco-Forero et al. 2009).

Isotropy is the most frequently addressed type of non-stationarity in literature (Journel and Huijbregts 1978, Cressie 1993). It is mainly used when data suggest a different behaviour in orthogonal directions, for instance, caused by strong wind currents or significant topographical gradients. Experimental variograms using preferential directions are used to address the anisotropy of the field (Bohling 2005).

Although the assumption of stationarity does not necessarily lead to inferior model performance, it may lead to unrealistic estimations of the interpolation variance (Bardossy 2006). Interpolation variance depends on the spatial correlation structure (Journel and Alabert 1989, Chiles and Delfiner 1999) and the station network configuration, but it does not depend on the particular value of measurements. Consequently, the estimations of interpolation

uncertainty are accurate as long as the process holds the same assumptions of the model (Bardossy and Li 2008).

2.3.3 **Methods to handle non-stationarity in random fields**

Techniques to handle temporal non-stationarity include seasonal (Woolhiser and Roldan 1986) and adaptive variograms (Mardia et al. 1998). For spatial stationarity, dimension expansion (Bornn et al. 2012), spatial deformation (Schmidt and O'Hagan 2003), spatially smoothed local models (Brunsdon et al. 1998), generalised covariance functions (Kitanidis 1993, Crujeiras and van Keilegom 2010), basis function expansion (Sampson and Guttorp 1992, Hannachi et al. 2007), moving window (Harris et al. 2010, Zhang et al. 2015), and the use of covariates (Hass 1996, Genton and Kleiber 2015). Most of these approaches use conventional interpolation tools after transforming the problem into a homogeneous and isotropic space.

For temporal non-stationarity, seasonal variograms (Bastin et al. 1984, van de Beek et al. 2009) suggest that the covariance structure has to consider specific climatological factors (i.e. wet or dry seasons). Adaptive variograms (Chen and Li 2012) update the covariance structure in a feed-forward loop, by assimilating the new observations into the variogram.

For spatial non-stationarity, dimension expansion methods (Bornn et al. 2012) map the problem into a higher dimensional space, in which the problem can be assumed to be stationary. Spatial deformation methods (Schmidt and O'Hagan 2003) use an alternative definition of the distance kernel (Higdon et al. 1998), homogenising the interpolation space. Spatially smoothed methods, including moving window approaches, (Brunsdon et al. 1998, Harris et al. 2010, Zhang et al. 2015) construct local models, which are stationary in its vicinity, providing a piecewise approximation, resolving thus an issue of non-stationarity. Generalised covariance functions assume that the mean of the process is not constant, but possess a trend in any of the dimensions of the problem (Starks and Fang 1982, Kitanidis 1993, Putter and Young 2001). A combination of these methods for handling spatial non-stationarity is also considered by Nott and Dunsmuir (2002). Applications in the mapping of precipitation fields using non-stationary approaches are significantly limited (Lloyd 2009).

2.4 Simulation of Rainfall-runoff processes using lumped conceptual models

Rainfall-runoff (RR) models are a sub-set of hydrological models which are used to simulate the catchment response to precipitation, by estimating discharge at specific locations. One important feature of RR models is that is not necessary a complete description of the internal processes which generate runoff, as the target of the models is not on the representation of ungauged states of the catchment, but to generate accurate discharge estimations (Devia et al. 2015, Seibert 1999). This simplification fostered the use of diverse modelling techniques such as conceptual and data-driven models (Solomatine and Wagener 2011), which are of use, especially in operational hydrological simulation and forecasting systems.

2.4.1 **Lumped conceptual rainfall-runoff models**

Conceptual hydrological models propose a simplified representation of the processes within the catchment. The description of the processes within the catchment simplifies the spatial variability of the inputs and response of the catchment, by using areal averages.

Conceptual models assume that the catchment and its drivers are homogeneous for each response unit. The parameters are assumed constant in the response unit and are adjusted to minimise the error between observations and simulation of discharge at the concentration point of interest in the catchment (Gupta et al. 2009, Moussa and Chahinian 2009, Booij and Krol 2010). As a result in the flexibility in the representation of the hydrological processes, the parameterisation of the model is not necessarily unique to yield similar simulation performance. Additionally, as a consequence of this incomplete description of the physical system, the internal parameters of the model are to be numerically defined, instead of being measured in the field. Considering these reasons, model parameterisation is a major uncertainty source in conceptual hydrological models (Beven and Freer 2001, Beven 2012).

In this document, an empirical RR model and 2 conceptual RR models are used: Linear Reservoir (Zeeuw 1973), Tank (Sugawara 1961) and HBV96 (Lindström et al. 1997). These models mean to represent 3 different conceptual models with different complexities, from the simplest linear reservoir, to a more elaborate description of internal processes such as the HBV.

The Linear Reservoir is used as the simplest tool for RR modelling. It assumes that the catchment acts as a reservoir which discharge is controlled by the water level inside of it (Figure 2.2). As such, the states of the model corresponds to the water level (and consequently, the previous discharge), the inputs are effective precipitation (*P*) and the output is discharge (*Q*). The model has a unique parameter (*k*), which controls the discharge rate, and thus, modulates the response of the catchment.

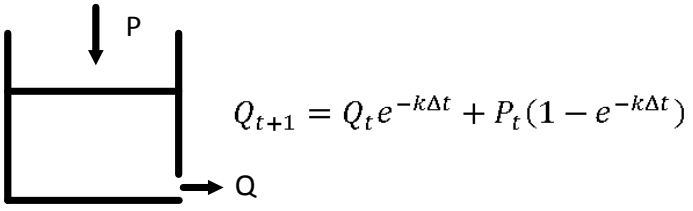

Figure 2.2 Linear reservoir hydrological model

Where *Q* is the discharge, *P* is effective precipitation, *k* is the model parameter and Δt is the size of the model time step.

The Sugawara (Sugawara 1961) tank is an extension of the Linear Reservoir model which uses several (linear or non-linear) tanks. The flexibility in the selection of the number of tanks, and its response, provides a more complex representation of the phenomena, which not necessarily

yields better simulation results. A 2 linear tanks Sugawara model is presented in Figure 2.3, however the configuration of the tanks is arbitrary and has to be defined by the modeller.

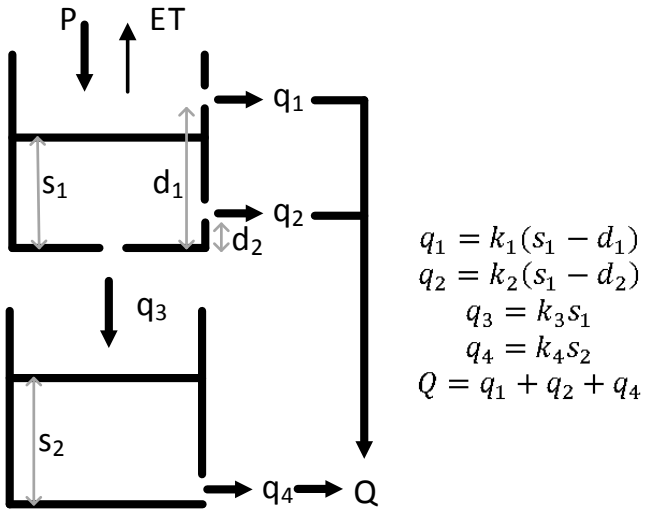

Figure 2.3 Sugawara (2 tank) model

Where *P* stands for precipitation and *ET* for evapotranspiration. *S1* and *S2* are the model states, represented by the water level in each of the tanks. *d1* and *d2* are the position of the outlets in the top tank. And $k_1$to k_4 represent the flux constants. Therefore, *d* and *k* are the model parameters to be determine during calibration. The description of the model components is presented in Table 2.1. The HBV-96 (Lindström et al. 1997) is a widely used conceptual method for flow simulation which conceptualise hydrological process for the simulation of discharge. The simulated processes are infiltration, snow dynamics, soil moisture dynamics, capillary flux, percolation to the deeper aquifer, fast and slow response of the catchment, among others. A conceptualisation of the HBV96 model is presented in Figure 2.4.

Table 2.1 Sugawara (2 tanks) model fluxes, states, inputs and parameters

Type	Variable	Description
Fluxes	q1	Upper outlet top tank discharge
	q2	Lower outlet top tank discharge
	q3	Bottom outlet top tank discharge
	q4	Bottom tank discharge
States	S1	Top tank water level
	S2	Bottom tank water level
Inputs	P	Effective precipitation
	ET	Evapotranspiration
Parameters	d1	Top tank upper outlet position
	d2	Top tank lower outlet position
	k1	Top tank upper outlet discharge coefficient
	k2	Top tank lower outlet discharge coefficient
	k3	Top tank bottom outlet discharge coefficient
	k4	Bottom tank discharge coefficient

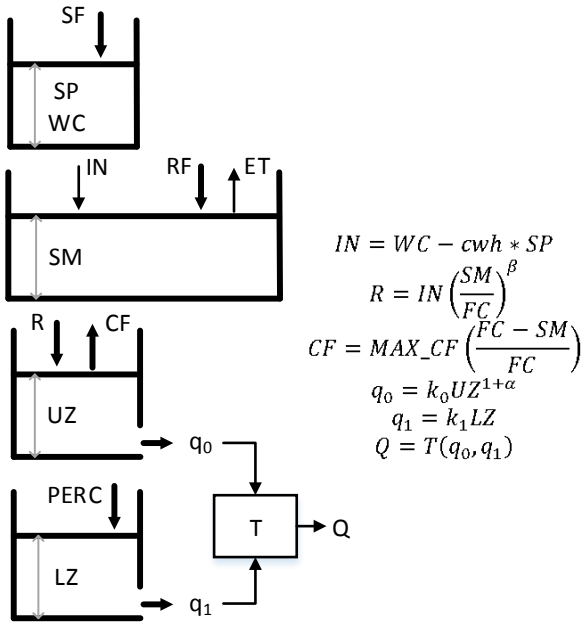

Figure 2.4 HBV hydrological model

Where the variables as described as (Table 2.2):

Table 2.2 HBV96 model fluxes, states, inputs and parameters

Type	Variable	Description
Fluxes	IN	Infiltration
	R	Recharge
	CF	Capillary flux
	PERC	Percolation
	q0	Fast response
	q1	Slow response
States	SP	Snow pack
	WC	Snow pack water content
	SM	Soil moisture
	UZ	Upper zone
	LZ	Lower zone
Inputs	SF	Snowfall
	RF	Rainfall
	ET	Evapotranspiration
Parameters	cwh	Snow pack water holding capacity
	MAX_CF	Maximum capillary flow
	FC	Field capacity
	α	Fast response exponent
	ß	Soil moisture yield exponent
	k0	Quick response parameter
	k1	Slow response parameter

2.4.2 **Role of measurements in rainfall-runoff modelling**

The typical data flow for hydrological rainfall-runoff modelling can be summarised as in Figure 2.5. For discharge simulation, precipitation and evapotranspiration are the most common data requirements (WMO 2008a, Beven 2012), while discharge data is commonly employed for model calibration, correction and update (Sun et al. 2016). Data-driven hydrological models may use measured discharge as input variables as well (Solomatine and Xue 2004, Shrestha and Solomatine 2006). Methods for updating of hydrological models have been widely used in discharge forecasting as data assimilation, using the model error to update the model states. In this way, more accurate discharge estimates can be obtained (Liu et al. 2012, Lahoz and Schneider 2014). In real-time error correction schemes, typically, a data-driven model of the error is employed which may require as input any of the mentioned variables (Xiong and OConnor 2002, Solomatine and Ostfeld 2008).

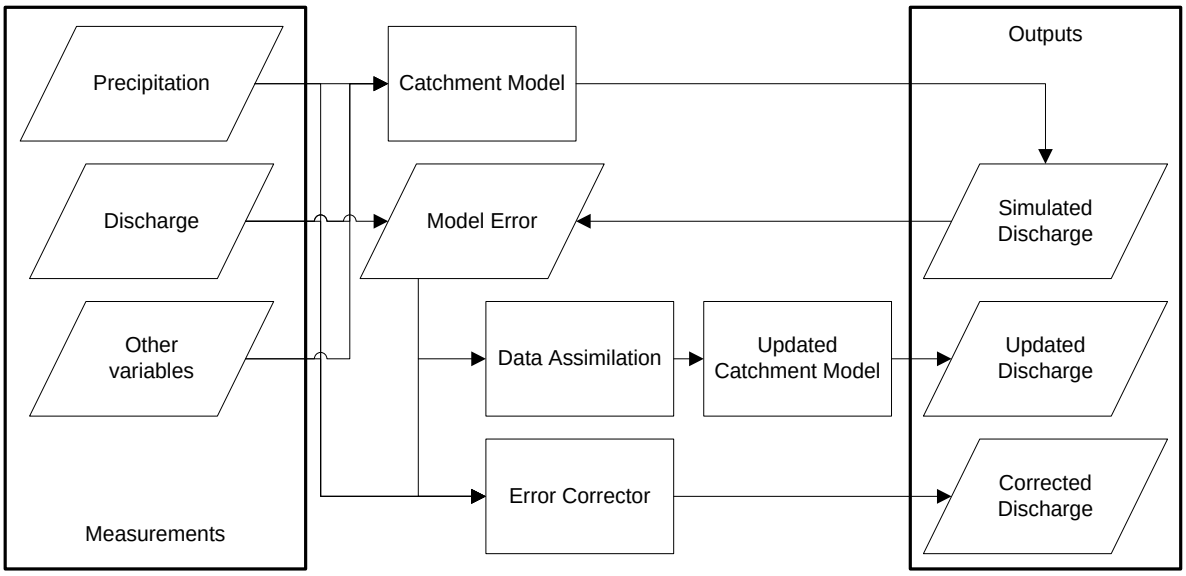

Figure 2.5 Typical data flow in discharge simulation with hydrological models

In a conceptual way, we can express the quantification of discharge at a given station as (Solomatine and Wagener 2011):

$$Q = \hat{Q}(x, \theta) + \varepsilon \qquad \textit{Equation 2.3}$$

Where Q is the recorded discharge, $\hat{Q}(x,\theta)$ represents a hydrological model, which is function of measured variables (mainly precipitation and discharge, x) and the model parameters (ϑ). ε is the simulation error, which is ideally independent of the model, but in practice is conditioned by it. Considering that neither the measurements are perfect, nor the model unbiased, the variance of the estimates is proportional to the uncertainty in the model inputs, $\sigma^2(x)$, and the uncertainty in model parameters, $\sigma^2(\theta)$:

$$\sigma^2\left(\hat{Q}(x,\theta)\right) \alpha\, \sigma^2(x), \sigma^2(\theta) \qquad \textit{Equation 2.4}$$

2.5 Classification of approaches for sensor network evaluation

There is a variety of approaches for the evaluation of sensor networks, ranging from theoretically sound to more pragmatic. In this section, we provide a general classification of these approaches, and more details of each method are given in the next section.

Although most of the approaches for the design of sensor networks make use of data, some rely solely on experience and recommendations. Therefore, a first tier in the proposed classification consists of recognising both measurement-based and measurement-free approaches (Figure 2.6). The former make use of the measured data to evaluate the performance of the network (Tarboton et al. 1987, Anctil et al. 2006), while the latter use other data sources (Moss and Tasker 1991), such as topography and land use.

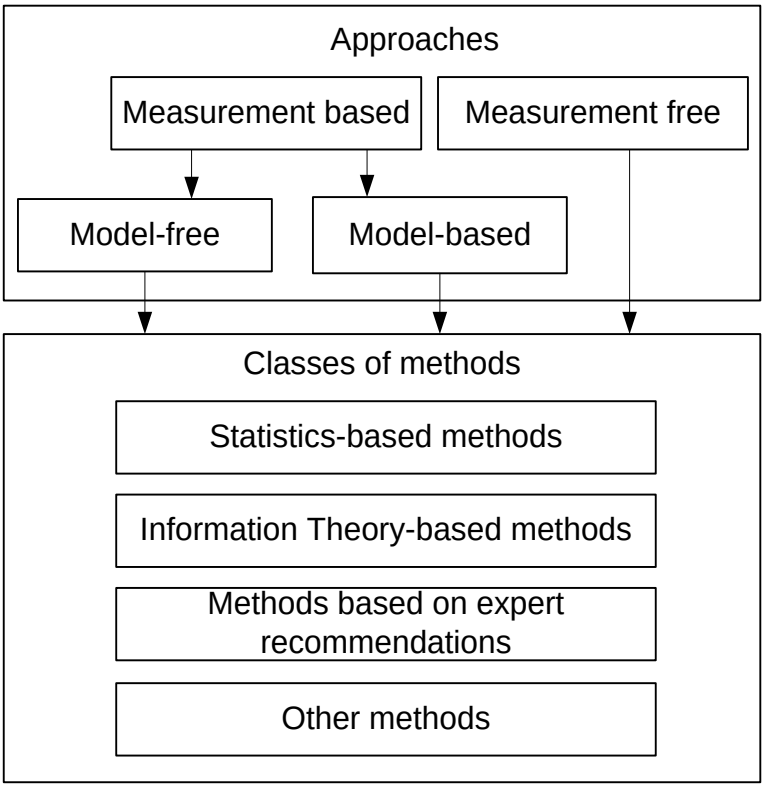

Figure 2.6 Proposed classification of methods for sensor network evaluation

2.5.1 **Sensor network evaluation**

As it is seen from its name, this approach does not require the previous collection of data of the measured variable to evaluate the sensor network performance. The evaluation of sensor networks is based on either experience or physical characteristics of the area such as land use, slope or geology. In this group of methods, the following can be mentioned: case-specific recommendations (Bleasdale 1965, Wahl and Crippen 1984, Karasseff 1986, WMO 2008a) and physiographic components (Tasker 1986, Laize 2004). This approach is the first step towards any sensor network development (Bleasdale 1965, Moss et al. 1982, Karasseff 1986, Nemec and Askew 1986).

In this section, we classify the methods used to quantify the performance of the sensor networks based on the mathematical apparatus used to evaluate the network performance. These methods can be broadly categorised in statistics-based, information theory-based, expert recommendations, and others.

The measurement-based approach can be furtherly subdivided into model-free and model-based approaches (Figure 2.6), depending on the use of modelling results in the performance metric. In model-free approaches, water systems and the external processes that drive their behaviour are observed through measurements, without the use of catchment models. Then, metrics about amount and quality of information in space and time are evaluated with regards to the management objectives and the decisions to be made in the system. Some performance metrics in this category are joint entropy (Krstanovic and Singh 1992a, 1992b), Information Transfer (Yang and Burn 1994), interpolation variance (Delhomme 1973, Pardo-Igúzquiza 1998, Cheng

et al. 2007) and autocorrelation (Moss and Karlinger 1974), among others. Figure 2.7 presents the scheme for the case when precipitation and discharge, as main drivers of catchment hydrology are considered, in model-free network evaluation (WMO 2008).

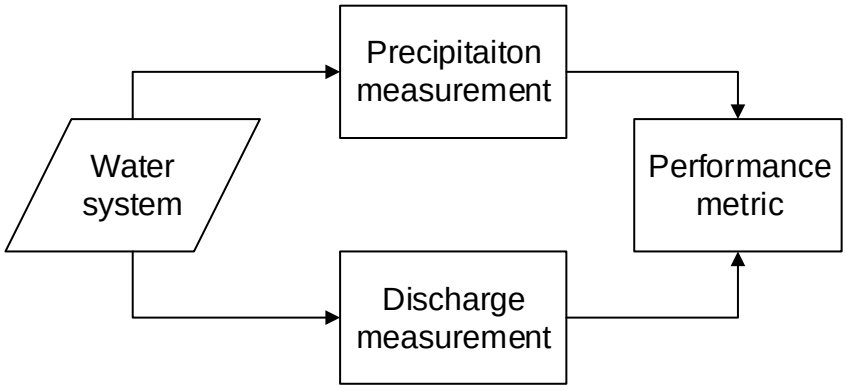

Figure 2.7 General procedure for Model-free sensor network evaluation

Fundamentally, the model-free approach aims to minimise the variance of the measured variable, therefore, (and in theory) minimising the variance in the estimation. However, a design that is optimal for estimation is not necessarily also optimal for prediction (Chaloner and Verdinelli 1995).

$$\min \sigma^2 \left(\hat{Q}(x,\theta)\right) \; \alpha \; \min\left(\sigma^2(x)\right) \qquad \textit{Equation 2.5}$$

Application of model-free approaches can be found in Krstanovic and Singh (1992a), Nowak et al. (2010), Li et al. (2012). Model-free evaluations are suitable for sensor network design aiming mainly to water resources planning, in which diverse water interests must be balanced. Due to the lack of a quantitative performance metric that relates simulated discharge, this kind of evaluations do not necessarily improve rainfall-runoff simulations.

In the model-based approach, the performance of sensor networks is carried out using a catchment model (Dong et al. 2005, Xu et al. 2013). In this case, measurements of precipitation are used to simulate discharge, which is compared to the discharge measurements at specific locations. Therefore, any metric of the modelling error could be used to evaluate the performance of the network. Figure 2.8 presents a generic model-based approach for evaluating sensor networks.

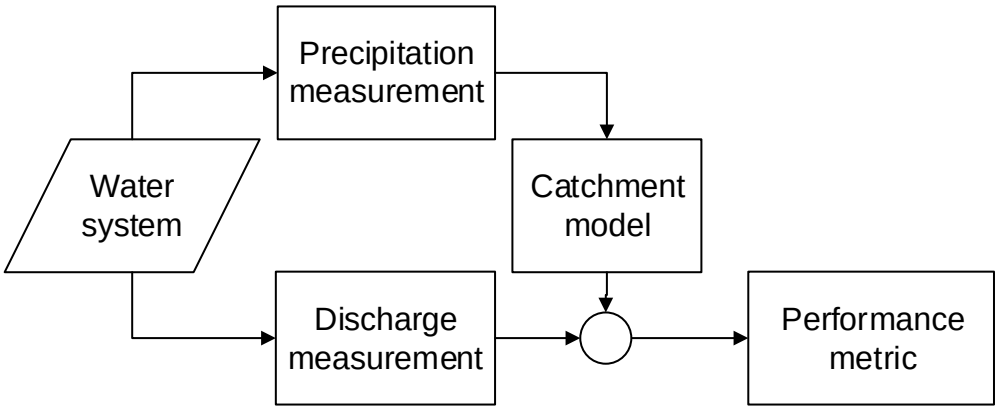

Figure 2.8 General procedure for Model-based sensor network evaluation

In the model-based design of sensor networks, it is assumed that the model structure and parameters are adequate. Therefore, it is possible to identify a set of measurements (x) which minimise the modelling error as.

$$\min \sigma^2(\epsilon) \ \alpha \min\left(\left|Q - \hat{Q}(x,\theta)\right|\right) \qquad \textit{Equation 2.6}$$

The need for the catchment model and possible high computational efforts for multiple model runs are some disadvantages of this approach. The computational load is especially critical in case of complex distributed models. It is worth mentioning particular model error metrics (Nash and Sutcliffe 1970, Gupta et al. 2009) may qualify the network by its ability to capture certain hydrological processes (Bennett et al. 2013), affecting the network evaluation.

2.5.2 **Statistics-based methods**

Statistics-based methods refer to methods where the performance of the network is evaluated with statistical uncertainty metrics of the measured or simulated variable. These methods aim to minimise either interpolation variance (Delhomme 1973, Rodriguez-Iturbe and Mejia 1974, Bastin et al. 1984, Bastin and Gevers 1985, Pardo-Igúzquiza 1998, Bonaccorso et al. 2002), cross-correlation (Maddock 1974, Moss and Karlinger 1974, Tasker 1986), or model error (Dong et al. 2005, Xu et al. 2013).

Interpolation variance (geostatistical)

Methods to evaluate sensor networks considering a reduction in the interpolation variance assume that for a network to be optimal, the measured variable should be as certain as possible in the domain of the problem. To achieve this, a stochastic interpolation model that provides uncertainty metrics is required. Geostatistical methods such as Kriging (Journel and Huijbregts 1978, Cressie 1993, Cressie 2015), or Copula interpolation (Bardossy 2006) have an explicit estimation of the interpolation error. This characteristic makes it suitable to identify areas with expected poor interpolation results, (Bastin et al. 1984, Pardo-Igúzquiza 1998, Grimes et al. 1999, Bonaccorso et al. 2002, Cheng et al. 2007, Nowak et al. 2010, Shafiei et al. 2014). The PDF of the field provides a framework to identify areas with deficiencies in spatial coverage of the network (Bogárdi et al. 1985).

The variance of the interpolation error σ^2 is determined by the covariance structure (C) of the measurements, and the distance between the stations and the interpolation target $(u_\alpha - u)$ (Journel and Huijbregts 1978, Cressie 1993) as:

$$\sigma^2(u) = C(0) - \sum_{\alpha=1}^{n} \lambda_\alpha(u)\big(\mathrm{C}\,(u_\alpha - u)\big) - \mu(u) \qquad \textit{Equation 2.7}$$

where C is the covariance function, $C(0)$ is the autocovariance of the random field, $C(u_\alpha - u)$ is the covariance between station α and the interpolation target u. In the design of precipitation sensor networks, the optimal network is such that minimises the average Kriging (interpolation) variance (AKV) (Rodriguez-Iturbe and Mejia 1974, Pardo-Igúzquiza 1998) over a considered area Ω as:

$$AKV = \frac{1}{U}\sum_{u=1}^{\Omega} \sigma^2(u) \qquad \textit{Equation 2.8}$$

Alternatively, the optimal network can also be defined as such that minimise the maximum (min-max) interpolation variance (MKV) (Barca et al. 2015) as:

$$MKV = \max \sigma^2(u)\,;\, u\epsilon\Omega \qquad \textit{Equation 2.9}$$

Bastin and Gevers (1985) optimised a precipitation sensor network at pre-defined locations to estimate the average precipitation for a given catchment. Their selection of the optimal sensor location consisted of minimising the normalised uncertainty by reducing the network. The main drawback of their approach is that the network can only be reduced and not augmented. Similar approaches have also been used by Rodriguez-Iturbe and Mejia (1974), Bogárdi et al. (1985), and Morrissey et al. (1995). Pardo-Igúzquiza (1998) advanced this formulation by removing the pre-defined set of locations (allowing augmentation). Instead, rain gauges were allowed to be placed anywhere in the catchment and its surroundings. A simulated annealing algorithm is used to search for the find the optimal set of sensors to minimise the interpolation uncertainty.

Copula interpolation is a geostatistical alternative to Kriging for the modelling of spatially distributed processes (Bardossy 2006, Bardossy and Li 2008, Bardossy and Pegram 2009). As a geostatistical model, the copula provides metrics of the interpolation uncertainty, considering not only the location of the stations and the model parameterisation but also the value of the observations. Li et al. (2011) use the concept of copula to provide a framework for the design of a monitoring network for groundwater parameter estimation, using a utility function, related to the cost of a given decision with the available information.

In the case of copula, the full conditional probability distribution function of the variable is interpolated. As such, the interpolation uncertainty depends on the confidence interval, measured values, parameterisation of the copula and the relative position of the sensors in the

domain of the catchment. More details on the formulation of copula-based design can be found in Bárdossy and Li (2008)

Cheng et al. (2007), as well as Shafiei et al. (2014), recognised that the temporal resolution of the measurements affects the definition of optimality in minimum interpolation variance methods. This change in the spatial correlation structure occurs due to more correlated precipitation data between stations in coarser sampling resolutions (Krajewski and Duffy 1986, Ciach and Krajewski 2006). For this purpose, the sensor network has to be split into two parts, a base network and non-base sensors. The former should remain in the same position for long periods, to characterise longer fluctuation phenomena, based on the definition of a minimum threshold for an area with acceptable accuracy. The latter is relocated to improve the accuracy of the whole system, and should be relocated as they do not provide a significant contribution to the monitoring objective.

Recent efforts have used minimum interpolation variance approaches to consider the non-stationarity assumption of most geostatistical applications in sensor network design (Chacon-Hurtado et al. 2014). To this end, changes in the precipitation pattern and its effect on the uncertainty estimation were considered during the development of a rainfall event.

Cross-correlation

The objective of minimum cross-correlation methods is to avoid placing sensors at sites that may produce redundant information. Cross-correlation was suggested by Maddock (1974) for sensor network reduction, as a way to identify redundant sensors. In this scope, the objective function can be written as:

$$\rho(X_i, X_j) = \sum_{i=1}^{n} \sum_{j=i+1}^{n} \frac{cov(x_i, x_j)}{\sigma(x_i)\sigma(x_j)} \qquad \textit{Equation 2.10}$$

Where *cov* is the covariance function between a pair of stations *(i, j)*, and σ is the standard deviation of the observations.

Stedinger and Tasker (1985) introduced the method called Network Analysis Using Generalized Least Squares (NAUGLS), which assesses the parameters of a regression model for daily discharge simulation based on the physiographic characteristics of a catchment (Stedinger and Tasker 1985, Tasker 1986, Moss and Tasker 1991). The method builds a Generalised-Least-Square (GLS) covariance matrix of regression errors to correlate flow records and to consider flow records of different length, so the sampling mean squared error can be expressed as:

$$SMSE = \frac{1}{n} \sum_{i=1}^{j} X_i^T (X^T \Lambda^{-1} X)^{-1} X_i \qquad \textit{Equation 2.11}$$

Where *X [k, w]* is the matrix of the (*k*) basin characteristics in a window of size *w* at discharge measuring site *i*. Λ is the GLS Weighting matrix, using a set of *n* gauges (Tasker 1986).

A comparable method was proposed by Burn and Goulter (1991), who used a correlation metric to cluster similar stations. Vivekanandan and Jagtap (2012) proposed an alternative for the location of discharge sensors in a recurrent approach, in which the most redundant stations were removed, and the most informative stations remained using the Cooks' D metrics, a measure of how the spatial regression model at a particular site is affected by removing another station. The result of these type of sensors is sparse, as the redundancy of two sensors increases with the inverse of the distance between them (Mishra and Coulibaly 2009).

Model output error

RR models are used to transform the measurements of precipitation into estimates of discharge at the outlet of a catchment. RR models are divided into physically-based, conceptual and data-driven models (Solomatine and Wagener 2011). Physically-based models describe rigorously the processes within the catchment, by maintaining the energy, momentum and mass-conservations of the system. Conceptual models use simplified representation of the hydrological processes within the catchment, usually aiming to represent a few states of interest. Data-driven models are built over the relationship of the data itself, making it suitable in simulation and forecasting environments, but limiting the possibility of assessing any of the hydrological processes. Different RR models have different data requirements, depending on the type of measured variables, spatial and temporal resolution, and purpose of the model, among others.

Conceptual models are widely used for RR modelling (Solomatine and Wagener 2011, Beven 2012). Depending on the spatial aggregation, conceptual models are furtherly divided into lumped, semi-distributed and distributed models, depending on the internal topology of the catchment. For the purpose of flow forecasting, the accuracy of lumped models is typically comparable to physically-based and distributed conceptual models (Carpenter and Georgakakos 2006, Ortiz and Guna 2009, Hassan et al. 2013, Devia et al. 2015).

The evaluation of the simulation models is usually carried out in metrics that describe the simulation error. NSE (Equation 2.12) is a score introduced by Nash and Sutcliffe (1970) which compares the variance of the model residuals over the variance of the measurements (Krause et al. 2005, Gupta et al. 2009). NSE is bound between minus infinity and one. In practice, values of NSE smaller than 0 indicate that the predicting capability of the model lies below the average of the data. On the other end, a score of 1 indicates a perfect fit.

$$NSE = 1 - \frac{\sum(Q_s - Q_r)^2}{\sum\left(\bar{Q}_r - Q_r\right)^2} \qquad \textit{Equation 2.12}$$

Where Q_s is the simulated, and Q_r is the recorded discharge. NSE is the efficiency using the inputs from the reduced network, and the. Another performance metric consists in the

evaluation of the average error of the model (Franz and Hogue 2011, Beven 2012), also known as bias. This metrics indicates the deviation from the mean of the residuals. Ideally, the residuals should be unbiased (bias = 0). To use the model bias as an objective function for sensor network design, absolute bias is preferred, considering that there are no different consequences from a positive or negative bias in the results (Equation 2.13).

$$BIAS = \frac{1}{k}\left|\sum Q_s - Q_r\right| \qquad \textit{Equation 2.13}$$

Finally, according to Dong et al. (2005) the optimal sensor network is such that maximises the correlation between the average precipitation and the recorded discharge (Equation 2.14). These results come from an experimental study and are furtherly explored in this document.

$$CPQ = \rho(\bar{P}, Q_r) \qquad \textit{Equation 2.14}$$

Where $\bar{P}$ is the average precipitation in the catchment and Q_r is the recoded discharge, and ρ is the correlation function.

Another application is provided by Dong et al. (2005) who proposed to evaluate the rainfall network using a lumped HBV model. They found that the model performance does not necessarily improve when extra rain gauges are placed. A similar approach was presented by Xu et al. (2013) who evaluated the effect of diverse rain gauge locations on runoff simulation using a similar hydrological model. It was found that rain gauge locations could have a significant impact and suggest that a gauge density less than 0.4 stations per 1000 km2 can negatively affect the model performance.

Anctil et al. (2006) aimed at improving lumped neural network rainfall-runoff forecasting models through mean areal rainfall optimisation, and concluded that different combinations of sensors lead to noticeable streamflow forecasting improvements. Studies in other fields have also used this method. For example, Melles et al. (2009, 2011), obtained optimal monitoring designs for radiation monitoring networks, which minimise the prediction error of mean annual background radiation. The main drawback of this approach is that multiple error metrics are considered, as specific objectives relate to different processes

2.5.3 **Information Theory-based methods**

The use of Information Theory (Shannon 1948) in the design of sensor networks for environmental monitoring is based on Communication Theory, which studies the problem of transmitting signals from a source to a receiver throughout a noisy medium. Information Theory provides the possibility of estimating probability distribution functions in the presence of partial information with the less biased estimation (Jaynes 1957). Some of its concepts are analogous to statistics concepts, and therefore similarities between entropy and uncertainty, as mutual

information and correlation, etc., can be found (Cover and Thomas 2006, Alfonso et al. 2010, Singh 2013).

Information Theory-based methods for designing sensor networks mainly consider the maximisation of information content that sensors can provide, in combination with the minimisation of redundancy among them (Krstanovic and Singh 1992a, 1992b, Mogheir and Singh 2002, Alfonso 2010, Alfonso et al. 2010, 2013, Singh 2013). Redundancy can be measured by using either Mutual Information (Singh 2000, Steuer et al. 2002), Directional Information Transfer (Yang and Burn 1994), Total Correlation (Alfonso et al. 2010, Fahle et al. 2015), among others.

Information Theory (IT) provides a framework to measure the information content of a random variable as well as the amount of shared information among a set of them, based on its (joint) probabilities (Jaynes 1957, Kolmogorov 1965, Shannon 1948). The information-based metrics can either represent information content (e.g. entropy) or information redundancy (e.g. mutual information), which are the foundation for the metrics of sensor network performance (Li et al. 2012).

Entropy

The Principle of Maximum Entropy (POME) is based on the premise that probability distribution with the largest remaining uncertainty (i.e., the maximum entropy) is the one that best represent the current stage of knowledge (Penfeld 2003). POME has been used as a criterion for the design of sensor networks, by allowing the identification of the set of sensors that maximises the joint entropy among measurements (Krstanovic and Singh 1992a). In other words, to provide as much information content, from the Information Theory perspective, as possible (Jaynes 1988).

Entropy (*H*) is a measure of the amount of information contained in a single random variable (Cover and Thomas 2006). Due to its roots in communication theory, information-theory estimates are suited for discrete variables, thus, continuous variables have to be quantised. Quantisation, refers to the methods to convert a continuous into a discrete variable (Gray and Neuhoff 1998). The information content (entropy, *H*) for a discrete variable can then be estimated as (Equation 2.15).

$$H(X) = -\sum_{x}^{I} p(x)\log p(x) \qquad \textit{Equation 2.15}$$

where $p(x)$ is the probability of the variable X taking the discrete value x, or, the probability of variable X being in the interval x.

For multiple random variables, the information contained in the set is not necessarily independent. Joint entropy (*JH*) measures the amount of non-redundant information which is

captured by the sensor network (set). Therefore, the measurement of the joint entropy can provide information about the diversity of measurements that the network is able to capture. The joint entropy (*JH*) can be calculated for a set of n discrete variables as (Equation 2.16).

$$JH(X_1, \dots, X_n) = -\sum_{x_1}^{I} \dots \sum_{x_n}^{I} p(x_1, \dots, x_n) \log p(x_1, \dots, x_n) \qquad \textit{Equation 2.16}$$

where $p(x_1,\dots, x_n)$ is the joint probability of the n variables $X_1,\dots, X_n$. For the case of two variables, the formulation can be simplified to Equation 2.17 as:

$$JH(X_1, X_2) = -\sum_{x_1}^{I} \sum_{x_2}^{I} p(x_i, y_j) \log p(x_i, y_j) \qquad \textit{Equation 2.17}$$

Due to the computational complexity of calculating the joint probability distribution of a highly dimensional space, an approximated estimation of the multivariate joint entropy is provided by the sum of the pair-wise joint entropy. This joint entropy is the sum of the joint entropies between the potential combinations of pairs of sensors (*PJH*) as (Equation 2.18):

$$PJH = \sum_{i=1}^{n-1} \sum_{j=i+1}^{n} JH(X_i, X_j) \qquad \textit{Equation 2.18}$$

The joint entropy is (by definition) always smaller or equal to the sum of the individual entropies (Cover and Thomas 2006). From the information theory perspective, an optimal network is such in which the shared information between sensors is minimum. For an optimal network, is expected that the pair-wise joint entropy (*PJH*) may not considerably diverge from the multivariate joint entropy (*JH*).

Krstanovich and Singh (1992a, 1992b) presented a concise work on rainfall network evaluation using entropy. They used POME to obtain multivariate distributions to associate different dependencies between sensors, such as joint information and shared information, which was used later either reduce the network (in the case of high redundancy) or expand it (in the case of lack of common information).

Fuentes et al. (2007) proposed an entropy-utility criterion for environmental sampling, particularly suited for air-pollution monitoring. This approach considers Bayesian optimal sub-networks using an entropy framework, relying on the spatial correlation model. An interesting contribution of this work is the assumption of non-stationarity, contrary to traditional atmospheric studies, and relevant in the design of precipitation sensor networks.

The use of hydraulic 1D models and metrics of entropy have been used to select the adequate spacing between sensors for water level in canals and polder systems (Alfonso et al. 2010,

Alfonso 2010). This approach is based on the current conditions of the system, which makes it useful for operational purposes, but it does not necessarily support the modifications in the water system conditions or changes in the operation rules. Studies on the design of sensor networks using these methods are on the rise in the last years (Alfonso 2010, Alfonso et al. 2013, Ridolfi et al. 2013, Banik et al. 2017).

Benefits of POME include the robustness of the description of the posterior probability distribution since it aims to define the less biased outcome. This is because neither the models nor the measurements are completely certain. Li et al. (2012) presented, as part of a multi-objective framework for sensor network optimisation, the criteria of maximum (joint) entropy, as one of the objectives. Other studies in this direction have been presented by Lindley (1956), Caselton and Zidek (1984), Guttorp et al. (1993), Zidek et al. (2000), Yeh et al. (2011) and Kang et al. (2014).

More recently, Samuel et al. (2013) and Coulibaly and Samuel (2014), proposed a mixed method involving regionalisation and dual entropy multi-objective optimisation (CRDEMO), which is a step forward if compared to single-objective optimisation for sensor network design.

Mutual information (trans-information)

Mutual information is a measurement of the amount of information that a variable contains about another. This is measured as the *relative entropy between the joint distribution and the product distribution* (Cover and Thomas 2006). In the simplest expression (two variables), the mutual information can be defined as:

$$I(X_1, X_2) = H(X_1) + H(X_2) - H(X_1, X_2) \qquad \textit{Equation 2.19}$$

where $H(X_1)$ and $H(X_2)$ is the entropy of each of the variables, and $H(X_1, X_2)$ is the joint entropy between them. The extension of the mutual information for more than two variables should not only consider the joint entropy between them, but also the joint entropy between pairs of variables, leading to a significantly complex expression for the multivariate mutual information. Regarding this issue, the multivariate mutual information can be addressed as a nested problem, such that:

$$I(X_1, X_2, \dots, X_n) = I(X_1, X_2, \dots, X_{n-1}) - I(X_1, X_2, \dots, X_{n-1} | X_n) \qquad \textit{Equation 2.20}$$

Where $I(X_1, X_2, \dots, X_n)$ is the multivariate mutual information among n variables, and $I(X_1, X_2, \dots, X_{n-1} \mid X_n)$ is the conditional information of n-1 variables with respect to the n^{th} variable. The conditional mutual information can be understood as the amount of information that a set of variable share with another variable (or variables). The conditional mutual information of two variables (X_1 and X_2) with respect to a third one (X_3) can be quantified as:

$$I(X_1, X_2 | X_3) = H(X_1 | X_3) - H(X_1 | X_2, X_3) \qquad \textit{Equation 2.21}$$

Where $H(X_1 \mid X_3)$ is the conditional entropy of X_1 to X_3 and $H(X_1 \mid X_2, X_3)$ is the conditional entropy of X_1 with respect to X_2 and X_3 simultaneously. The conditional entropy can be understood as the amount information that a variable does not share with another. The joint entropy between two variables can be quantified as:

$$H(X_1|X_2) = \sum_{i=1}^{k}\sum_{j=1}^{m} p(X_{1i}, X_{2j}) \log \frac{p(X_{1i})}{p(X_{1i}, X_{2j})} \qquad \textit{Equation 2.22}$$

where $p(X_1, X_2)$ is the joint probability, for k and m discrete values, of $X_1$and X_2.

An optimal sensor network should avoid collecting repetitive or redundant information, in other words, it should be such that reduces the mutual (shared) information between sensors in the network. Alternatively, it should maximise the transferred information from a measured to a modelled variable at a point of interest (Amorocho and Espildora 1973). Following this idea, Husain (1987) suggested an optimisation scheme for the reduction of a rain sensor network. His objective was to minimise the trans-information between pairs of stations. However, assumptions of the probability and joint probability distribution functions are strong simplifications of this method. To overcome these assumptions, the Directional Information Transfer (*DIT*) index was introduced (Yang and Burn 1994) as the inverse of the coefficient of non-transferred information (*NTI*) (Harmancioglu and Yevjevich 1985). Both *DIT* and *NTI* are a normalised measure of information transfer between two variables (X_1 and X_2).

$$DIT = \frac{I(X_1, X_2)}{H(X_1)} \qquad \textit{Equation 2.23}$$

Particularly for the design of precipitation sensor networks, Ridolfi et al. (2011) presented a definition of the maximum achievable information content for designing a dense network of precipitation sensors at different temporal resolutions. The results of this study show that there exists a linear dependency between the non-transferred information and the sampling frequency of the observations.

Entropy estimations are relative to the measured variables and its study case. The average information transfer (*AIT*) between a pair of stations, normalise the entropy estimations, by scaling the joint entropy over one of the variables (or station) simultaneously (Yang and Burn 1994). This normalisation permits an unbiased comparison of results between different case studies. The optimal sensor network is such that minimises the *AIT* (Equation 2.24).

$$AIT = \frac{1}{n^2}\sum_{i=1}^{n}\sum_{j=1}^{n} \frac{JH(X_i, X_j)}{H(X_i)} \qquad \textit{Equation 2.24}$$

Total Correlation (*C*) is an alternative measure of the amount of shared information between two or more variables, and has also been used as a measure of information redundancy in the design of sensor networks ((Alfonso et al. 2010, Alfonso 2010, Leach et al. 2015) as:

$$C(X_1, \dots, X_n) = \sum_{i=1}^{n} H(X_i) - H(X_1, \dots, X_N) \qquad \textit{Equation 2.25}$$

Where $C(X_1, X_2, \dots, X_n)$ is the total correlation among the *n* variables, $H(X_i)$ is the entropy of the variable *i*, and $H(X_1, X_2, \dots, X_n)$ is the joint entropy of the *n* variables. Total Correlation can be seen then as a simplification of the multivariate mutual information, where only the interaction among all the variables is considered. In the design of sensor networks, it is expected that the mutual information among the different variables is minimum, therefore, the difference between the total correlation and multivariate mutual information tends to be minimised as well. The advantage of total correlation is the computational advantage that represents assuming a marginal value for the interaction among variables.

Another information theory objective function used in the design of sensor networks is to minimise the amount of redundant information. Total correlation (Alfonso et al. 2010) is a measure of the amount of redundant information between a set of variables (or sensors on a network) and is quantified as the difference between the sum of all the individual entropies and the joint entropy (Equation 2.26). Consequently, the optimal sensor network is such that minimises the total correlation (*TC*).

$$TC = \sum_{i=1}^{n} H(X_i) - JH\ (x_1, \dots, x_n) \qquad \textit{Equation 2.26}$$

A method to estimate trans-information fields at ungauged locations has been proposed by Su and You (2014), employing a trans-information-distance relationship. This method accounts for spatial distribution of precipitation, supporting the augmentation problem in the design of precipitation sensor networks. However, as the relationship between trans-information between sensors and their distance is monotonic, the resulting sensor networks are generally sparse.

2.5.4 **Methods based on expert recommendations**

Physiographic components

Among the most used planning tools for hydrometric network design are the technical reports presented by the WMO (2008), in which a minimum density of stations depending on different physiographic units, are suggested (Table 2.3). Although these guidelines do not provide an indication about where to place hydrometric sensors, rather they recommend that their distribution should be as uniform as possible and that network expansion has to be considered. The document also encourages the use of computationally aided design and evaluation of a more comprehensive design. For instance, Coulibaly et al. (2013) suggested the use of these guidelines to evaluate the Canadian national hydrometric network.

Table 2.3 Recommended minimum densities of stations (area in Km² per station) – Adopted from WMO [2008]

Physiographic unit	Precipitation		Evaporation	Streamflow	Water Quality
	Non-recording	Recording			
Coastal	900	9,000	50,000	2,750	55,000
Mountains	250	2,500	50,000	1,000	20,000
Interior plains	575	5,750	5,000	1,875	37,500
Hilly/undulating	575	5,750	50,000	1,875	47,500
Small islands	25	250	50,000	300	6,000
Urban areas	–	10–20	–	–	–
Polar/arid	10,000	10,000	100,000	20,000	200,000

Moss et al. (1982) presented one of the first attempts to use physiographic components in the design of sensor networks in a method called Network Analysis for Regional Information (*NARI*). This method is based on relations of basin characteristics proposed by Benson and Matalas (1967). *NARI* can be used to formulate the following objectives for network design: minimum cost network, maximum information and maximum net benefit from the data-collection program, in a Bayesian framework, which can be approximated as:

$$\log \sigma\left(S\left(\left|\hat{Q} - Q\right|\right)^{\alpha}\right) = a + \frac{b_1}{n} + \frac{b_2}{y} \qquad \textit{Equation 2.27}$$

where the function $S(|\hat{Q} - Q|)^{\alpha}$ is the α percentile of the standard error in the estimation of Q, a, b_1 and b_2 are the parameters from the *NARI* analysis, n is the number of stations used in the regional analysis, and y is the harmonic mean of the records used in the regression.

Laize (2004) presented an alternative for evaluating precipitation networks based on the use of the Representative Catchment Index (*RCI*), a measure to estimate how representative a given station in a catchment is for a given area, on the stations in the surrounding catchments. The author argues that the method, which uses datasets of land use and elevation as physiographical components, can help identifying areas with an insufficient number of representative stations on a catchment.

Practical case-specific considerations

Most of the first sensor networks were designed based on expert judgement and practical considerations. Aspects such as the objective of the measurement, security and accessibility are decisive to select the location of a sensor. Nemec and Askew (1986) presented a short review of the history and development of the early sensor networks, where it is highlighted that the use of "basic pragmatic approaches" still had most of the attention, due to its practicality in the field and its closeness with decision makers.

Bleasdale (1965) presented a historical review of the early development process of the rainfall sensor networks in the United Kingdom. In the early stages of the development of precipitation sensor networks, two main characteristics influencing the location of the sensors were identified: at sites that were conventionally satisfactory and where good observers were located. However, the necessity of a more structured approach to select the location of sensors was underlined. As a guide, Bleasdale (1965) presented a series of recommendations on the minimal density of sensors for operational purposes, relating the characteristics of the area to be monitored and the minimum required a number of rain sensors, as well as its temporal resolution.

In a more structured approach, Karasseff (1986) introduced some guidelines for the definition of the optimal sensor network to measure hydrological variables for operational hydrological forecasting systems. The study specified the minimum requirements for the density of measurement stations based on the fluctuation scale and the variability of the measured variable by defining zonal representative areas

From a different perspective, Wahl and Crippen (1984) as well as Mades and Oberg (1986) proposed a qualitative score assessment of different factors related to the use of data and the historical availability of records for the evaluation of sensor value. Their analyses aimed at identifying candidate sensors to be discontinued, due to their limited accuracy.

User survey

These approaches aim to identify the information needs of particular groups of users (Sieber 1970), following the idea that the location of a certain sensor (or group of sensors) should satisfy at least one specific purpose. To this end, surveys to identify the interests for the measurement of certain variables, considering the location of the sensor, record length, frequency of the records, methods of transmission, among others, are executed.

Singh et al. (1986) applied two questionnaires to evaluate the streamflow network in Illinois: one to identify the main uses of streamflow data collected at gauging stations, where participants described how data was used and how they would categorise it in either site-specific management activities, local or regional planning and design, or determination of long-term trends. The second questionnaire was used to determine present and future needs for streamflow information. The results showed that the network was reduced due to the limited interest about certain sensors, which allowed for enhancing the existing network using more sophisticated sensors or recording methods. Additionally, this redirection of resources increased the coverage at specific locations.

2.5.5 **Other methods**

There are also other methods that cannot be easily attributed to the previously mentioned categories. Among them, Value of Information, fractal, and network theory-based methods can be mentioned.

Value of Information

The Value of Information (*VOI*), (Howard 1966, Hirshleifer and Riley 1979) is defined as the value a decision-maker is willing to pay for extra information before making a decision. This willingness to pay is related to the reduction of uncertainty about the consequences of making a wrong decision (Alfonso and Price 2012).

The main feature of this approach is the direct description of the benefits of additional piece of information, compared with the costs of acquiring that extra piece of information (Black et al. 1999, Walker 2000, Nguyen and Bagajewicz 2010, 2011, Alfonso and Price 2012, Ballari et al. 2012). The main advantage of this method is that provides a pragmatic framework in which information have a utilitarian value, usually economic, which is especially suited for budget constraint conditions.

One of the assumptions of this type of models is that a prior estimation of consequences is needed. If *a* is the action that has been decided to perform, *m* is the additional information that comes to make such a decision, and *s* is the state that is actually observed, then the expected utility of any action a can be expressed as:

$$u(a, P_s) = \sum_S P_s u(C_{as}) \qquad \textit{Equation 2.28}$$

where P_s is the perception, in probabilistic terms, of the occurrence of a particular state (*s*) among a total number of possible states (*S*), and *u* is the utility of the outcome C_{as} of the actions given the different states. When new information (i.e., a message *m*) becomes available, and the decision-maker accepts it, his prior belief P_s will be subject to a Bayesian update. If $P(m|s)$ is the likelihood of receiving the message *m* given the state *s* and P_m is the probability of getting a message *m* then:

$$P_m = \sum_S P_s P(m|s) \qquad \textit{Equation 2.29}$$

The value of a single message *m* can be estimated as the difference between the utility, *u*, of the action, a_m that is chosen given a particular message *m* and the utility of the action, a_0, that would have been chosen without additional information as:

$$\Delta_m = u\big(a_m, P(s|m)\big) - u\big(a_0, P(s|m)\big) \qquad \textit{Equation 2.30}$$

The Value of Information, *VOI*, is the expected utility of the values Δ_m:

$$VOI = E(\Delta_m) = \sum_M P_m \Delta_m \qquad \textit{Equation 2.31}$$

Following the same line of ideas, Khader et al. (2013) proposed the use of decision trees to account for the development of a sensor network for water quality in drinking groundwater applications. *VOI* is a straightforward methodology to establish present causes and consequences of scenarios with different types of actions, including the expected effect of additional information. A recent effort by Alfonso et al. (2016) towards identifying valuable areas to get information for floodplain planning consists of the generation of VOI maps, where probabilistic flood maps and the consequences of urbanisation actions are taken into account to identify areas where extra information may be more critical.

Fractal-based

Fractal-based methods employ the concept of Gaussian self-affinity, where sensor networks show the same spatial patterns at different scales. This affinity can be measured by its fractal dimension (Mandelbrot 2001). Lovejoy et al. (1986) proposed the use of fractal-based methods to measure the dimensional deficit between the observations of a process and its real domain. Consider a set of evenly distributed cells representing the physical space, and the fractal dimension of the network representing the number of observed cells in the correlation space. The lack of non-measured cells in the correlation space is known as the fractal deficit of the network. Considering that a large number of stations have to be available at different scales, the method is suitable for large networks, but less useful in the deployment of few sensors in a catchment scale.

Lovejoy and Mandelbrot (1985) and Lovejoy and Schertzer (1985) introduced the use of fractals to model precipitation. They argued that the intermittent nature of the atmosphere can be characterised by fractal measures with fat-tailed probability distributions of the fluctuations, and stated that standard statistical methods are inappropriate to describe this kind of variability. Mazzarella and Tranfaglia (2000) and Capecchi et al. (2012) presented two different case studies using this method for the evaluation of a rainfall sensor networks. The former study concludes that for network augmentation, it is important to select the optimal locations that improve the coverage, measured by the reduction of the fractal deficit. However, there are no practical recommendations on how to select such locations. The latter proposes the inspection of seasonal trends as the meteorological processes of precipitation may have significant effects on the detectability capabilities of the network.

A common approach for the quantification of the dimensional deficit is the box-counting method (Song et al. 2007, Kanevski 2008), mainly used in the fractal characterisation of precipitation sensor networks. The fractal dimension of the network (*D*) is quantified as the ratio of the logarithm of the number of blocks (*NB*) that have measurements and the logarithm of the scaling radius (*R*).

$$D = \frac{\log(NB(R))}{\log(R)} \qquad \textit{Equation 2.32}$$

Due to the scarcity of measurements of precipitation type of networks, the quantification of the fractal dimension may result unstable. An alternative fractal dimension may be calculated using a correlation integral (Mazzarella and Tranfaglia 2000) instead of the number of blocks, such that:

$$CI(R) = \frac{2}{B(B-1)} \sum_{i=1}^{B} \sum_{j=1}^{B} \Theta\left(R - \left|u_{\alpha i} - u_{\alpha j}\right|\right) : for\ i \neq j \qquad \textit{Equation 2.33}$$

In which *CI* is the correlation integral, *R* is the scaling radius, *B* is the total number of blocks at each scaling radius, and U_α is the location of station α. Θ is the Heaviside function. A normalisation coefficient is used, as the number of estimations of the counting of blocks considers each station as a centre.

The consequent definition of the fractal dimension of the network is the rate between the logarithm of the correlation integral and the logarithm of the scaling radius. This ratio is calculated from a regression between different values of *R*, for which the network exhibit fractal behaviour (meaning, a high correlation between log(*CI*) and log(*R*)).

$$D = \frac{\log(CI)}{\log(R)} \qquad \textit{Equation 2.34}$$

The Maximum potential value for the fractal dimension of a 2-D network (such as for spatially distributed variables) is two. However, this limit considers that the stations are located on a flat surface, as elevation is consequence of the topography, and is not a variable that can be controlled in the network deployment.

Network theory-based

Recently, research efforts have been devoted to the use of the so-called network theory to assess the performance of discharge sensor networks (Halverson and Fleming 2015, Sivakumar and Woldemeskel 2014). These studies analyse three main features, namely average clustering coefficient, average path length and degree distribution. Average clustering is a degree of the tendency of stations to form clusters. Average path length is the average of the shortest paths between every combination of station pairs. Degree distribution is the probability distribution of network degrees across all the stations, being network degree defined as the number of stations to which a station is connected. Halverson and Fleming (2015) observed that regular streamflow networks are highly clustered (so the removal of any randomly chosen node has little impact on the network performance) and have long average path lengths (so information may not easily be propagated across the network).

In hydrometric networks, three metrics are identified (Halverson and Fleming 2015): degree distribution, clustering coefficient and average path length. The first of these measures is the average node degree, which corresponds to the probability of a node to be connected to other

nodes. The metric is calculated in the adjacency matrix (a binary matrix in which connected nodes are represented by 1 and the missing links by 0). Therefore, the degree of the node is defined as:

$$k(\alpha) = \sum_{j=1}^{n} a_{\alpha,j} \qquad \textit{Equation 2.35}$$

Where *k(α)* is the degree of station *α*, *n* is the total number of stations, and *a* is the adjacency matrix.

The clustering coefficient is a measure of how much the nodes cluster together. High clustering indicates that nodes are highly interconnected. The clustering coefficient (*CC*) for a given station is defined as:

$$CC(\alpha) = \frac{2}{k(\alpha)(k(\alpha)-1)} \sum_{j=1}^{n} a_{\alpha,j} \qquad \textit{Equation 2.36}$$

Additionally, the average path length refers to the mean distance of the interconnected nodes. The length of the connections in the network, provide some insights in the length of the relationships between the nodes in the network.

$$L = \frac{1}{n(n-1)} \sum_{\alpha=1}^{k(\alpha)} \sum_{j=1}^{n} d_{\alpha,j} \qquad \textit{Equation 2.37}$$

As can be seen from the formulation, the metrics of the network largely depends on the definition of the network topology (adjacency matrix). The links are defined from a metric of statistical similitude such as the Pearson r or the Spearman rank coefficient. The links are such pair of stations over which statistical similitude is over a certain threshold.

According to Halverson and Fleming (2015), an optimal configuration of streamflow networks should consist of measurements with small membership communities, high-betweenness, and index stations with large numbers of intracommunity-links. Small communities represent clusters of observations, thus, indicating efficient measurements. Large numbers of intra-community links ensure that the network has some degree of redundancy, and thus, resistant to sensor failure. High-betweenness indicates that such stations which have the most inter-communal links are adequately connected, and thus, able to capture the heterogeneity of the hydrological processes at a larger scale.

2.6 Proposed framework for sensor network design

Table 2.4 summarises the sensor network design classes and approaches, with the selected references to the relevant papers in each of the categories for further reference. It is of special

interest in the review to highlight the lack of model-based information theory methods, as well as the low number of publications in network theory-based methods. Also, quantitative studies in the comparison of different methodologies for the design of sensor networks are limited. It is suggested, therefore, that a pilot catchment is used for the scientific community to test all the available methods for network evaluation, and to establish similarities and differences among them.

Table 2.5 summarises the main advantages and disadvantages for each of the design and evaluation methods. These recommendations are general, but take into account the most general points in the design considerations of sensor networks. Some of the advantages of these methods have been exploited in combined methodologies, such as those presented by Yeh et al. (2011), Samuel et al. (2013), Barca et al. (2015), Coulibaly and Samuel (2014), and Kang et al. (2014).

Table 2.4 Classification of sensor network design criteria including recommended reading.

		Approaches		
		Measurement-based		**Measurement-Free**
		Model-free	**Model-based**	
Classes	**Statistics-based**			
	Interpolation variance	Pardo-Iguzquiza (1998) Bardossy and Li (2008) Nowak et al. (2010)		
	Cross-correlation	Maddock (1974) Moss and Karlinger (1974)	Vivekanandan and Jagatp (2012)	
	Model error		Tarboton et al. (1987) Dong et al. (2005)	
	Information Theory			
	Entropy	Krstanovic and Singh (1992a, 1992b) Alfonso et al. (2014)	Pham and Tsai (2016)	
	Mutual information	Husain (1987) Alfonso (2010)	Coulibaly and Samuel (2014)	
	Expert recommendations			
	Physiographic components	Samuel et al. (2013)	Moss and Karlinger (1974) Moss et al. (1982)	Laize, 2004
	Practical case-specific considerations			Wahl and Crippen (1984) Nemec and Askew (1986) Karaseff (1986)
	User survey			Sieber (1970) Singh et al. (1986)
	Other methods			
	Value of information	Alfonso and Price (2012)	Black et al. (1999) Alfonso et al. (2016)	
	Fractal characterisation			Lovejoy and Mandelbrot (1985) Capecchi et al. (2012)
	Network theory	Sivakumar and Woldemeskel (2014) Halverson and Fleming (2015)		

Table 2.5 Advantages and disadvantages of sensor network design methods

	Advantages	***Disadvantages***
Statistics-based		
Interpolation variance	Useful to assess data scarce areas No event-driven Minimise uncertainty in spatial distribution of measured variable	Heavily rely on the characterisation of the covariance structure No relationship with final measurement objective
Cross-correlation	Useful for detecting redundant stations Computationally inexpensive	Augmentation not possible without additional assumptions Limited to linear dependency between stations
Model error	Has direct relationship with the measurement objectives	Biased towards current measurement objectives Biased towards model and error metrics
Information Theory		
Entropy	Assess non-linear relationship between variables Unbiased estimation of network performance	Formal form is computationally intensive Quantising (binning) of continuous variables lead to different results Optimal networks are usually sparse Difficult to benchmark Data intensive
Mutual information	Idem	Idem
Expert recommendations		
Physiographic components	Well understood Functional for heterogeneous catchments with few available measurements Useful at country/continental level	Not useful for homogeneous catchments No quantitative measure of network accuracy
Practical case-specific considerations	No previous measurements are required Useful to observe specific variables	Biased towards expert Collected data does not influence selection Biased towards current data requirements
User survey	Pragmatic Cost-efficient	Extensive user identification Biased towards current data requirements
Other methods		
Value of information	Provides a full economical assessment	Hard to quantify Usually decisions are made with available information Biased towards a rational decision model

Fractal characterisation	Efficient for large networks Does not require data collection	Not suitable for small networks or catchments Does not consider topographic or orographic influence
Network theory	Provides insight in interconnected networks	Not useful for augmentation purposes Data intensive

Based on the presented literature review, a first contribution towards a unified, general procedure for sensor network design is presented. Such procedure, which is currently lacking due to the diversity of cases, criteria, assumptions, and limitations, logically link in a flowchart various methods in the form of a procedure, following measurement-based approaches (Figure 2.9). The flowchart suggests two main loops: one to measure the network performance (optimisation loop), and the other to represent the iterations required in either augmentation or reduction scenarios. Most of the measurement-based methods, as well as most of the design scenarios can be seen as particular cases of this generalised algorithmic flowchart. A review of some potential optimisation methods (some of which are later used in this document) are presented in ANNEX 1.

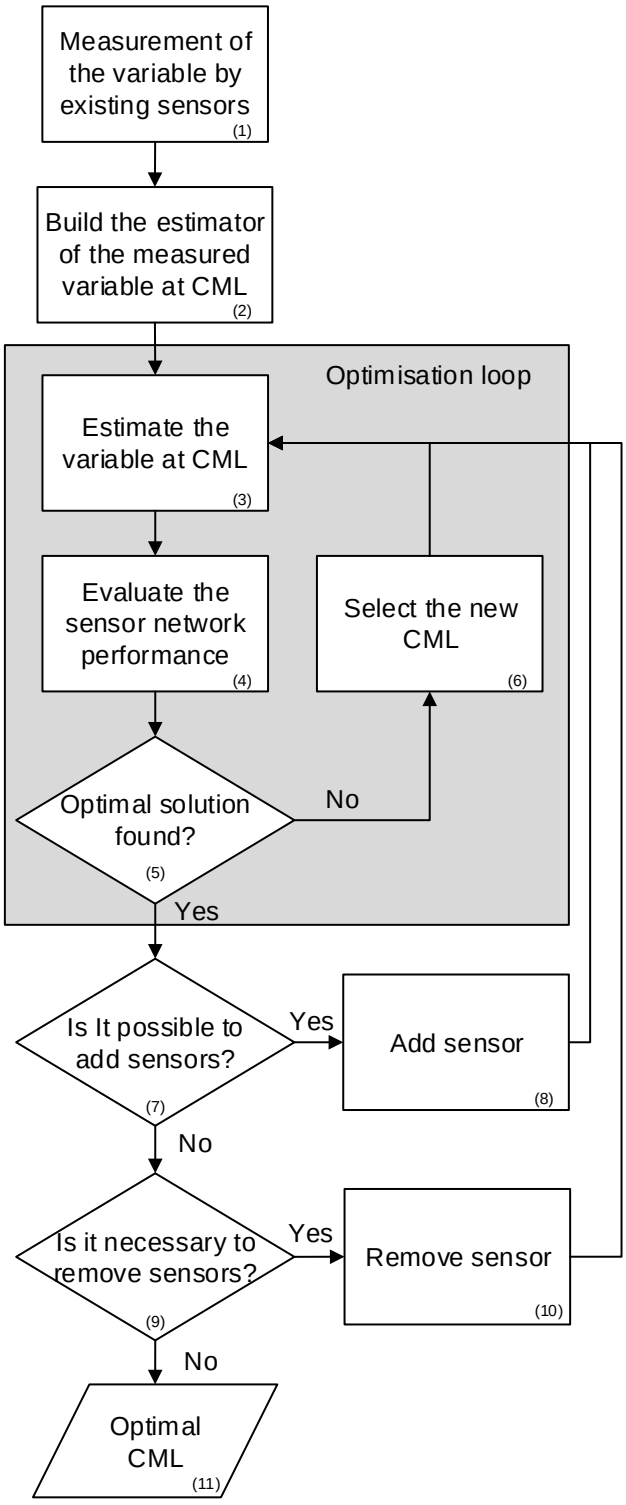

Figure 2.9 Sensor network (re) design flow chart. (CML=candidate measurement locations)

The general procedure consists of 11 steps (boxes in Figure 2.9). In the first place, physical measurements (1) are acquired by the sensor network. This data is used to parameterise an estimator (2), which will be used to estimate the variable at the Candidate Measurement Locations (*CML*) using, for instance, Kriging (Pardo-Igúzquiza 1998, Nowak et al. 2010), or 1D hydrodynamic models (Neal et al. 2012, Rafiee et al. 2012, Mazzoleni et al. 2015). The sensor network reduction does not require such estimator as measurements are already in place.

The selection of the *CML* should consider factors such as physical and technical availability, as well as costs related to maintenance and accessibility of stations, as illustrated by the WMO (WMO 2008) recommendations. The selection of *CML* can also be based, for example, on expert judgement. These limitations may be a model as constraints in the optimisation problem.

Then an optimisation loop starts (Figure 2.9), by the estimation of the measured variable at the *CML* (3), using the estimator built in (2). Next, the performance of the sensor network at the *CML* is evaluated (4), using any of the previously discussed methods. The selection of the method depends on the designer and its information requirements, which also determines if an optimal solution is found (5). The stopping criteria in the optimisation problem can be set by a desired accuracy of the network, some non-improved number of solutions or a maximum number of iterations. As pointed out in the review, these performance metrics can be either model-based or model-free and should not be confused with the use of a (geostatistical) model of the measured variable.

In case the optimisation loop is not complete, a new set of *CML* is selected (6). The use of optimisation algorithms may drive the search of the new potential *CML*. The decision about adequate performance should not only consider the expected performance of the network but also, recognise the effect of a limited number of sensors.

Once the performance is optimal, an iteration over the number of sensors is required. If the scenario is for network augmentation (7), then a possibility of including additional sensors has to be considered (8). The decision to go for an additional sensor will depend on the constraints of the problem, such as a limitation on the number of sensors to install, or on the marginal improvement of performance metrics.

The network reduction scenario (9) is inverse: due to diverse reasons, mainly of financial nature, networks require to have fewer sensors. Therefore, the analysis concerns what sensors to remove from the network, within the problem constraints (10).

Finally, the sensor network is selected (11) from the results of the optimisation loop, with the adequate number of sensors. It is worth mentioning that an extra loop is required, leading to re-evaluation, typically done on a periodical basis, when objectives of the network may be redefined, new processes need to be monitored, or when information from other sources is available, and that can potentially modify the definition of optimality.

2.7 Conclusions

Most of the sensor network methodologies aim to minimise the uncertainty of the variable of interest at ungauged locations and the way this uncertainty is estimated varies between different methods. In statistics-based models, the objective is usually to minimise the overall uncertainty about precipitation fields or discharge modelling error. Information theory-based methods aim to find measurements at locations with maximum information content and minimum

redundancy. In network theory-based methods, estimations are generally not accurate, resulting in less biased estimations. In methods based on practical case-specific considerations and value of information, the critical consequences of decisions dictate the network configuration.

However, in spite of the underlying resemblances between methods, different formulations of the design problem can lead to rather different solutions. This gap between methods has not been deeply covered in the literature and therefore a general agreement on sensor network design procedure is relevant.

In particular, for catchment modelling, the driving criteria should also consider model performance. This driving criterion ensures that the model adequately represents the states and processes of the catchment, reducing model uncertainty and leading to more informed decisions. Currently, most of the network design methods do not ensure minimum modelling error, as often it is not the main performance criteria for design.

Furthermore, in the last years, the rise of various sensing technologies in operational environments have promoted the inclusion of additional design considerations towards a unified heterogeneous sensor network (New et al. 2001). These new sensing technologies include, e.g., passive and active remote sensing using radars and satellites (Schuurmans et al. 2007, Wagner et al. 2009, Thenkabail 2015), microwave links (Giuli et al. 1991, Messer et al. 2006, Leijnse et al. 2007, Zinevich et al. 2008, Overeem et al. 2011, 2012, Rayitsfeld et al. 2012), mobile sensors (Haberlandt and Sester 2010, Dahm et al. 2014), crowdsourcing and citizen observatories (Huwald et al. 2013, Lanfranchi et al. 2014, Alfonso et al. 2015). These information sources have the potential to complement conventional networks, by exploiting the synergies between the virtues and reducing limitations of various sensing techniques, and at the same time, require the new network design methods allowing for handling the heterogeneous dynamic data with varying uncertainty.

The proposed classification of the available network design methods was used to develop a general framework for network design. Different design scenarios, namely relocation, augmentation and reduction of networks are included, for measurement-based methods. This framework is open and offers “placeholders” for various methods to be used depending on the problem type.

Concerning the further research, from the hydrological modelling perspective, we propose to direct efforts towards the joint design of precipitation and discharge sensor networks. Hydrological models use precipitation data to provide discharge estimates, however as these simulations are error-prone, the assimilation of discharge data, or error correction, reduces the systematic errors in the model results. The joint design of both precipitation and discharge sensor networks may help to provide more reliable estimates of discharge at specific locations.

Another direction of research may include methods for designing dynamic sensor networks, given the increasing availability of low-cost sensors, as well as the expansion of citizen-based data collection initiatives (crowdsourcing). These information sources are on the rise in the last

years, and one may foresee appearance of interconnected, multi-sensor heterogeneous sensor networks shortly.

The presented review has also shown that limited effort has been devoted to considering changes in long-term patterns of the measured variable in the sensor network design. This assumption of stationarity has become more relevant in the last years due to new sensing technologies and increased systemic uncertainties, e.g. due to climate and land use change and rapidly changing weather patterns. Although this topic has been recognised for quite some time already (Nemec and Askew 1986), the number of publications presenting effective methods to deal with them is still limited.

3. Case studies

3.1 Introduction

This chapter introduces the case studies in which the proposed methods have been tested. The cases are the Brue and Don River catchments in the UK, and the Bacchiglione River in Italy. The Brue catchment has been used due to the large amount of data, derived from the observations setup for the HYREX project (Wood et al. 2000). The Don and Bacchiglione River catchments are associated to the WeSenseIt project, which founded this study, which also have quite different monitoring conditions.

Conveniently, the three case studies show diverse hydro-meteorological, hydrological, and monitoring conditions, which allows for exploration of different scenarios in the deployment of dynamic sensor networks. For instance, the Brue catchment is the smallest catchment in the study, containing at the same time the largest amount of sensors. These characteristics makes it interesting for the analysis of precipitation patterns at a higher spatial resolution. In contrast, the Bacchiglione River catchment has an area of about four times the Brue catchment, and has a moderate observation network, standard for operational purposes in the catchments of the region. Its high elevation and its precipitation characteristics are useful to represent the potential use of sensors in different climatological regimes. Lastly, the Don River catchment is the largest among the case studies, with an area almost as double as Bacchiglione, and with the least number of precipitation sensors. This case is used to evaluate the methods in ungagged basins.

3.2 Bacchiglione River

The Bacchiglione River (Italy) is located in north Italy, in the Veneto region. This river can be considered as the tributary of a big and complex drainage network which covers a large part of the Vicenza area. This area is characterised by a steep slopes in the upper part of the catchment, to a more gentle slopes towards the concentration point. The elevation in this catchment ranges from 2150 msl close to Valli del Pasubio, to approximately 40 msl at Vicenza. The catchment area of the Bacchiglione River at Vicenza is about 540 km².

The data for this case study was supplied by the Alto Adriatico Water Authority (AAWA) in the context of the WeSenseIt project. The supplied data contained precipitation data that spans from 2000 to 2009 at an hourly resolution. The average precipitation of approximately 1660 mm/year, with higher precipitation rates during the warmer months.

The precipitation sensor network is composed by 16 precipitation stations which record hourly precipitation estimates. The stations used in this case study does not necessarily lie within the catchment bounds (Figure 3.1), however they are used as they make part of the operational

forecasting system of the region. The reference system for the coordinates of the stations is the Monte Mario, Italy zone 1.

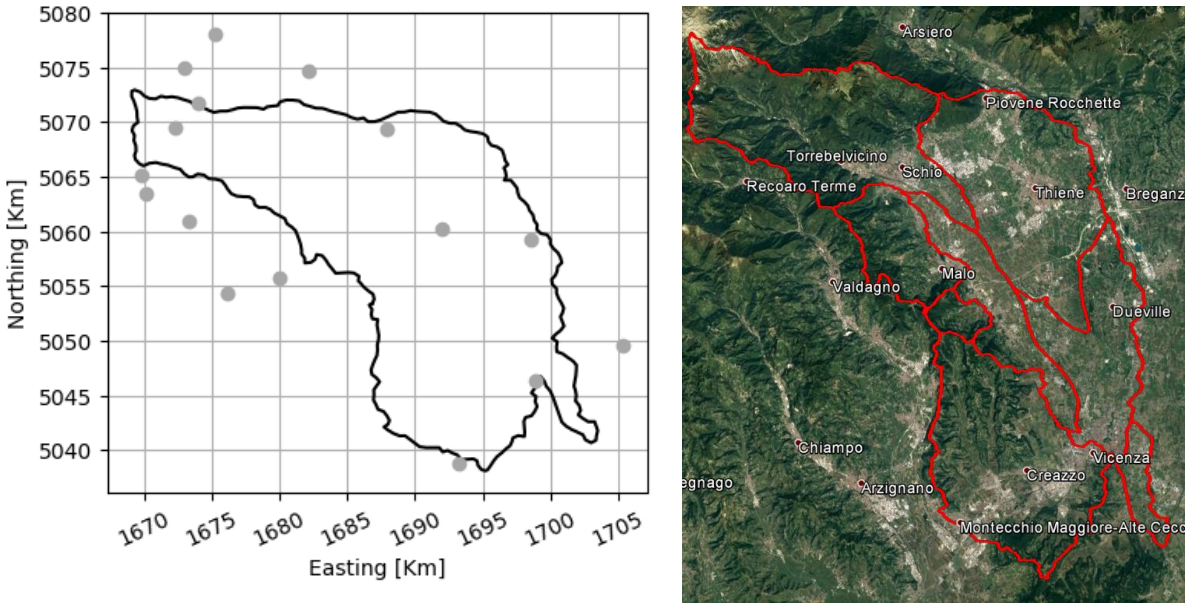

Figure 3.1 Scheme of the Bacchiglione River catchment with location of precipitation sensors (left) and some locations of interest (right)

In the case of the Bacchiglione River catchment it was decided to explore the high precipitation events. The high precipitation events are highlighted in Figure 3.2, in the overview of the complete dataset. From this dataset, two events were selected. The precipitation in mid-2002 was not considered as one of the case studies, as it is shows a peak in the variability of the precipitation data in the event, leading to the conclusions that may be consequence of a data point of dubious quality. A zoom-in of the events is presented in Figure 3.3.

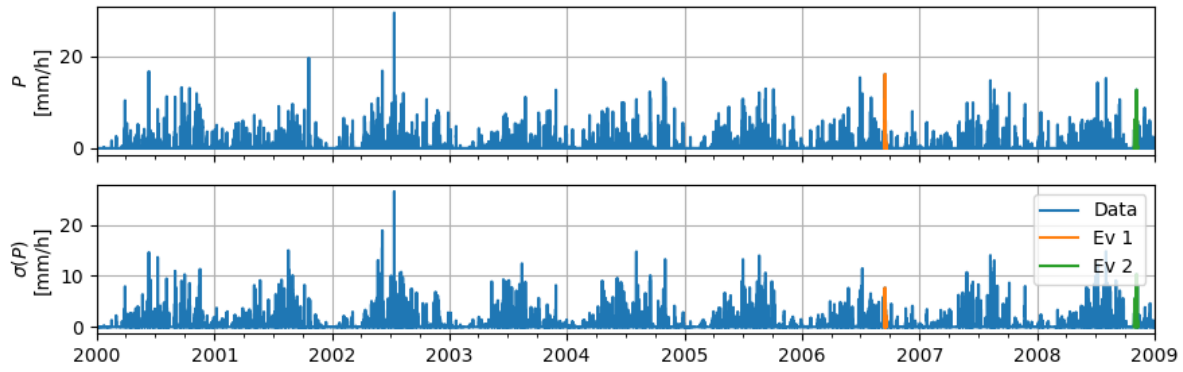

Figure 3.2 Overview selected high precipitation events in the Bacchiglione River catchment

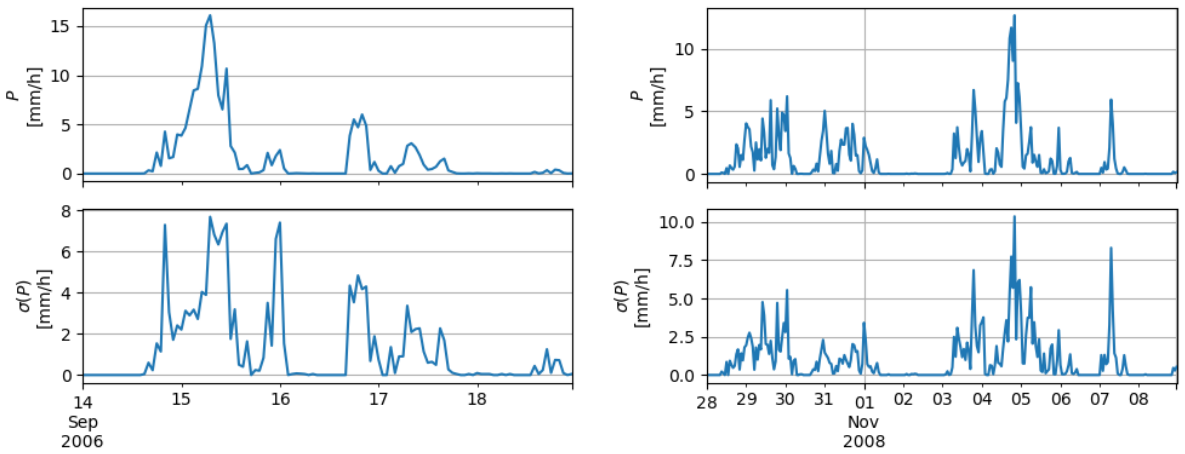

Figure 3.3 Detail of high precipitation events in the Bacchiglione River catchment

Finally, the events are summarised in Table 3.1. The selected events vary in length from 4 to 11 days, providing insight of the potential scheduling of sensors at different time scales.

Table 3.1 Summary of the precipitation events selected for the Bacchiglione River catchment

Start	End	Length (days)
14/09/2006	18/09/2006	4
28/10/2008	08/11/2008	11

3.3 Brue Catchment

Brue catchment is located in Somerset, South West of England with predominantly rural use and modest slope (Moore et al. 2000). The drainage area of the catchment is 135 km² approximately, with a concentration time of about 10 to 12 hours at Lovington. Hourly precipitation data are available at 48 automatic precipitation stations, in the context of the HYREX project (Wood et al. 2000), where the used data spans from 1993 to 2000. Figure 3.4 shows the location of the precipitation sensors, with respect to the projected British National Grid.

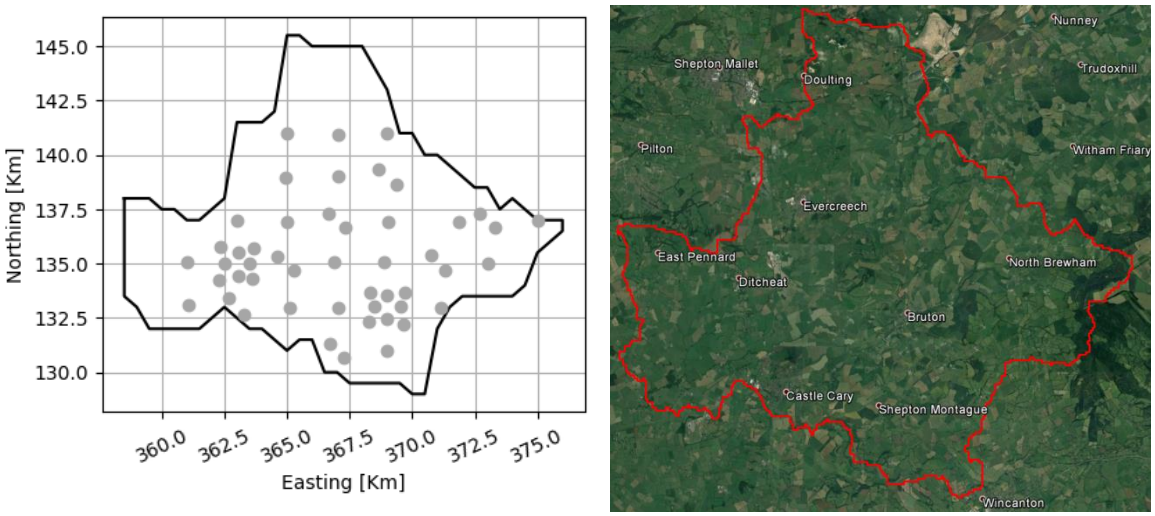

Figure 3.4 Scheme of Brue catchment with location of precipitation sensors (left) and some locations of interest (right)

A general overview of the available data for the catchment is presented in Figure 3.5. From the figure it can be seen that some missing data has been filled with constant values at the end of 1998 for discharge, as well as in early spring 1994, summer 1996, late 1997 and late 1999 for temperature and late 1997 for evapotranspiration. As the amount of missing data is considerably small, there is no special handling of the missing data.

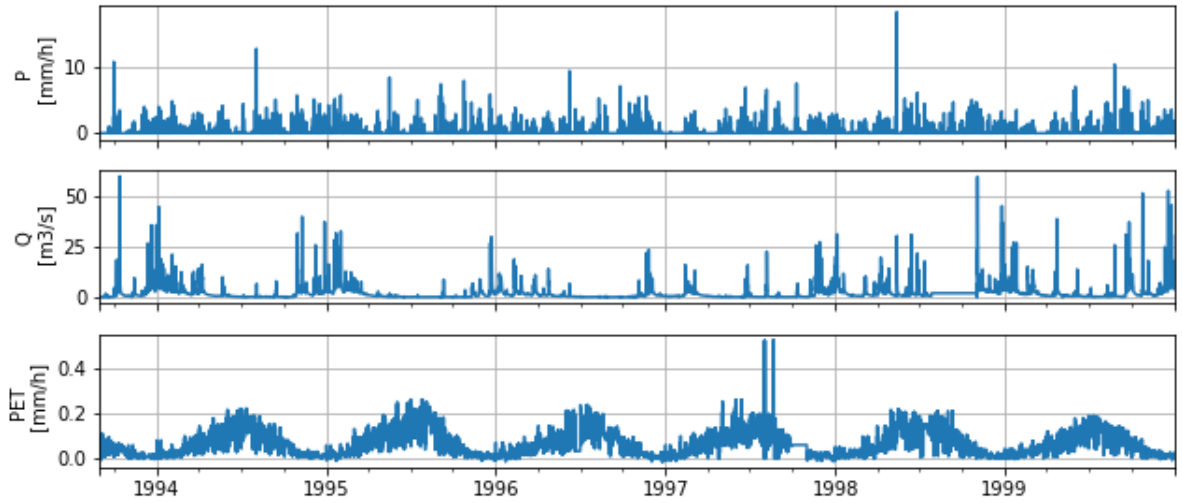

Figure 3.5 Overview of the experimental dataset

Figure 3.6 shows the overview of the dataset for the Brue Catchment, highlighting the events of interest, highlighting 3 variables, average precipitation (P), standard deviation of the precipitation measurements (σ(P)) and discharge (Q). The selection of the events are driven by maximum discharge values, precipitation variability, and length. In this regard, it is possible to observe in Figure 3.7 a zoom-in of the selected events.

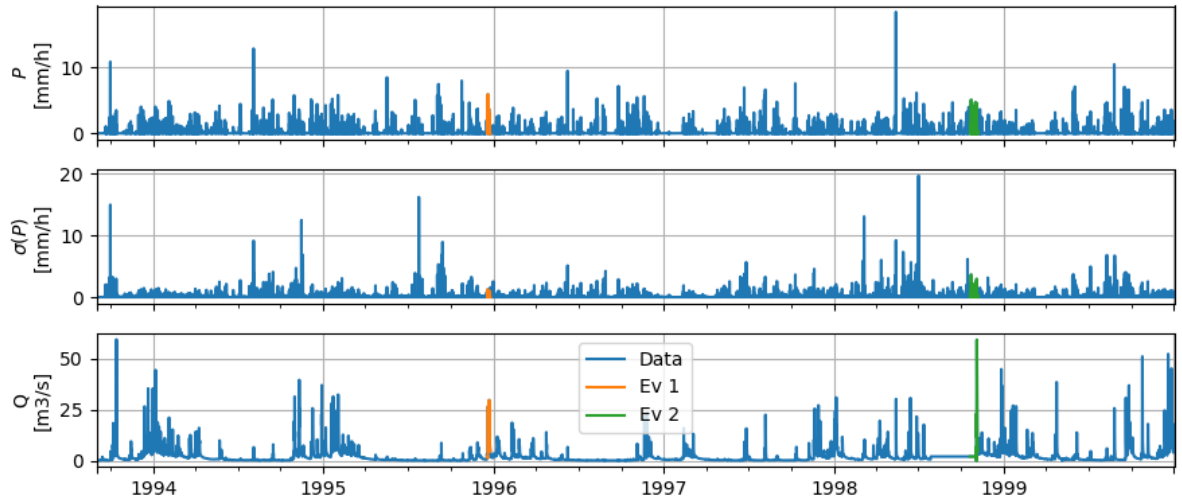

Figure 3.6 Overview selected high discharge events in the Brue catchment

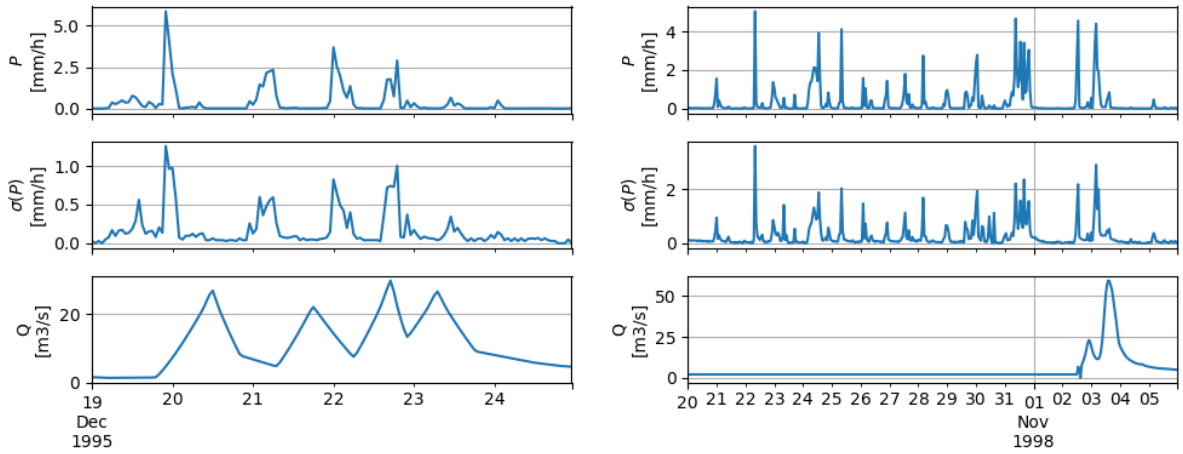

Figure 3.7 Detail of high discharge events in the Brue catchment

It is possible to visually asses that the precipitation events which are selected due to the high variability of the observation in the network does not consider the highest fluctuation event, as this behaviour may be triggered by an inconsistent measurement, as it is a single peak. The selection of the events also considers a consistent time frame, which allows for sensors to be deployed. The selected events are resumed in Table 3.2.

Table 3.2 Summary of the precipitation events selected for the Brue catchment

Begin	End	Length (days)
19/12/1995	24/12/1995	5
20/10/1998	05/11/1998	16

3.4 Don River

The Don River catchment is located in England, in the South Yorkshire and Derbyshire counties. The catchment drains from the areas in the Peak district to the Ouse River, right next to the North Sea. The catchment is mostly of agricultural use, in its headwater, but highly urbanised towards the valley. Due to this, there are control structures for high discharge in the main tributaries (Rother and Dearne), however they are not operated in a regular basis. The catchment also contains the cities of Sheffield, Rotherham and Doncaster. The total length of the river is about 110 Km, in a catchment area of approximately 1247 Km², yielding an average discharge of 19 m³/s.

The available sensor network in the area is comprised by 3 precipitation sensors (as described in Figure 3.8), providing hourly measurements for the operational forecasting system of the South-west Yorkshire region. The data for this case study spans from August 2011 to January 2015. The average precipitation for the area is of approximately 1586 mm/year, without considerably seasonal effects. The projection used in the location of the catchment and sensors is WGS84 zone 32N.

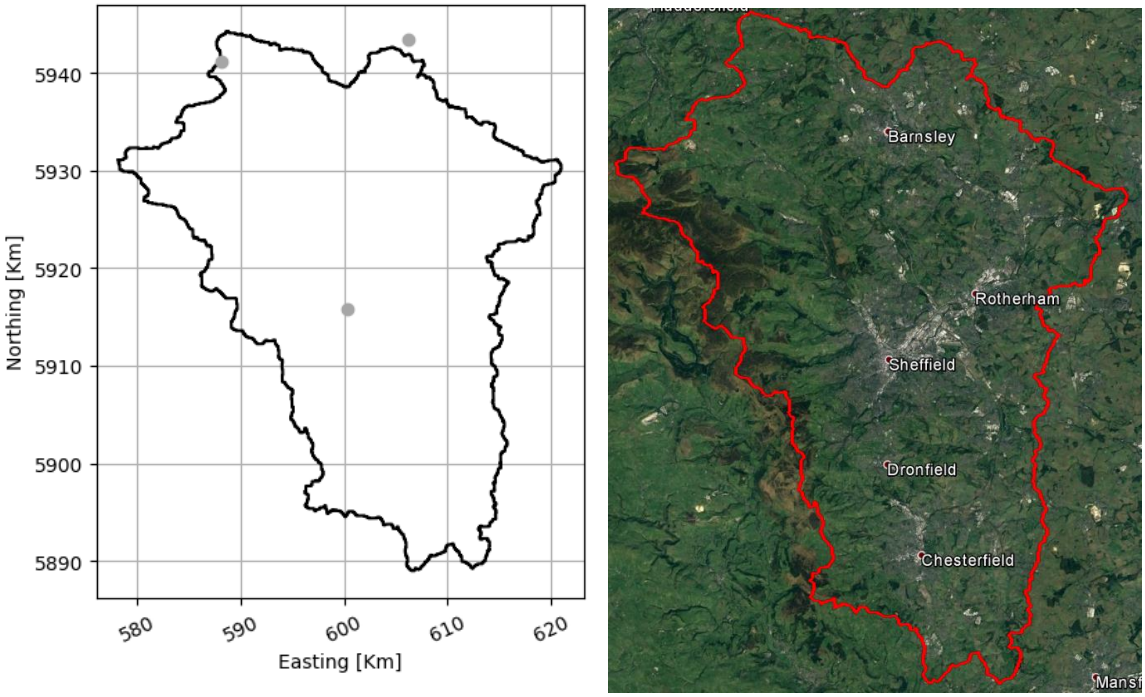

Figure 3.8 Scheme of the Don River catchment with location of precipitation sensors and some locations of interest (right)

The events selected in the catchment were selected based on high precipitation rates and high discharge, over extended periods of time (Figure 3.9). These criteria were are selected as making a valid approximation of the precipitation variability by only using three sensors may not be meaningful, and it is supported in the fact that was not possible to visually identify peaks in the precipitation variation using the provided data. The selected events using the high precipitation criteria are highlighted in Figure 3.9, and the details of these events are presented in Figure 3.10. Table 3.3 summarises the selected events for the Doncaster River case study.

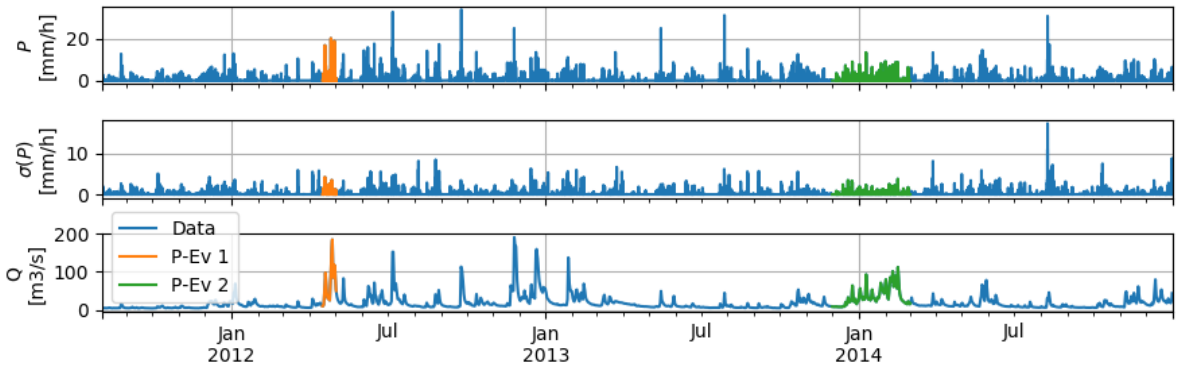

Figure 3.9 Overview selected high precipitation events in the Don River catchment

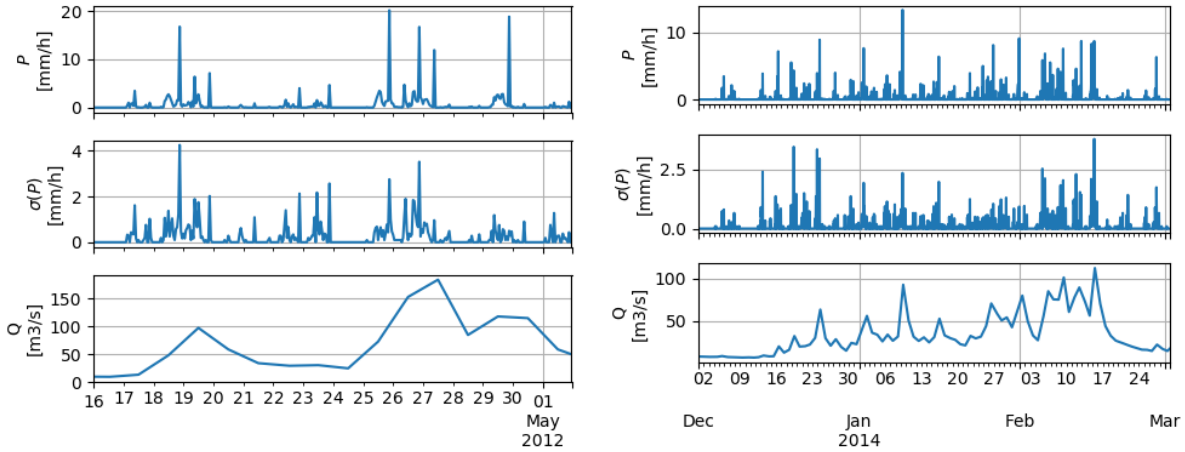

Figure 3.10 Detail of high precipitation events in the Don River catchment

Table 3.3 Summary of the precipitation events selected for the Don River catchment

Begin	End	Length (days)
30/03/2012	15/05/2012	46
01/12/2013	01/03/2014	90

4. Advancing Kriging methods for merging heterogeneous data sources in non-stationary precipitation fields

4.1 Introduction

Including precipitation observations from dynamic sensors and citizen observatories using geostatistical models, requires the revision of some of the most common assumptions (Journel and Alabert 1989). This chapter describes and revises three of these assumptions, namely homogeneity in measurement uncertainty, average temporal distribution of the precipitation within the observation interval, and spatial stationarity.

The first assumption occurs in when the observational error is neglected, or assumed to be homogeneous for all observations, as in the Kriging framework. The classical approach to include observation uncertainty in Kriging, is to make it part of the covariance structure. As such, this factor is introduced via the variogram Nugget (Wackernagel 1998). However, this approach is not usable with heterogeneous observations, such as citizen observatories, as the nugget is a property of the field and not of the observations.

The second assumption is directly related to representing the total volume of precipitation at a given location. In the context of dynamic sensors, it is expected that a sensor moves considerably faster than the temporal resolution of the model, thus measurements have to be extrapolated from partial observations in time. As a consequence, dynamic sensors add an extra uncertainty source that may be critical in the usability of the observations.

Finally, the dimensions of the problem requires that the assumption of stationarity is revised. Although temporal stationarity assumptions may be suitable for the modelling of precipitation fields at hourly scale, assumptions about spatial, and intensity stationarity are not adequate. The findings regarding the testing of stationarity assumptions and a framework to relax such assumptions are developed through this Chapter.

This chapter starts by exploring the formulations of Kriging with variable measurement uncertainty, and therefore building a framework for the usability of heterogeneous observations. Next, the partial temporal recording of observations is quantified, based on the high temporal resolution data acquired for the Brue catchment. Then, the stationarity of the precipitation field are evaluated, and followed by the description of the proposed method for incorporating the

spatial and intensity non-stationarity, which is developed and tested and later applied in Chapter 6. Finally, conclusions and recommendations are presented.

4.2 Dealing with data of variable measurement uncertainty

4.2.1 The Kriging system with noisy measurements

Kriging is the best linear unbiased estimator. It estimates a given variable at a location (u), by using a linear combination of the observations at stations (α):

$$Z(u) = \sum_{\propto=1}^{n} \lambda_\alpha Z_\alpha \qquad \textit{Equation 4.1}$$

The Kriging system aims to identify the optimal set of weights (λ) such that the variance of the estimates are minimum (Cressie 1993, Deutsch and Journel 1998). To achieve this purpose, the weights are found as:

$$\lambda = K^{-1}k \qquad \textit{Equation 4.2}$$

Where K is the covariance matrix of the measurements and k is the covariance vector of the measurements towards the interpolation target. The covariance matrix of the measurements can be derived from the measurement itself, but the variance towards an ungauged location requires defining a function that relates the variance and the position of the target with respect to the sensor network (Bohling 2005). This function is known as the (semi) variogram, or inversely, correlogram.

In its more simple form, the variogram is a measure of covariance with respect to the distance between 2 observations (Cressie 1993). This relationship has to be empirically adjusted to the data, using a licit (or valid) covariance model, to ensure that the statistical properties of the covariance function are preserved. These properties include: symmetry, positive semi-definiteness, and positive real values, which necessarily leads to positive eigenvalues and determinant. These characteristics ensure that the covariance matrix can be inverted, and therefore, that the Kriging system has always a unique solution.

For the case of different observational error, the observational errors are added as proposed by Mazzetti and Todini (2009). In this framework, the variogram (Γ) is built over a modified estimation of the original variogram (γ), such that the variance of the measurements is included directly on the observations, and not as a part of the random field. This leads to:

$$\Gamma_{i,j} = \gamma_{i,j} + \frac{1}{2}\left(\sigma_{\varepsilon i}^2 + \sigma_{\varepsilon j}^2\right) \qquad \textit{Equation 4.3}$$

$$\Gamma_{i,i} = 0 \qquad \textit{Equation 4.4}$$

$$\Gamma_{i,0} = \gamma_{i,0} + \frac{1}{2}(\sigma_{\varepsilon i}^2) \quad \textit{Equation 4.5}$$

4.2.2 **Acceptable observation errors in the Kriging context**

The variogram function ($\Gamma_{i,j}$) range exist between zero to sill (C_0). The addition of the measurement variance ($\sigma_{\varepsilon i}^2 + \sigma_{\varepsilon j}^2$), will consequently lead to semi-variance values which are higher than the sill, and thus negative covariance, as the measurement variance is always positive.

$$C_{i,j} = C_0 - \Gamma_{i,j} \quad \textit{Equation 4.6}$$

$$C_{i,0} = C_0 - \Gamma_{i,0} \quad \textit{Equation 4.7}$$

$$if\ h \geq R \rightarrow \Gamma_{i,j} \geq C_0\ ;\ \Gamma_{i,0} \geq C_0 \quad \textit{Equation 4.8}$$

A negative covariance does not have a physical meaning, as covariance is always a positive quantity in the Kriging context. By adding measurements with relatively high error ($\sigma_{\varepsilon i}^2 + \sigma_{\varepsilon j}^2$), or considerably far away from other sensors ($h \geq R$) or to the interpolation target, will artificially increase the variance of the estimates, beyond the natural variability of the process.

Now, it is necessary to determine the limit in the accuracy of the measurements. In principle, the variance of the measurement error should be less than the variance of the process which is measured. Otherwise, measurements have a higher error than the model prediction, and thus, increase the uncertainty in the estimation. Considering that the covariance is always a positive ($C_{i,j} \geq 0$) we have that:

$$C_0 - \left(\gamma_{i,j} + \frac{1}{2}\left(\sigma_{\varepsilon i}^2 + \sigma_{\varepsilon j}^2\right)\right) \geq 0 \quad \textit{Equation 4.9}$$

Therefore, reorganising the previous equations, and considering that the semi-variogram and the measurement error variance are always positive, the admissible sum of the measurement error variance between a pair of gauges should be:

$$\sigma_{\varepsilon i}^2 + \sigma_{\varepsilon j}^2 \geq 2\left(C_0 - \gamma_{i,j}\right) \quad \textit{Equation 4.10}$$

Considering that two limiting cases are present when $i = j$ (meaning two sensors are in the same location), and the distance between a couple of sensors is equal to the fluctuation scale (r) of the process (or semi-variogram range). For these cases, one can say that the permissible sum between a pair of sensors range from$[0, 2(C_0 - N)]$, however, the admissible value of the sum of a pair of error covariance depends on the distance between stations.

Additionally, a similar constraint is imposed on how far can efficiently be from the interpolation target. Following the same principles as before, the maximum admissible variance of the measurement error is given by:

$$\sigma_{\varepsilon i}^2 \geq 2\left(C_0 - \gamma_{i,0}\right) \qquad \textit{Equation 4.11}$$

These equations also reveal that the admissible variance of the error measurements is directly linked to the distance in which these measurements are useful. In the Kriging formulation, in which measurement errors are neglected, the measurements can be used for infinitely long distances. In practice, the covariance function takes care of this by asymptotically reducing the weights of the measurements, as the semi-variogram approaches the sill, and therefore, including such measurements does not cause instabilities in the algorithm.

4.3 Estimating uncertainty due to partial recording

One of the uncertainty sources in the measurement using dynamic sensors comes from the fact that there is partial information about the total amount of precipitation that is recorded in a time step. In the case of static sensor networks, there is no error, as the precipitation measurements are integrated over the complete time. In the case of dynamic sensors, the information is partially recorded, as it will require some time for the sensor to be moved to another location.

As consequence, it is required to estimate the increase in the variance of the measurements, by extrapolating partial records. For this purpose, the intra-hourly variability of precipitation was investigated. The methodology consisted in integrating the total recoded volume in the gauge in 5 minute intervals (τ), and exploring how much of the total hourly volume is recorded ($\hat{P}$), and how much will be the error (P_ϵ) of extrapolating the currently measured volume (P_τ) towards the estimation of the total volume in an hour ($\dot{P}_{t|\tau}$).

$$\hat{P}_{t|\tau} = P_\tau \frac{t}{\tau} \qquad \textit{Equation 4.12}$$

$$P_\epsilon = \hat{P}_{t|\tau} - P_t \qquad \textit{Equation 4.13}$$

The results obtained for the data in the Brue catchment (Figure 4.1) provides insight regarding the incurred errors due to partial temporal measurements. The collected precipitation volume varies along the development of the precipitation event, in which there seem not to be a particular time lapse in which the precipitation occur. This yields heavily tailed probability distributions of the total recorded volume towards the beginning and end of the integration time, while shows a fairly well distributed probability distribution function towards the centre, indicating a normal distribution of the precipitation in the each of the intervals. Additionally, assuming that the recorded intensity in for different integration time does not seem to be an inadequate approach, as the results show that the volumetric error, incurred by such are relatively mostly unbiased, but with errors which may be significantly high, rising the suspicion in inflated statistics due to the tendency of low precipitation events occurring.

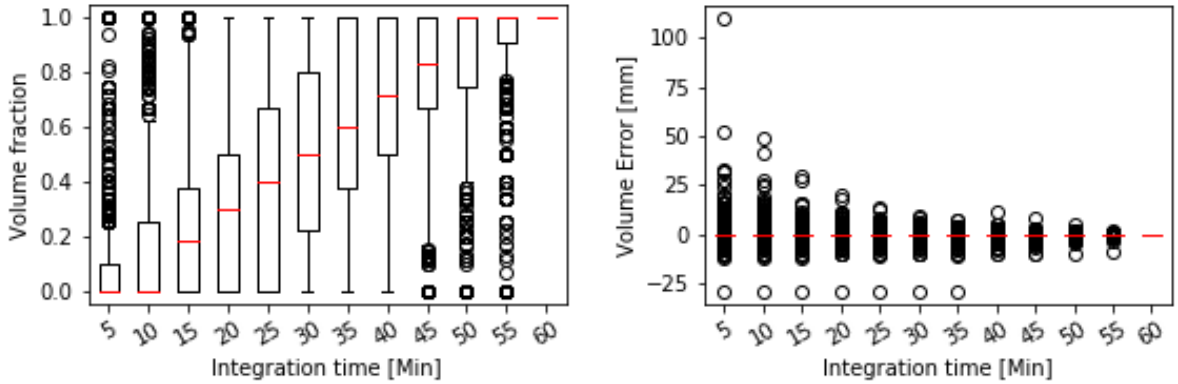

Figure 4.1 Volume error estimation due to partial measurement of the precipitation

To further explore the intra-hour variability, the average and variance of the observations in the estimation of the total model error as:

$$\bar{P}_\epsilon|\tau = \frac{1}{T}\sum_{t=1}^{T} \hat{P}_{t|\tau} - P_t \qquad \textit{Equation 4.14}$$

$$\sigma^2(P_\epsilon|\tau) = \frac{1}{T}\sum_{t=1}^{T} \left(\hat{P}_{t|\tau} - P_t\right)^2 \qquad \textit{Equation 4.15}$$

Where $\bar{P}_\epsilon$ is the average estimation error and $\sigma^2(P_\epsilon)$ is the estimation variance. In this context, it becomes clearer that the model does not suffice to explain the high errors, especially in short integration time, as the variability may seem reduced by the amount of observations in the low range.

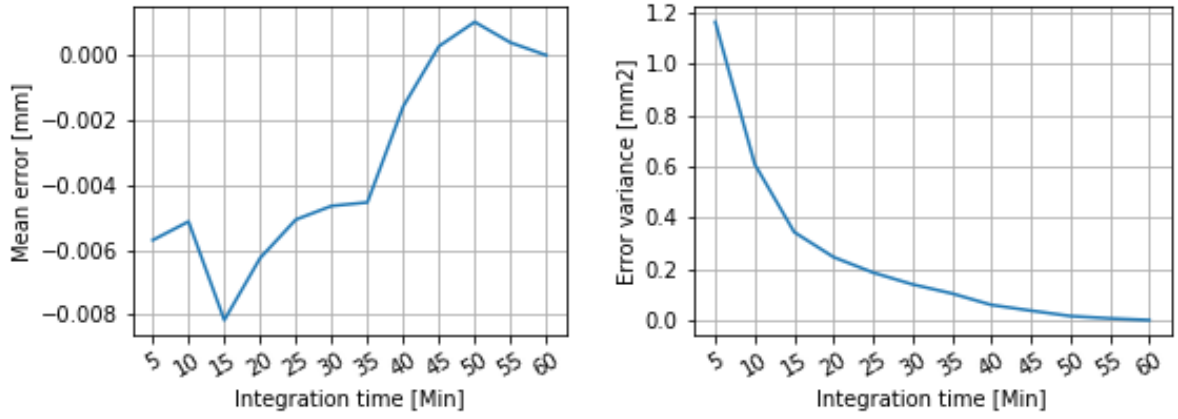

Figure 4.2 Long term average of mean and variance of volumetric error at different integration time

To overcome the bias in the amount of precipitation, a conditioned variance estimation, based on the total accumulated volume is proposed as:

$$\sigma^2(P_\epsilon|\tau, \hat{P}_{t|\tau}) = \frac{1}{T}\sum_{t=1}^{T}\left(\hat{P}_{t|\tau} - P_t\right)^2 |\hat{P}_t \in \tau \qquad \textit{Equation 4.16}$$

Figure 4.3 shows how the desegregation of the accumulated precipitation in the variance estimates is able to provide insight, by conditioning the estimates. In other words, if extremely high precipitation occur during the first 5 minutes of the hour, using this value to extrapolate to the complete hour will incur in a high variance of the error. On the contrary, low precipitation estimates during the integration period yield lower variance, as the probabilities of low precipitation to yield low overall precipitation volumes are a fair estimate.

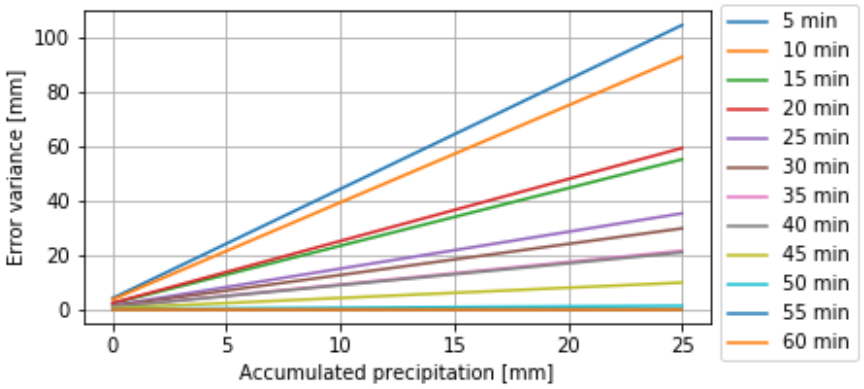

Figure 4.3 Error variance conditioned to accumulated precipitation for different integration time

In the implementation, the experimental results are approximated by a response function of the form:

$$z = ax_1 + bx_2 + cx_1x_2 \qquad \textit{Equation 4.17}$$

As such, the optimal coefficients are defined in a curve-fitting approach, by minimising the difference between the error variance observations and the response function. The independent variables of the response function are the total precipitation that the sensor measures in the time interval which is placed, and time interval that the sensors remains in the measurement location. The optimal set of parameters can be approximated by:

$$EV = \max(3.74P_{T|t} + 0.000497T - 0.0739\ P_{T|t}T;\ 0) \qquad \textit{Equation 4.18}$$

The results of this equation can be visualised in Figure 4.4, where the colour indicates the error variance in the extrapolation of the precipitation estimates. These results are obtained for the Brue catchment, but will be used in all the other case studies due to the lack of data at a resolution sufficient to carry out these analyses.

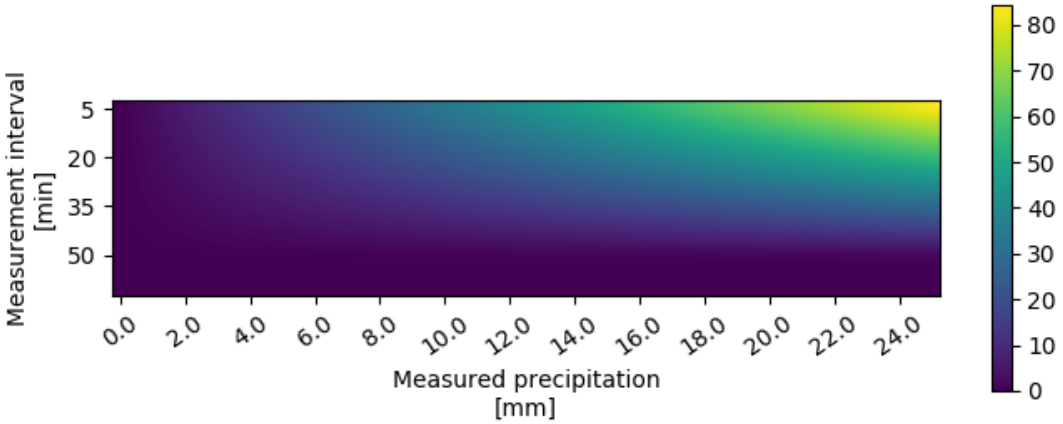

Figure 4.4 Variance of approximation error by partial observations of precipitation estimates

4.4 Handling Non-stationarity in the kriging framework

The proposed methodology is based on using a (revised) generalised covariance function. It employs a unique parameterisation of the variogram at each sensor in the network under different precipitation intensities. Figure 4.5 shows a flowchart with the three steps of the methodology, which includes parameterisation of the centrosymmetric (CS) variograms, evaluation of stationarity assumptions, and the interpolation procedure which, depending on the results of the type of stationarity test, could be conventional Kriging, or the proposed non-stationary Kriging.

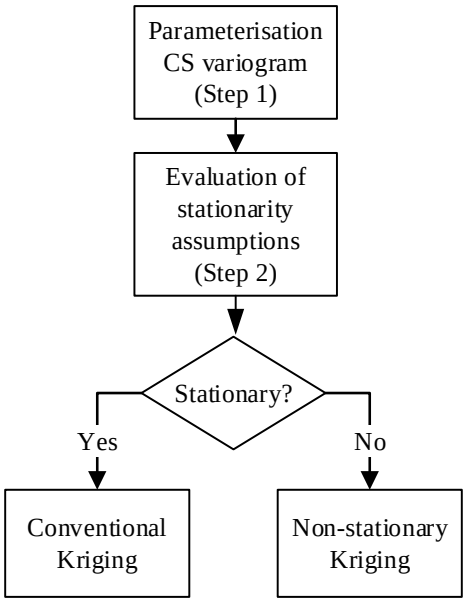

Figure 4.5 General structure of the proposed methodology

4.4.1 Evaluation of stationarity assumptions

The evaluation of stationarity assumptions is carried out to determine which assumptions are valid in the modelling of precipitation fields (Jun and Genton 2012). Here, we assess the temporal, spatial and intensity stationarity. The temporal stationarity evaluates the change of

the statistical properties of the precipitation in time. The spatial stationarity evaluates the change in mean and variance of the measurements, as well as the changes in the covariance structure at different locations. Finally, the Intensity stationarity evaluates the change of the covariance structure in different precipitation regimes.

The tests to assess the stationarity of the precipitation field are summarised in Table 4.1. Temporal (*T1*), spatial (*T2 - T7*) and intensity (*T8 – T9*) stationarity tests are carried out. Temporal stationarity is evaluated for each of the stations, using the *ADF* test (Dickey and Fuller 1979). Spatial stationarity is evaluated comparing different properties of experimental and theoretical centrosymmetric (*CS*) correlograms, by testing the assumptions of stationarity. The intensity stationarity evaluates the similitude of *CS* correlograms in the different precipitation regimes. The hypotheses are evaluated at a significance level of 0.05.

Table 4.1 Hypothesis tests for assessing different types of stationarities of spatially distributed variables

Index	**Test type**	**Null hypothesis (H0)**	**Alternative hypothesis (H1)**	**Type of stationarity**
T1	ADF test	The precipitation series for α is non-stationary	The precipitation series for α is stationary	Temporal
T2	t-test	The mean of station α_i and α_j are statistically equivalent	The mean of station α_i and α_j are not statistically equivalent	Spatial
T3	Levene test	The variance of station α_i and α_j are statistically equivalent	The variance of station α_i and α_j are not statistically equivalent	
T4	t-test	The mean between CS experimental variogram in station α_i and α_j are statistically equivalent	The mean between CS experimental variogram in station α_i and α_j are not statistically equivalent	
T5	t-test	The mean between CS theoretical variogram in station α_i and α_j are statistically equivalent	The mean between CS theoretical variogram in station α_i and α_j are not statistically equivalent	
T6	t-test	The mean between the sill of the CS theoretical variogram in station α_i and α_j are statistically equivalent	The mean between the sill of the CS theoretical variogram in station α_i and α_j are not statistically equivalent	
T7	t-test	The mean between the range of the CS theoretical variogram in station α_i and α_j are statistically equivalent	The mean between the range of the CS theoretical variogram in station α_i and α_j are not statistically equivalent	
T8	t-test	The mean between the sill of the CS theoretical variogram in high and low precipitation are statistically equivalent	The mean between the sill of the CS theoretical variogram in high and low precipitation are not statistically equivalent	Intensity
T9	t-test	The mean between the range of the CS theoretical variogram in high and low precipitation are statistically equivalent	The mean between the range of the CS theoretical variogram in high and low precipitation are not statistically equivalent	

The Augmented Dickey-Fuller (*ADF*) test (Said and Dickey 1984) is used to evaluate the temporal stationarity of the precipitation (*T1*). In short, this test seeks for a unit root using an autoregressive model. If the data has a unit root, the process is non-stationary, meaning that the

residuals of the autoregressive model have similar statistical properties in time over a sliding window. We apply this tests to each station separately.

Spatial stationarity requires that the mean and variance of the measurements are equal, as well as the covariance correlogram, regardless of its position in the catchment. Also, the correlogram should only depend on separation, meaning that under stationarity conditions all the CS correlograms should be equal. We use a t-test to assess the equivalence of the mean between stations (*T2*), and the Levene test (Levene 1960) to assess the equivalence of the variance between stations (*T3*). The t-test is used to evaluate the equivalency between both, experimental (*T4*) and theoretical correlograms (*T5*). Also, we use the t-test is to further test the equivalence of the sill (*T6*) and range (*T7*) of CS theoretical correlogram.

Intensity stationarity requires that the parameters of the CS correlograms are statistically equal regardless of the precipitation regime. For this study, the precipitation regime is defined as a threshold that discriminates between low and high precipitation. We use a t-test to evaluate the statistical equivalence of the mean of the sill (*T8*) and range (*T9*) for *CS* correlograms in the different precipitation regimes. In the stationary case, there should be no statistical difference in the correlogram parameters, independent of the precipitation regime.

4.4.2 **Non-stationary centro-symmetric (CS) variogram**

A variogram for each station can be parameterised separately, depending on different conditions. For precipitation, such conditions refer to different precipitation regimes. Traditionally, the experimental variogram with n stations is calculated with the number of possible combinations of pairs of stations $Nd = n\,(n - 1) / 2$ in the monitoring network. The proposed approach consists of configuring a variogram using n stations, by considering the distance between a station α ($\alpha = 1, 2\ldots$ n) and the remaining stations in the network.

The pseudocode in Figure 4.6 proposes the algorithm for the parameterisation of a generalised covariance structure for non-stationary interpolation. Conditions (i), Stations (α) and Data (d) are the inputs. The conditions (i) are a set of I number of situations for which the system is expected to show different statistical behaviours. For precipitation, the conditions i are defined as an intensity threshold of the measured variable. Data (D) consists of time series of D number of records of the variable to be interpolated at each station. Also, a data pool ($P_{i,\alpha}$), is defined as a collection of records that meets the condition i at station α, used to fit a theoretical variogram ($V_{i,\alpha}$).

SET *Conditions,* $\iota = \{1, 2, \ldots, I\}$
SET *Stations,* $\alpha = \{1, 2, \ldots, n\}$
SET *Data,* $D = \{1, 2, \ldots, N_r\}$
FOR each *Station* (α)
  FOR each *Condition* (i)
    INIT P
      IF D_α meets ι **THEN**
        $P_{i,\alpha} = D_{i,\alpha}$
      END IF
    Fit $V_{i,\alpha}$ to $P_{i,\alpha}$
  END FOR
END FOR

Figure 4.6 Proposed algorithm for the parameterisation of CS variograms ($V_{i,\alpha}$) at each station (α) in different conditions (i)

The algorithm results in a variogram per station and condition, $V_{i,\alpha}$. This covariance structure does not rely on the assumption of a constant mean, but it is constructed by the superposition of local variograms. The use of local variograms in the parameterisation of the covariance structure, leads to a kriging estimator which is not only valid for regionalised variables. In the ideal case when there is no difference in the variogram parameterisation between stations and conditions (regionalised variable), the generalised covariance structure will be equivalent to the variogram.

4.4.3 **Interpolation with Non-Stationary Kriging (NSK)**

The objective of the Kriging interpolation is to simulate a precipitation field (Z), which is optimal under assumptions of stationarity, linearity and Gaussianity. If the outcome of the stationarity evaluation is that the field is stationary in all its aspects, the current method will reduce to the conventional Kriging approximation, and therefore, it should be preferred due to parsimony. However, if such outcome indicates that the field is non-stationary, then the proposed Non-Stationary Kriging (NSK).

NSK is based on the same formulations of the conventional Kriging, which are modified to take into account spatial non-stationarity. Consequently, the value of the precipitation field Z, in the position u, can be expressed as:

$$Z(u) = \sum_{\propto=1}^{n} \lambda_{\alpha|i}(u) Z(u_\alpha) \qquad \textit{Equation 4.19}$$

where Z is the precipitation field, u is the target position in which the value of precipitation is unknown. λ corresponds to the weights assigned to each station (α), given the precipitation regime i, to interpolate the field in the location u. The values of Z_α correspond to the value of the field in the position of the measurements, therefore, the measurements themselves.

Contrary to the conventional Kriging interpolation, in the proposed NSK, the weights λ in Equation 4.19 not only depend on the covariance structure and the position of the interpolation target (*u*), but also on the precipitation regime. Under non-stationary conditions, there are no single values of field auto covariance (*C(0)*) or the Lagrangian parameter (*μ(u)*), as they are subject to each precipitation regime. Therefore, the estimation of the interpolation variance $\sigma^2\big(Z(u)\big)$ can then be expressed as:

$$\sigma^2(Z(u)) = \sum_{\propto=1}^{n} \lambda_{\alpha|i}(u)(C_{\alpha|i}(0) - C_{\alpha|i}(u_\alpha - u)) - \mu_{\alpha|i}(u) \qquad \textit{Equation 4.20}$$

Where $C_{\alpha|i}(0)$ is the variance and $\mu_{\alpha|i}$ is the Lagrangian parameter in the Ordinary Kriging at station α, for precipitation regime, i and u_α is the location of the station (α). It is worth noting that the conventional Kriging interpolation variance can also be used, by assuming a constant mean employed. In this case, the Lagrangian parameter would not be considered. This approach is an extension of the static nature of the interpolation variance in the conventional Kriging for different regimes and locations.

A drawback of the proposed method is the expected inconsistency between covariance estimations between pairs of stations. This occurs because each station has its particular parameterisation of the correlogram function, which implies an asymmetric covariance matrix of the measurements, meaning that the covariance between a pair of stations (*A* and *B*) follows:

$$Cov(A,B) \neq Cov(B,A) \qquad \textit{Equation 4.21}$$

As a result, the covariance matrix (*K*) is not positive definite (Christakos 1984); in consequence, the Kriging system may not have a unique solution. To overcome asymmetry, it is suggested to replace *K* by the average covariance (average bi-directional), $\overline{K}$ formulated as:

$$\overline{K} = \frac{1}{2}(K + K^T) \qquad \textit{Equation 4.22}$$

The resulting average bi-directional covariance matrix is now symmetric, but as do not come from a licit covariance model (Christakos 1984), it cannot be ensured that is actually a positive semi-definite matrix. In this case, it is opted for approximating the matrix to its closest semi-definite matrix using the spectral decomposition method proposed by Rebonato and Jäckel (2011), approximating the covariance matrix by minimising the norm between the original and the approximation, that ensure positive eigenvalues. As result, the solution of the Kriging system is always possible. Then, the set of weights λ for each regime *i* can be obtained as:

$$\lambda_{i|u} = \overline{K_i}^{-1} k_u \qquad \textit{Equation 4.23}$$

where k_u is the covariance vector between the stations and the location *u*.

4.5 Application in the Brue Catchment

Before applying the proposed methodology, a variogram model for the case study is set up as a baseline for the analysis as presented in Figure 4.7. The fitting of the theoretical variogram minimises the RMSE between the regularised experimental and the theoretical variogram. The results show that the PDF of the sill and range are fairly symmetrical and normally distributed, while the nugget effect shows a more uniform behaviour than the other two variables (Figure 4.8). The nugget effect, which is directly related to the measurement error, was not identifiable in the analysis.

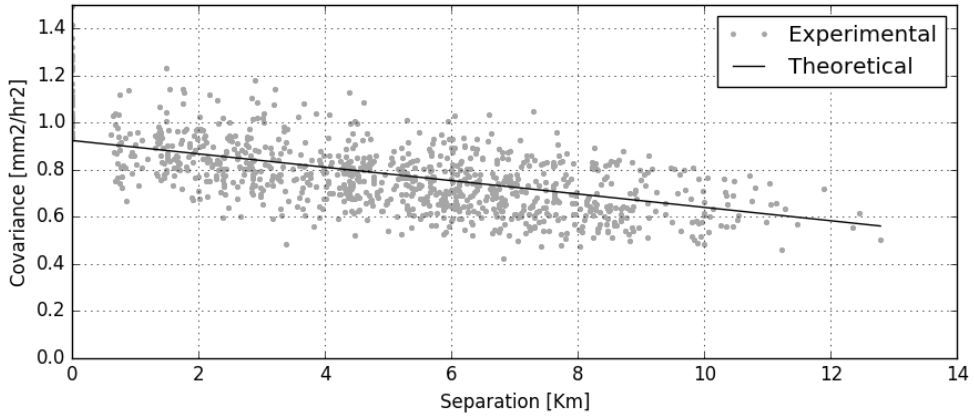

Figure 4.7 Conventional variogram estimation

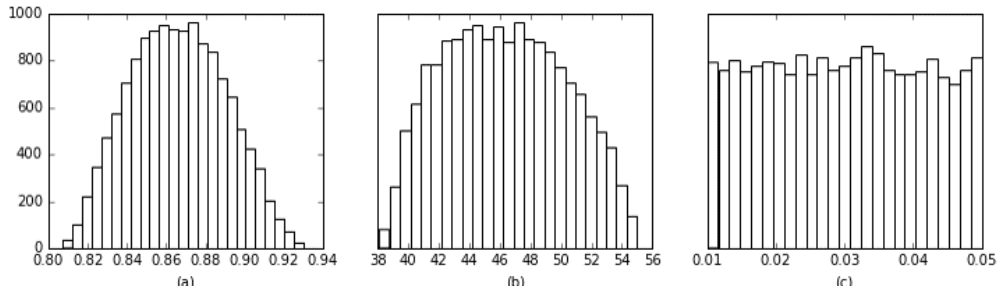

Figure 4.8 Identifiability analysis of spherical variogram parameters in conventional analysis (a) Sill, (b), range and (c) nugget

4.5.1 CS variogram in single precipitation regime

CS variograms are fitted using the relative distance from each sensor to the rest of the network. Figure 4.9 shows the results for CS equifinal variograms, which suggest that the CS variograms are inconsistent with the baseline, as the CS sill values fluctuate in wider ranges. The range is hardly identifiable, and far more variable than the range in the baseline. Similarly to the baseline, the nugget was not clearly identified in the CS variogram. These results indicate that the selection of a unique variogram to represent the covariance structure may not be an adequate hypothesis.

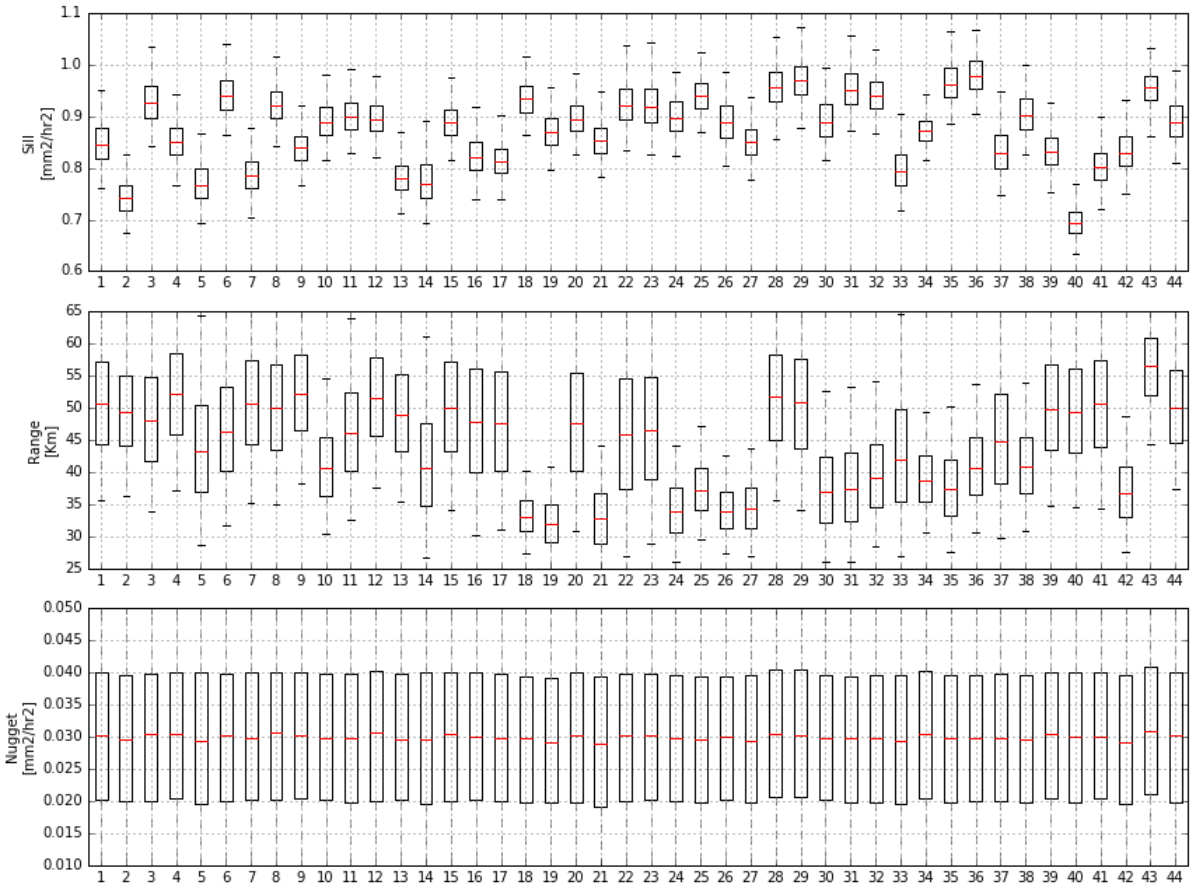

Figure 4.9 Identifiability analysis of centrosymmetric variogram parameters (top) Sill, (mid) Range, and (bottom) Nugget

4.5.2 **CS variograms in several precipitation regimes**

The precipitation regimes used in this study are denoted as low (*L*) and high (*H*) precipitation. These regimes are considered as the conditions (*i*) for the variogram parameterisation, as presented. The threshold for the separation between low and high precipitation is set to 2.0 mm/hr, and corresponds to 10 times the minimum resolution of the stations, and approximately 90th percentile of the precipitation data (Figure 4.10). The selection of the threshold is arbitrary at this point, but the analysis can be easily extended to more than one precipitation threshold.

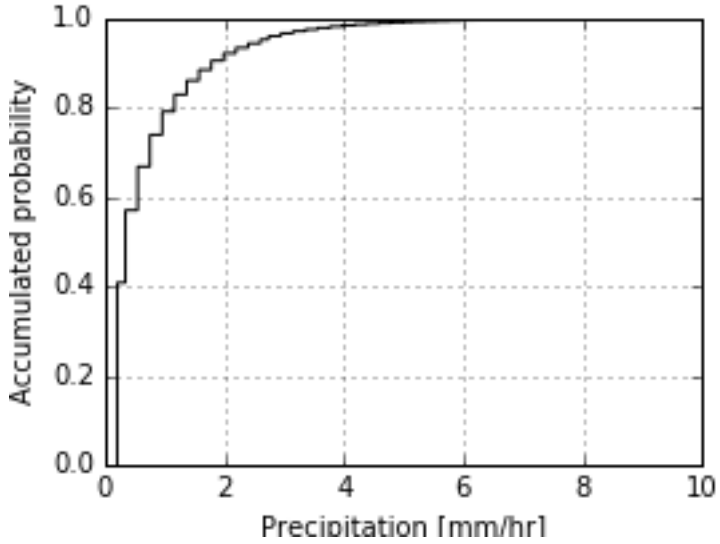

Figure 4.10 Accumulated probability distribution of precipitation data

Results for the CS sill indicate a clear difference between *L* and *H* regimes (Figure 4.11). The difference in the parameterisation between the two regimes is considerable, which differs from the results obtained for the baseline. In comparison, *L* is characterised by a significantly lower sill than *H* and the baseline. In practice, this is reflected in a smaller interpolation uncertainty for lower precipitation intensities, and a larger one for higher precipitation intensities. This result is expected, as the variance grows exponentially with the magnitude, and thus it is conditioned by the selection of the precipitation regime.

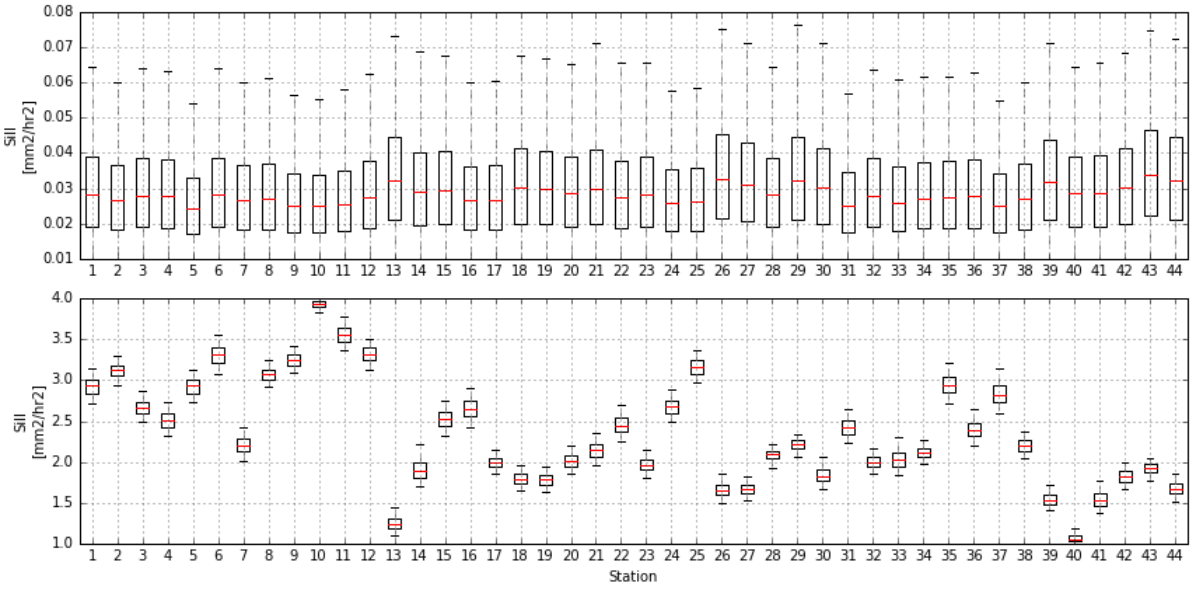

Figure 4.11 Identifiability of the CS Sill in Low (top) and High (bottom) precipitation regimes

The results for the CS variograms at different precipitation intensities (Figure 4.12) reveal a shorter range of the CS variogram for *L*, and longer for *H*. The results expose a smaller spread of the results for *H* in comparison with *L* and the baseline. The spread of the low precipitation range can be explained by the little sensitivity of this parameter when the process is noisy. On

the contrary, the range in the high precipitation variogram is relatively well bounded, and thus, less uncertain than the baseline.

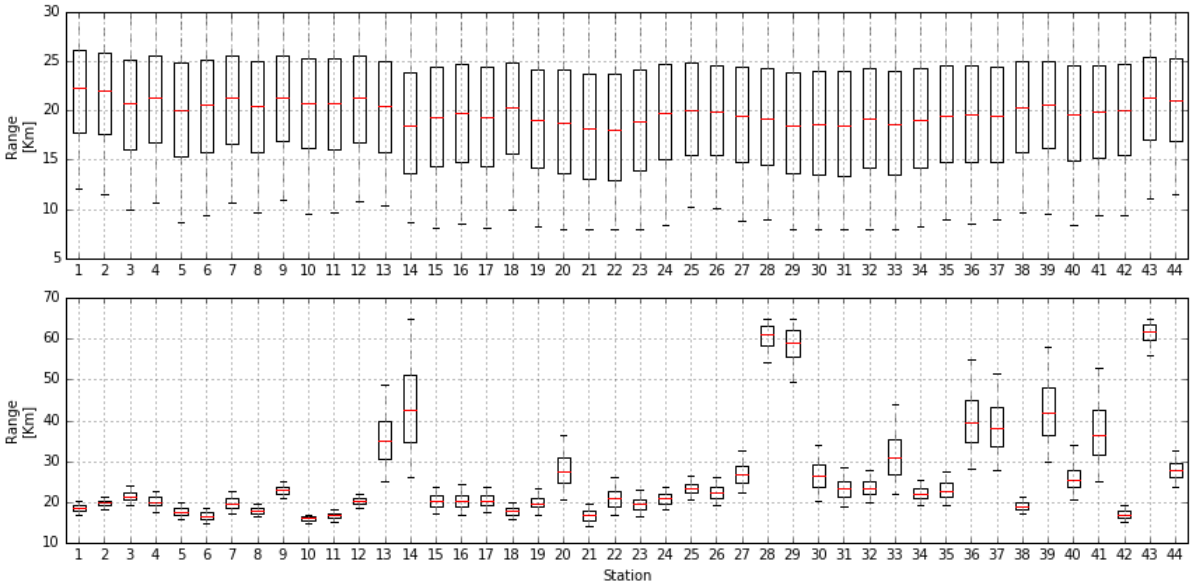

Figure 4.12 Identifiability of the CS range in Low (top) and High (bottom) precipitation regimes

The results obtained for the nugget (Figure 4.13) reveal that this parameter is not identifiable regardless of the precipitation regimes.

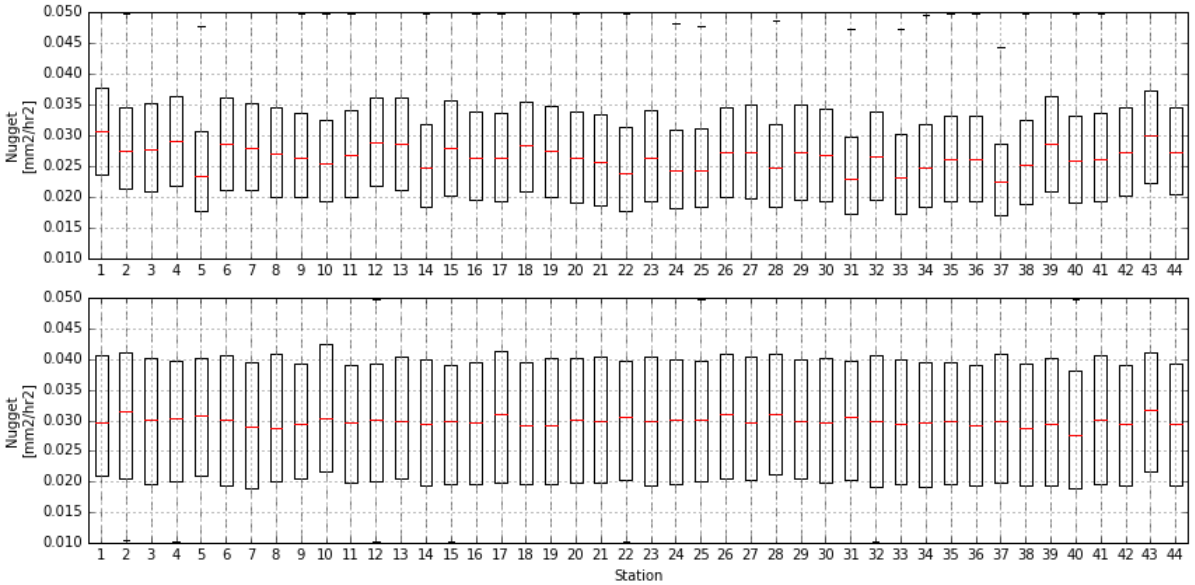

Figure 4.13 Identifiability of the CS Nugget in Low (top) and High (bottom) precipitation regimes

4.5.3 **Stationarity tests**

The results of the hypothesis tests described in the methodology are presented in Table 4.2.

Table 4.2 Results of the hypothesis tests for non-stationarity of the precipitation field

Index	Description	Test	Accepted H0	Rejected H0
T1	Temporal non-stationarity	ADF	0.00%	100.00%
T2	Equal mean between stations	t-test	30.23%	69.77%
T3	Equal variance between stations	Levene	59.51%	40.49%
T4	Equal average of CS experimental variogram	t-test	29.07%	70.93%
T5	Equal average of CS theoretical variogram	t-test	0.00%	100.00%
T6	Equal mean of the theoretical CS Sill	t-test	0.01%	99.99%
T7	Equal mean of the theoretical CS Range	t-test	3.38%	96.62%
T8	Equal mean of CS Sill in high and low precipitation	t-test	0.00%	100.00%
T9	Equal mean of CS Range in high and low precipitation	t-test	2.27%	97.73%

The results of the ADF test reveal that precipitation is temporarily stationary. For this, test, the selection of the time lag for the ADF test was set between 2 and 3 hours, considering that the autocorrelation beyond this point is marginal (Figure 4.14). The result was lower than -50 in the ADF for all stations, which practically yields a p-value of 0.0, rejecting the null hypothesis. Meaning that a 95% level of confidence, the hypothesis of non-stationarity can be rejected, and assume the precipitation is temporarily stationary at temporal operational scale.

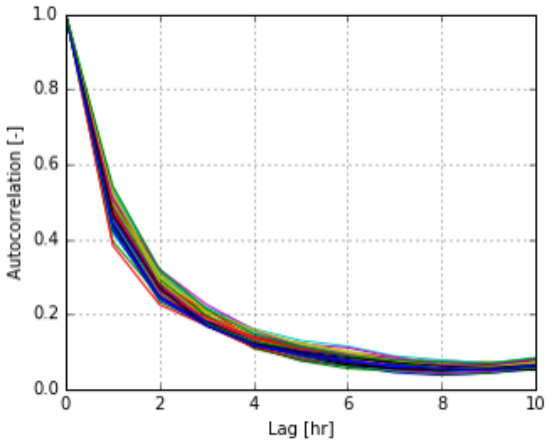

Figure 4.14 Autocorrelation of the precipitation time series for all stations in the Brue Catchment

Spatial stationarity refers to the fact that, independently of the position in space, the statistical properties of the process must remain statistically equal. The results obtained for every possible combination of stations reveals that in approximately 30% of the cases, the precipitation average is equal for the stations, thus the null hypothesis is rejected in 70% of cases. *T2* evaluates the null hypothesis that the variance between a pair of observations is equal, which is the requirement to assess spatial homogeneity. The variance between a pair of stations is equal in almost 60% of the cases, while is rejected in 40% of them.

The testing of the homogeneity of the experimental and theoretical variograms also reveals that the assumptions of spatial homogeneity in the variograms are not adequate. The stationarity tests for the spatial homogeneity of the variograms (*T4 – T7*) reject the hypothesis of equality of means and parameters of CS variograms at different stations in the catchment. These results contradicts the assumption of spatial stationarity, as the rejection rate of these tests is considerably high.

Additionally, the assumption of stationarity between low and high precipitation thresholds was rejected. The hypothesis of statistically equivalent parameters between precipitation regimes was rejected most of the times for the sill and range. The test was not carried out for the nugget, but the relatively little effect of the interpolation and the lack of identifiability of this parameter in every condition will end up in the acceptance of the equivalence of the nugget in different precipitation regimes.

4.5.4 **Comparison of conventional Kriging and NS-Kriging**

To evaluate the performance of the proposed methodology a leave-one-out approach is used (Cressie 1993, Kanevski 2008, 2010), where precipitation estimates are carried out at each station, without using the measurements of said station for building up the model. To summarise the interpolation error, two deterministic metrics are used: the root mean squared error (RMSE) and the mean absolute error (MAE), as:

$$RMSE = \frac{1}{n}\sum_{\alpha=1}^{n}\sqrt{\frac{1}{T}\sum_{t=1}^{T}\left(P_{\alpha,t} - \hat{P}_{\alpha,t}\right)^2} \qquad \textit{Equation 4.24}$$

$$MAE = \frac{1}{n}\sum_{\alpha=1}^{n}\frac{1}{T}\sum_{t=1}^{T}\left|P_{\alpha,t} - \hat{P}_{\alpha,t}\right| \qquad \textit{Equation 4.25}$$

where n is the total number of stations (α), T is the total number of observations in the time series, P is the recorded and $\hat{P}$ is the estimated precipitation in step t at station α.

Additionally, two descriptors of the estimation variance are assessed: the Mean Prediction Interval (MPI), and the Prediction Interval Coverage Probability (PICP) (Shrestha et al. 2009, Dogulu et al. 2015). MPI measured the average width of the prediction interval, for a given confidence interval, while the PICP determines how many of the observations actually fall within the confidence bounds. Making use that the Kriging estimates of the error are Gaussian, the formulation of these indicators can be presented as:

$$MPI = \frac{1}{n}\sum_{\alpha=1}^{n}\frac{1}{T}\sum_{t=1}^{T}2k_f\sigma_{\alpha,t} \qquad \textit{Equation 4.26}$$

$$PICP = \frac{1}{n}\sum_{\alpha=1}^{n}\frac{1}{T}\sum_{t=1}^{T}\theta\left(k_f\sigma_{\alpha,t} - \left|P_{\alpha,t} - \hat{P}_{\alpha,t}\right|\right) \qquad \textit{Equation 4.27}$$

where σ is the standard deviation of the interpolation error, k_f is the coverage factor (which is directly related to the confidence level of the estimates) and θ is the Heaviside function. Again, P represents the observations and $\hat{P}$ the estimates of precipitation at time t and station α.

Finally, the model results are evaluated in a probabilistic framework, using normed residuals (Kitanidis 1983, Samper and Neuman 1989, Lee 1997). For this purpose, the normed mean residuals (*S1*) and normed mean-variance (*S2*) are used as:

$$S1 = \frac{1}{n}\sum_{\alpha=1}^{n}\frac{1}{T}\sum_{t=1}^{T}\frac{P_{\alpha,t} - \hat{P}_{\alpha,t}}{\sigma_{\alpha,t}} \qquad \textit{Equation 4.28}$$

$$S2 = \frac{1}{n}\sum_{\alpha=1}^{n}\frac{1}{T}\sum_{t=1}^{T}\left(\frac{P_{\alpha,t} - \hat{P}_{\alpha,t}}{\sigma_{\alpha,t}}\right)^2 \qquad \textit{Equation 4.29}$$

where σ is the standard deviation of the interpolation error, P are the observations and $\hat{P}$ the estimates of precipitation at time t in station α.

The results for RMSE and MAE show comparable results (Figure 4.15) between OK and NSK. In most of the cases, a marginally better performance is observed for the conventional Kriging, although in practice both are equally accurate, considering that the resolution of the measurements is 0.2 mm.

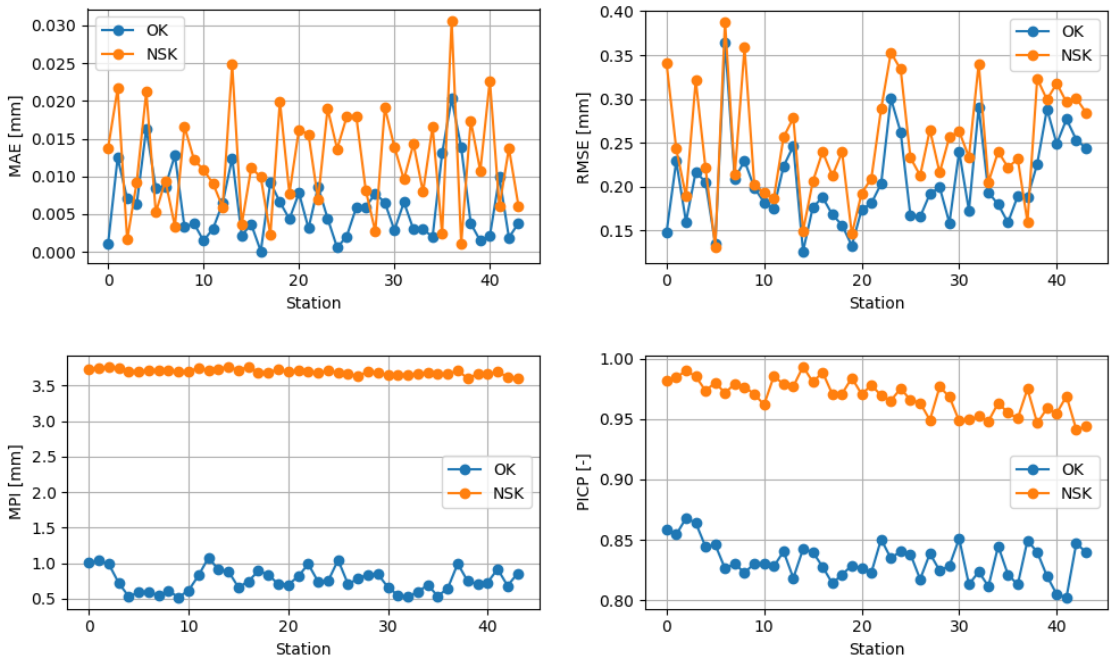

Figure 4.15 Error and prediction interval metrics of conventional (OK) and (proposed) non-stationary Kriging (NSK)

The MPI accounts for the length of the mean prediction interval, while the PICP accounts for the frequency that observations lie within the prediction interval. The results (Figure 4.15) show that the prediction interval of the OK is considerably smaller than NSK. However, evaluation of the PICP reveals a systematic underperformance of the indicator, as OK averages 82% of hits inside the prediction intervals, while NSK lies around 97%.

Finally, the normed residuals account for errors which are proportional to the prediction interval. Ideally, S1 should be equal to zero to satisfy the unbiasedness condition, and S2 should be equal to 1 to ensure the adequacy of the prediction interval (Samper and Neuman 1989). The results for S1 (Figure 4.16) reveal significantly less variable results regarding the prediction intervals for the proposed methodology, as the metrics for the error are consistent between methods. The results of NSK for S2 are several orders of magnitude better.

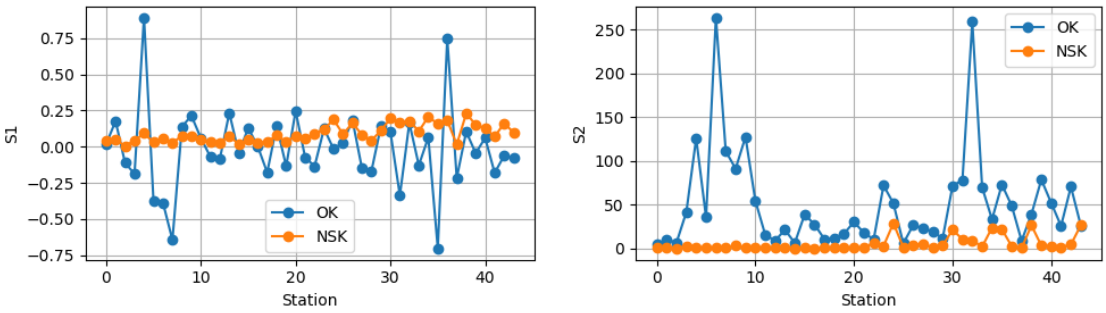

Figure 4.16 Normed errors of Ordinary Kriging (OK) and (proposed) non-stationary Kriging (NSK)

The previous analyses show that OK provides mean estimations which are as good as those obtained by NSK. However, the OK consistently underestimates the prediction intervals. In consequence, the stationarity assumptions do not necessarily lead to larger interpolation errors but, may result in a systematic misrepresentation of the interpolation error. Table 4.3 and Table 4.4 presents a complete overview of the results.

Table 4.3 Results for the average performance of different precipitation performance metrics among the cross-validation results

	MAE [mm]	RMSE [mm]	MPI [mm]	PICP [mm]	S1 [-]	S2 [-]
OK	0.006	0.205	0.763	0.833	-0.012	49.20
NSK	0.012	0.250	3.693	0.969	0.090	5.132

Table 4.4 Results for the coefficient of variation of different precipitation performance metrics among the cross-validation results

	MAE [mm]	RMSE [mm]	MPI [mm]	PICP [mm]	S1 [-]	S2 [-]
OK	0.732	0.241	0.208	0.018	-22.595	1.108
NSK	0.569	0.244	0.011	0.014	0.664	1.612

Additionally, a similar analysis is carried out for several (extended) cross-validation scenarios, where sets of 30, 35 and 40 stations randomly left out. As the size of the leave-one-out analysis

grows exponentially with the number of stations left out, a sample of 100 random combinations were tested. The results of the average absolute model error and prediction intervals are presented in Figure 4.17, where it is possible to observe that the deterministic performance of both models decrease in terms of RMSE, as long as the number of stations left out increases, while the MAE shows higher values when only one station is left out, thus indicating that the inaccuracies of the model results in low precipitation conditions inflate the absolute error. Also, it is interesting to observe how the MPI, and consequently PICP, increases with the number of stations left out in the OK. In this case, the network becomes sparser, yielding higher estimation error variance. In contrast, the average values for MPI and PICP remain almost constant for NSK. It has to be noted that in practice both models have a similar performance, as the order of magnitude of the error among models may be negligible.

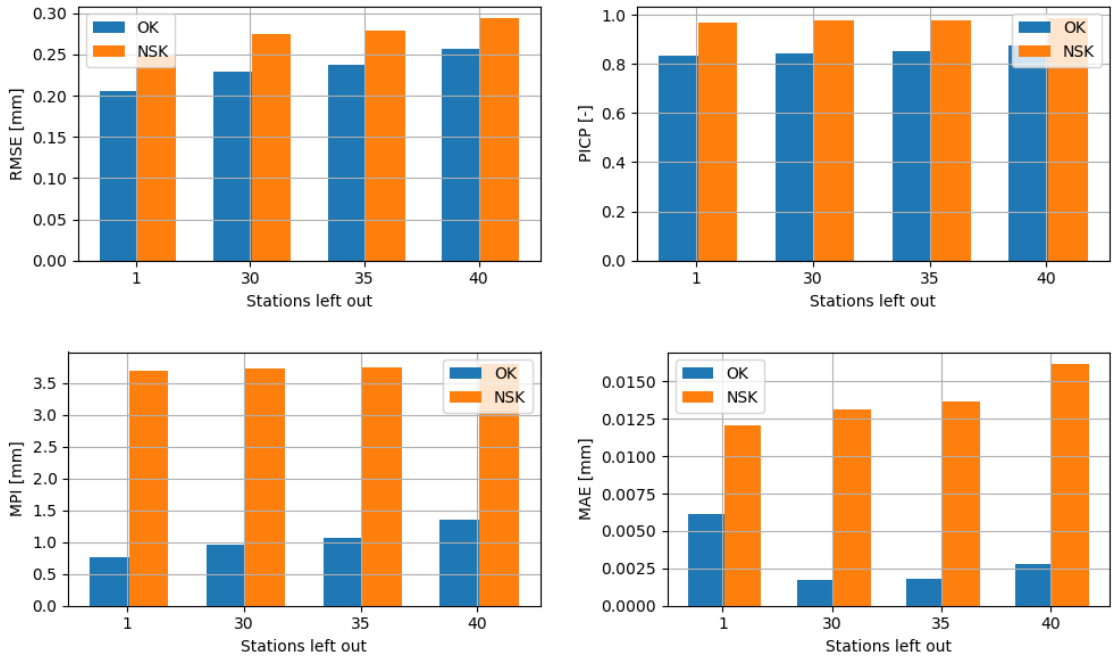

Figure 4.17 Error and prediction interval metrics of Ordinary Kriging (OK) and (proposed) non-stationary Kriging (NSK) for various cross-validation scenarios

Figure 4.18 shows the results of the mean absolute normed errors for the extended cross-validation scenario. The results show that the values of S1 for OK are only superior in the leave-one-out cross-validation, but not when a higher number of stations are left out, indicating that only in areas with high sensor density, the OK outperforms NSK in this particular objective. In contrast, values of S2 are considerably lower for NSK in comparison with OK, indicating that NSK provides a more meaningful estimation of the interpolation error.

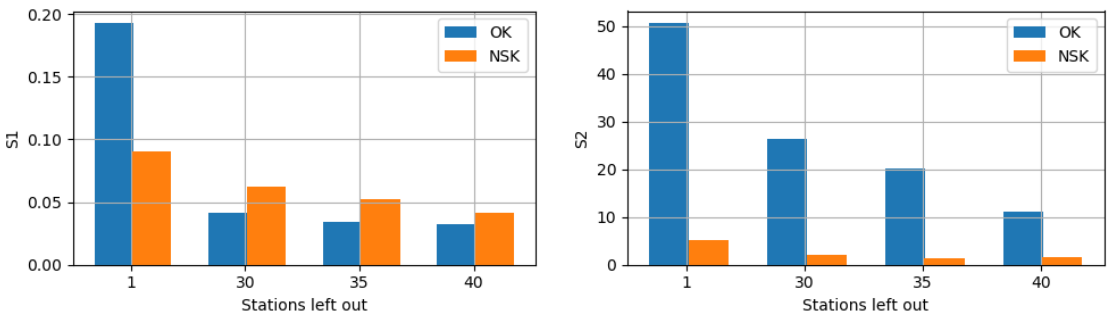

Figure 4.18 Normalised errors of Ordinary Kriging (OK) and (proposed) non-stationary Kriging (NSK) for various cross-validation scenarios

4.6 Conclusions

This chapter explores in depth the characteristics of modelling of random fields through Kriging-type formulations. This includes the redefinition of the fundamental ordinary Kriging to account for the individual measurement uncertainty in heterogeneous networks as a result of different partial recording times, the use of diverse instruments, among others. The results indicate that there is indeed a great role in the observation uncertainty in the results of the Kriging estimates, as observations with a higher uncertainty that the precipitation field itself, are not suitable for use in these type of models.

The data analysis revealed that in the Brue catchment, the temporal variability of the precipitation plays a significant role in the uncertainty estimation. The experimental results indicate that the uncertainty due to partial recording grows exponentially with the non-recorded time. As consequence, dynamic sensors should be restricted in its displacement to provide observations of acceptable quality. As a side effect, displacement in highly observed areas require longer observations to yield valid results, and therefore, dynamic sensors have less displacement capacity in such environments. These results are to be validated for the other case studies, but it is assumed that the uncertainty due to partial recording has the same characteristics in all the case studies.

Additionally, an alternative method for the parameterisation of a generalised covariance structure which is neither fixed in time or space is presented and tested (CS variogram). The results in the modelling of precipitation field yield similar cross-validation errors than the Ordinary Kriging. However, it describes better the errors estimation. This has a direct implication in the design of dynamic sensor networks, as the purpose of sensors in the geostatistical design, aims to minimise the spatial uncertainty in the Kriging estimation.

In the proposed method, the covariance structure is not selected using a maximum-likelihood approach. Therefore, the parameterisation is not biased by assuming that a fixed variogram represents the covariance function. Consequently, the method provides a framework to assess the parametric uncertainty, in contrast with the maximum-likelihood approach to estimate the covariance function.

This study has a number of limitations. The proposed method has been tested only on one case study, and further exploration on other cases is required. Considering that the terrain of the case study is relatively flat, without preferential precipitation areas, the assumptions of spatial stationarity at a first glance may seem to be reasonable. However, the analysis suggests that this assumption may not be adequate for precipitation fields at hourly resolution. Consequently, it is foreseen that the assumptions regarding spatial stationarity may be inadequate to characterise the interpolation error for hourly precipitation using conventional Kriging estimates.

Another specific (limiting) characteristic of the considered case study is the relatively high density of stations. Using sparse networks in the evaluation of stationarity is a major challenge, as the number of data points for the assessment of the correlogram decreases significantly from $n(n-1)/2$ to n. Therefore, a smaller number of points in the correlogram parameterisation may result in more uncertain estimates of the covariance function, and identifying areas of applicability of the presented method is one of the future challenges as well.

5. Optimisation of static precipitation sensor networks and robustness analysis

5.1 Introduction

Static (conventional) sensor networks are the heart of any hydrological monitoring system (WMO 2008, 2009). They are formed by standardised instruments with well-established operation and maintenance protocols. Static sensor networks, therefore, permit continuous observation of variables during extended periods of time at designed locations, and are the main data source for hydrological and hydraulic models.

The design of static precipitation sensor networks have been traditionally driven by aspects such as the minimisation of interpolation estimations (Pardo-Igúzquiza 1998, Barca et al. 2015, Bardossy and Pegram 2009), the even spatial distribution of the sensors and the maximisation of information content they provide (Ridolfi et al. 2011, Coulibaly and Samuel 2014). However, there are some aspects that have not been given enough attention in previous studies and that can eventually have effects on the traditional analyses, especially in the context of citizen observatories.

This Chapter starts with the formulation of the optimisation problem, starting with the analysis of the encoding of decision variables. The experiments are carried out for the Brue catchment. First, the selection of the decision variable encoding is selected between two alternatives, namely Cartesian and local-polar. The optimisation algorithm was selected between four classic candidates, namely Genetic Algorithms, Particle Swarm, Simulated Annealing and Harmony Search, for a sample objective function.

Following, the relationship between some of the most frequently used objective functions from the literature are evaluated. The experiment consists in a Monte Carlo experiment with 100 000 runs for three to seven sensors. The final outcome of this experiment is to identify similitudes and differences between objective functions, as well as their trade-offs. It is of especial interest to explore the dependence between model-free and model-based methods, aiming to provide guidelines for development of monitoring plans in previously ungauged catchments.

Next, the problem of designing optimal sensor networks is solved for all of the objective functions. These experiments are carried out with three to five sensors for each objective function. The results show the optimal network configurations for each case.

Finally, an analysis of robustness of the optimal solutions is carried out. This analysis aims to understand how robust are each of the previously found optimal solutions to the location of the sensors. The general idea is to evaluate the changes in the objective function in the vicinity of the optimal solution at different distances, and analyse its relative change. This may help in the selection of an objective function for the design of sensor networks, and also provide support for the selection of potential objective functions in the design of dynamic sensor networks. The outcomes of this Chapter are fundamental for formulating the objective functions in Chapter 6.

5.2 Formulation of decision variable encoding

The problem of designing an optimal sensor network consists of defining optimal network configurations such that minimise (or maximise) a predetermined objective function (Chacon-Hurtado et al. 2017). Regardless the objective function, the decision variables of the optimisation problem are the position of sensors, and therefore they are directly related to a coordinate system. An important question that arises is to what extent the performance of the optimisation procedures for sensor network design depends on the selection of a coordinate system that defines the decision variables, knowing that one single design network solution can be represented in different ways. We called this the *encoding problem*. Two alternative solutions for the encoding problem are presented below, namely Cartesian and local-polar coordinate systems, followed by an experimental setup to evaluate the performance of both alternatives using different optimisation algorithms. The results are used as part of to design static and dynamic sensor networks, later in this thesis, as presented in Chapter 6.

5.2.1 Sensor location defined in Cartesian coordinates

The problem of optimal location of sensors within a catchment can be posed assuming an arbitrary Cartesian coordinate system, in which each sensor locations is defined by its coordinates (*x, y*). Figure 5.1 shows a simple network of three sensors.

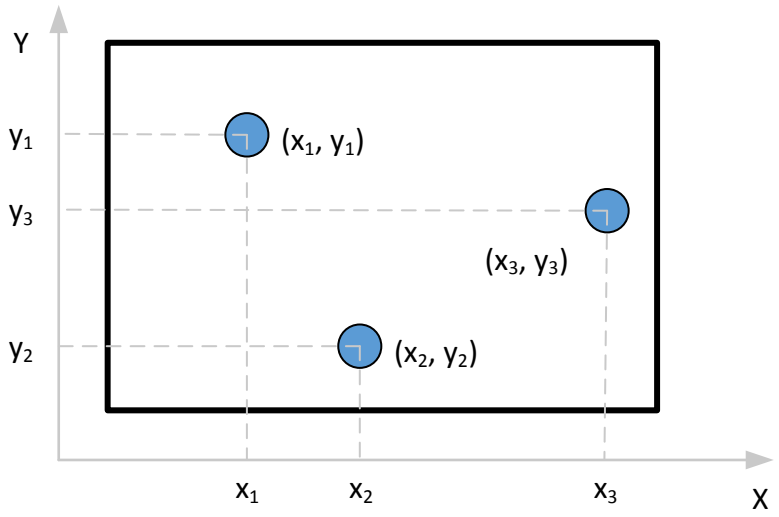

Figure 5.1 Sensor network problem posing with an arbitrary Cartesian coordinate system

As consequence we can define the decision variable vector as:

$$s\{x_1, x_2, \dots, x_n, y_1, y_2, \dots, y_n\}$$

Conditioned to:

$$(x_i, y_i) \in \Omega \; for \; i \in \Omega$$

Where *s* is the decision variable set of *n* sensors, *x* and *y* are the coordinates of sensor *i*, and *Ω* is the domain of the catchment.

However, one single design network solution can be represented by different vectors *s*, as shown in Figure 5.2. The network at the left can be represented by the vector s_L = {1, 2, 3, 4}, whereas the network at the right can be represented by the vector v_R = {4, 2, 3, 1}. Both s_L and S_R are identical from the point of view of sensor location, but are encoded differently. The implication of this non-uniqueness in the encoding leads to a lack of a meaningful metric to recognise similar solutions. This may lead to complications (and most likely higher epistasis variance) in the optimisation procedure, in particular in the crossover operator of GA methods, and in the distance operator in the particle swarm method.

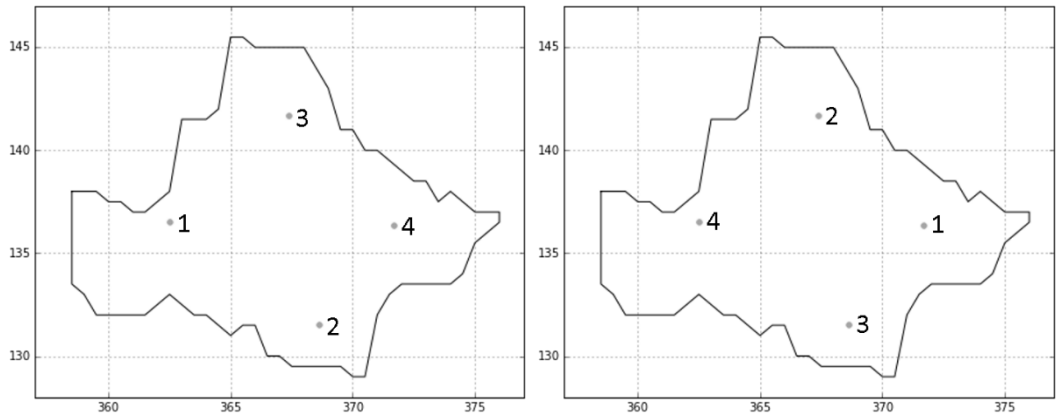

Figure 5.2 identical sensor networks with different sensor encoding

To overcome this situation, a methodology for re-arranging vector *s* is proposed. This will allow to create a quasi-unique representation of each sensor network, facilitating their comparison. The methodology consists of sorting the solutions based on distances, as described below and using Figure 5.3:

- Create a polygon containing the catchment, with a number of vertices (*V1, V2, V3, V4*) equal to the number of sensors (*a, b, c, d*).
- Assign arbitrarily to each sensor a polygon vertex and calculate the distance between each sensor and its assigned vertex (e.g., distances between *a* and *V1*, *b* and *V2*, *c* and *V3*, *d and V4* in Figure 5.3)
- Sum up the individual distances between sensors and vertices, obtaining a total distance.

- Iterate over all the possible combinations of nodes and vertices to find the combination with the minimum total distance between sensors and vertices.

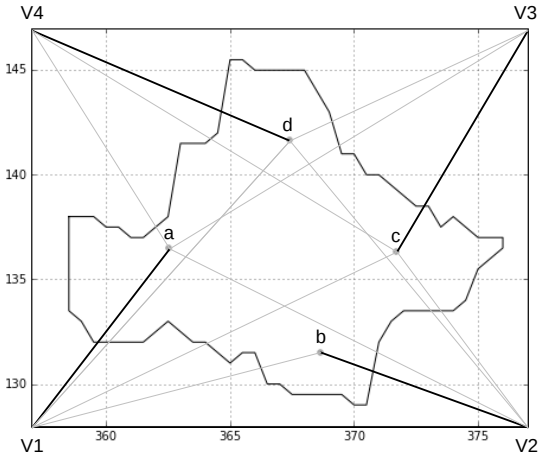

Figure 5.3 Sorting algorithm schematisation

It is clear that the proposed combinatorial problem may be inefficient. However, there are two main reasons to support its use: first, distance functions are cheap to calculate, and second, the number of stations in the selected case studies make it possible to apply the approach in a reasonable time frame. Figure 5.4 illustrates the advantage of the methodology, using normalised coordinates, showing eight similar sensor network configurations (each line is a network). It can be seen that without sorting the vector, the identification of similar networks is extremely difficult, whereas similar networks can be easily identified after the sorting is performed.

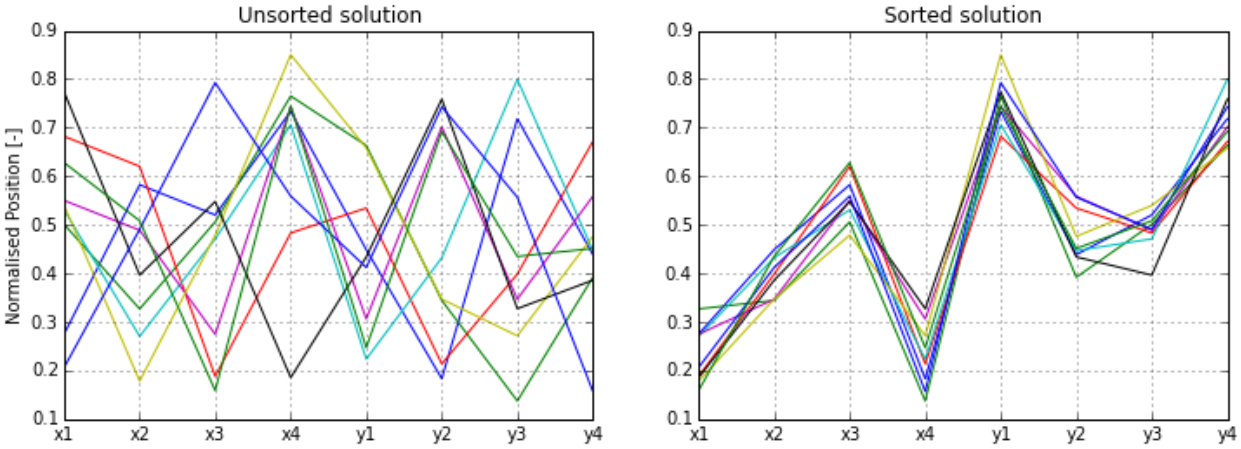

Figure 5.4 Unsorted (left) and sorted (right) solutions for the position of eight different sensor networks

5.2.2 **Sensor location defined in local-polar coordinates**

An alternative way to define the position of the sensors is by using a local-polar coordinate system (Figure 5.5), which means that there are as many coordinate system origins (grey circles) as sensors (blue circles), and therefore the vector s is unique for the same networks, solving the encoding problem. The optimal set of sensors in polar coordinates (r, θ), from an arbitrary origins denoted as (x^*, y^*) is now given by the vector:

$$s\{r_1, r_2, \dots, r_n, \theta_1, \theta_2, \dots, \theta_n\}$$

Conditioning the results to be within the catchment limits as:

$$(x_i^* + r_i \cos\theta_i \, , y_i^* + r_i \sin\theta_i) \in \Omega \; for \; i \in \Omega$$

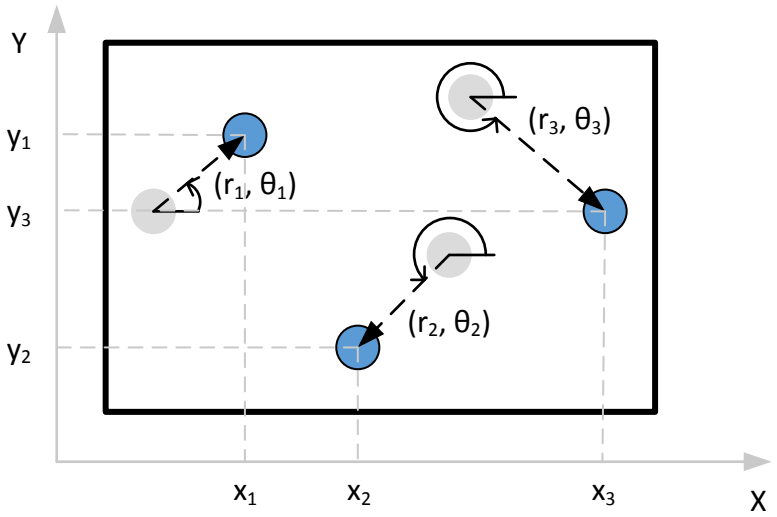

Figure 5.5 Sensor network problem posing in a local-polar coordinate system

However, as the sensors have their own local-polar coordinates, there is still the need to place them within a global coordinate system. Assuming that the design of a completely new sensor network is required, a methodology to conveniently select (i.e., uniformly distributed in the area) candidate locations of each local-polar coordinate origin is proposed. It consists of a random subset of nodes coming from a hexagonal lattice in the domain of the catchment. As lattices are regular structures, a hexagonal one will ensure that there is a minimum distance among the potential origins, which guarantees an overall adequate spread.

The lattice is built iteratively, as described in Figure 5.6. The first step consists in defining the (rectangular) bounds of the catchment in a Cartesian plane, (*H*, *L*), where H is the shortest, and *L* is the longest dimension respectively. Then, a hexagonal lattice is built, using as distance between the nodes half of the longest dimension (*L*/2) of the catchment bounds (represented as grey nodes). If the number of nodes within the domain of the catchment is below the minimum number of sensors, a new lattice is built using half of the distance of the previous (represented as green nodes).

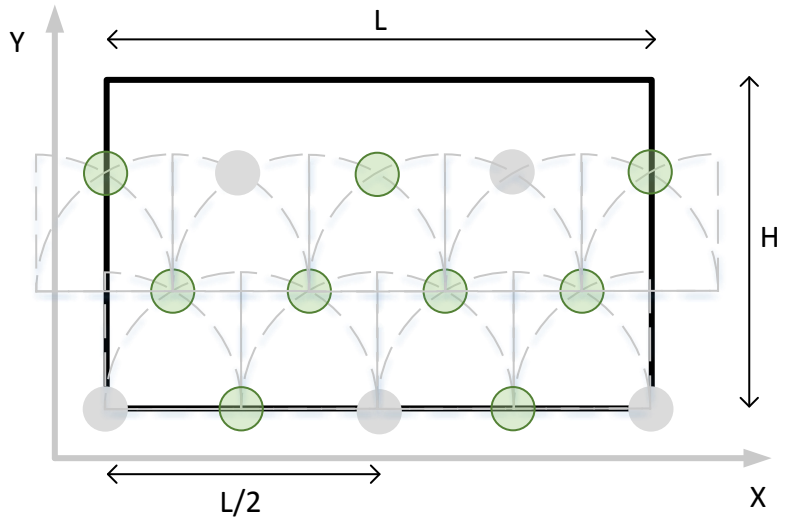

Figure 5.6 Hexagonal lattice for initialisation of sensor positions

Due to the exponential growth in the number of nodes in the lattice, it is likely that it surpasses the amount of gauge origins (orange) for the sensors in the catchment (blue polygon), as shown in Figure 5.7. The iteration finishes when the number of origins is equal or larger to the number of sensors. It can be demonstrated that few iterations are required to generate more nodes than the required initial locations, as the number of nodes in the lattice grows exponentially in each iteration.

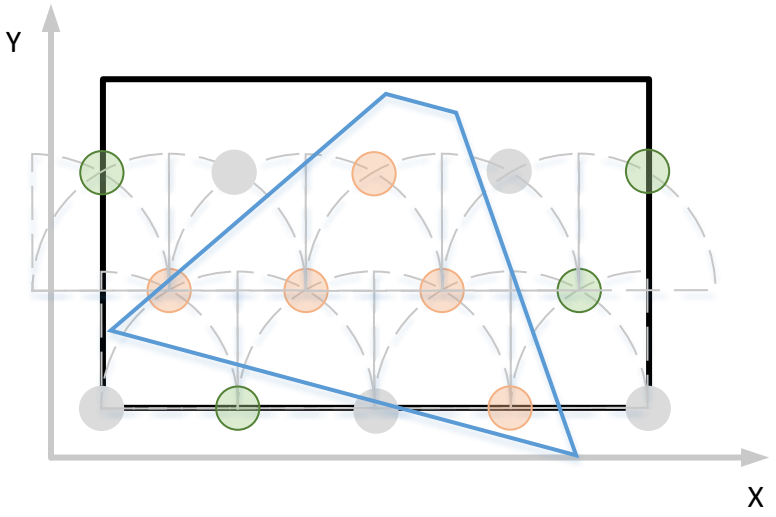

Figure 5.7 Selection of coordinate system origins in the local-polar coordinate system

5.3 Selection of decision variable encoding and of optimisation algorithm

An experimental setup to evaluate the performance of the two alternative solutions for the encoding problem presented above, namely Cartesian and local-polar coordinate systems is presented. The experiment consists of evaluating four different optimisation algorithms to find the optimal configuration of three sensors in the Brue Catchment, to minimise the average Kriging variance (AKV). The test is carried out using the Cartesian coordinate posing and the

local-polar coordinate posing. Details of the algorithms can be found in Annex 1, and their corresponding parameters used in the experiments are presented in Table 5.1.

Table 5.1 Optimisation algorithms for the minimisation of AKV in the Brue catchment

Algorithm	Acronym	Max Iterations	Parameters
Particle Swarm	PSO	5000	Swarm size = 50
Harmony Search	HSO	5000	Pitch adjustment rate = 0.65
Genetic Algorithms	GA	5000	Population = 50
Simulated Annealing	SA	5000	Mutation rate = 0.5

The results of the evolution of the minima are presented in Figure 5.8. The evident first result is that in both cases, SA is underperforming, and it is especially evident when using the local coordinate system. In both cases, GA shows to be the second worst algorithm to converge to the optimal solution, and failing to reach the minima of the other optimisation algorithms in the local coordinate system. HSO and PSO show a relatively good performance in both cases, being able to reach to the minimum of the objective function. It can be stated that solutions found using local coordinate system converge about 66% faster than those using global coordinate system.

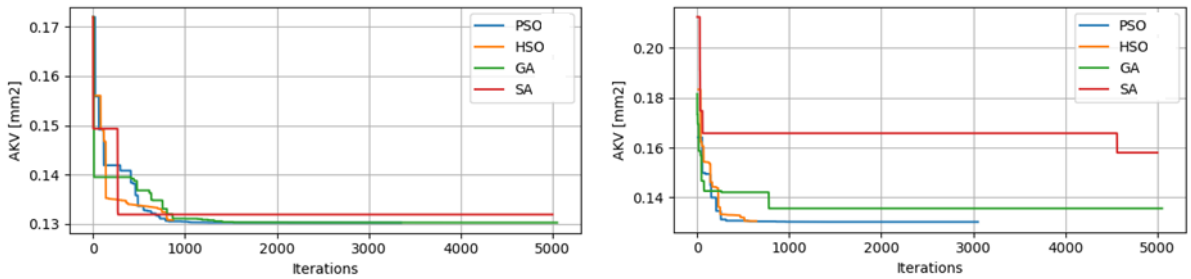

Figure 5.8 Evolution of the optimisation process for Cartesian (left) and Local-polar (right) coordinate systems

Additionally, it is possible to see that in the amount of valid solutions that are generated by each optimisation algorithm, varies depending on how the problem is posed (Figure 5.9).

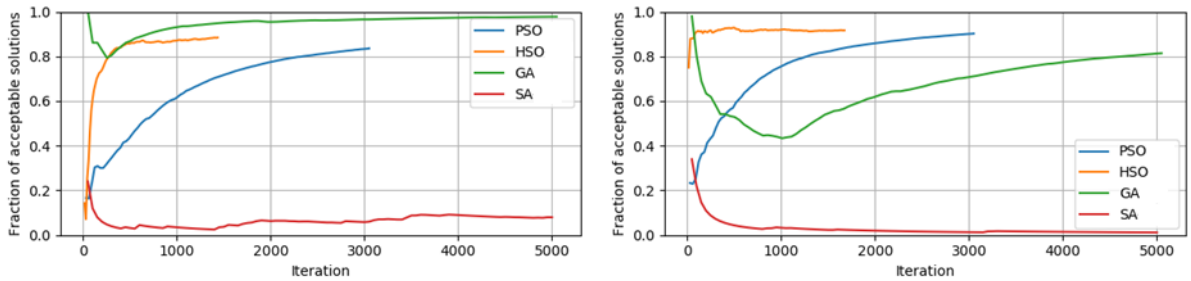

Figure 5.9 Evolution of the fraction of valid generated solutions for Cartesian (left) and Local-polar (right) coordinate systems

It can be observed that HSO and PSO are able to generate far more valid solutions when using the local-polar coordinate system than when using the Cartesian coordinate system. On the

contrary, GA and SA are able to generate more valid solutions when using the global coordinate system.

The solutions generated using the Cartesian coordinate system have larger random jumps, indicating that may help in finding the local minima due to randomisation (or mutation in GA), instead of refinement of the solutions. As consequence, methods that generate better solutions (HSO and PSO) converge earlier to the optimal in the local-polar coordinate system. Based on these results, PSO is used as optimisation algorithm for the design of the sensor networks, using a local-polar coordinate system in Section 5.4 and also in Chapter 6.

5.4 Exploring relationships between various objective functions

A second aspect worth exploring relates to the lack of consensus in the criteria for the design of sensor networks, some of them shown in the reference column in Table 5.2. In this section, functional relationships and hidden links between the different objective functions for optimal design of precipitation monitoring networks are presented. Table 5.2 summarises the objective functions to be contrasted in the trade-off analysis.

Table 5.2 Summary of selected objective functions

Type	Method	Metric	Unit	Reference	Description of objective function
Model free	Geostatistics	AKV	mm^2	Pardo-Iguzquiza 1998	Minimise the average interpolation variance over the precipitation field.
		MKV	mm^2	Barca et al. 2015	Minimise the maximum interpolation variance over the precipitation field.
	Information Theory	JH	nat	Krstanovic and Singh 2000	Maximise information content of the monitoring network.
		PJH	nat	Krstanovic and Singh 2000	Maximise information content of the monitoring network, estimated with pairs of sensors.
		TC	nat	Alfonso 2010, Alfonso et al. 2010	Minimise the total correlation of the monitoring network
		AIT	-	Yang and Burn 1994	Minimise the normalised information transfer
Model based	RR model	NSE	-	Xu et al. 2013	Maximise Nash and Sutcliffe Efficiency
		BIAS	m^3/s	-	Minimise the absolute average model error

		CPQ	-	Dong et al. 2005	Maximise correlation between average precipitation and discharge

A schematic representation of the methodology is shown in Figure 5.10. The inputs of the methodology are a base precipitation field generated with all the avaliable rainfall data, a rainfall runoff (RR) model of the catchment and the observed discharge data at the outlet of the catchment. The methodology consists of the random positioning of *S* sensors within the catchment (S-network). A Monte Carlo experiment which yields 100 000 S-networks is carried out. These steps are repeated for a varying number of sensors in the network, from three (3) to seven (7). The steps of the methodology in Figure 5.10 are described in detailed in the following sections.

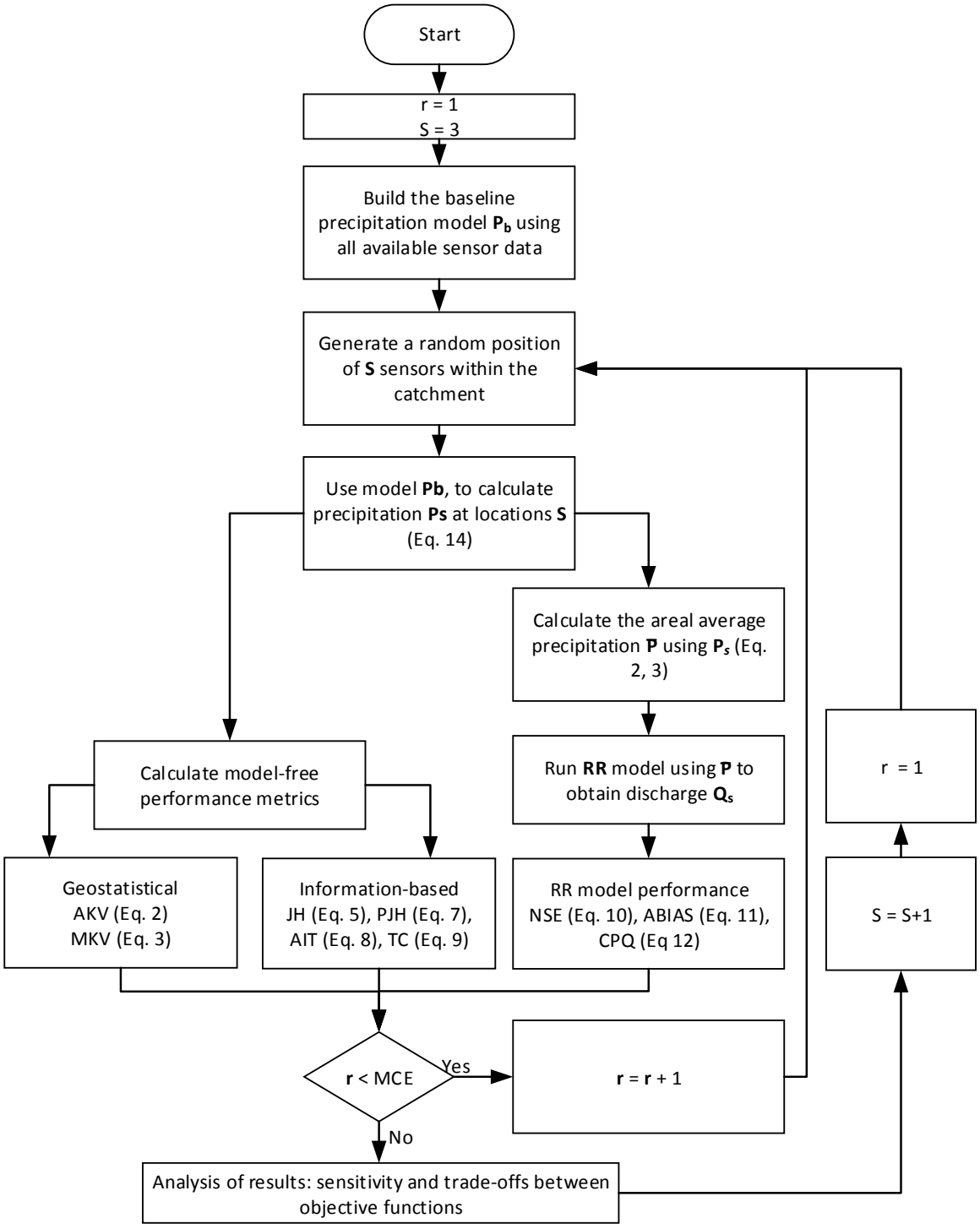

Figure 5.10 Methodology flowchart for the analysis of different objective functions for the design of sensor networks

Where *S* is the number of sensors which are going to be used in the deployment of each *S-Network*; *r* corresponds to the run number in the Monte Carlo experiment, that has a maximum (*MCE*) of 100 000 runs.

The first step is the construction of the baseline precipitation P_b using all the available information of the case study. The second step is to generate an *S-network* (network with

random position of *S* sensors) within the catchment. The third step is to generate the precipitation data for *the S-network* (P_s) using the baseline precipitation model, P_b. The fourth step is to calculate the average areal precipitation $\bar{P}$ over the catchment using a linear combination of the interpolated values at each sensor location of the S-network (Equation 5.1, Equation 5.2).

$$\bar{P} = \sum_{\alpha=1}^{S} w_\alpha P_\alpha \qquad \textit{Equation 5.1}$$

$$w_\alpha = \left[\sum_{j=1}^{S} cov(P_\alpha, P_j) cov\left(O_\alpha, O_j\right)\right]^{-1} cov(P', P_\alpha) \qquad \textit{Equation 5.2}$$

where $\bar{P}$ is the average precipitation over the catchment calculated using the sensor locations of the *S-network*, w_α is the weight of each station (α), P_α is the recorded precipitation at α, *O* is the observation error and *P'* is a first estimate of the precipitation at station *j*. The set of weights (w_α) is identified by the BLUE approach, minimising the variance of the estimated precipitation error (Equation 5.2). This method is widely used in meteorological (Daley 1991) and hydrological modelling applications (Lindström et al. 1997).

Finally, for each S-network produced, the objective functions summarised in Table 5.2 are calculated. The model-free objective functions (geostatistical and information theory based) are calculated using P_s whereas model-based objective functions use $\bar{P}$ to run the RR model and calculate the simulated discharge (Q_s).

The Monte Carlo experiments are the base for trade-off and sensitivity analysis for each S-network. Monte Carlo can also be seen as random search for optimal solutions, albeit neither the most efficient nor effective one. These set of close-to-optimal solutions will be used for further analysis. For each pair of objective functions we will be identifying sets of non-dominated solutions. Trade-offs are evaluated by comparing pairs of objective functions for each S-network configuration, whereas sensitivity reflects the degree of change in objective functions for different network configurations.

We propose a method to quantitatively evaluate the trade-off between a pair of objective functions, based on the shape of the relation between them. The objective is to describe the upper and lower limits of the plots, to measure how conflictive the functions (*f1*, *f2*) are. The method consists in rotating a set of local axes, until a given number of solutions *NS* below the rotated axis is reached. The origin of the local axes corresponds to the minimum of both objective functions.

$$f1', f2' = f1 - \min(f1), f2 - \min(f2) \qquad \textit{Equation 5.3}$$

We use the concept of rotation matrix (*R*) to perform a rotation in the Euclidean space as:

$$R(\theta) = \begin{pmatrix} \cos(\theta) & -\sin(\theta) \\ \sin(\theta) & \cos(\theta) \end{pmatrix} \quad \textit{Equation 5.4}$$

where θ is any angle of rotation of the axes. The matrix with the coordinates of the sensor network (*[n, 2]*) is rotated around the minimum of each function, yielding the transformed functions f^*:

$$\begin{aligned} f1^*(\theta1), f2^*(\theta1) &= [f1', f2']R(\theta1) \\ f1^*(\theta2), f2^*(\theta2) &= [f1', f2']R(\theta2)^T \end{aligned} \quad \textit{Equation 5.5}$$

Finally, the fraction of the solutions that remain in the negative side of the rotated axis is calculated using the Heaviside function (Θ, Equation 5.6). It has to be noted that the matrix is being transposed for *θ2*, in order to maintain the sign of the vector.

$$\begin{aligned} g(\theta1) &= \frac{1}{MCE}\sum_{i=i}^{MCE}\Theta\left(-f2_i^*(\theta1)\right) \\ g(\theta2) &= \frac{1}{MCE}\sum_{i=i}^{MCE}\Theta\left(-f1_i^*(\theta2)\right) \end{aligned} \quad \textit{Equation 5.6}$$

Finally, the solutions (g) are compared with the fraction of solutions which are negative in each axis (NS/MCE). As the problem is not explicitly solvable, an iterative procedure for the selection of the θ index is required. As the g-function is smooth and convex, it has been found out that the definition of the θ index can be efficiently solved using a Newton-Raphson solution such that:

$$\left| g(\theta) - \frac{NS}{MCE} \right| \cong 0 \quad \textit{Equation 5.7}$$

A schematisation of the method is presented in Figure 5.11. In this figure it is possible to observe three of the most common cases of relations between two objective functions. Figure 5.11(a) shows a sparse relation between f1 and f2, and how θ1 and θ2 are defined with respect to the corresponding axis. Figure 5.11(b), shows a strong inverse relation between f1 and f2, making θ1 and θ2 close to 0. Finally, Figure 5.11(c), shows a strong direct relation between f1 and f2, meaning that the minimisation of f1 leads to the minimisation of f2. In this case, both θ1 and θ2 have relative high values.

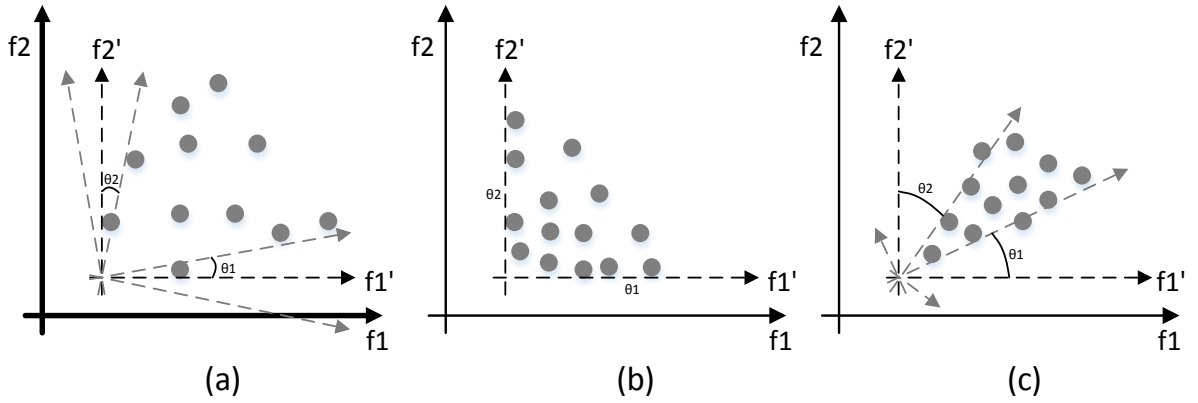

Figure 5.11 Three common cases in the trade-off evaluation of objective functions in the design of sensor networks. (a) mildly-conflicting, (b) highly-conflicting, and (c) cooperative

5.4.1 **Relationship between model-free objective functions**

Figure 5.12 presents the PDF of the results as box-plot for the geostatistical methods, based on Equation 2.8 and Equation 2.9. The average Kriging variance (AKV) has a positive skewness, indicating that the probability of having an S-network with low AKV is high, if the position of the sensors is randomly selected. On the contrary, the maximum Kriging variance (MKV) shows almost no skewness. As the number of sensor increases, there is a reduction of both AKV and MKV, as well as a reduction in the range of the AKV values.

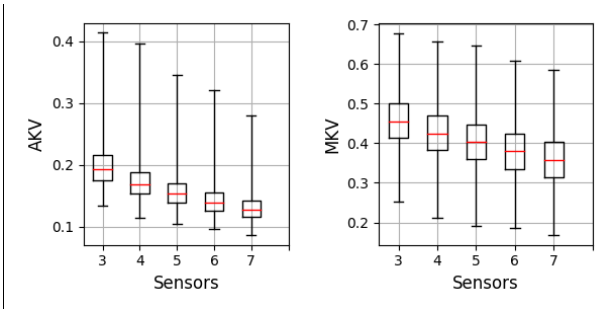

Figure 5.12 Sensitivity of the average (AKV) and maximum (MKV) Kriging variance for varying number of sensors

Figure 5.13 presents the comparison between AKV and MKV for five different network sizes by plotting all the generated networks in the objective function space (with the Pareto optimal set indicated by black points). It can be seen that there is a strong direct relation between them. Note that the size of the Pareto front is small in all cases, which means that the minimisation of one of the objective functions leads to the minimisation of the other. It has to be noticed that the reduction in the AKV may not necessarily lead to correspondingly lower MKV, however if both are minimised, their trade-off reduces (an indication of dependency). Also, it is possible to observe that the direct relation between average and maximum Kriging variance strengthens as the number of sensors increases. From the geostatistical perspective, one can think of the network with low AKV as a fairly well distributed network, as the Kriging variance is a function of the separation between the interpolation target (catchment) and the sensor network.

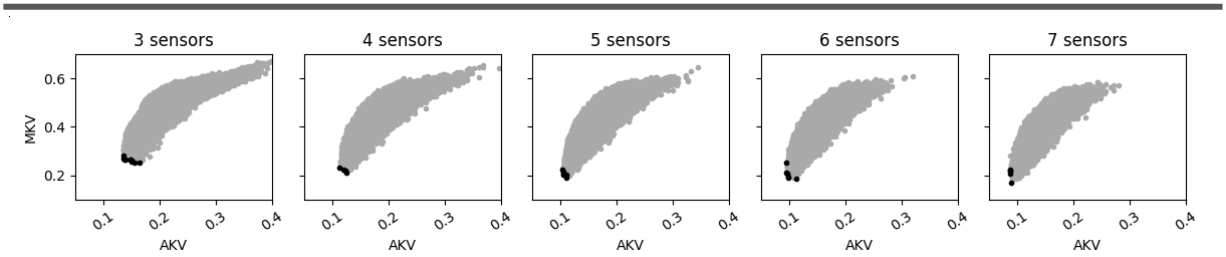

Figure 5.13 Results of Monte Carlo simulation: trade-off between geostatistical objective functions for varying number of sensors

Figure 5.14 presents the histograms for the results of the information-based objective function for different number of sensors. These metrics are calculated using Equation 2.16, Equation 2.18, Equation 2.24 and Equation 2.26 respectively. The sign of the joint entropy metrics (JH and PJH) have been reversed to pose the optimisation problem as minimisation. In consequence, the best solutions are located towards the bottom of the boxplots. The results for JH and PJH reveal that random networks yield centred distributions disregarding the number of sensors. The results show high correlation between JH and PJH; the differences in their values rise the number of sensors increases, and this can be explained by their formulations. Figure 5.14 also shows that the objective functions of information redundancy (AIT and TC) depend on the number of sensors in the system: more sensors share more information.

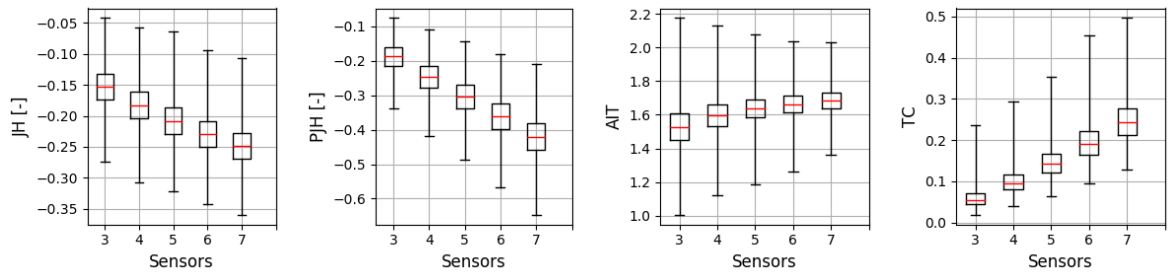

Figure 5.14 Sensitivity of the Multivariate joint entropy (JH), pair-wise joint entropy (PJH), average information transfer (AIT) and total correlation (TC) for varying number of sensors

The results of Monte Carlo simulations between JH and PJH (Figure 5.15) show a directly proportional relationship, thus suggesting that maximising PJH is almost equivalent to maximising JH. The simplification from JH and PJH is especially relevant, because the complexity of computing multivariate joint probabilities increases exponentially as the number of sensors. It can also be seen that the larger the number of sensors, the lower the correlation and the higher the differences between JH and PJH. All the other objective functions show conflicting indirect relations as can be seen in Annex 1.

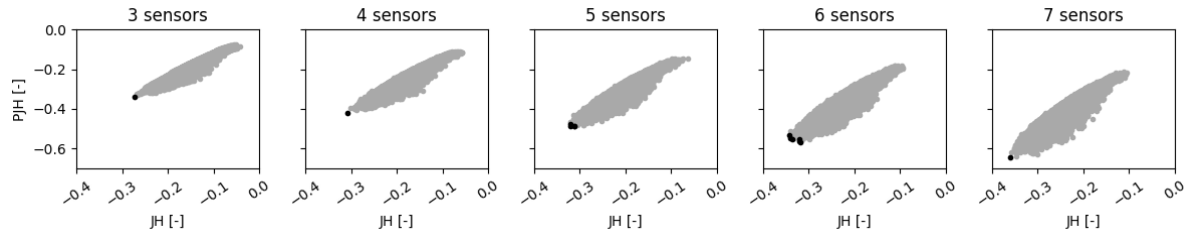

Figure 5.15 Trade-off between joint entropy (JH) and pair-wise joint entropy (PJH) for varying number of sensors

5.4.2 **Relationship between model-based objective functions**

The results for absolute bias (BIAS) and correlation between the average precipitation and discharge (C-PQ) are symmetrically distributed, while NSE is positively skewed (Figure 5.16). The skewness of the NSE can be explained by the fact that the RR processes act as a low-pass filter (Blöschl and Sivapalan 1995, Beven 2012) from precipitation to discharge. The C-PQ does not exhibit a significant variation with regards to the position of the sensors.

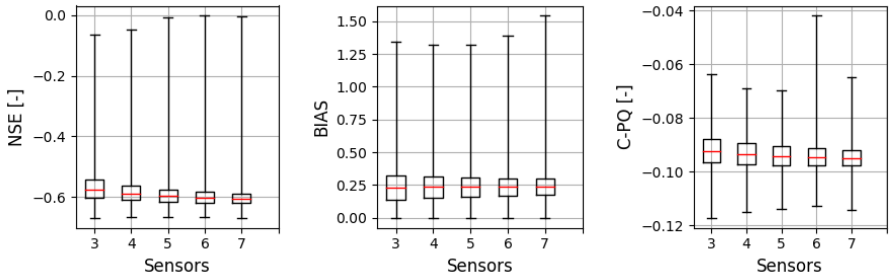

Figure 5.16Sensitivity of the N-NSE, BIAS, and C-PQ for varying number of sensors

The comparison between of NSE with respect to BIAS and CP-Q shows general trade-offs (Figure 5.17). Although the relation between BIAS and NSE shows little dependency, especially for a small number of sensors, the maximisation of NSE implies the minimisation of BIAS. However, the minimisation of BIAS does not necessarily lead to a maximisation of NSE.

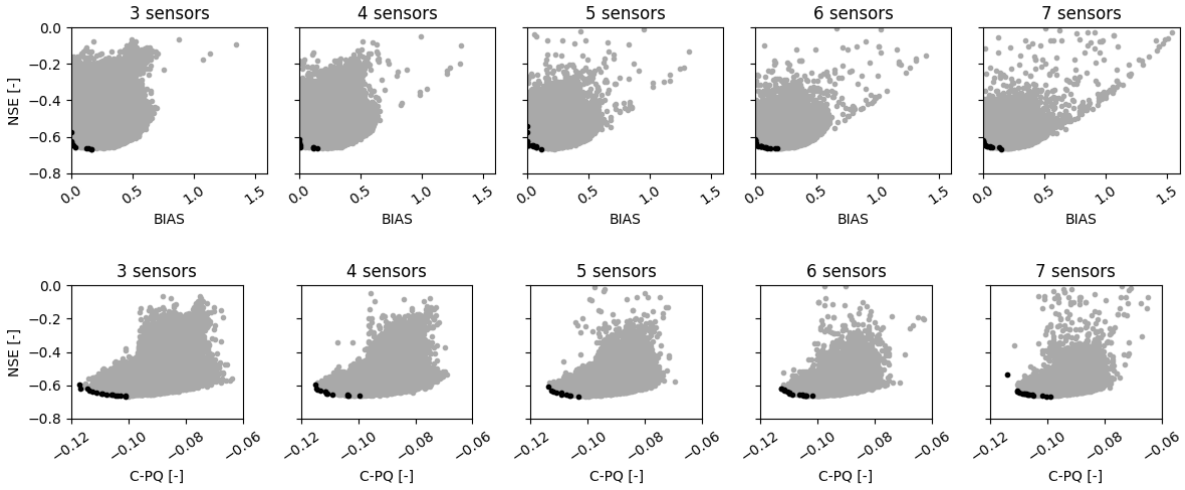

Figure 5.17Trade-off between model-based objective functions for varying number of sensors

The maximisation of C-PQ seems to have a relationship with NSE, especially when the number of sensors is limited. The results show a reduction in the interval of the NSE for higher values of C-PQ, indicating a possible trend connecting these two objective functions. However, a trade-off among these two functions can still be observed. Additionally, there are models close to the optimal for almost every value of C-PQ, regardless the number of sensors. Also, optimal networks for NSE may have any corresponding value of C-PQ, but networks with higher values of C-PQ are less likely to correspond to networks with low NSE.

5.4.3 **Relationship between all objective functions**

We also analysed the relationships between the various types of objective functions: geostatistical, information theory and model-based. In particular, the relationship between model-free and model-based approaches may unveil relationships that are valuable for the deployment of sensor networks for hydrological modelling applications, and this may allow for approximating the model-based design without previously building a RR model of the catchment.

Figure 5.18 presents the relationship between the geostatistical objective functions (AKV and MKV) and the total correlation (TC) (the results for all the objective functions are presented in Annex 1). It can be concluded that generally there is no evidence of a strong functional relationship. Only for a low number of sensors, one can see some interdependency between the AKV and MKV on one hand, and TC on the other (indicated by a smaller Pareto front if compared to the one for a larger number of sensors). This interdependency can be explained as the amount of shared information among a limited number of independent variables seem to be related to the adequate selection of locations in geostatistical sense. Therefore, as the number of sensors increases and the amount of information shared becomes larger, these functions become more and more conflicting.

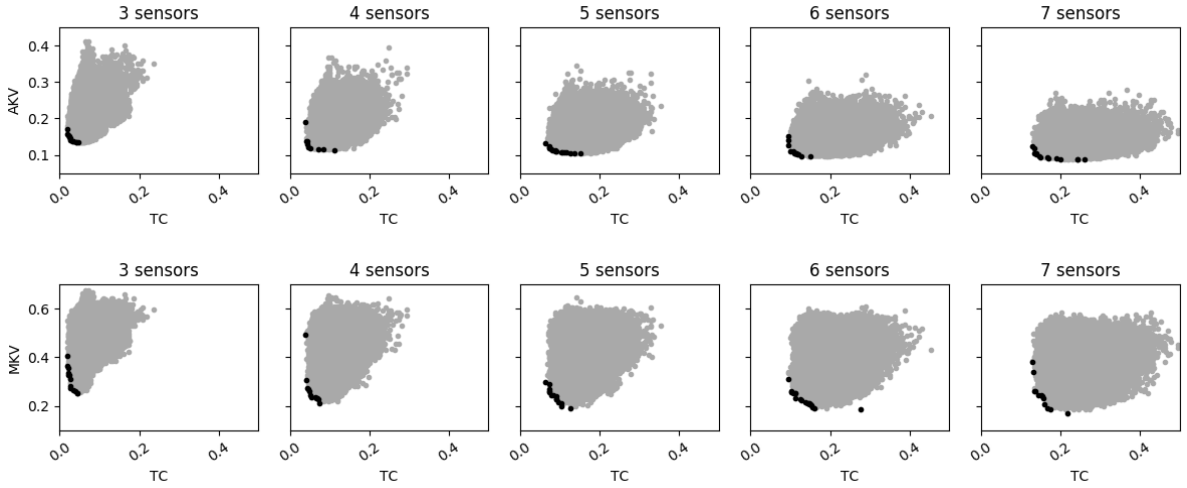

Figure 5.18 Trade-off between total correlation (TC) and geostatistical objective functions (AKV and MKV) for a varying number of sensors

The comparison between the geostatistical and model performance functions reveal that the functions are not conflicting (Figure 5.19). The results for AKV on NSE reveal that the minimisation of AKV leads to the maximisation of NSE, as both functions tend to converge to the same minimum despite the number of sensors. The minimisation of MKV does not necessarily yield better NSE, but the reduction of this metric significantly reduces the range of the potential NSE. These results indicate that the minimisation of MKV may yield better RR model performance, but it does not mean that is a requisite for a network to yield optimal simulation metrics. In contrast, the minimisation of AKV tends to yield sensor networks with a higher NSE performance.

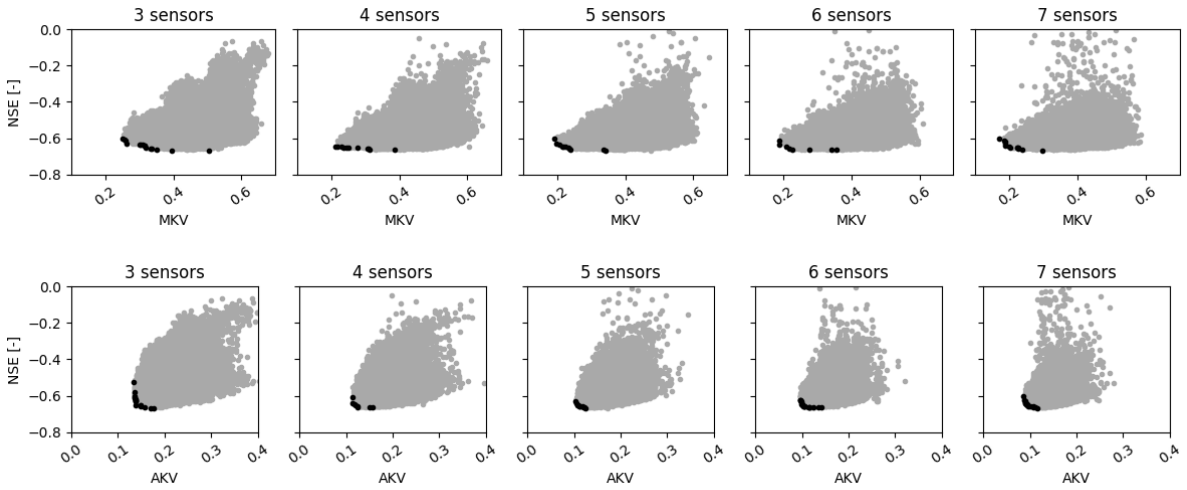

Figure 5.19Trade-off between geostatistical objective functions and NSE for a varying number of sensors

The relationship between JH (and consequently PJH) and TC was also compared with the hydrological model performance (Figure 5.20). From Figure 5.20 it can be seen that high NSE values can appear for a wide range of JH, but low NSE values do not occur alongside with high JH values. In this regard, the maximisation of the JH will lead to a smaller range of NSE, but it is not a requirement to find a network with adequate performance. Additionally, minimisation of TC yields sensor networks with low NSE scores as the number of sensors increase. However, close to good NSE values correspond to a wide range of TC values. AIT did not exhibit any relationship to NSE or absolute bias.

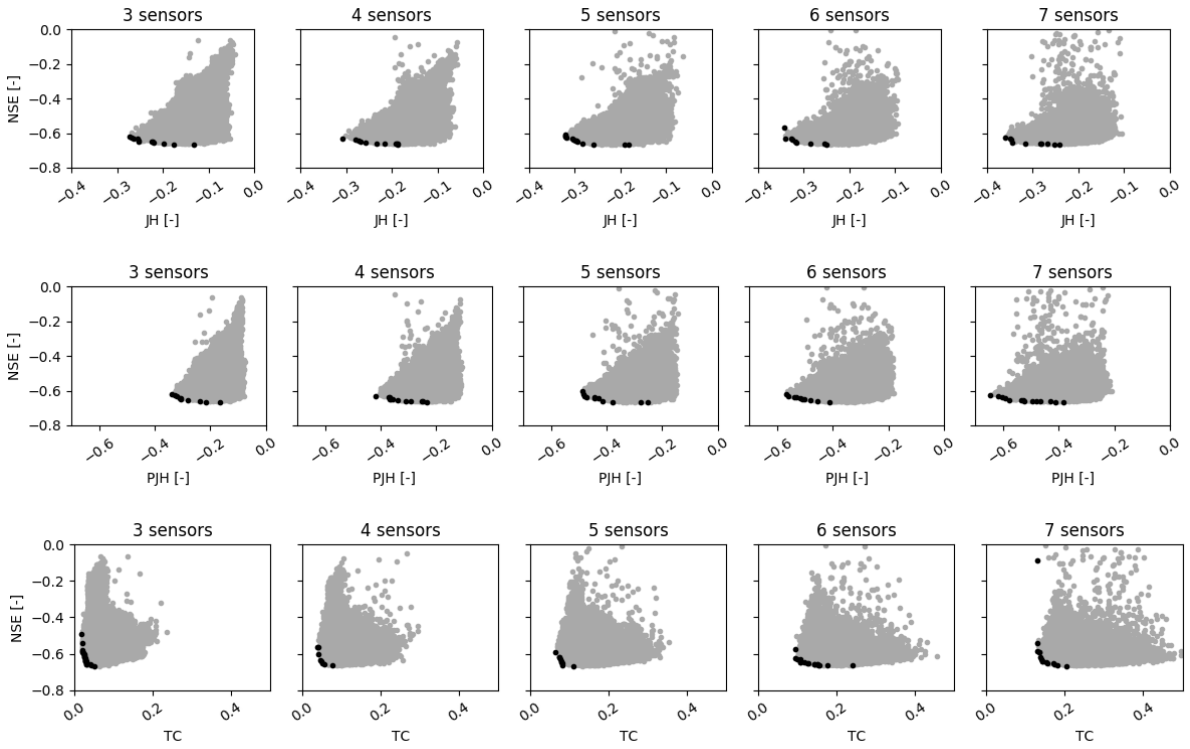

Figure 5.20Trade-off between information-based objective functions and NSE for a varying number of sensors

5.4.4 Can we use model-free instead of model-based objective functions in designing networks for hydrological modelling?

One of the main drivers of this study is to evaluate the possibility of designing sensor networks using model-free methods, which can provide data for accurate hydrological models. The purpose lies in the development of sensor networks in areas where hydrological models are inexistent, so it is possible to develop monitoring plans which lead to adequate performance of such. To this end, the model-free objective functions were used to assess the θ1 and θ2 indexes to estimate NSE (Figure 5.21) and absolute bias (Figure 5.22), using as threshold 0.1% of the total number of solutions.

The results in Figure 5.21 show that there is not a clear indication among the model-free objective functions, which can ensure adequate results of the hydrological model in terms of NSE. It is important to notice that the highest score in this regard belongs to AKV, indicating that approximating the design of the sensor networks using this objective function can lead to an adequate performance of RR models. Additionally, it is possible to observe that most of the model-free objective functions have high θ1values for low number of sensors, indicating that the discrimination of network configurations that yield good hydrological model performance decreases as the number of sensors increases.

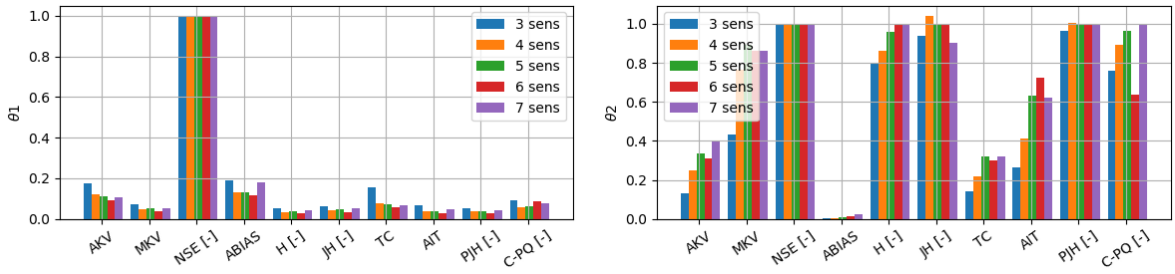

Figure 5.21 θ1 and θ2 coefficients for assessing NSE

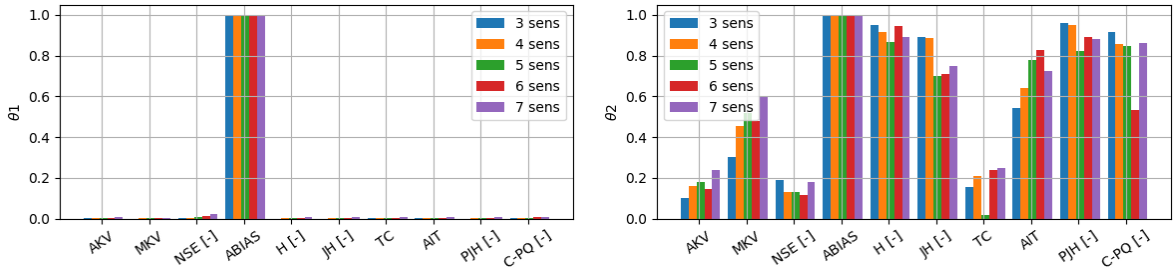

Figure 5.22 θ1 and θ2 coefficients for assessing ABIAS

In contrast, it is possible to establish that the information theory-based objective functions are able to discriminate sensor networks that yield poor NSE values. This is especially evident for the metrics of joint entropy (JH and PJH). Also, it is interesting to observe how the simplified formulation from JH to PJH has almost no effect in the discriminative capacity of the objective function. It can be concluded that the simplifications of PJH may be adequate for the design of sensor networks for catchments with the characteristics of the present case study. Additionally, it is possible to see how all of the objective functions are able to better discriminate low-performance NSE networks, as long as the number of sensors increases.

The assessment of the hydrological model bias is essential to provide information in mid and long-term planning, as the interest is mainly focused on average precipitation volumes, in contrast with a perfect description of the hydrograph characteristics. In this regard, it was found that none of the model-free or any of the other model-based performance objective functions were able to discriminate sensor networks that yield a low absolute bias. In other words, the values of θ1 are close to 0. In contrast, it seems to be possible to identify networks that yield a low performance in terms of absolute bias, indicated by high values of θ2. Among these techniques, the information-based metrics show a relationship, especially the total pair-wise entropy (*H*) and joint entropy (JH and PJH). In other words, entropy metrics can be used to assess inadequate sensor networks.

5.5 Solving the optimal design problem for the selected objective functions

5.5.1 Using model-based objective functions

Although precipitation sensor networks provide data to simulation models, an aspect worth exploring is how the precipitation sensor networks would look like if they were designed to improve these models. In principle, the use of hydrological models in the design of sensor networks has a fundamental limitation, as the sensor network design is driven by the error structure of the hydrological model. The consequence of this is reflected in a specific network for each hydrological model, and period of analysis, leading to a reduced possibility of generalising the results from one network to another, or from one analysis period to another.

The optimisation problem is selecting the optimal sensor locations such that maximise the performance of a hydrological model measured in terms of Nash-Sutcliffe Efficiency (NSE). Three hydrological models are used: an empirical model (linear reservoir, LR) and two conceptual hydrological models, the Sugawara (SUG) and HBV-96. Details about the set-up of the models are presented in Annex 2.

The results of the optimal configuration of the sensor network for each of the models are presented in Figure 5.23, (the connecting lines are drawn to facilitate the visualisation of the different resulting networks). From here it can be seen that the optimal configuration of the network largely depends on the selection of hydrological model. The results for the HBV-96 model (left in Figure 5.23), show a strong tendency to cluster stations towards the centroid of the catchment. In contrast, linear reservoir model (right) that clusters the sensors towards the Eastern part of the catchment, and away from the catchment outlet. For the Sugawara model (bottom), the sensors were clustered towards the centre and East part of the catchment.

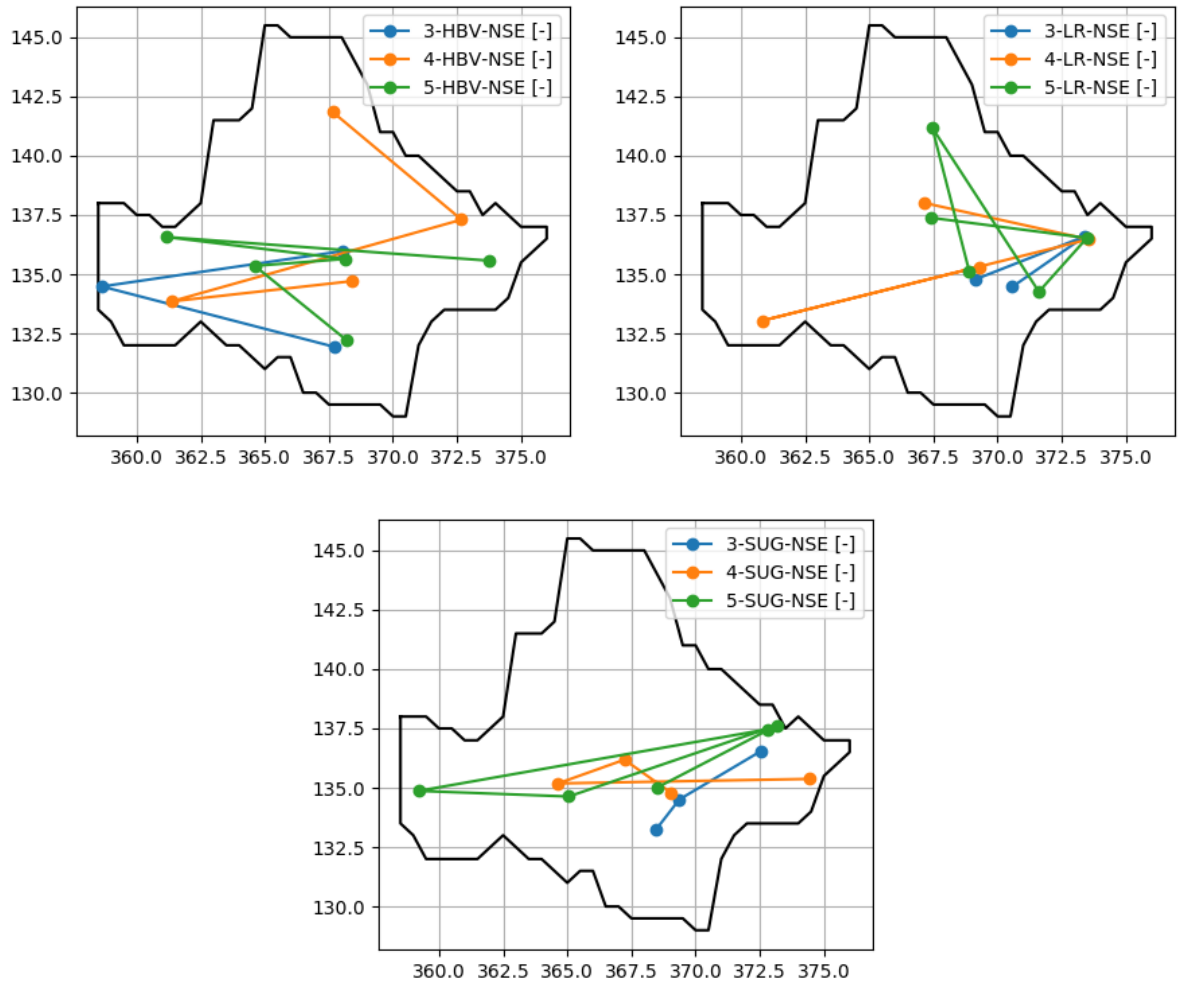

Figure 5.23 Results of optimal sensor networks using 3 sensors for HBV (left), LR (right) and Sugawara (bottom) in the Brue catchment

As a conclusion, it can be seen that there is a relationship between the optimal sensor networks, and the used hydrological model. These conclusions are supported in the evidence that sensors are clustered towards different areas of the catchment. This behaviour can be interpreted by the fact that different structures of the hydrological models lead to different errors, and therefore, the sensor networks aim to compensate this error.

5.5.2 **Using model-free objective functions**

In this stage the optimal deployment of static sensor networks for three to five sensors are explored in the Brue Catchment in a model-free optimisation. The large availability of precipitation records makes the Brue catchment case suitable to make the following analyses as the sensor baseline is large enough to keep a low uncertainty in the estimation of precipitation values at ungauged locations.

Optimal sensor networks using geostatistical measures

The geostatistical measures which are the average (AKV) and maximum (MKV) Kriging variance. The results of the optimisation are presented in Figure 5.24, where it can be seen that

for a low number of sensors, convergence occurs with fewer iterations in the AKV; in contrast, the convergence is faster when a larger number of sensors are used in MKV.

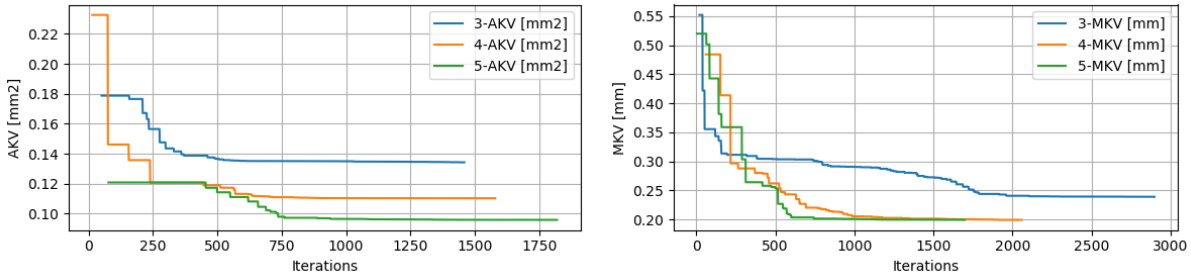

Figure 5.24 Evolution of optimal finding for Average (left) and Maximum (right) Kriging variance

The resulting configuration of the optimal location of sensors is presented in Figure 5.25. From the results it is possible to observe spatially well distributed networks for both AKV and MKV within the catchment. The optimal MKV networks are closer to the edge of the catchment, which yields estimations with a low absolute variance due to the fact that extrapolation (outside the convex hull of the sensors) is reduced. In contrast, the average (AKV) pushes the sensors away from the boundaries of the catchment, to generate an overall lower variance fields.

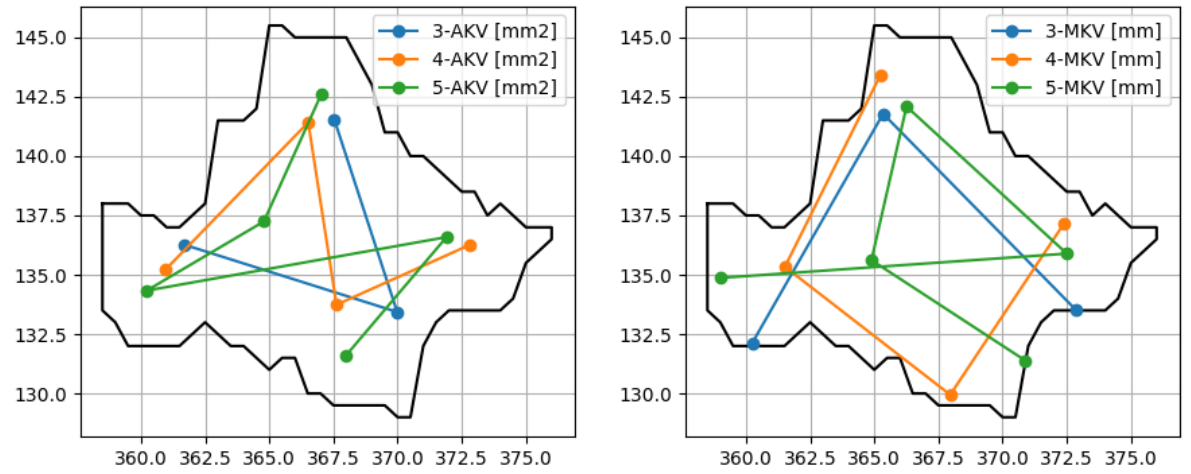

Figure 5.25 Optimal sensor location for Average (left) and Maximum (right) Kriging variance

Optimal sensor networks using information theory metrics

The results of the optimisation problem for the design of sensor networks using information metrics are presented in Figure 5.26. The figure reveals that most of the objective functions tend to require about 1000 model runs to reach values close to the overall minimum. Also, it is possible to observe how the minimum joint entropy (JH, top left) takes a larger number of model runs, in comparison with the pair-wise joint entropy (PJH, top right). Additionally, the total correlation (TC, bottom right) discriminates better the assessments of redundancy than average information transfer (AIT, bottom left), showing larger differences among the networks with 3 and 4 sensors.

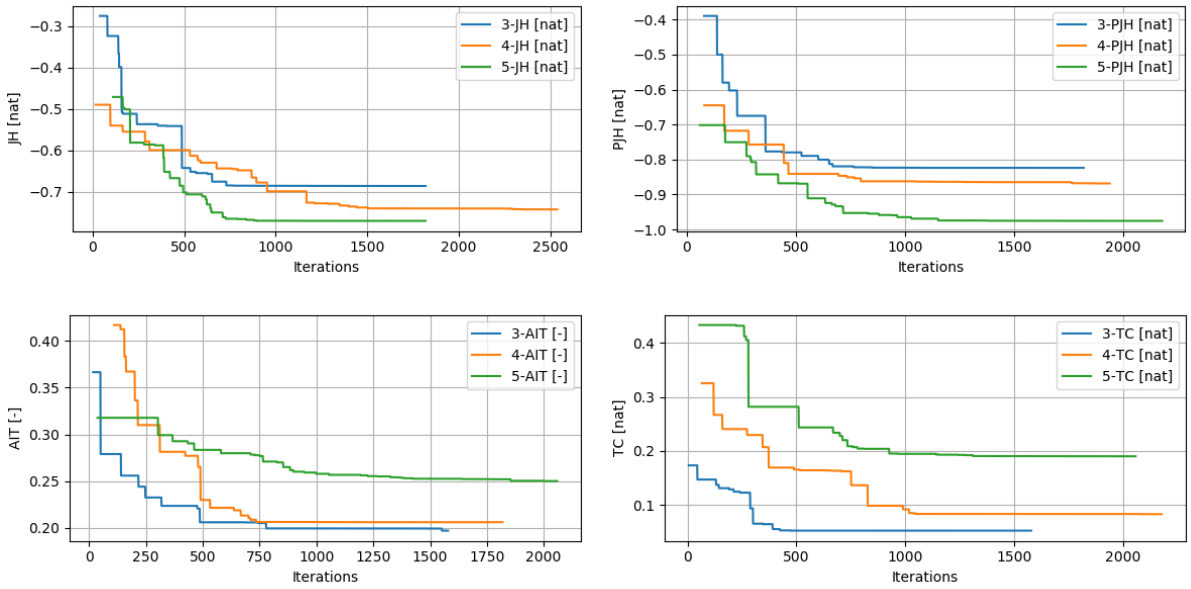

Figure 5.26 Evolution of optimal finding for Joint Entropy (JH), Pair-wise Joint Entropy (PJH), Average Information Transfer (AIT) and Total Correlation (TC)

The results of the optimal sensor networks are presented in Figure 5.27. The results show some interesting features about the optimal configuration of the networks, as they are not well distributed within the catchment. First, the results between JH and PJH are considerably different, while the formulations are similar, indicating that despite the apparent similitude of both functions for a low number of sensors, the location of the sensors differ largely. This differences may probably be triggered by instabilities when computing the information metrics. These differences may appear in the optimisation problem when using multivariate joint entropy to maximise its performance.

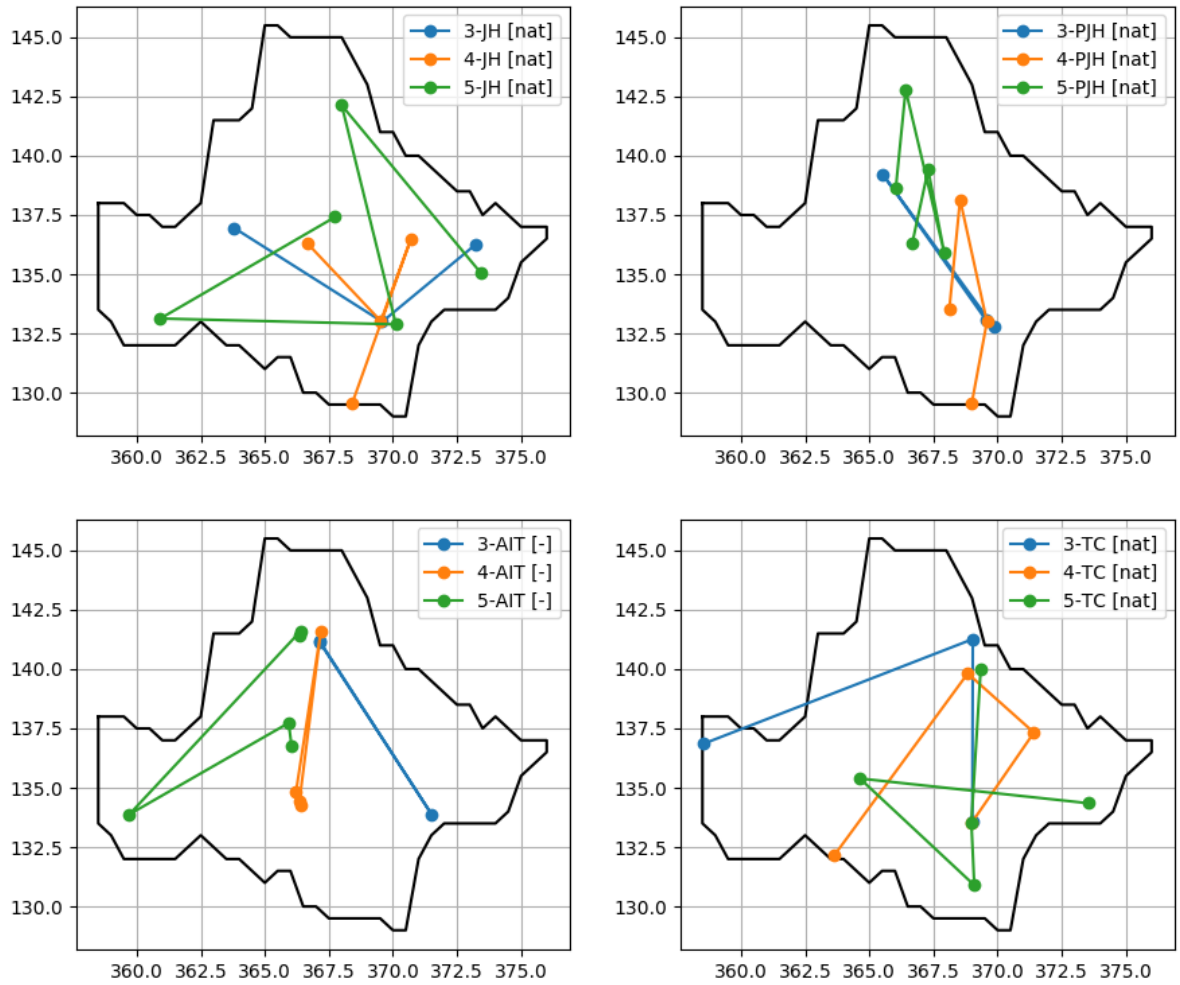

Figure 5.27 Optimal sensor location for Joint Entropy (JH), Pair-wise Joint Entropy (PJH), Average Information Transfer (AIT) and Total Correlation (TC)

The sensor networks in the information based context, aim to augment the information content of the measurements. The analysis reveals an important variability of precipitation towards the north of the catchment, which is capitalised by most of the objective functions. The pair-wise information metrics (PJH and AIT) exploit this information sink, generating the maximum relationship towards this area, leading to inflated metrics of the performance function, if the multivariate entropy is neglected. On the contrary, information metrics which are able to address the multi-variate entropy (JH and TC) are able to produce much sparser networks. In conclusion, the use of information theory metrics requires accounting for the multi-variate entropies for the design of sensor networks, even if the number of sensors appears to be low.

5.6 Analysis of robustness

The fourth aspect to discuss is the robustness of static sensor networks. If a small change in the position of a sensor produces a large reduction in the performance of the objective function, it is said that the network is not robust. This aspect is further explored in this section by means of analysis of robustness of the optimal position of the sensors.

The analysis consists of evaluating the susceptibility of the objective functions to the position of sensors in its neighbourhood. If the solution lies in a smooth minima, the variations of the objective function are gradually increasing as the sensors take position in locations which are nearby to the optimum. On the contrary, if the objective function changes rapidly by locating the sensors in the vicinity of the optimal location, it is possible that the minima has found a solution that is numerically better, but perhaps far from the optimum.

To this end, the following method is proposed: first, a random sampling of the position of the sensors (*s*) at different distances is carried out. This can be visualised as concentric rings (of radius *rs*) around the optimal position of the sensors, as depicted in Figure 5.28. For each of the configuration of sensors in the random sampling, the objective function (*OF*) is calculated and four indicators are produced: range variation (*rv*), intra-ring standard deviation (*stdv*), minimum (*minv*) and maximum (*maxv*) variation. The formulations of these indicators are shown as follows:

$$minv_i = \min OF(s) \; \forall \; s \; \in S_i \qquad \textit{Equation 5.8}$$

$$maxv_i = \max OF(s) \; \forall \; s \; \in S_i \qquad \textit{Equation 5.9}$$

$$rv_i = \frac{maxv_i - minv_i}{rs_{i+1} - rs_i} \qquad \textit{Equation 5.10}$$

$$stdv_i = \frac{\sqrt{\frac{1}{S}\sum OF(s) - \overline{OF(S)}}}{rs_{i+1} - rs_i} \qquad \textit{Equation 5.11}$$

Where *OF* is the value of the objective function, S_i is the set of all the position of the sensors α between distance rs_{i+1} and rs_i and *s* is each of the individual position of the sensors. The range variation (*rv*) explores the distance between the minimum and maximum values of the objective function for a given ring, indicating the rate of change of the objective function. The standard deviation variation (*stdv*) accounts for the intra-variability of the results within the ring. In addition, min and max are included for reference.

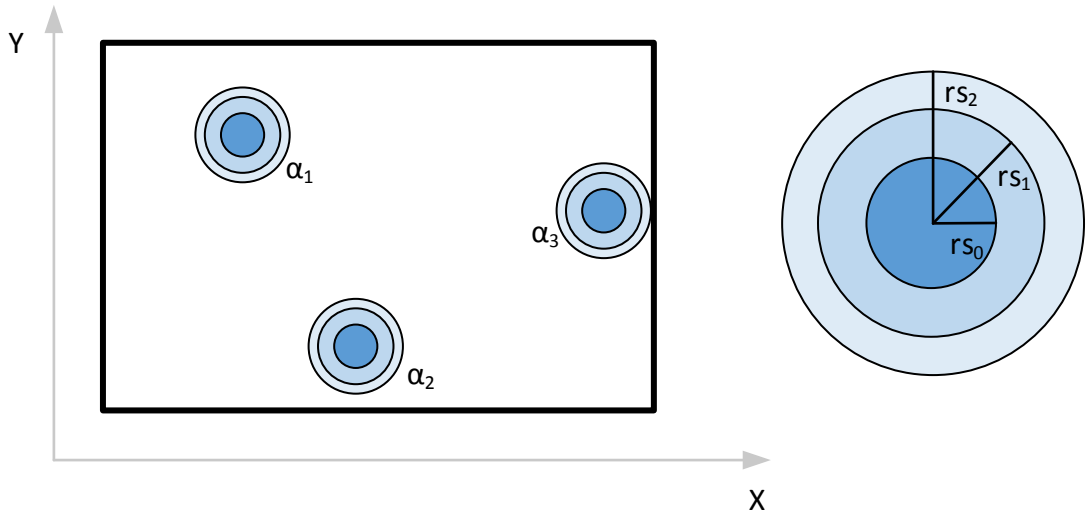

Figure 5.28 Methodology to analyse robustness of optimal sensor networks. Concentric rings correspond to the distance in which the random samples are generated for the robustness analysis.

Once the indicators are calculated for a ring, the process is repeated for each of the remaining rings. The rate of change of each indicator provides insights about the behaviour of the objective function in the vicinity of the optimal solution. A flowchart of the robustness analysis methodology is presented in Figure 5.29.

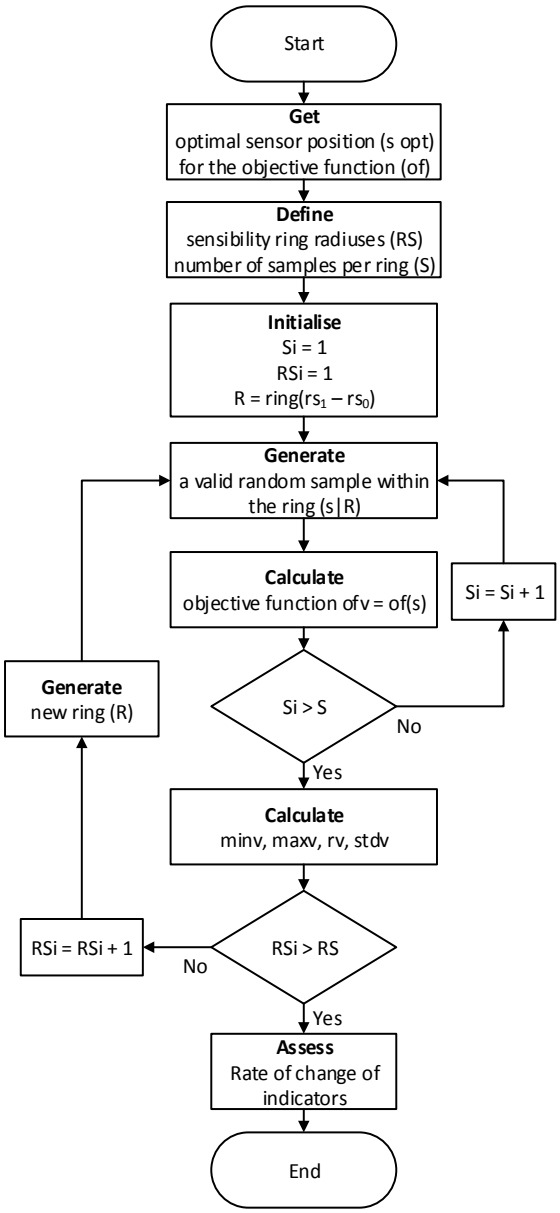

Figure 5.29 Flowchart for the robustness analysis of optimal solutions for sensor networks

To evaluate the sensitivity of the optimisation results, the methodology was applied to the optimised networks found in the previous section. In this experiment, the number of rings is set to 10, each having a radius varying from 0.1 to 1Km. The number or samples per ring (*S*) is set to 500. An independent sample set is generated for each objective function.

The results for *rv* are presented in Figure 5.30. The analysis reveals that the objective functions with the highest divergence from the optimal set are the model-based metrics, especially the HBV and SUG, followed by the joint entropy measures, JH and PJH. The robustness of the model-based performance metrics indicates that the design of sensor networks using hydrological models may end up in solutions that are optimal, but far from being robust. In consequence, these optimal sensor networks may be unreliable, and even more considering that hydrological models are uncertain. Also, it is possible to observe how the sensitivity of the optimal networks obtained using model-based methods reduces as the number of sensors increase.

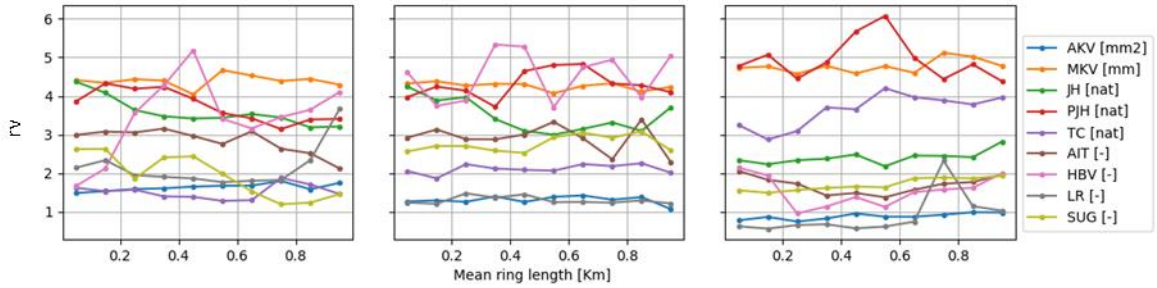

Figure 5.30 Range variability (rv) for the optimal configuration of sensor networks for 3, 4 and 5 sensors respectively

The JH and PJH show a similar sensitivity as long as the number of sensor is low. This means that the role of multivariate joint entropy is important in the design. In addition, the presence of larger multi-variate entropies influences the sensitivities of the estimates when the number of sensors increase. PJH is more sensible than JH in the case of redundant networks (with more sensors).

For the geostatistical measures AKV and MKV, the *rv* gradient does not greatly change among the different rings. This occurs due to the linearity of the Kriging model, suggesting stable solutions for the minima.

Additionally, Figure 5.31 shows the intra-variability (*stdv*) of the solutions within the ring (Eq. 77). This metric evaluates the consistency of the solutions generated in each of the rings. If the solutions are rather insensible to the position of the sensors the score will be the lowest, while higher variability among the rings will generate a higher score. In this regard, the geostatistical metrics vary greatly, being among the highest (MKV) and lowest (AKV), regardless of the number of sensors, but keeping an almost constant index in all of the rings.

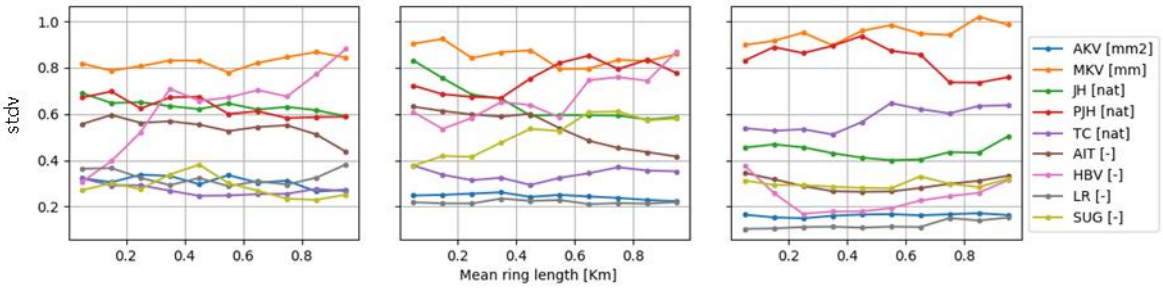

Figure 5.31 Intra-ring standard deviation (stdv) for the optimal configuration of sensor networks for 3, 4 and 5 sensors respectively

The model-based performance statistics show diverse behaviours to the variability of the performance of hydrological models. The HBV shows a great variability of the solutions, which is reduced as long as the number of sensors in the network increases, indicating that the sensitivity to the performance of the model largely depends on the number of sensors. Basically, indicating that the model becomes less sensitive to the position of the sensors as long as its number grow.

On the other end of the spectrum, the LR model shows little variation among the different rings, indicating that the optimal solution does not vary significantly from the optimal in each of the rings. Part of this behaviour can be attributed to the fact that the optimal solution for this objective function tends to be clustered towards the same area at the east of the catchment, making the objective function almost insensible to the sensors in the vicinity of the optimal.

In the case of SUG, the performance of the model seems to be more susceptible when using four sensors in comparison to three and five sensors. This behaviour can be attributed to the optimal position, as it is possible to observe that the network with three sensors is considerably clustered towards the east of the catchment, and the network with 5 sensors find its optimal by having 2 sensors lying extremely close to each other, reducing the effect in the performance variability during the sensitivity analysis.

As in the *rv*, metrics of JH and PJH tend to diverge as the number of sensors increases due to a more clustered set of sensors in for PJH, in contrast with the sparser network found for JH. The result of the instability of the PJH arises as the minima of the objective function is considerably erratic in the position of nearby sensors, indicating that the solution may be consequence of the numerical approximation in calculating joint entropies.

5.7 Conclusions

This chapter explored the problem of optimal design of static sensor networks. The first conclusion in this direction, is that using a local-polar coordinate system together with the particle swarm optimisation algorithm, are the most efficient way to solve the problem of the optimal network configuration that minimises the average Kriging variance. This problem formulation and optimisation algorithms are used in the experiments of this Chapter, as well as in the optimal scheduling of dynamic sensors in the next Chapter.

From the relationship between objective functions, it was found that the design of precipitation sensor networks is a determinant factor in the performance of hydrological models. The number of sensors in did not affect the best performance configuration, as the same performance was achieved with 3, 4, and 5 sensors. However, a larger number of sensors reduces considerably the probabilities of selecting an inadequate configurations of the network, increasing its reliability. These results confirm those obtained by Dong et al. (2005) and Xu et al. (2013), which also highlights that the impact of the position of the sensors in the hydrological model performance is inversely proportional to the available number of sensors. In conclusion, networks with less sensors require a more careful design, while networks with more sensors make the hydrological model performance less sensitive to the final configuration of the sensor network.

The results also show that the bias is less sensitive to the position of the sensors than the other error metrics. Therefore, optimal sensor networks are more critical for applications that use information in short-time windows, such as early warning systems and real-time control. Long-time window applications such as water resources planning, do not require sensor networks to

be as refined. This can be explained as the systematic errors in the precipitation measurement are filtered out in the long-term average, thus having a lesser impact in the model bias with respect to metrics such as NSE. As conclusion, the monitoring objectives control to a large extent the final results of the optimal sensor networks.

The trade-off analysis between the average Kriging variance and the hydrological model performance, reveal a weak dependence between these two objectives. In the literature this property has been speculated, but has not been confirmed. However, we confirm that the minimisation of the average Kriging variance leads to the maximisation of the NSE (and consequently reduction in the bias) in the Brue Catchment. As consequence, the objective functions for scheduling of dynamic sensors in the following Chapter, will aim to minimise metrics of average spatial variability of the precipitation field.

Additionally, it was found out that the results for maximum NSE performance were located in areas with a low MKV. However, using MKV for the design of sensor networks does not guarantee that the performance of the hydrological model is optimal, as acceptable results for NSE were found with every single value of MKV, but models with bad performance were always found in areas with high MKV. Therefore, this index may be used as a secondary objective to consider, as it is useful in identifying sensor networks that yield poor model performance. Similar conclusions can be derived for C-PQ, as the inter-relationship with NSE is similar to MKV.

Signs of over/under gauging (and therefore indication of the adequacy of the number of sensors) can be detected in the relationship between some objective functions. Particularly, the relationship between AKV and TC show a dependency which varies in function of the number of sensors. Also, the relationship between the JH and PJH reveals the amount of information that overlaps between measurements. If the catchment is over gauged, the JH and PJH should differ considerably, as the joint entropy for more than two variables cannot be neglected. On the contrary, if the catchment is under gauged, the information overlapping between more than two variables is expected to be minimum, and therefore, estimations of JH and PJH will be more strongly correlated.

The optimal configuration of sensor networks for the different objective functions of this Chapter, show great differences in the solutions. These results indicated that, unless the objective functions are part of a generalised field property (such as the correlogram in AKV and MKV), may be susceptible to singularities in the data. In particular, information-based metrics, are quite susceptible to this feature. Therefore, it is possible that smoothed precipitation fields (in time and space), may provide a more consistent dataset for the design of sensor networks with to be used in the other information-theory objective functions.

Finally, it was found that the AKV show a relatively high robustness, among all of the model-free objective functions and number of sensors. This result indicates that the changes in the objective function vary gradually with the position of the sensors, indicating that the function is indeed concave in the vicinity of its optimal locations, making it relatively insensible to small

deviations from its optimal location, in contrast to information-based metrics. This conclusion reinforce the use of formulations based on the minimisation of interpolation variance as objective function in the design of sensor networks with dynamic components, as will be considered in Chapter 6.

6. Optimisation of dynamic precipitation sensor networks

6.1 Introduction

Measurements of hydrological variables are carried out to extract information about water systems with various aims, including the understanding of processes and the improvement in decision making (Hart and Martinez 2006). A side objective is, therefore, the minimisation of the uncertainty in the estimation of hydrological variables (Loucks et al. 2005). Conventional measurements of hydrological variables are carried out using stations which remain in the same location for extended periods of time (WMO 2008a).

Currently, observations methods have evolved from ground stations to remote observations and dynamic sensors, including those carried by citizens (citizen observatories) (Lanfranchi et al. 2014, Alfonso et al. 2015). The latter data source implies that the observations are carried out at an irregular sampling frequency, are scattered in space (Mazzoleni et al. 2015), and which may vary according to the level of engagement of the participants (Mazzoleni et al. 2018). Although one of the reasons for using citizens for monitoring is the potential of larger scalability (with the help of volunteers), with respect to conventional observation methods. There are well-known challenges that make it difficult to generate sustainable citizen observatories (Gharesifard and When 2016, 2017, de Vos et al. 2017, Aceves-Bueno et al. 2017).

To include citizen's observations into conventional data streams, these are treated as if were taken using dynamic sensors. From the measurement side, these are heterogeneous observations, and handled as described in sections 4.2 and 4.3. From the scheduling side, means that we assume that citizens are highly engaged, and therefore, they will always be available to travel to any place, at any given moment. In case that these latter assumption is not valid, the data from citizens will only be opportunistic (anything that is send is added to the data stream). In this document, we use the term citizen sensors to denote not scheduled observations, while using the term dynamic sensors for schedulable observations.

Following the structure of the previous chapters, we explore two main alternatives for scheduling the position of dynamic sensors, based on model-based and model-free approaches. Model-based approaches minimise the error of lumped hydrological models to schedule the position of dynamic sensors, and is tested in section 6.3.1. Also, model-free approaches are tested and three alternatives are proposed, based on the minimisation of average volumetric uncertainty based on Kriging variance (6.3.2), non-stationary Kriging variance (6.3.3), and based on the discrepancy of a set of an ensemble of different families of models (6.3.4).

To ensure the maximum utility of the dynamic sensors, it is necessary to develop a methodology for optimal scheduling of the position of the set of dynamic sensors. The scheduling strategy defines the posing of the optimisation problem and the rules which govern the position of the dynamic sensors. In the context of this thesis, finding the optimal location of the sensors is denoted as a deployment strategy, while the general set of rules that control the overall movement of the sensors is defined as the scheduling strategy.

This chapter is organised as follows. First, we present the optimal scheduling strategy and the framework for dynamic sensor deployment. Second, the different objective functions for the deployment are presented and discussed. Third, the experimental setup to test the deployment strategies is discussed. Lastly, results of the scheduling for each of the deployment strategy are presented, and compared against each other. Finally, conclusions, recommendations, limitations and further work is discussed.

6.2 Posing the optimisation problem

The formulation of the problem for the optimal scheduling of dynamic sensor networks (DSN) requires the set of conventions that are shown in Figure 6.1. The rectangle represents the spatial area that needs to be monitored, the orange triangles (SS) represent the static sensors in the network, the grey circles represent the current position of each dynamic sensor (DS), and the blue circles represent their target position. The variables that describe the new position of a sensor are the distance from the initial position of the sensor (R), and its angle (θ). Therefore, the problem is formulated in local-polar coordinates, as described in Section 5.2.2. Additionally, each dynamic sensor belongs to a base (B), indicated by the green hexagons in the figure, which acts as a resting place for the sensors when is not active.

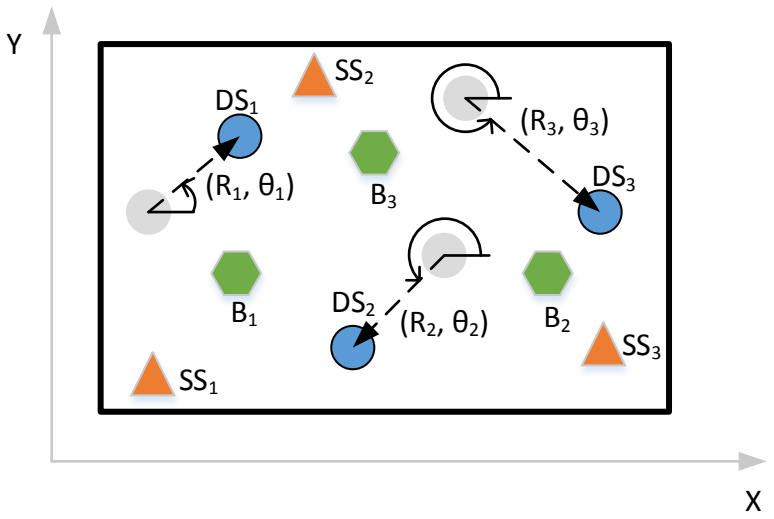

Figure 6.1 Conventions in the optimal scheduling of dynamic precipitation sensor networks

The scheduling of dynamic sensors is intended to actively respond to precipitation events (Haberlandt and Sester 2010). These sensors will be used to carry out measurements in areas and times that can potentially yield useful observations, and should be at base position when

are not required. One of the criteria set is that the sensors will only leave base (and therefore collect data) once the average areal precipitation ($\bar{P}$) calculated using the static sensor network (SSN) is over a threshold *tr*. A general overview of the strategy for the operation of the sensor network is presented in Figure 6.2.

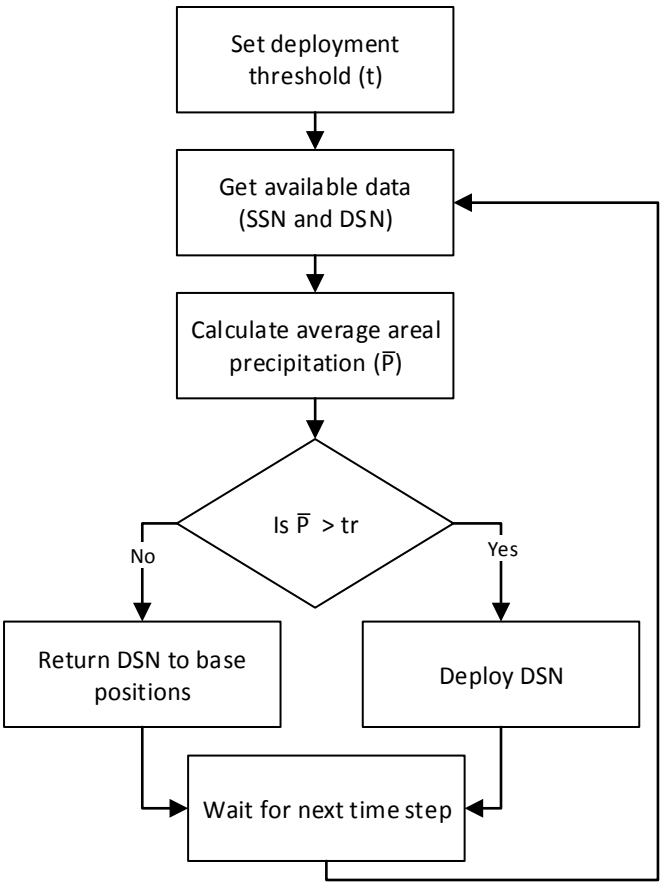

Figure 6.2 Overview of the general scheduling strategy of DSN

The deployment strategy is the central points in this study. It aims to minimise a function related to the uncertainty of the total precipitation volume. The uncertainty in the precipitation estimations comes from two main sources: measurement uncertainty and interpolation uncertainty. The former accounts for instrumental errors and the completeness of the observation, and consequently, is directly affected by the displacement of a dynamic sensor. As shown in section 4.3, the uncertainty in the measurements is affected by the fraction of time in which the sensor is static at a specific site. The latter accounts for the errors coming from the interpolation exercise with limited sensors, and it is quantified using field estimations.

To deploy the DSN, three approaches are developed and tested: including the minimisation of uncertainty metrics based on 1) stationary Kriging (KVP), 2) non-stationary Kriging (NKVP, 0), and 3) multi-model discrepancy (MMD). The first two strategies are based on a metric that relates the total volumetric uncertainty, under the assumptions of ordinary and non-stationary Kriging, while the latter use concepts of equifinality and model ensemble to achieve conceptually similar estimates. The formulation and details of these strategies are presented in the following sections.

The methodology for the deployment of dynamic sensor networks (DSN) is proposed in Figure 6.3. The first step consists of obtaining the current position of the DSN, which can differ from the planned one due to factors such as accessibility, traffic or others that may constrain the placement of the sensors. This thesis does not consider any of these aspects, and assume that the sensors are always satisfactorily deployed in their target locations.

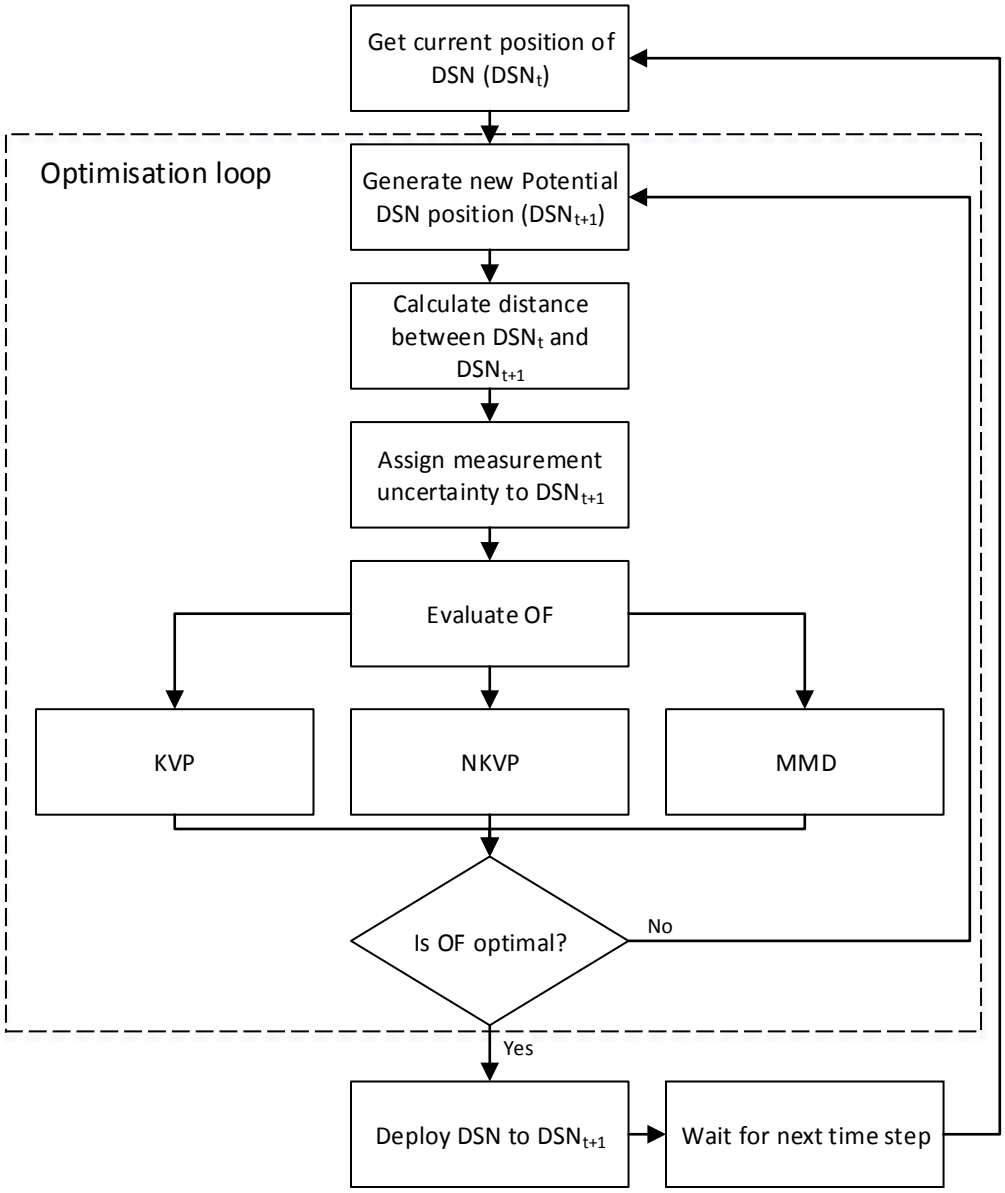

Figure 6.3 Methodology for the deployment of dynamic sensor networks (DSN)

The second step constitutes the generation of a new position for the DSN. These new positions may be selecting by using an optimisation algorithm, and is the beginning of the optimisation loop. The new set of solutions are given for each of the dynamic sensors, and consequently are used to calculate the distance between the current and the next position of the DSN. Additionally, defines the initial position of the sensors for the coming time step.

The third step is to add uncertainty to the DSN measurements, depending on how much time the sensor remains in the target position (DSN_{t+1}). Assuming that dynamic sensors have a fixed velocity, the time available for the sensor to take measurements in the target position can be estimated as:

$$t_i = 1 - \frac{R_i}{v} \qquad \textit{Equation 6.1}$$

where *t* is the time that the sensor *i* remains in the target position, *R* represents the total displacement and *v* is the velocity of sensor *i*. Consequently, the uncertainty due to the incomplete observation in time is directly proportional to the amount of recorded precipitation and inversely to the fraction of the time that the sensor resides in the measurement location.

In the fourth step, the objective functions to schedule the DSN are evaluated. Depending on the deployment strategy, one of the objective functions is evaluated for the new position of the sensor network. In case the value of the objective function is not optimal, the process will re-start again, otherwise the sensors will be deployed to their target positions and the problem will re-start in the following time step.

6.3 Objective functions and corresponding strategies for deployment

In this point, we evaluate strategies that are categorised in two approaches, based on model-based and model-free formulations. In general, model-based design aims to define the position of the dynamic sensors, which directly minimise the error of a hydrological model; in the context of this thesis, using lumped hydrological models. In this section we explore the potential use of the error of lumped hydrological models as a driver for defining the optimal sampling strategy by analysing the error propagation in hydrological models (6.3.1). In model-free formulations, the objective solely rely on information derived from the data itself. As previously discussed, these metrics will be based on the minimisation of the overall uncertainty of the precipitation volume, as discussed in Section 6.1, based on the findings of Chapter 5.

6.3.1 Can model-based objective functions be used for model-based optimisation of dynamic sensor networks?

One of the possibilities to guide the deployment of dynamic sensor networks is to reduce the error in rainfall-runoff models. Ideally, better observations will reduce the model error. For this purpose, it is necessary to understand the relationship between the inputs and output of the model, considering that hydrological processes are often non-Markovian. Additionally, it is required to establish a way to map from the model error into the inputs (inverse model), and therefore to the position of the DSN. Applications of inverse models to establish precipitation estimates from discharge have been proposed (Herrnegger et al. 2015, Volkmann 2011, Kunstmann et al. 2006).

The current approaches for estimating precipitation from discharge (inverse models), assume that the processes are Markovian (Herrnegger et al. 2015), and therefore, only a previous condition and a perturbation of the inputs is required to yield the next outputs and states. This assumption is valid as long as the model states converge close to the models of the forward model, implying that the effects of the precipitation variation are only immediately seen. In case the model is not Markovian, the model errors will accumulate over time.

As result, it will limit the use of the model error at the current time, rendering it unusable to determine the optimal network configuration in the previous step. Additionally, inverse models only provide information about the value of (average) precipitation that the model requires to adjust its error, but do not offer insights (and do not seem required at that point), of where sensors should be.

To understand the error propagation in a real case study, the Brue catchment is used and modelled with three different hydrological models: HBV96, Sugawara and linear reservoir. An analysis to precipitation perturbations is carried out for three different hydrological models. The analysis consists of comparing the difference in discharge estimates, by adding a perturbation of 1 mm of precipitation at each time step of a model run window and evaluating the difference along the time series.

If the perturbations on the discharge add up linearly, then the model is Markovian, and the effect of the perturbations should not affect the discharge estimations retrospectively. On the contrary, if the states of the model influence the precipitation estimates, the discharge at a given time step comes from different precipitation patterns, and therefore render the problem unsolvable.

The results for the HBV96 model (Figure 6.4) show that the perturbation in the precipitation time series has a long impact in the precipitation estimations, which largely spreads in time. The differences in discharge vary greatly, especially after high precipitation events, indicating that higher variations tend to decrease in time, but are conditioned to the initial conditions of the system. Besides, the magnitude of the error is directly linked with the evolution of the precipitation event, as errors which are induced in dry spells of the catchment are more significant in posterior steps.

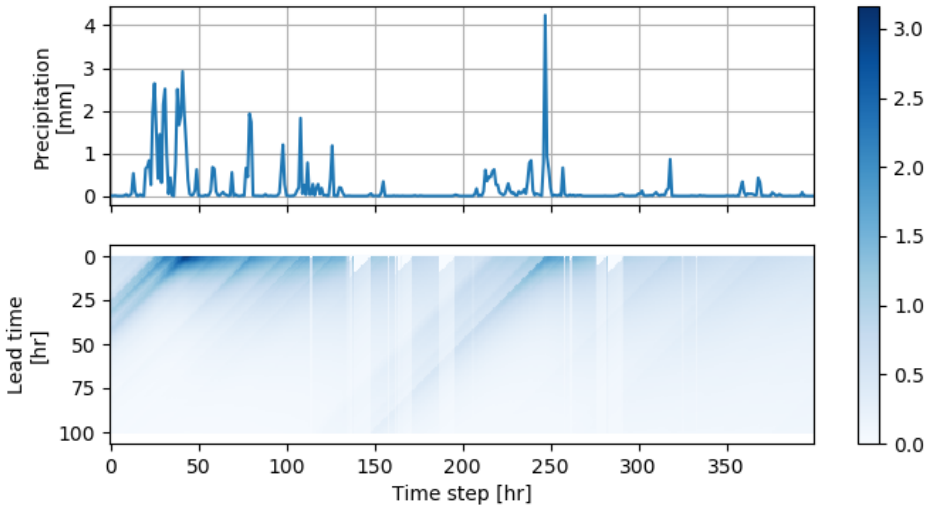

Figure 6.4 Propagation of precipitation errors in the HBV96 model. Scale bar shows the difference in discharge between original and perturbed model [m³/s]

The results of the Sugawara model (Figure 6.5) shows a different behaviour to the propagation of precipitation errors in the model. In this case, it is possible to observe a decreasing trend in the magnitude of the simulation error, which is propagated in time, depending on the preceding states of the model (especially upper tank) at the moment of the error propagation. This explains the lack of response of the model for the dry spell; as soon as the upper tank (see Section 2.4.1) has enough volume, the errors in the model increase significantly, but not in function of the discharge.

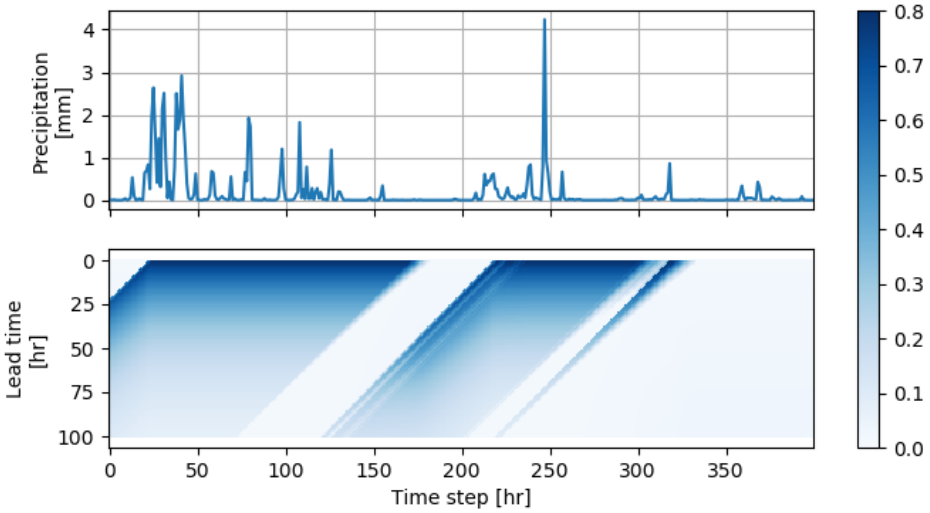

Figure 6.5 Propagation of precipitation errors in the Sugawara model. Scale bar shows the difference in discharge between original and perturbed model [m³/s]

In contrast with the HBV96 and Sugawara, the linear reservoir model (Figure 6.6) shows a monotonic response to the measurement errors in the precipitation estimates. In this figure a constant and decreasing error value occurs in discharge estimates, which are not conditioned by the dynamics of the discharge of precipitation in future steps. In this situation, it is possible to determine that both, the forward and inverse hydrological model are Markovian, and thus, only one step is required to go forward or backwards in time.

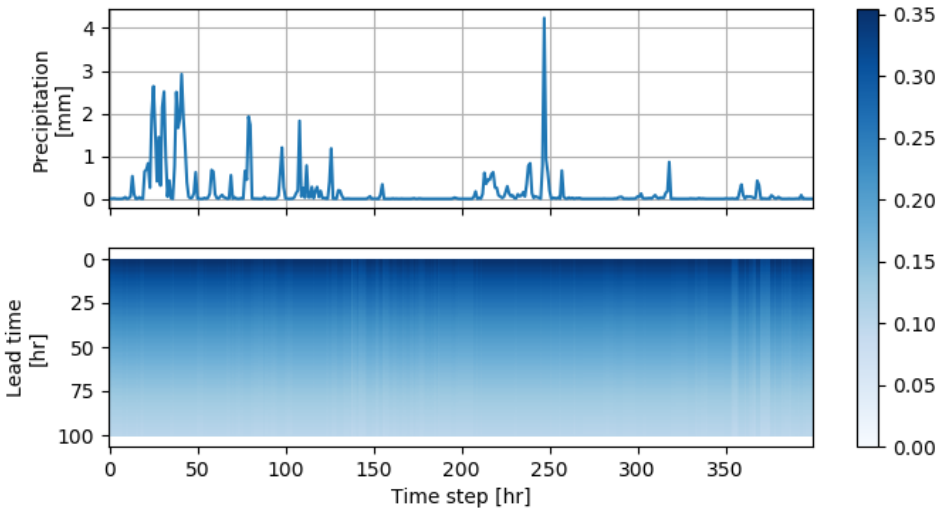

Figure 6.6 Propagation of precipitation errors in the linear reservoir model. Scale bar shows the difference in discharge between original and perturbed model [m³/s]

As a conclusion, it is not possible to assess the influence of the precipitation errors based on the last discharge measurement, using a hydrological model consisting of more than one tank. The conclusion is reached as there exist thresholds for the behaviour of the multi-tank system, which prevents the response surface of the model from being smooth, inducing larger errors, especially in quick response processes. Additionally, the response of any lumped hydrological model can only account for the errors in the overall areal precipitation error, but does not provide a logical framework to deploy dynamic sensor networks.

6.3.2 **Kriging Variance (KVP)**

One of the suggested objectives to design dynamic sensor networks is to minimise the uncertainty of the estimation in the precipitation volume. This objective function is equivalent to the minimisation of the Kriging variance in the design of static sensor networks, acknowledging that precipitation is not homogeneous in the catchment, but changes as the precipitation event develops.

This method can be understood as a generalisation of the minimisation of the Average Kriging Variance minimisation (Pardo-Igúzquiza 1998, Coulibaly et al. 2013, Chacon-Hurtado et al. 2017), without the assumption that the variance value is homogeneous in all the catchment. As such, the objective function is defined as the minimum of the overall volumetric uncertainty of the estimation at a given coverage (confidence) level (k), as:

$$\min: \int_{\Omega} p(u) * k\sigma(u) \qquad \textit{Equation 6.2}$$

where p is the precipitation at the location u, k is the confidence level, which represents the number of standard deviations which are used to compute the volumetric uncertainty, which varies from 0 (no coverage) to a value of approximately 6.0 (a coverage of approximately 99%), as the Kriging error is Gaussian. σ corresponds to the standard deviation of the simulation error

in the position *u*, calculated in the ordinary Kriging estimator. Finally, *Ω* represents the spatial domain of the catchment.

To produce a robust deployment strategy, the sensors should increase its measurement time in the target locations, to reduce its uncertainty. To this end, it is possible to trade optimal locations at a given step, to be in a better position for the next step, leading to a larger impact in the objective function in a time window. In other words, it is possible to allow the sensors to displace ahead of time to areas where observations are expected to be of higher importance. The problem is formulated in a time window (*w*), such that the objective function can be written as:

$$\min: \sum_{t=1}^{w} \int_{\Omega} p_t(u) * k\sigma_t(u) \qquad \textit{Equation 6.3}$$

6.3.3 **Non-stationary Kriging Variance (NKVP)**

Similarly to the previous method, the deployment of the dynamic sensors can be driven by the minimisation of the total precipitation volume uncertainty, now considering that the precipitation field is modelled as non-stationary. The formulation is basically the same as for KVP. However, the estimations of precipitation and error of the estimations are calculated using non-stationary estimates as discussed in Chapter 3:

$$\min: \int_{\Omega} P^*(u) * k\sigma^*(u) \qquad \textit{Equation 6.4}$$

where *P** is the precipitation at the location *u* estimated using a non-stationary approach (see Section 4.4.3). *k* is the confidence level, which represents the number of standard deviations which are used to compute the volume uncertainty, which varies from 0 (no coverage) to approximately 6, for a coverage of approximately 99% of the PDF, making clear Gaussianity assumptions. σ* corresponds to the standard deviation of the simulation error in the position u, calculated using the non-stationary Kriging estimator. *Ω* represents the spatial domain of the catchment.

Similarly to KVP, the problem can also be posed in a time-window, such that it is possible to trade measurements for preferential positions. Better position means that sensors can stay longer in the target locations, and therefore, reduce the uncertainty due to the partial observation of the precipitation. In this respect, the optimisation can be carried out in a time window (*w*), such that:

$$\min: \sum_{t=1}^{w} \int_{\Omega} p_t^*(u) * k\sigma_t^*(u) \qquad \textit{Equation 6.5}$$

6.3.4 **Multi-Model Discrepancy (MMD)**

Typically, precipitation models are data-driven, so several models can describe the process with similar accuracy. This is known as equifinality (Beven and Freer 2001), which occurs because the models are either statistical or mathematical approximations, parameterised with incomplete information, from noisy measurements, using likelihood metrics that may be biased. As consequence, there is not a single best model that is best in each condition to represent the phenomena, and therefore, an ensemble of equifinal models may be useful to provide insights regarding the spatial uncertainty in the precipitation field.

These equifinal models can be used to build ensembles of models which have similar explanatory capabilities about the precipitation field. Assuming that there is no superior model in the ensemble, it is possible to estimate the interpolation uncertainty, by measuring the divergence of the estimations.

Considering that the models are tied to observations, the measurement of the divergence of the ensemble is a metric of the lack of quality in the interpolation. This divergence between models can be directly associated with uncertainty in the spatial interpolation, which not only depends on the distance between measurements and interpolation targets, but also by the gradients between observations. The optimal location of dynamic sensors is a problem that can be formulated as the minimisation of the divergence of the equifinal model ensemble:

$$min: \frac{1}{m}\sum_{u=1}^{m}\sqrt{\frac{\sum_{i=1}^{E}\left(e_{u,i}-\overline{e_u}\right)^2}{E}} \qquad \textit{Equation 6.6}$$

Where E is the total number of ensembles, e is the ensemble i at location u and m is the total number of discrete interpolation targets in the catchment, used to construct the precipitation field. In the same manner, as with the other strategies, the problem can be posed in a time-window (w), such that is possible to trade measurement opportunities, for better positions in the overall time window. Therefore, the objective can be posed as:

$$\text{min: } \sum_{t=1}^{w}\frac{1}{m}\sum_{u=1}^{m}\sqrt{\frac{\sum_{i=1}^{E}\left(e_{u,i}-\overline{e_u}\right)^2}{E}} \qquad \textit{Equation 6.7}$$

In this particular case we use an ensemble of 9 different types of models. These models are: simple Kriging, squared simple Kriging, ordinary Kriging, squared ordinary Kriging, cubic and linear interpolation, radial basis functions, inverse distance weighting and nearest neighbours.

6.4 Experimental setup and solution of the optimisation problem

The experiments aim to explore the optimal deployment of dynamic sensors under different time-windows and different artificial perturbations in the baseline precipitation field. Additionally, each strategy is tested for two different precipitation events in the Brue, and

Bacchiglione case studies, while KVP and MMD are tested in the Doncaster case study, due to the limited size of the baseline network (3 sensors) to make adequate estimations of non-stationary variograms.

To implement the algorithm shown in Figure 6.3, several assumptions have been made. First, the threshold for the deployment of dynamic sensors is set at 1.0 mm/hr, using the data from the static sensor network. Second, the sensors return to their corresponding base as fast as possible. Third, the dynamic sensors do not acquire data while returning to its base position. Fourth, we assume a sensor velocity of 20 Km/h for Brue and Bacchiglione, and 30 Km/h for Don. More realistic definitions of the velocity of the sensors may be re-defined in subsequent studies.

The time window determines how the optimisation problem is posed. As such, each additional step in the window generates a new set of sensor positions in time. Consequently, the dimensions of the optimisation problem grow proportionally with the size of the window. As part of the experiment, the problem was run in batches of equal window size, for 1, 3 and 6 hours. It has to be noted that the optimisation problem is not re-started in each time step, but a new problem is solved at the end of each time window.

The base of the dynamic sensor network is defined to account for different conditions regarding the scheduling. In the Bacchiglione case study, the dynamic sensors were homogeneously distributed inside the catchment, with special interest towards ungauged areas. In the Brue catchment, the sensors were (on purpose) located close to each other, towards the North of the catchment, opening up a relatively large under-gauged area in the East of the catchment. In the Don River catchment, the base position of the sensor network was located in large under gauged areas, mostly outside of the convex hull of the limited static sensor network. Table 6.1 presents the base positions of each of the dynamic sensors in each of the case study. The colour in the top of the table corresponds to the colour of the sensors in the subsequent figures.

Table 6.1 Base position of the dynamic sensors in each case study (column colours for identification purposes in subsequent figures

	DS 1		DS 2		DS 3	
	N [Km]	E [Km]	N [Km]	E [Km]	N [Km]	E [Km]
Bacchiglione	1685.0	5065.0	1695.0	5061.0	1690.0	5045.0
Brue	367.7	140.3	365.2	142.1	-	-
Don	590.0	5930.0	605.0	5905.0	610.0	5920.0

The experiments are set in two sets, depending if artificial perturbations are added or not to the deployment strategy. In this direction, we describe several fields which are going to be used in setting up the experiments as shown in Figure 6.7. The baseline field corresponds to the field built with all available data in the case study, represented by the four static (black) sensors. The perturbation, is a spatially random auto-correlated field that affect the precipitation field. The sampling field is considered as "true", as all the observations during the experiments will be taken from here. Finally, the sampled field corresponds to the field that is built using the

observations coming from the sampling field, either being taken by static (grey) or dynamic sensors (orange).

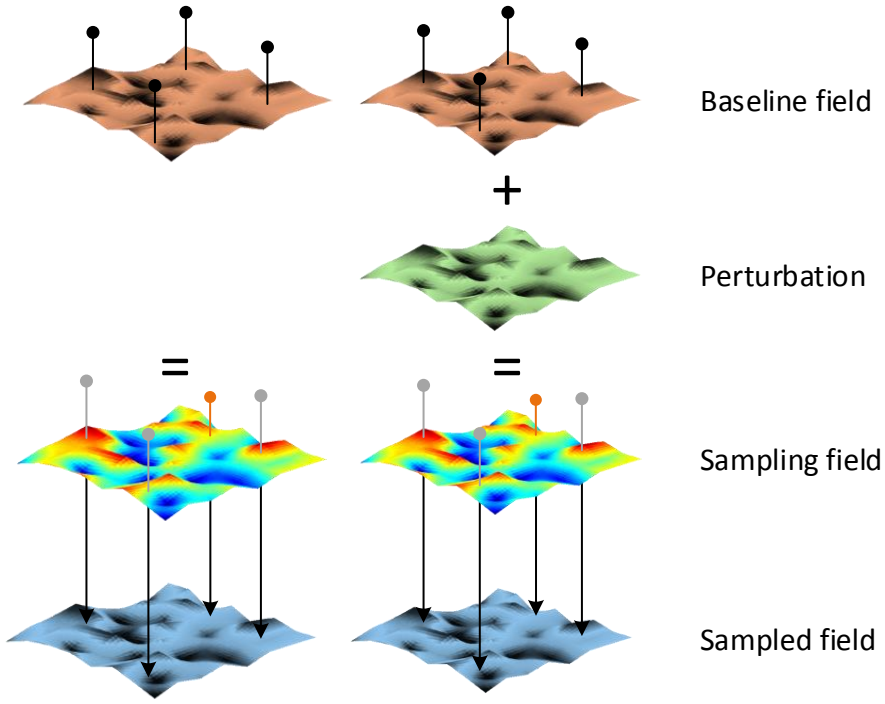

Figure 6.7 Schematisation of the baseline, perturbation, sampling and sampled precipitation fields

The sampled field is built the data coming from all static and dynamic sensors in Bacchiglione and Don, but uses data coming from a reduced static network for Brue. This decision is made due to the high density of static sensors in the area, which is far from any practical application, rendering the deployment of dynamic sensors unjustified. Therefore, a reduced static sensor network was selected for this case study, such that observation deficiencies occur in the East of the catchment. The final configuration of the static sensor network is presented in Figure 6.8.

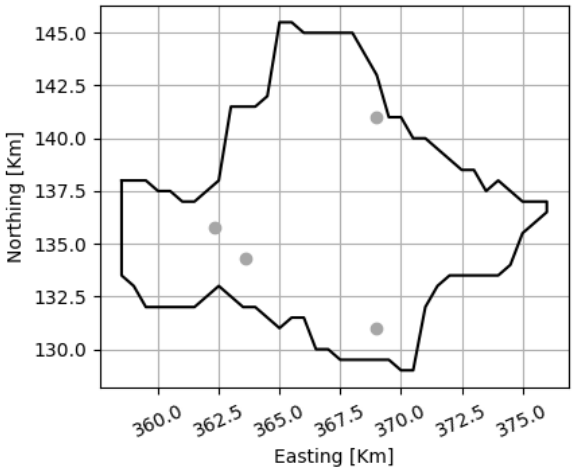

Figure 6.8 Reduced static sensor network in the Brue catchment

The first set of experiments consists in using the baseline precipitation field as the sampling field. The experimental setup for the scheduling of sensor networks in windows of 1, 3 and 6

hours, for 2 different precipitation events, are summarised in Table 6.2, where the blue cells represent the experiments carried out, and the grey cells the experiments which were not.

Table 6.2 Overview of the experimental setup for the deployment of dynamic sensors

Case study	Methods		
	KVP	NKVP	MMD
Bacchiglione			
Brue			
Don			

The second set of experiments consist in systematically modifying the baseline precipitation by introducing a spatially auto-correlated perturbation, as described in Annex 3. These experiments were carried out using different deployment strategies for a window size of 3 hours, in the precipitation event 1 only. The summary of the experiments is shown in Table 6.3, where blue indicates which methods were used in which case study.

Table 6.3 Overview of the experimental setup for experiments for the deployment of dynamic sensors using different perturbation scenarios

Case study	Methods		
	KVP	**NKVP**	**MMD**
Bacchiglione			
Brue			
Don			

The amplitude of the perturbation is set to 0.5 and 0.8 times the stationary variance for each case study. The fluctuation scale is set to 10 Km for short scale and; 20 Km for Brue and 30 Km for Bacchiglione and Don for long scale. These experiments are summarised in Table 6.4, and its parameterisation in Table 6.5.

Table 6.4 Perturbation scenarios classification in experiment set 2

	Fluctuation scale	
Amplitude	**Short**	**Long**
Mid	Ex1	Ex2
High	Ex3	Ex4

Table 6.5 Parameterisation of the perturbation for each of the scenarios to be tested in the case studies in experiment set 2

Case study	**Perturbation specification**			
	Ex1	**Ex2**	**Ex3**	**Ex4**
Bacchiglione	a = 0.5, f=10	-	-	a = 0.8, f=30
Brue	a = 0.5, f=10	a = 0.5, f=20	a = 0.8, f=10	-
Don	a = 0.5, f=10	a = 0.5, f=30	a = 0.8, f=10	-

6.5 Results and discussion

6.5.1 Scheduling of dynamic sensors using KVP

The results of scheduling the DSN using the KVP deployment strategy for window-size of 1, 3 and 6 hours are presented for the case study of Bacchiglione, Brue and Don River in the following sections. Additionally, the problem is solved for the different perturbation scenarios, as defined in Table 6.5. In this chapter, the path of each dynamic sensor is represented by a solid line with a different colour.

Bacchiglione

The results for a window size of 1 hour for precipitation events 1 and 2 in the Bacchiglione catchment are presented in Figure 6.9. The results show that the sensors do not go far from their base, with a frequent return of the sensors to their base position. Additionally, it is possible to observe that the sensors tend to stay in the vicinity of its base position. However, in the second event, DS_3 (green) overtakes at some point the position of DS_2 (orange), showing that the sensors are working in a cooperative manner when being scheduled.

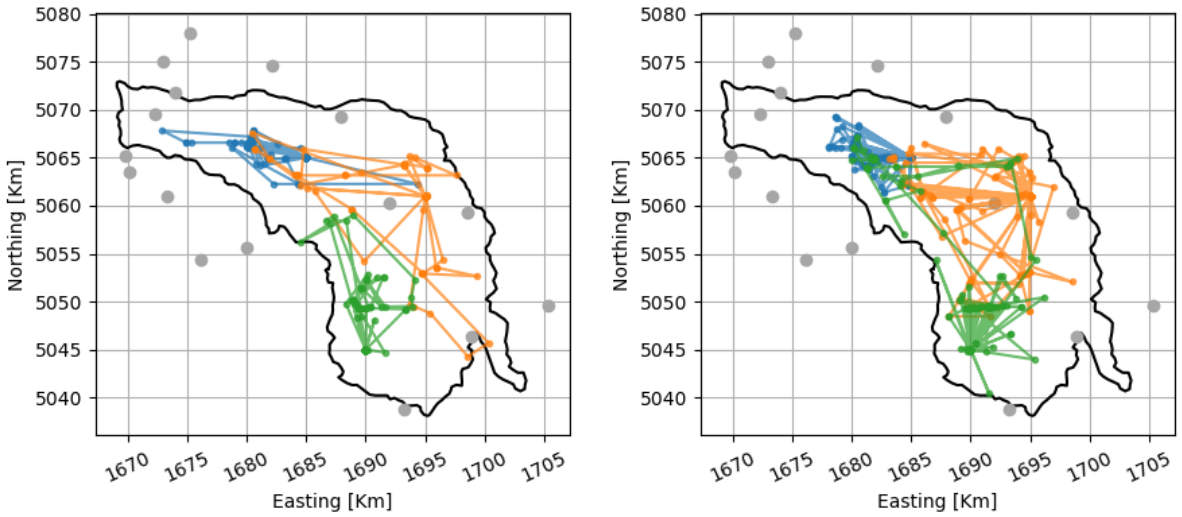

Figure 6.9 Scheduling of dynamic sensors using KVP strategy in Bacchiglione River for precipitation event 1 (left) and 2 (right), using one hour window size

For the with 3h window-size, it is possible to see a shifting from the original areas of influence of the sensors (Figure 6.10). In the first precipitation event, the sensors tend to move SE, towards areas with a lower density of static networks, which goes in contradiction with the results obtained for the deployment using a shorter time window. A similar behaviour is exposed in the second event, as the sensors enlarge its area of influence, and it is possible to see that DS_2 (orange), goes far in the direction NW, even in the presence of the DS_1 (blue), indicating that the deployment included several steps in order to reach such location. Additionally, the DS_3 (green) has a much more active role covering moving around the South of the catchment, especially towards the mountainous area located in the South-East of the catchment.

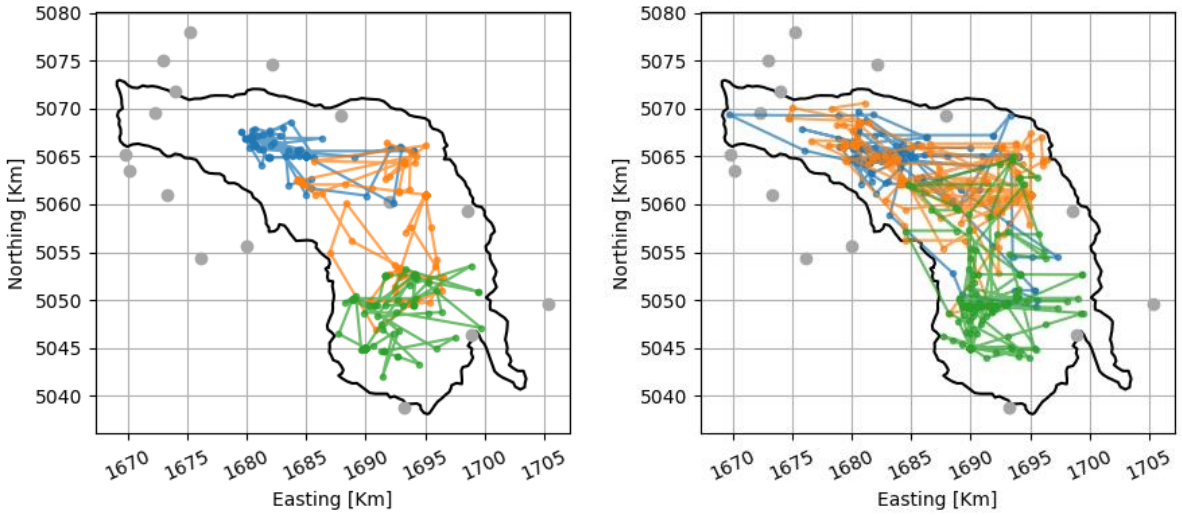

Figure 6.10 KVP deployment results in Bacchiglione for precipitation event 1 (left) and 2 (right), using three hours window size

Finally, the deployment of the dynamic sensors in a time-window of 6 hours, reveals a large overlap among sensors, in both events (Figure 6.11). One of the reasons is attributed to a more frequent deployment of the dynamic sensors, as well as a more relaxed limitation with respect to the displacement capabilities of the sensors. As it was previously shown, one of the largest uncertainty sources in the use of dynamic sensors is related to the fraction of the time that the sensor is able to remain in the same place, to carry out the measurement. As consequence, in a larger time-window, the sensors are deployed further, as the displacement limit increases proportionally with the time ahead that the sensor deployment is planned. In practice, this yields to more sparse deployments of the dynamic sensors, increasing the reach of the network.

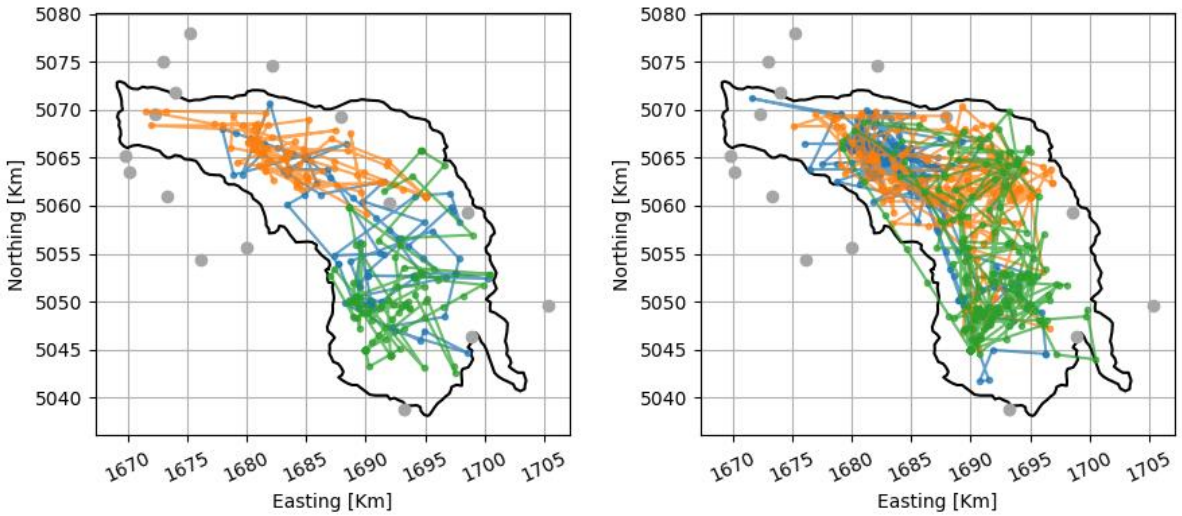

Figure 6.11 KVP deployment results in Bacchiglione for precipitation event 1 (left) and 2 (right), using six hours window size

Brue

The results for the deployment of the sensor networks in the Brue catchment using a time-window of 1 hour are presented in Figure 6.12. The results show the consistent re-visit of the

base for each of the sensors in both events. The reasons behind are the size of the catchment, which makes it possible to travel between two points within the catchment possible in one step, and also indicating intermittent precipitation, especially in event 1. On the contrary, the deployment of sensors for the second precipitation event seems to find a preferential area for the deployment, towards the Centre-East side of the catchment, which lies between the two most eastern sensors in the catchment. In the second event, there is also a constant re-visit to the base point.

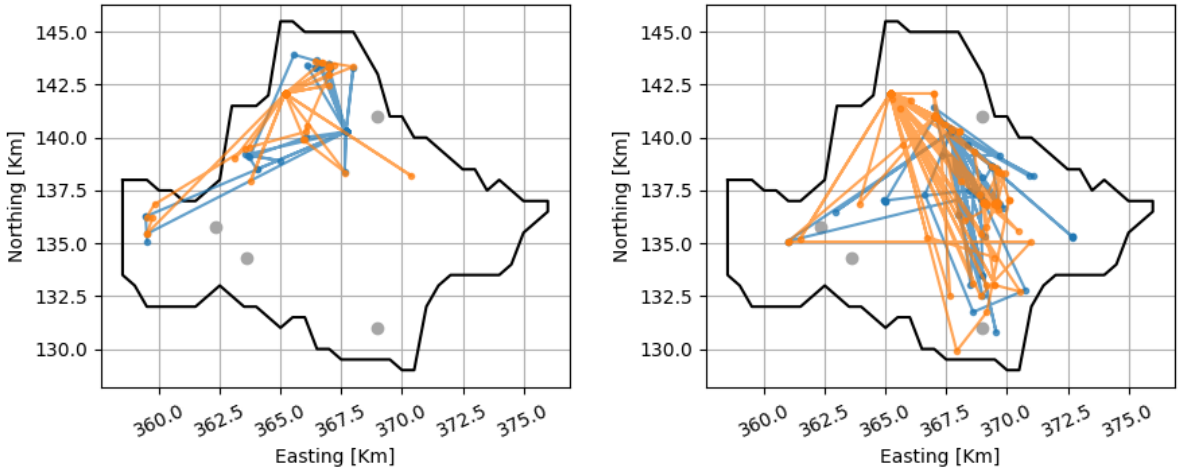

Figure 6.12 KVP deployment results in Brue for precipitation event 1 (left) and 2 (right), using one hour window size

When the window size increases to 3 hours (Figure 6.13), the results seem to diverge from the previous. In this case, the deployment of the sensors is more consistent. However, due to the size of the catchment, and the proximity of the base points of the two dynamic sensors, there is no clustering of the position of the dynamic sensors, and thus, no preferential location for none of them. As an example, it can be seen that in the first precipitation event, the DS_1 (blue) sensor, deploys towards the West end of the catchment, as the DS_2 (orange) deploys at the farthest eastern position.

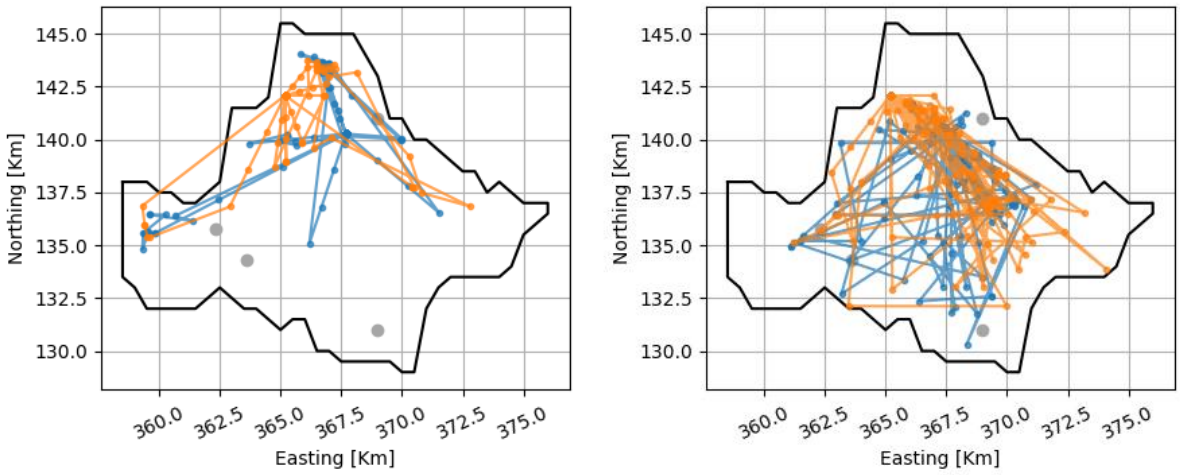

Figure 6.13 KVP deployment results in Brue for precipitation event 1 (left) and 2 (right), using three hours window size

In the 6-hour time-window interval, it is possible to observe that both sensors travel far from its original location. Also, it is possible to observe how returning to the base point is less frequent, as consequence of longer plan times. The reason for this behaviour can be attributed to the penalty in the objective function by arriving late to the scheduled optimal measurement point. As consequence, there is a higher uncertainty in the measurements due to the partial observation of the precipitation event in the target location. Therefore, it is possible to appreciate short displacements, preceded by long jumps.

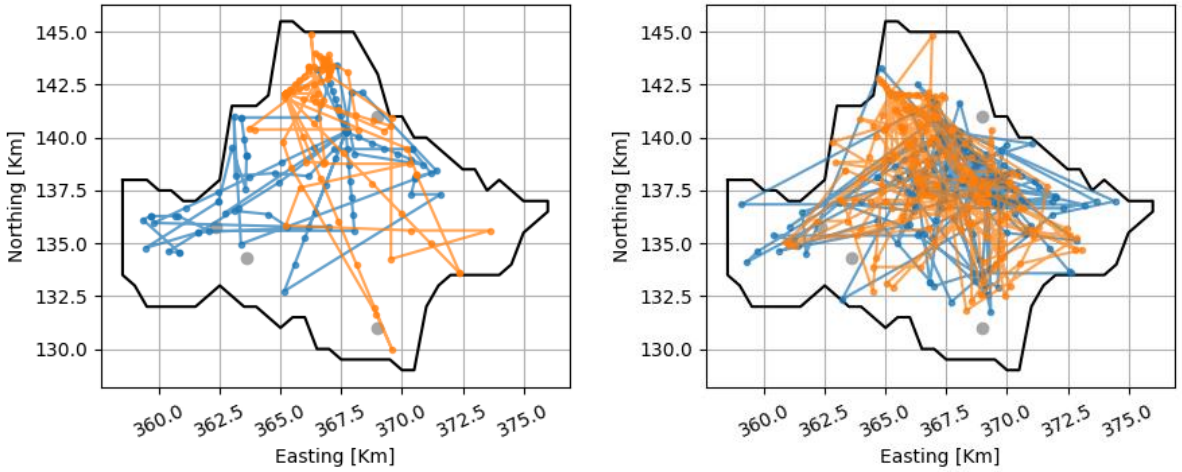

Figure 6.14 KVP deployment results in Brue for precipitation event 1 (left) and 2 (right), using six hours window size

Don

The results for the scheduling of dynamic sensors using KVP in the Don River catchment for a window size of 1 hour are presented in Figure 6.15. Due to the size of the catchment, it is possible to observe that the sensors are heavily constrained by the displacement capability, and the penalty on the objective function, due to the partial observation of the precipitation event. Consequently, the deployment of the sensors occurs only in the vicinity of the base position, and thus, there is little interaction among sensors. As result, there are no major differences in the deployment of the dynamic sensors between the two events.

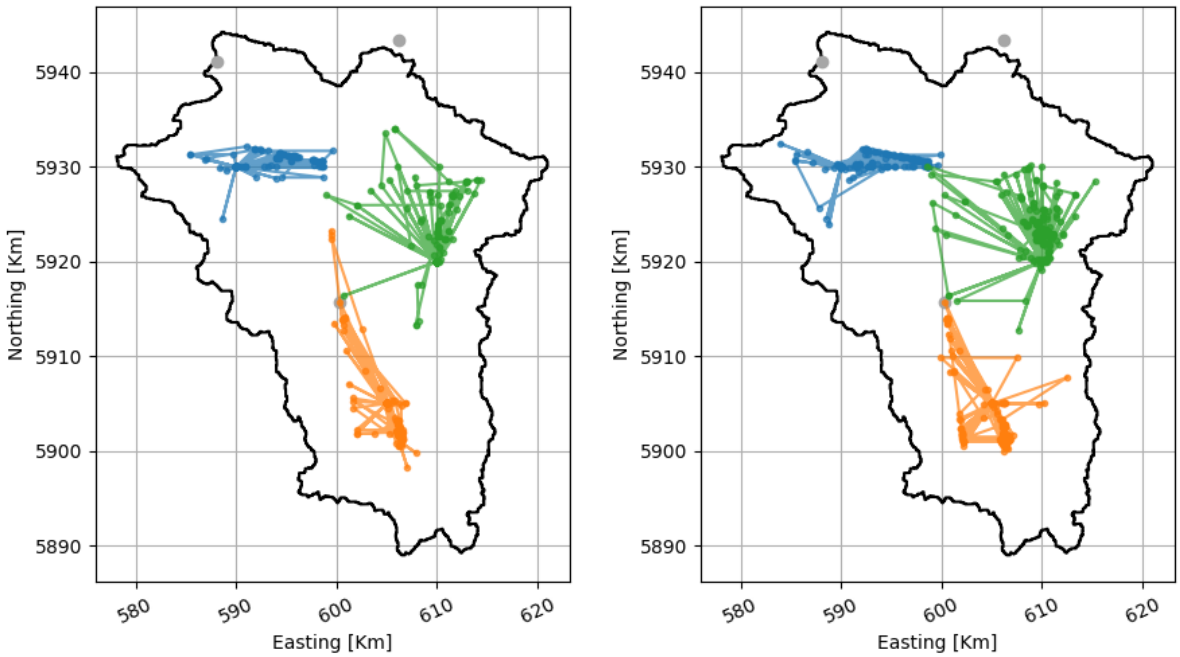

Figure 6.15 KVP deployment results in Doncaster for precipitation event 1 (left) and 2 (right), using one hour window size

When the time-window for the deployment increases from 1 to 3 hours, it is possible to observe a stronger interaction among dynamic sensors (Figure 6.16), especially between the blue and green sensors, which are the closest. The increase in the time-window in solving the optimal deployment problem makes possible to increase the reach of the network, and therefore, boost the area of influence of the dynamic sensors. However, it is possible to observe that clusters are mostly maintained, as eventually, sensors rotate around its base position.

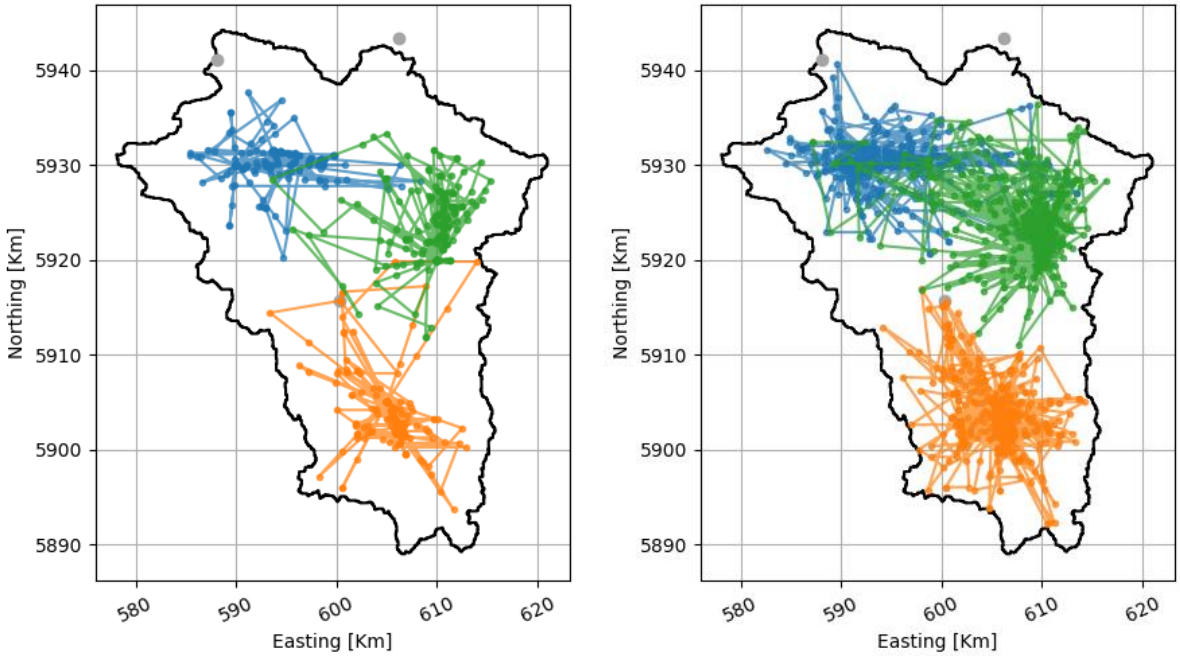

Figure 6.16 KVP deployment results in Doncaster for precipitation event 1 (left) and 2 (right), using three hours window size

When the time-window of the deployment problem increases from three to six hours (Figure 6.17), the deployment of the DSN seems to follow the same trends as previously. As in the previous time-window, it is possible to observe that the deployment of the sensors revolve around their base positions generating clusters, and rarely distant sensors overlap. It is possible to see that during these precipitation events, the orange and blue sensors get near to the base of each other, whereas the green sensor does, especially towards the blue cluster, indicating that there seem to be some parts dominated for each sensor, which may suggest that is possible to use soft constraints in the deployment of the dynamic sensors.

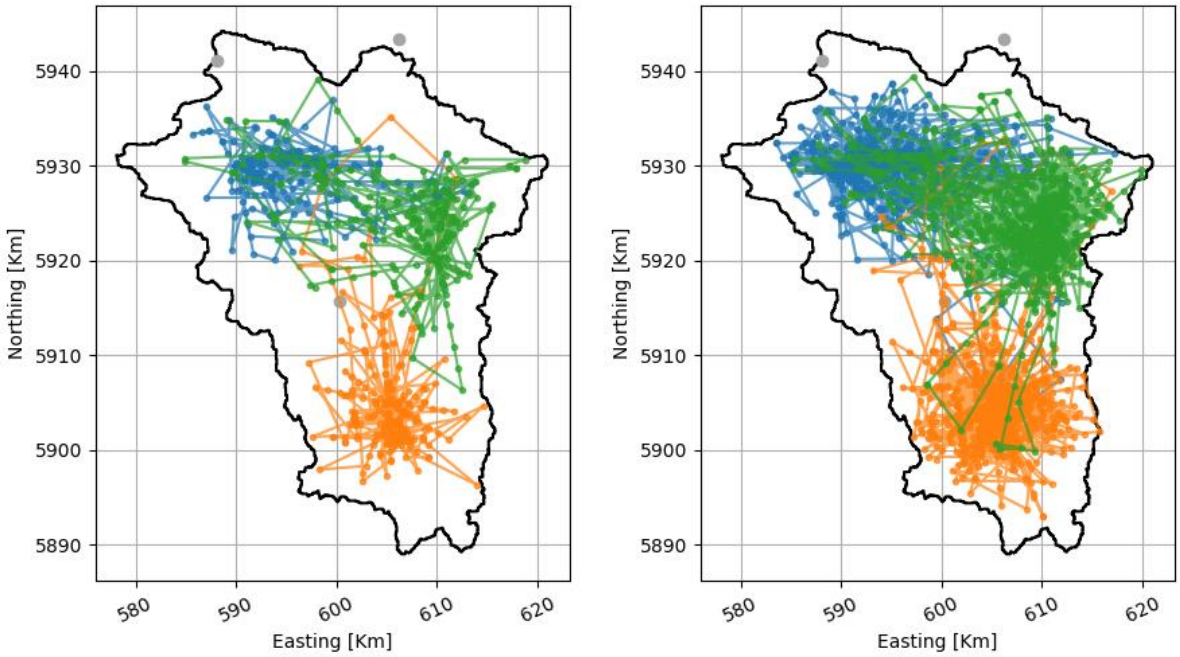

Figure 6.17 KVP deployment results in Doncaster for precipitation event 1 (left) and 2 (right), using six hours window size

6.5.2 **Scheduling of dynamic sensors using NKVP**

Bacchiglione

The scheduling of dynamic sensors using the NKVP strategy is carried out in the Bacchiglione and Brue catchments. Don River catchment is left out, because of the insufficient amount of baseline data to generate informative non-stationary variograms.

The results for the application of the NKVP to deploy the dynamic precipitation sensors using a time-window of one hour in for two precipitation events in the Bacchiglione catchment is presented in Figure 6.18. The results indicate a strong deployment of the sensors to remain in the areas far from the current monitoring network. Also, it is possible to observe that even for a single hour time-window, the deployment of the sensors is considerable. In this deployment scenario, it is possible to observe that sensors tend to revolve around its base positions, but with significant interactions among them.

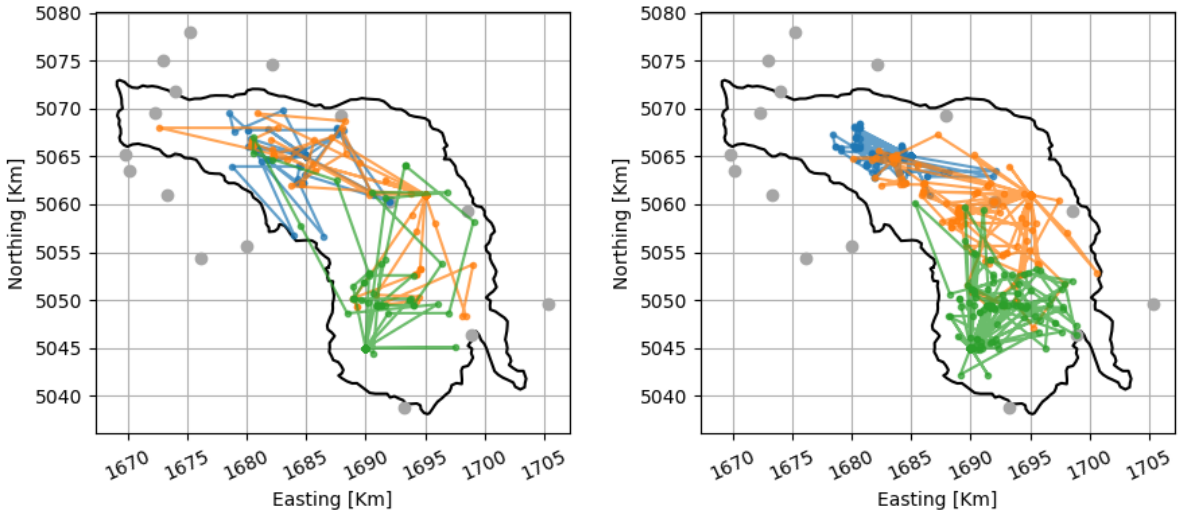

Figure 6.18 NKVP deployment results in Bacchiglione for precipitation event 1 (left) and 2 (right), using one hour window size

The results of the deployment in a time-window of 3 hours are presented in Figure 6.19. The results show that seems not to be a clustering of the scheduling of the dynamic sensors, as they are freely roaming through the catchment in both precipitation events. In a part of the events, it is possible to see that the sensor assigned to the most Southern base (DS_3, green), eventually goes past the most Northern base (DS_1, blue) in the first precipitation event. After the movement of the sensor is completed in this location, it finds the shortest route to return to its base, explaining the stop of the sensor in a point outside of the catchment, and as discussed, no measurements are being taken by the dynamic sensor in such conditions.

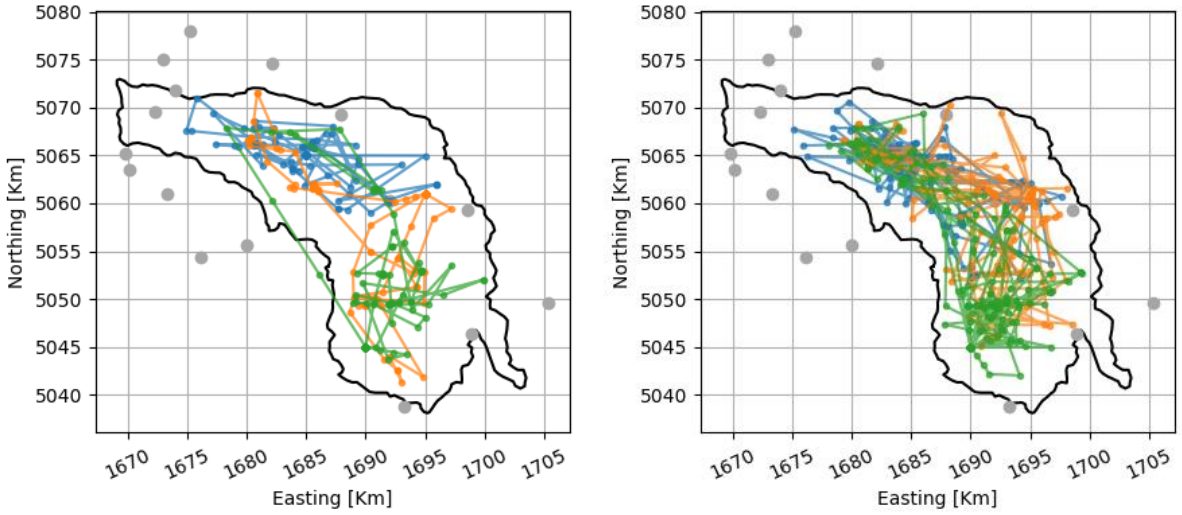

Figure 6.19 NKVP deployment results in Bacchiglione for precipitation event 1 (left) and 2 (right), using three hours window size

The 6-hour time-window deployment using the NKVP strategy (Figure 6.20), reveals that the influence clusters of the dynamic sensors are almost none, as the sensors do not seem to cluster towards particular areas. This can be understood that the deployment of the sensors responds to the precipitation dynamics, beyond the conditions forced by outside factors, such as rules for the return to base. Additionally, it is possible to assess that the interaction among sensors shows

a cooperative behaviour among them in the search for the optimal configuration of the whole sensor network at each time step.

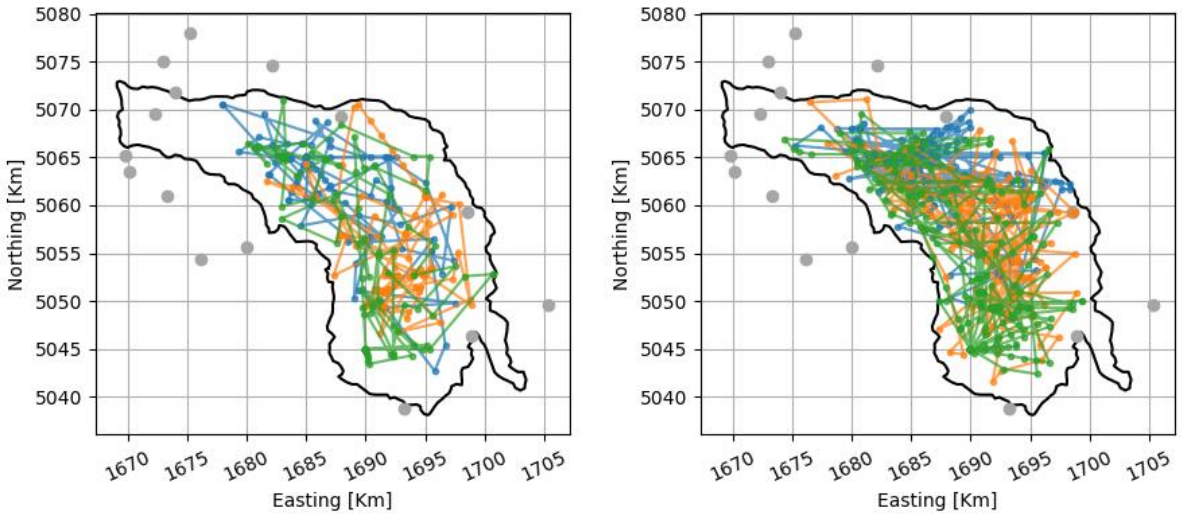

Figure 6.20 NKVP deployment results in Bacchiglione for precipitation event 1 (left) and 2 (right), using six hours window size

Brue

The results for the case of Brue are fundamentally different with respect to the results obtained for the Bacchiglione catchment. For the Brue catchment, it is possible to observe a tendency in the deployment of the dynamic sensors, using a one hour time-window (Figure 6.21), to be clustered towards the Centre-East of the catchment in the two precipitation events. This area can be seen as a potential target for localising sensors, due to the relatively low density of sensors in comparison with the rest of the catchment, purposely defined in the selection of the reduced sensor network for this experiment.

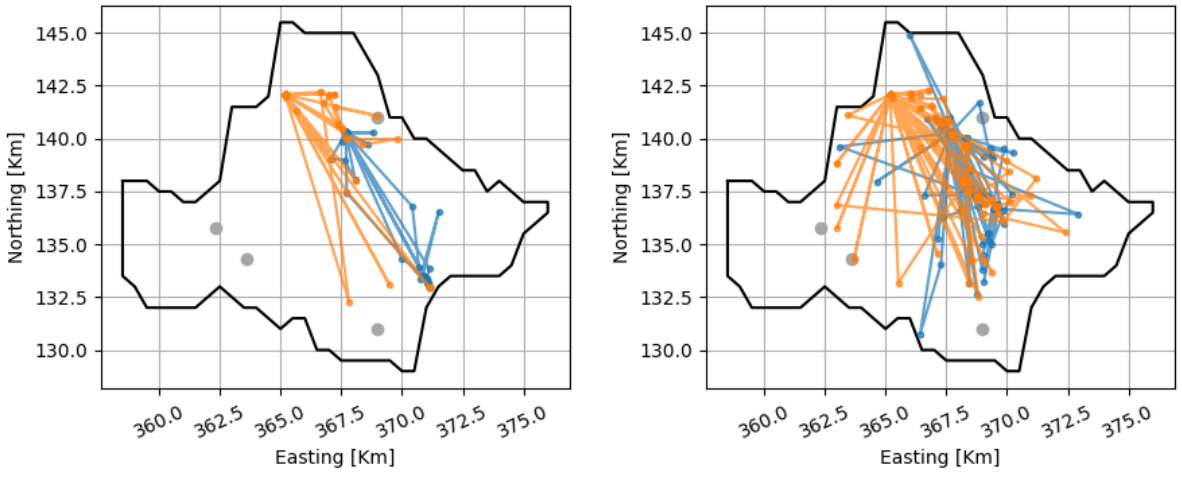

Figure 6.21 NKVP deployment results in Brue for precipitation event 1 (left) and 2 (right), using one hour window size

The results of using a time-window of 3 hours for scheduling the dynamic sensors are presented in Figure 6.22. The results show that indeed there is still a tendency on positioning the dynamic sensors towards the Centre-East are of the catchment, especially evident in the first event.

However, the second event reveals a more freely relocation of the sensors around the catchment, from which are of especial interest, the deployment of sensors towards the West end of the catchment. In this area, the density of sensors is maximum, but the lack of precipitation in other areas defines this place as optimal in this context.

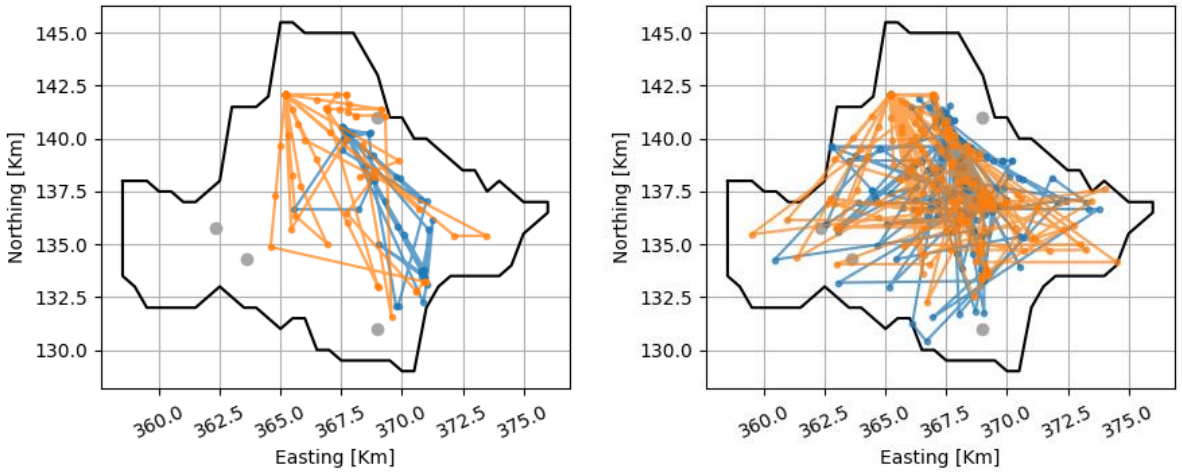

Figure 6.22 NKVP deployment results in Brue for precipitation event 1 (left) and 2 (right), using three hours window size

The results for the 6-hour time-window deployment of the dynamic sensors is presented in Figure 6.23. The results in the position of the sensors slightly differ from the previous case, with the condition that the reach of the sensors is increased. These results can be explained by the fact that in longer time windows, the sensors can be closer to the optimal point before the point becomes optimal, thus reducing the uncertainty associated with the partial recording of the precipitation, which is exponentially proportional to the travel distance. Additionally, sensors travel relatively further than in smaller time-windows, and therefore, return to the base position less often.

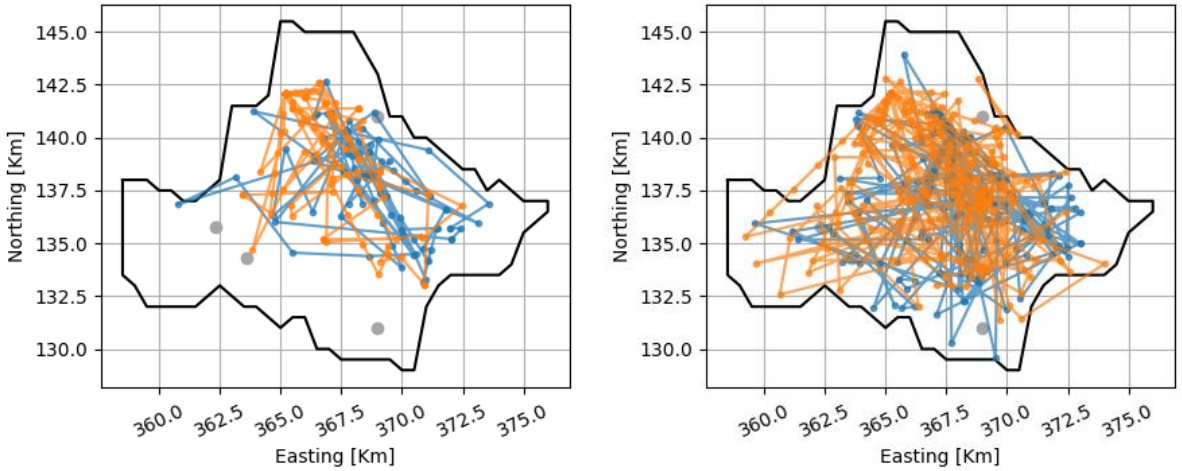

Figure 6.23 NKVP deployment results in Brue for precipitation event 1 (left) and 2 (right), using six hours window size

The experimental results for the 3-hour time windows suggest that the base position of the sensors can be improved. As discussed, the problem was purposely posed so that there are evident flaws in the design of the static sensor network, as well as the location of the base

position of the dynamic sensors. The results show a tendency of the dynamic sensors to relocate themselves to the Centre-East area of the catchment, indicating that this area may be of interest to locate the base of the dynamic sensors, thus reducing the displacement of the sensors. The reduction in the displacement distance has an effect on the overall cost of deployment of the sensors, as well as it reduces the uncertainty due to a partial recording of the precipitation event.

6.5.3 **Scheduling of dynamic sensor networks using MMD**

Bacchiglione

The results for the 1-hour time-window for the Bacchiglione case study are presented in Figure 6.24. It is possible to observe how the sensors are solely scheduled around its base position, without a particular preferential target around the catchment. It is possible to observe that the DS_3 (green) sensor prefers locations towards the south of its base position. Additionally, it is important to notice that the position of the sensors tends to drift away from the static sensors, which may reduce the search space in the optimal scheduling strategy.

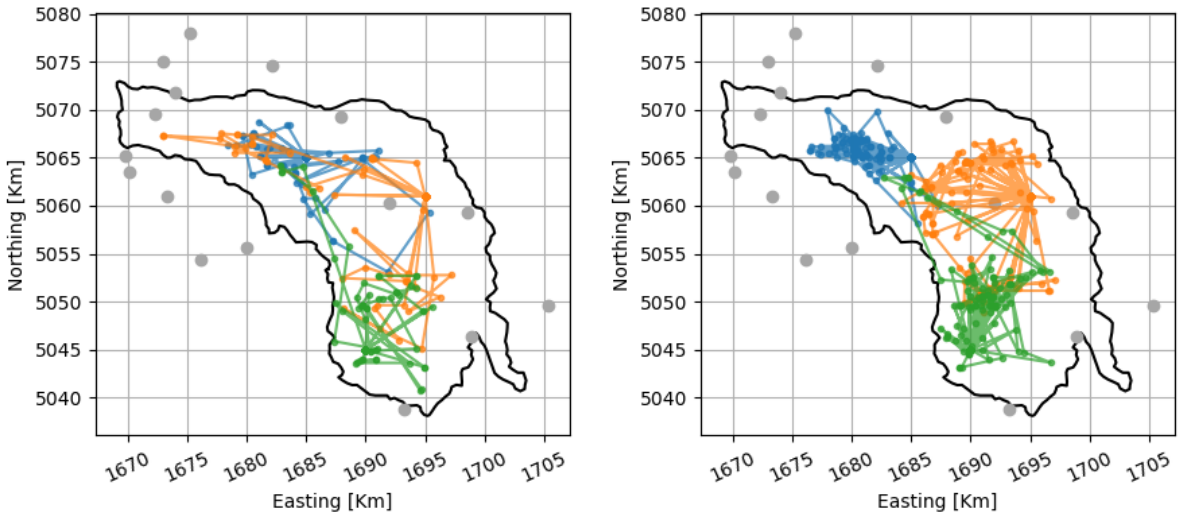

Figure 6.24 MMD deployment results in Bacchiglione for precipitation event 1 (left) and 2 (right), using one hour window size

The two case studies show a different behaviour in the deployment of the sensors in the 3-hour time-window deployment (Figure 6.25). In the first precipitation, the DS_3 (green) and DS_1 (blue) sensors remain in the vicinity of its base position, while DS_2 (orange) tends to freely roam along the catchment. In the second event, it is possible to observe the DS_3 sensor taking a more active role. As said before, DS_3 never scheduled towards the south of its position in the first precipitation event, while only a few times in the second event. In both events, the dynamic sensors are consistently deployed towards the large areas between sensors in the centre and North part of the catchment.

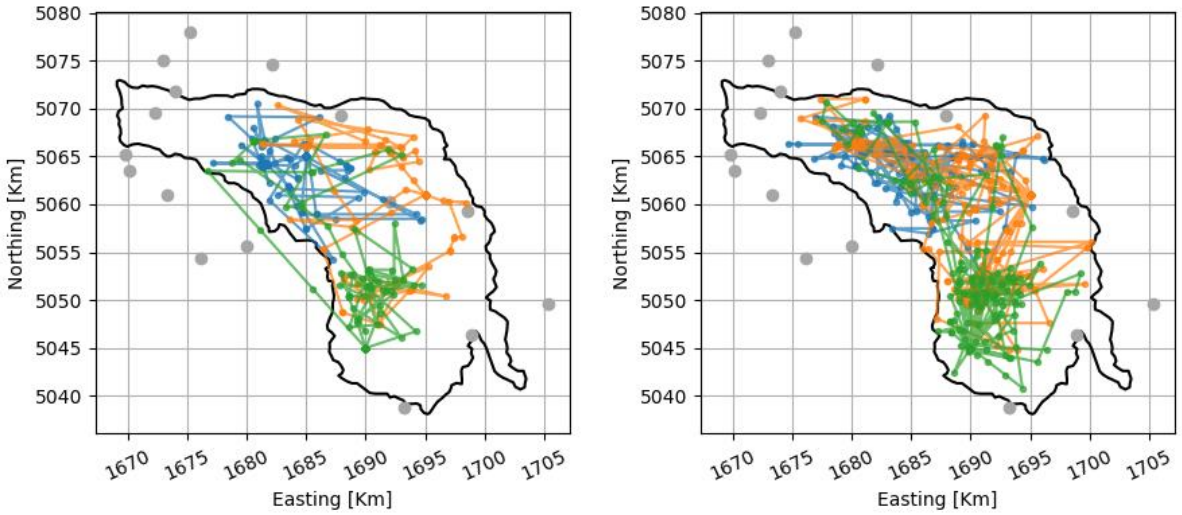

Figure 6.25 MMD deployment results in Bacchiglione for precipitation event 1 (left) and 2 (right), using three hours window size

Following the same trend in the deployment as the other techniques, and case studies, the deployment of sensors in the 6-hour time-window (Figure 6.26), driving the dynamic sensors from the vicinity of its base position. It is interesting to observe also how the positioning of the dynamic sensors gets closer to the static sensors in comparison with shorter time-windows. This indicates that it may be used as non-optimal positions to allow the sensors in posterior steps to be in a more adequate position, minimising the total discrepancy in the whole time-window. Also it is necessary to observe that there is little deployment of the sensors towards the South end of the catchment, in contrast with shorter time-windows, indicating that the optimal position of the sensors may be located away from this area, and that only it is measured in short time-windows, as it is not possible to effectively reach with the current displacement constraints.

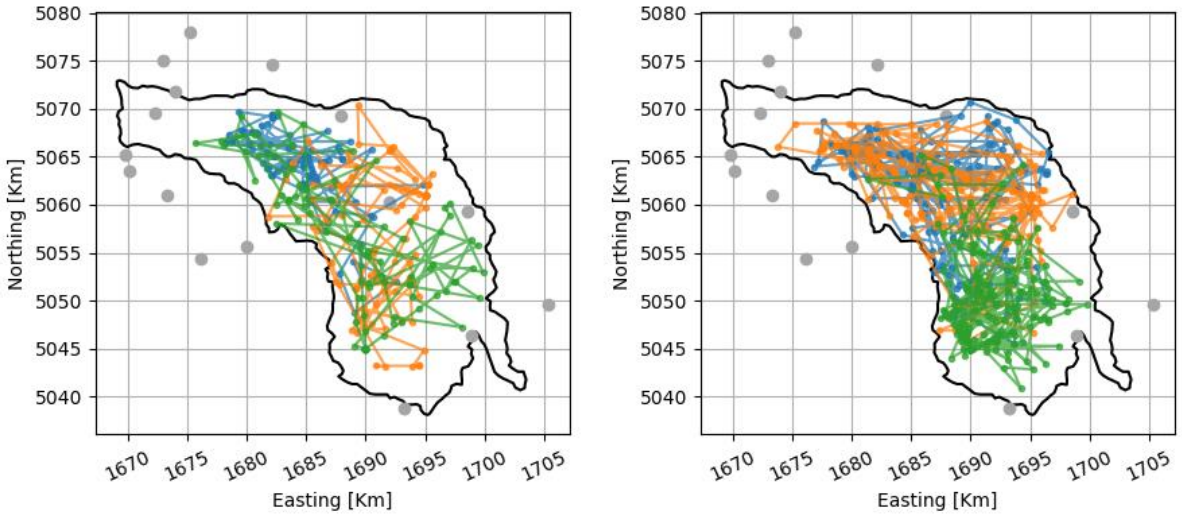

Figure 6.26 MMD deployment results in Bacchiglione for precipitation event 1 (left) and 2 (right), using six hours window size

Brue

The results for the deployment of dynamic sensor networks in the Brue catchment using the MMD approach in a 1-hour time-window are presented in Figure 6.27. For this case, it is possible to observe how the sensors tend to be deployed towards the North and East ends of the catchments, which corresponds to the areas with the less sensor coverage. In the cases where the sensors are deployed towards the West of the catchment, they tend to take extreme positions. However, the deployment towards these areas is scarce in comparison with the deployment towards the Centre and East.

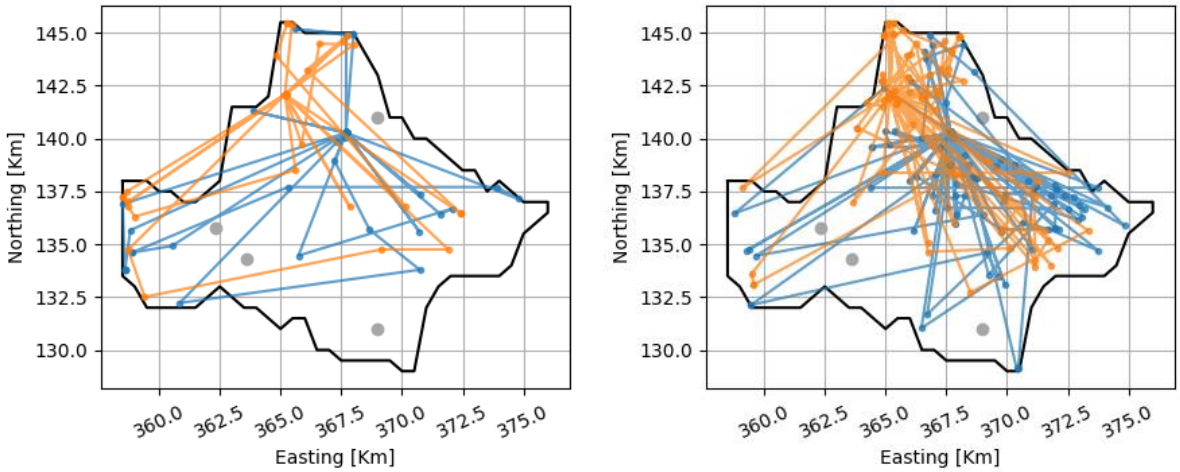

Figure 6.27 MMD deployment results in Brue for precipitation event 1 (left) and 2 (right), using one hour window size

The results for the deployment of sensors on a 3-hour time-window using the MMD methods are presented in Figure 6.28. The results show the deployment of the sensors in a more regular fashion in comparison with the one hour time window. It is also of interest to observe how areas that were previously of lesser interest in the deployment (such as the Centre-South), become more active, in scenarios with longer time-window. The reason for this may be justified by the use of this location as trampoline positions so that the overall discrepancy in the time window is minimised.

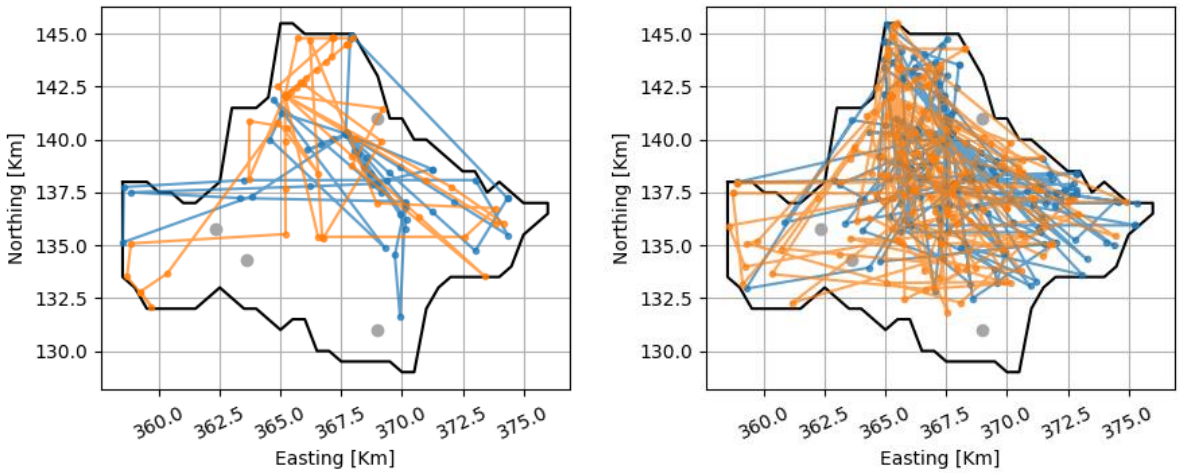

Figure 6.28 MMD deployment results in Brue for precipitation event 1 (left) and 2 (right), using three hours window size

To complete the experiment, Figure 6.29 shows the deployment of the dynamic sensors in the Brue catchment in a 6-hour time-window using the MMD method. In this case, as similarly to the other deployment methods, the reach of the sensor network has increased considerably, blurring the areas of special interest. However, it is possible to observe (especially in the first event) that there still exists a trend for deploying the sensors towards the Centre-East of the catchment.

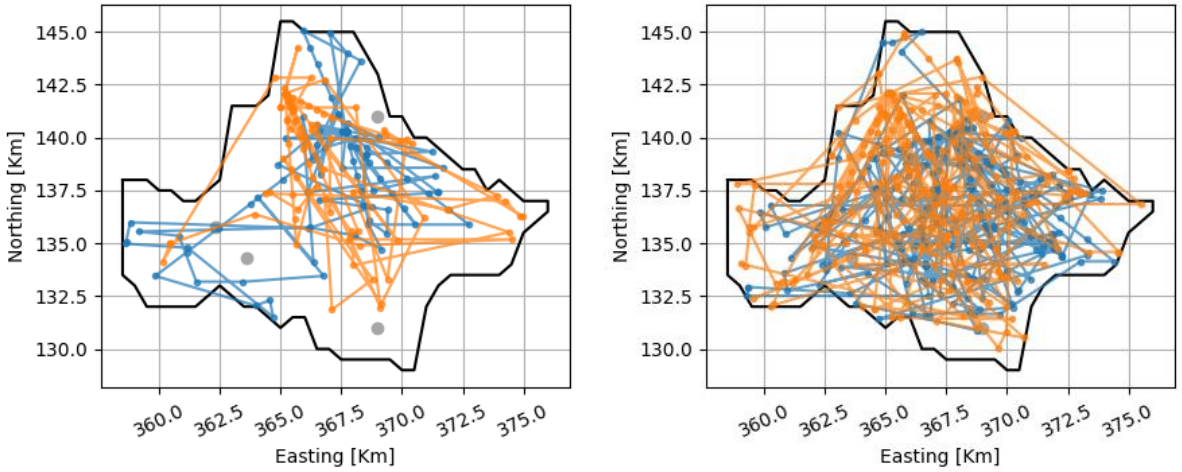

Figure 6.29 MMD deployment results in Brue for precipitation event 1 (left) and 2 (right), using six hours window size

Don

The results for the deployment of the dynamic sensors in the Don River catchment using a 1-hour time-window are presented in Figure 6.30. As discussed in previous stages, the characteristics of the Don River catchment is that is the largest case study in extension, and at the same time, has the lower amount of static sensors to guide the deployment of the dynamic sensors. As consequence, it is possible that the static sensor networks lack the proper coverage. As consequence, it is possible to observe, that the sensors tend to stay in their influence areas, much more than in the other case studies. Also, it is possible to observe that the algorithm position the sensors towards the edge of the catchment, as is evident in the most Southern sensor, DS_2 (orange), which deploys towards the Southern end of the catchment, while the most Eastern sensor, DS_3 (green) deploys preferably towards the North-East of its base position in both events.

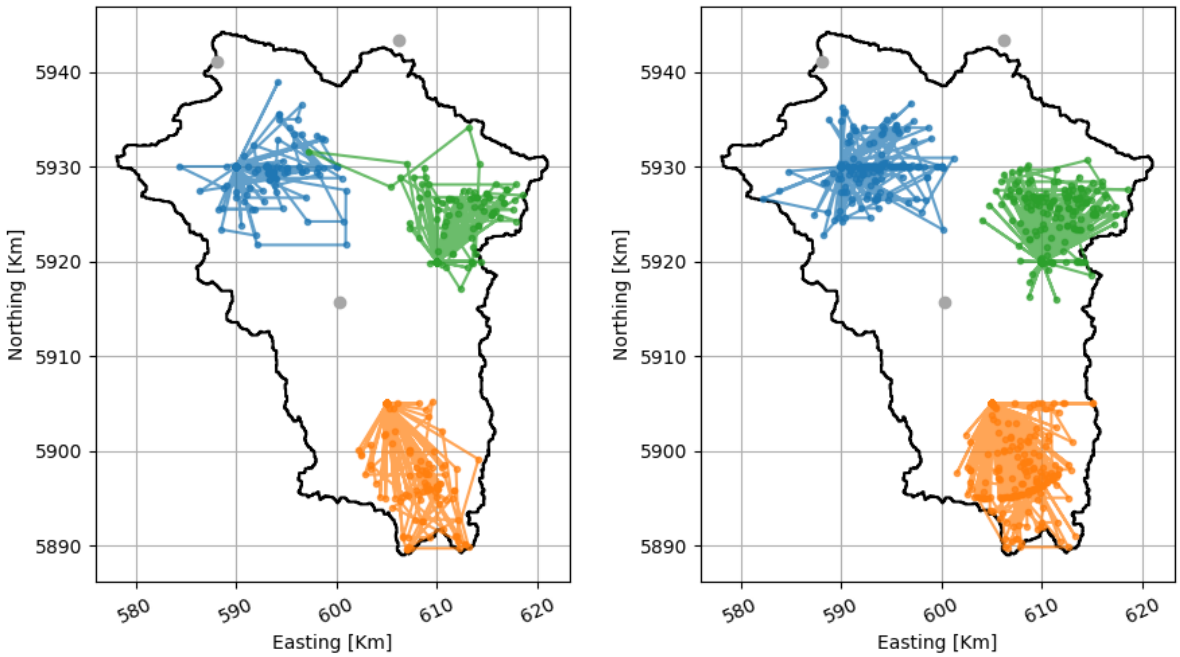

Figure 6.30 MMD deployment results in Don for precipitation event 1 (left) and 2 (right), using one hour window size

The results of the scheduling of dynamic sensors in a 3-hour time-window using MMD are presented in Figure 6.31. The results reveal a similar behaviour with respect to the 1-hour time window, indicating that there is no considerable overlap among sensors, showing that it is possible (at least to this time-window) to effectively assign dynamic sensors to specific parts of the catchment. Also, by extending the time-window to three hours, it was possible for the sensors to extend its reach, deploying furtherly, but radially towards their base positions. Additionally, it is possible to observe that the sensors start to cooperate, as there is a movement towards the centre of the catchment, especially evident in the second event.

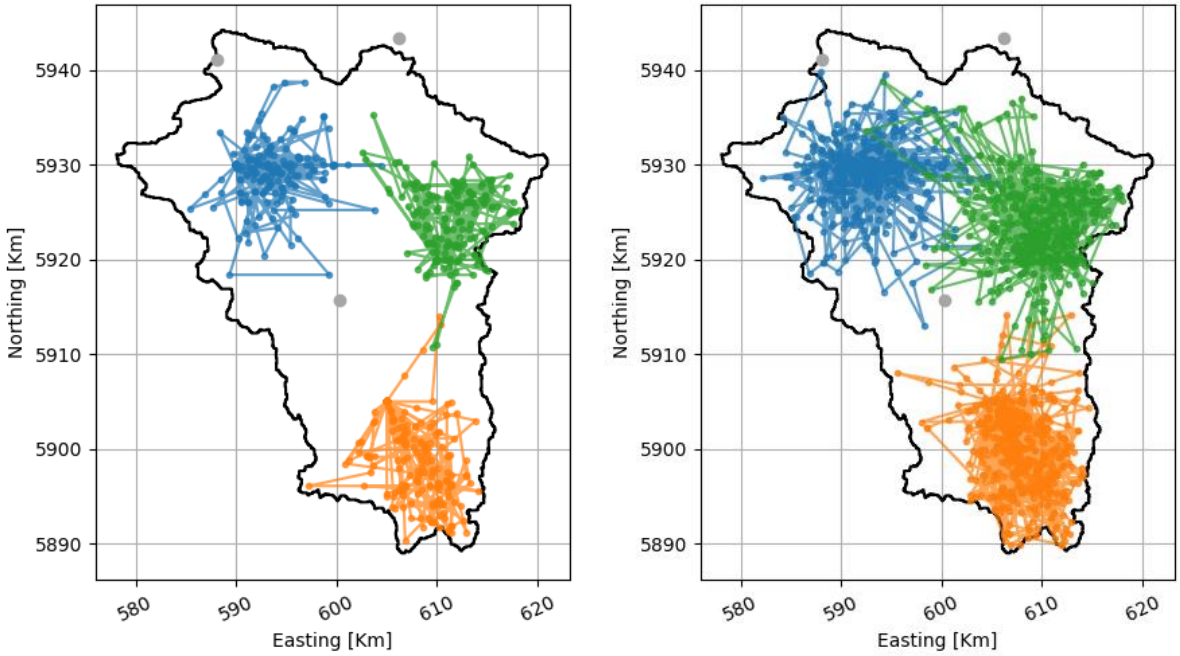

Figure 6.31 MMD deployment results in Don for precipitation event 1 (left) and 2 (right), using three hours window size

When the time-window extends to 6 hours (Figure 6.32), it is possible to observe a similar pattern to the 3-hour time-window. In this case, it is possible to see how the green and blue sensors merge their area of influence, while the orange sensors remain within its own area of influence. The cooperation can be understood as the North part of the catchment has a far greater coverage with respect to the South, and therefore, the orange sensor has to account for the dynamics of the precipitation field in this area, which is also explained by the lack of capacity of the models to agree (and consequently diverging) towards largely ungauged areas.

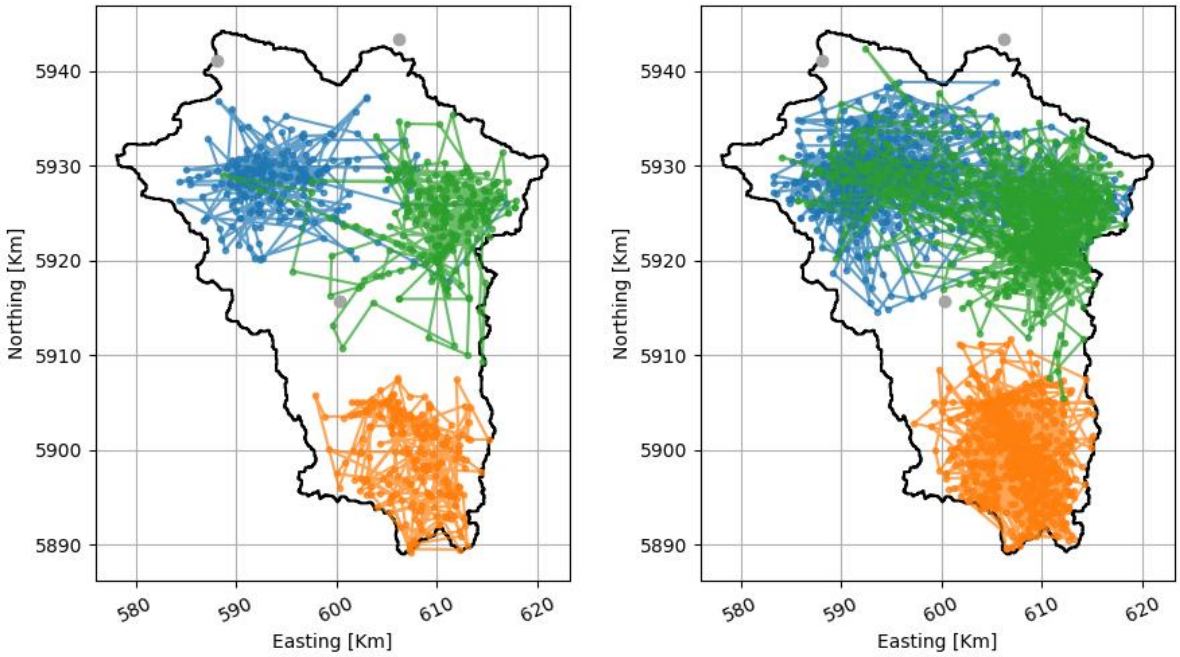

Figure 6.32 MMD deployment results in Don for precipitation event 1 (left) and 2 (right), using six hours window size

6.5.4 **Comparing solutions corresponding to different objective functions**

Due to the characteristics of the case studies, and the incompatibility of the deployment strategies, the results between approaches is not quantitatively compared. The analysis compares the value of the objective functions for the two precipitation events in three case studies, and for the three (where applicable) deployment strategies.

The results for the value of the objective functions for the three deployment methods in the Bacchiglione River catchment are presented in Figure 6.33, for the Brue Catchment in Figure 6.34 and for the Don River Catchment Figure 6.35. The results show that even if there is no correspondence of the units among methods, their own values tend to peak at similar times, indicating that there exists a correspondence among methods. Indubitably, the similitude between the objective function between KVP and NKVP is evident, differing mostly in the orders of magnitude of the variables. This can be explained by the fact that both are a measure of variance in the field, and therefore, the dynamics are controlled by those of the precipitation field and the deployment of the sensors.

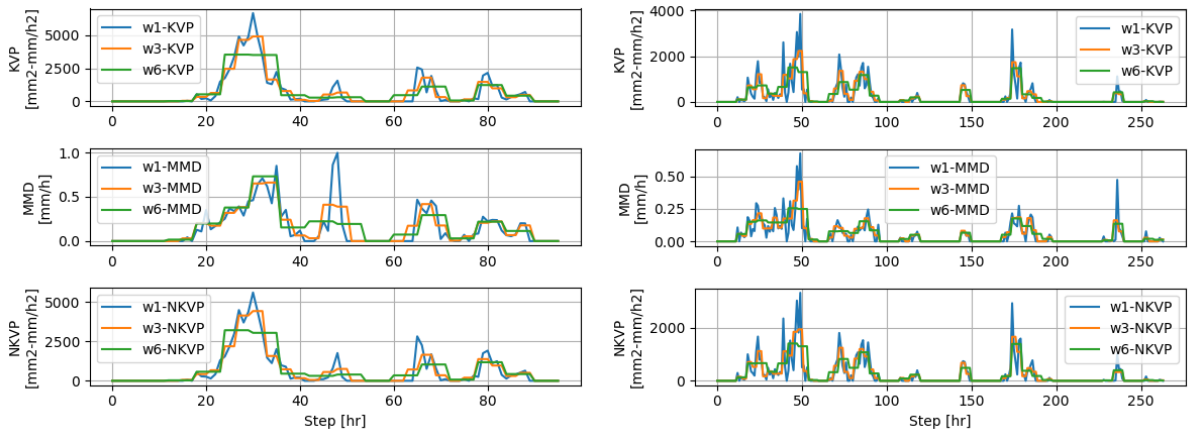

Figure 6.33 Objective function for event 1 (left) and event 2 (right) using different deployment methods and time-windows in the Bacchiglione River catchment

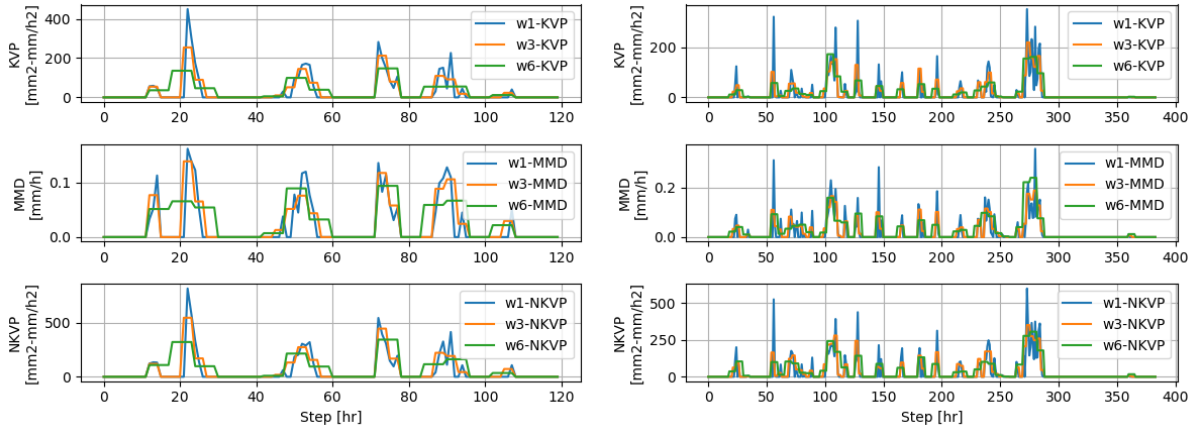

Figure 6.34 Objective function for event 1 (left) and event 2 (right) using different deployment methods and time-windows in the Brue catchment

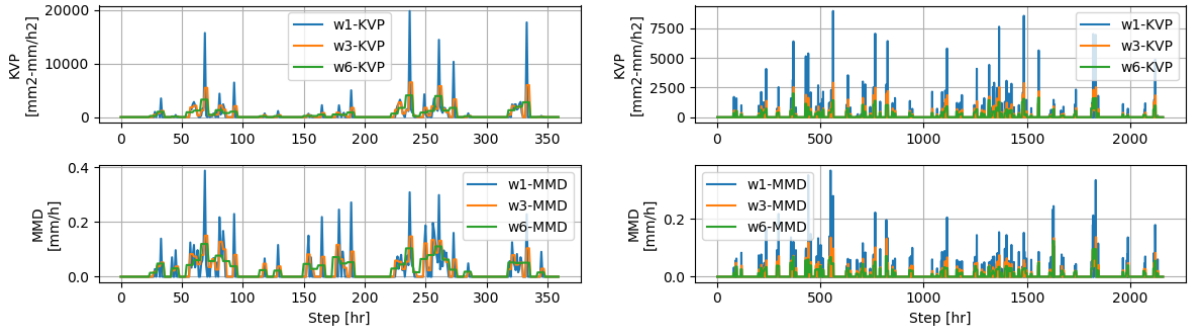

Figure 6.35 Objective function for event 1 (left) and event 2 (right) using different deployment methods and time-windows in the Don River catchment

Additionally, it is possible to observe that the increment in the time-window for the deployment of the sensors has an important effect in the optimality of the results. Longer time-windows show consistently lower peaks, and therefore, suggesting that the use of non-optimal location to deploy sensors may be of great importance to increase the reach of the sensors, and to reduce the uncertainty associated with the partial recording of the precipitation.

6.5.5 **Sensitivity of solutions to uncertainties in the generated precipitation field**

This section explores the effect of the deployment of dynamic sensors in cases where perturbations are added. This perturbation is artificially introduced, aiming to explore the effect unknown processes in the precipitation field. The results explore the experiments presented in Table 6.5, for the strategies in each case study as described in Table 6.4. The experiments are presented for the first precipitation event in each of the case studies. The results are presented by case study, perturbation experiment and finally deployment strategy.

Bacchiglione

The relative comparison of the results in the deployment for a time-window of three hours, for perturbations with mid amplitude and fluctuation scale (Ex 1), and high amplitude and long fluctuation scale (Ex4) using the KVP as deployment method are presented in Figure 6.36. The results of the two methods reveal significant differences in the deployment of the network. For Ex 1, the sensors explore freely the solution space, with a preference for the Centre-Southern end of the catchment, while Ex 4 drives the sensors to explore the catchment more uniformly.

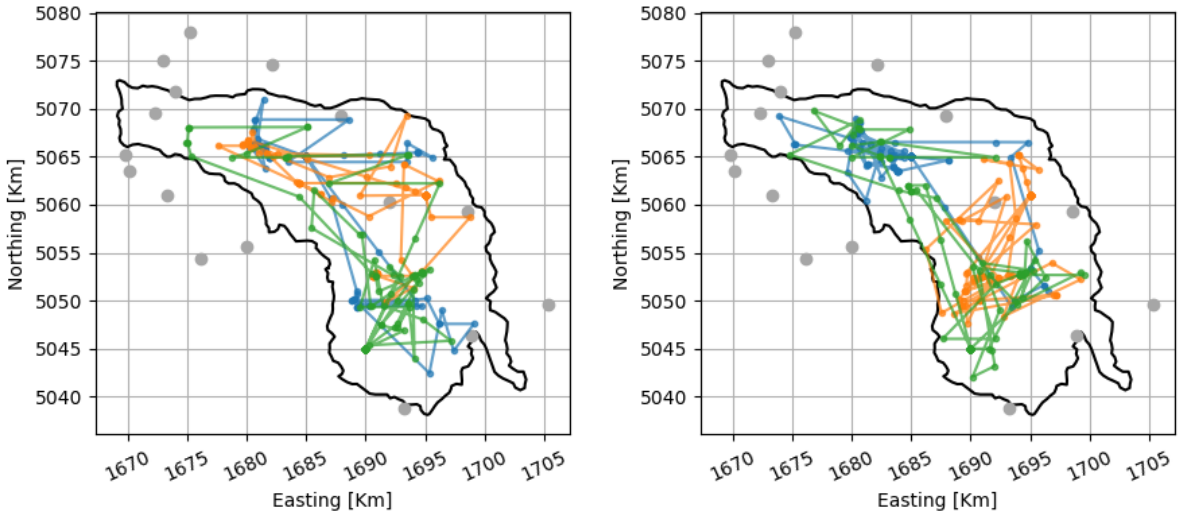

Figure 6.36 Optimal KVP deployment in Bacchiglione for Ex 1 (left) and Ex 4 (right)

The added perturbation foster the dynamic sensors to explore other areas that were not part in the original deployment, making the cooperation among sensors more evident. The effect that the fluctuation scale and amplitude of the perturbation increases (from Ex 1 to Ex 4) show that the results tend to locate the dynamic sensors towards smaller ungauged areas, which may result into smaller influence area of the static sensors.

The same experiment repeated for NKVP strategy, and the results are presented in Figure 6.37. The results show a similar behaviour for the first perturbation experiment (Ex 1), but a slightly different trend in the second (Ex 4). In the first, the deployment of the dynamic sensors occurs mostly towards the Centre-South of the catchment, where green and orange sensors have a more active role, while the blue sensor tends to monitor the North end. In the second perturbation experiment, the deployment occurs in more homogeneously, towards the ungauged areas in the centre of the catchment. This behaviour seems to highlight the importance that the spatial

correlation structure of that the perturbation has in the deployment of DSN. Considering this, it is possible to suggest that the effect of the fluctuation scale of the precipitation process has an important role in the definition of the deployment of dynamic sensors using the NKVP method.

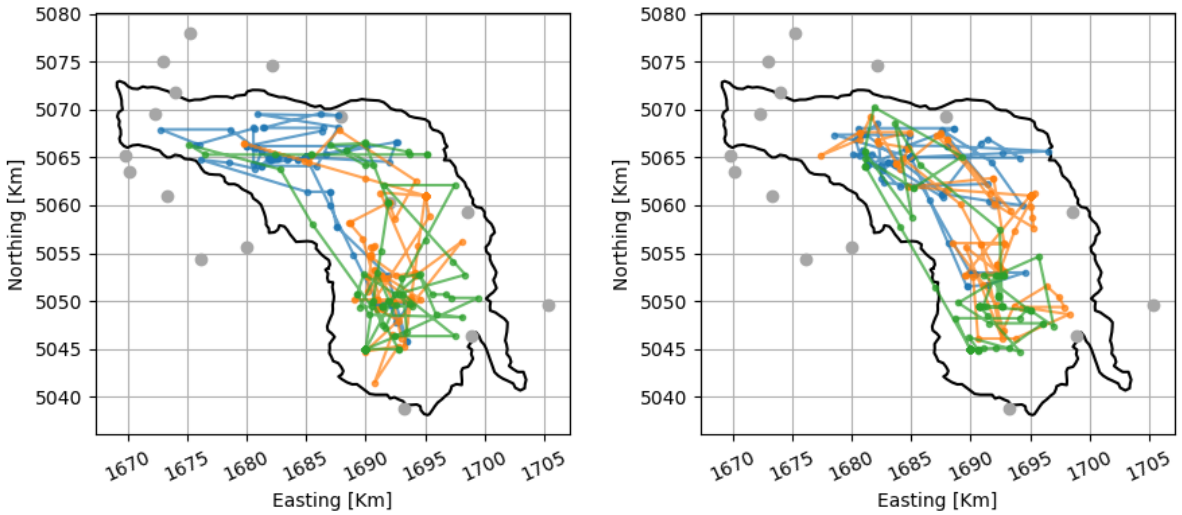

Figure 6.37 Optimal NKVP deployment in Bacchiglione for Ex 1 (left), Ex 4 (right)

Brue

The results for the deployment of dynamic sensors in three perturbations experiments (Ex 1, Ex 2, Ex 3) in the Brue catchment, using the KVP method are presented in Figure 6.38. The results show a tendency of the sensors to be located towards the North and East side of the catchment in the events with a short fluctuation scale, in contrast with the deployment in the events of perturbations with a long correlation scale. In other words, indicating that in short correlation scales, the variance of the estimation grows significantly faster, and therefore, the values of maximum precipitation are more relevant in the deployment of the DSN. On the other hand, if the fluctuation scale of the perturbation is longer, then is possible to make better assessments of the precipitation field, and therefore, it is more relevant to carry out measurements in areas with a low network density (East).

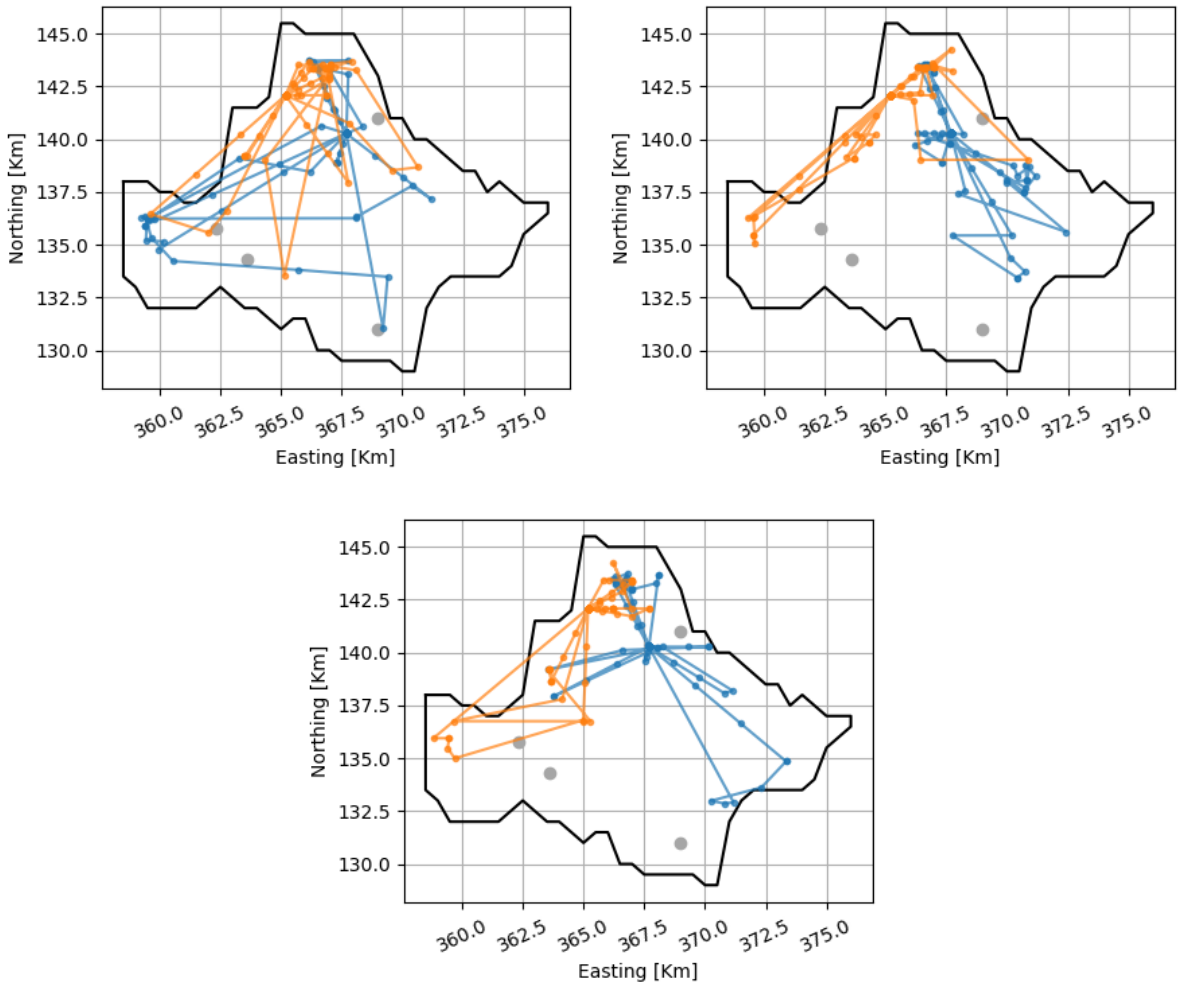

Figure 6.38 Optimal KVP deployment in Bacchiglione for Ex 1 (left), Ex 2 (right), and Ex 3 (bottom)

The optimal deployment of dynamic sensors using the NKVP method for the three noise scenarios is presented in Figure 6.39. The deployment of the sensor shows that there is a tendency of the sensors to be placed towards the ungauged parts of the catchment in the Centre-East. It is possible to observe how the increment in the amplitude of the noise lead to the deployment of sensors closer to the static sensor network in some occasions (Ex 3), indicating that probably the gain of the precipitation towards the static sensor in the North of the catchment is driving the deployment. However, it is also possible to observe that in all of the noise scenarios, there is always a visit towards the West side of the catchment, probably triggered by a precipitation located in this area.

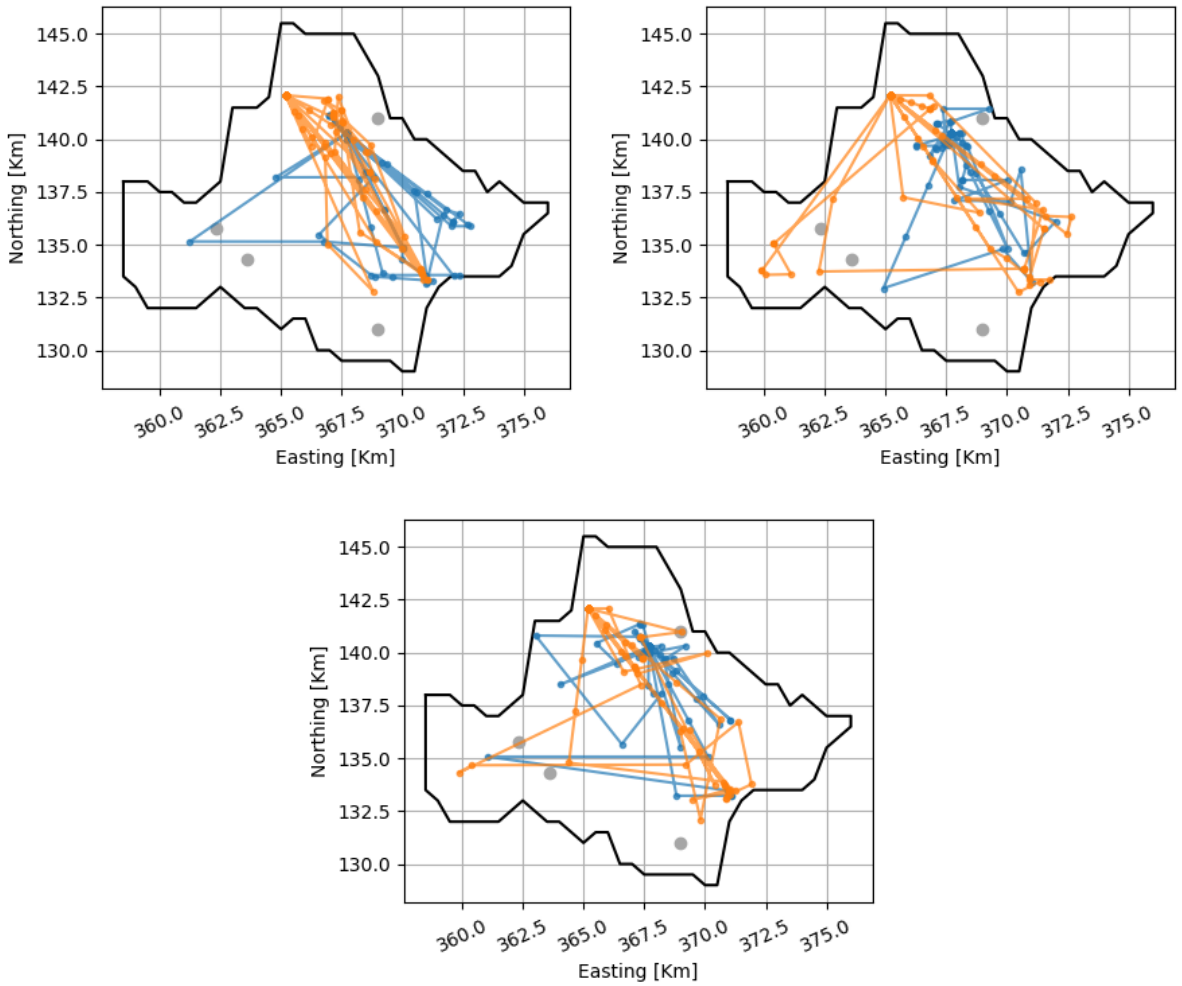

Figure 6.39 Optimal NKVP deployment in Bacchiglione for Ex 1 (left), Ex 2 (right), and Ex 3 (bottom)

The deployment of the dynamic sensors in the three noise scenarios using the MMD in the Brue Catchment are presented in Figure 6.40. The results show a more uniform distribution deployment of the sensor of the catchment, driving the optimal position of the sensor away from the static sensor network, proportionally to the fluctuation scale. In other words, there is deployment of dynamic sensors closer to static sensors in the experiments with low fluctuation scale of the noise (Ex 1 and Ex 3), while the deployment seems to be driven away from static sensors in the noise scenario with long fluctuation scale (Ex 2).

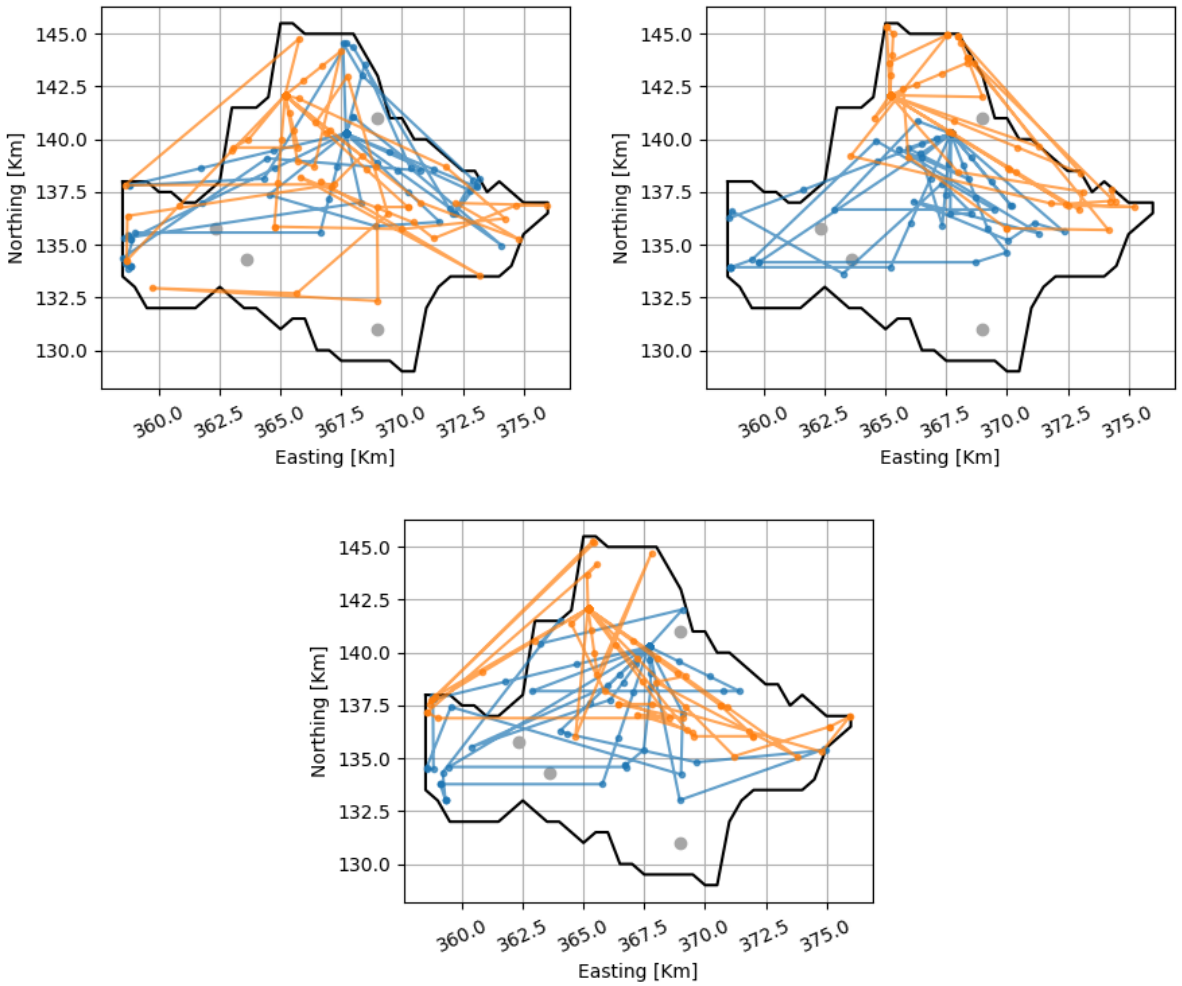

Figure 6.40 Optimal MMD deployment in Bacchiglione for Ex 1 (left), Ex 2 (right), and Ex 3 (bottom)

Additionally, it is possible to observe that extreme positions of the sensors are encouraged. This can be explained by the divergence of many of the models, especially towards important gradients in the sensor network. In the case of an important gradient in the observations, the presence of a sensor in the edge of the catchment serves as a sort of anchor, to reduce the spread of the models. Also, it can be seen as maximising the convex hull of the whole sensor network, if the gradient in the observations of the static network is pronounced. This can also be supported by the lack of deployment towards the South, where there is a sensor close to the boundary of the catchment in this direction.

Don

The results of the deployment using the KVP model in the three noise scenarios for the Don River catchment are presented in Figure 6.41. The results show that the deployment patterns change little with respect to the underlying noise field. This can be attributed to the lack of static networks which can actually generate a difference in the driving of the dynamic sensors under different noise conditions. In other words, seems not to be a noticeable difference in the deployment

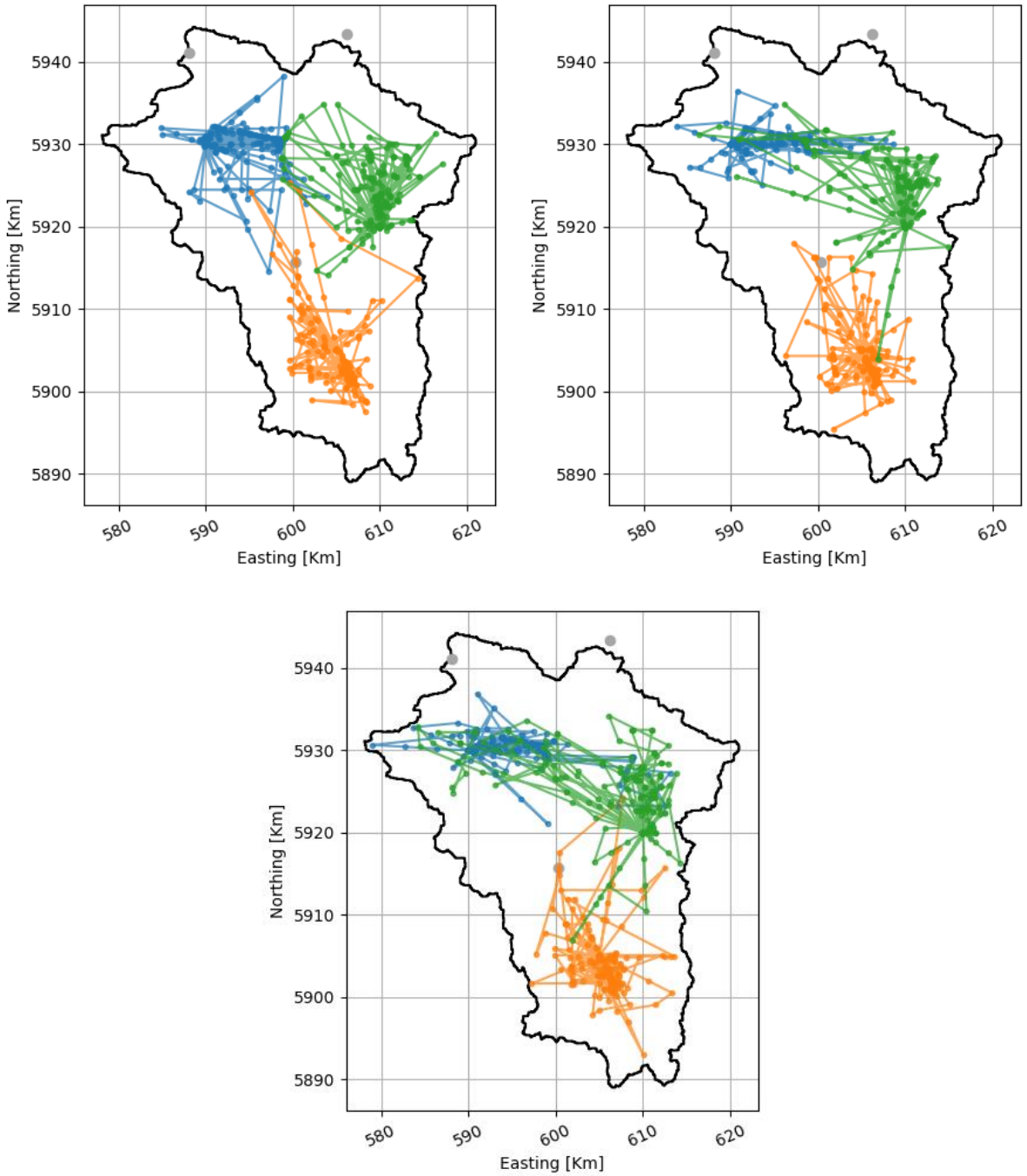

Figure 6.41 Optimal KVP deployment in Don for Ex 1 (left), Ex 2 (right), and Ex 3 (bottom)

The deployment of dynamic sensors using the MMD in the scenarios of artificial noise is presented in Figure 6.42. The results for the deployment of the network agrees with the results already observed in the previous noise scenario, meaning that the dynamics of the deployment are not altered by the presence of noise. In this regard, the sensors remain to a large extent around their base positions and are deployed mostly towards the boundaries of the catchment.

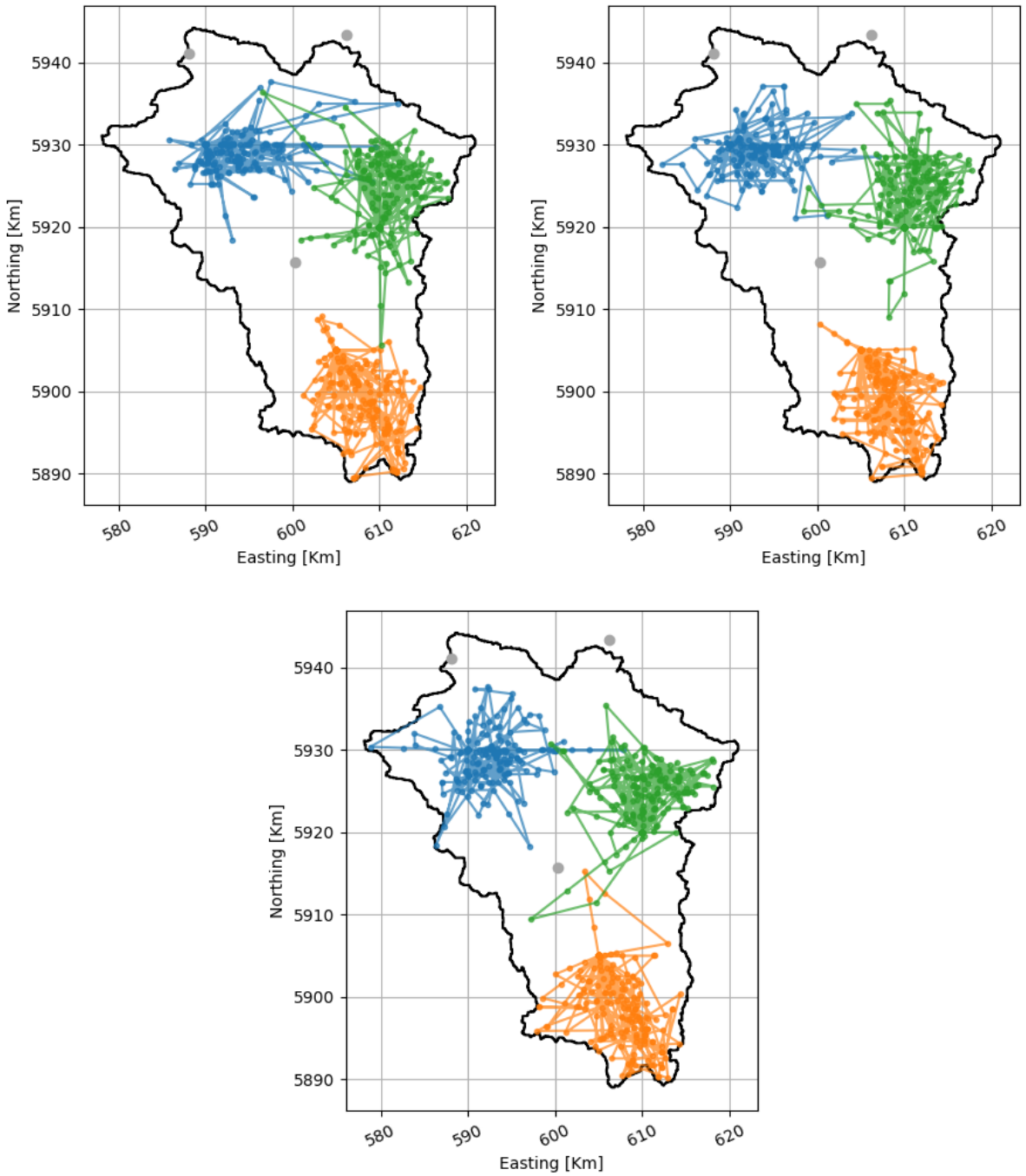

Figure 6.42 Optimal MMD deployment in Don for Ex 1 (left), Ex 2 (right), and Ex 3 (bottom)

6.5.6 **Additional considerations for practical deployment of dynamic sensors**

In the design of sensor networks, there are usually additional considerations that may constraint the development of a certain monitoring plan, such as cost and accessibility, among others (Loucks et al. 2005). This study is based on the fact that sensors are moving through the catchment for actively monitoring, and therefore, it is of interest to understand how far these sensors go. This travel distance is directly correlated with the cost of the operation of these sensors, and may be the base for making decisions such as the limiting threshold for the sensors to leave its base, or to constrain the total travel distance between observations.

Figure 6.43 presents the results of the total travel distance for each of the precipitation events in each of the case studies for the three different time-windows. The overall results show that the deployment of sensors using the MMD gives consistently longer displacement distance than KVP and NKVP, which are consistent with the different case studies. The results also show that the length of the time-window is directly proportional to the total travel distance. It is presumed that there is an asymptotic limit for the total travel distance with respect to the time-window, but it was not found in the results of this study.

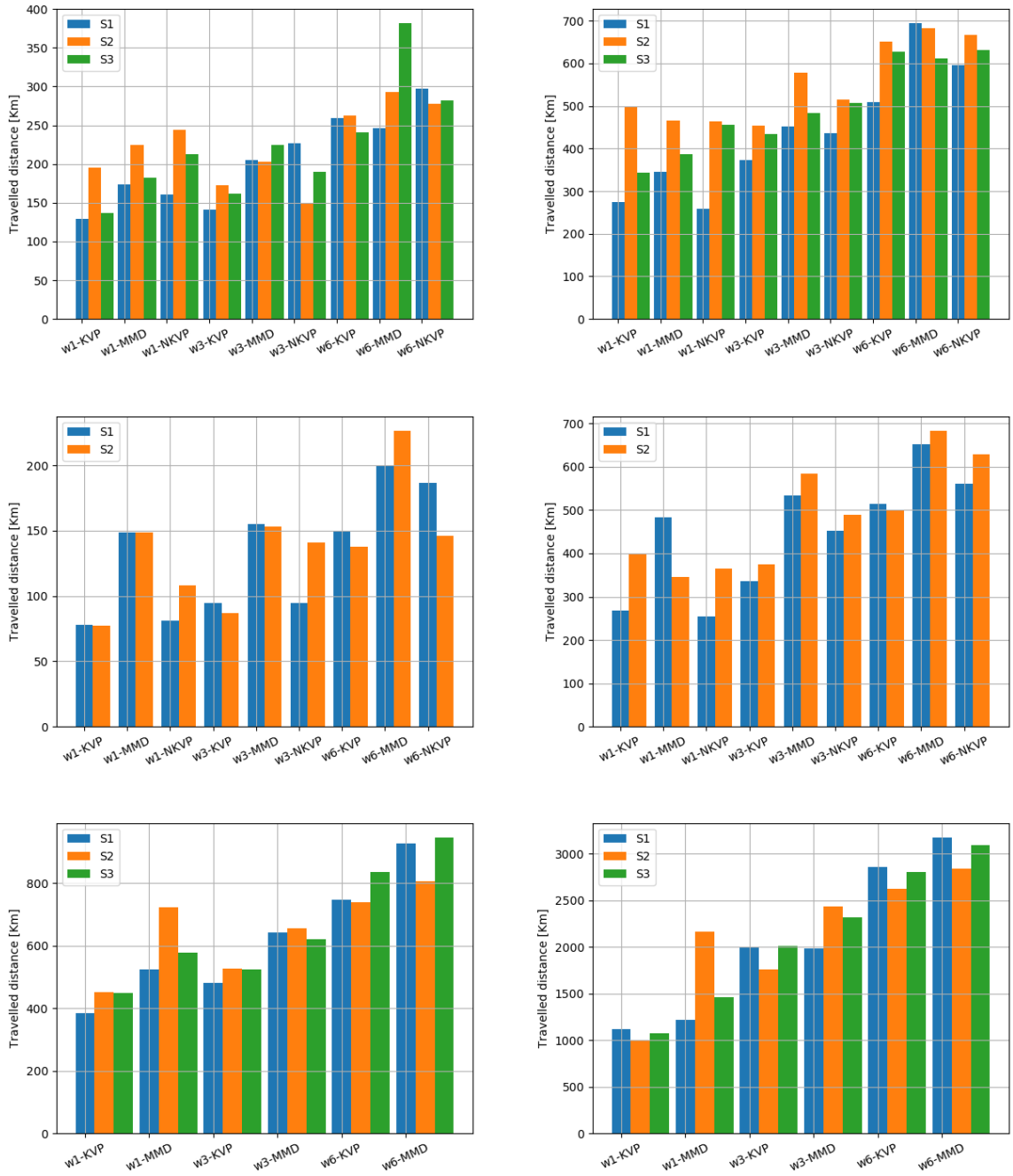

Figure 6.43 Travel distance for the deployment of sensors in the three case studies (top: Bacchiglione, mid: Brue, Bottom: Don) for the first (left) and second (right) precipitation event

6.6 Conclusions

In this chapter, three strategies for the scheduling of sensor networks for two different events in three case studies were tested. The overall results indicate that sensors indeed are generally directed towards areas with low coverage from the static sensor networks. However, it is common to find deviations from these rules, if the observations in the static sensor network suggest potentially high values of precipitation in ungauged areas. This last situation is minimised in the event that the static sensor network is relatively well distributed, as uncertainties in the spatial interpolation are considerably smaller.

To accentuate the monitoring in ungauged locations, NKVP tends to schedule sensors to areas with low monitoring, in contrast with KVP. The reason can be attributed to a more realistic estimation of the precipitation variance, which drives the sensors using NKVP to remain in areas of higher variance, and far from the points of maximum precipitation, which correspond to measured variables. As consequence, the optimal value for the location of the sensor in similar precipitation conditions, will result in DSN which are closer to the static sensors, when using KVP, and farther, when using NKVP.

In non-stationary Kriging-type interpolation, 'hot' areas for dynamic sensors are identified, and trend to enlarge the coverage of the network. The average precipitation is better represented by measurements that are located in the areas of higher uncertainty. In contrast with the Kriging-based methods, the MMD strategy tends minimise the overlap of the dynamic sensors, developing a cluster in which the sensors should be. This clustering is the result variance estimates which do not account for the precipitation intensity, but instead by the relative differences between precipitation estimations.

The result in the position of the dynamic sensors for the Brue catchment reveals minor discrepancies between the Kriging-based and the MMD strategies. The results for the Kriging based methods cluster towards North-west and the east end of the catchment, where measurements are more uncertain due to the distance to the sensors. As ensemble methods react to the patterns in the precipitation, the clusters vary, without following a clear pattern. In general, the discrepancies between methods depend on the amount of available information and the interpolation tools to simulate the precipitation field.

In contrast, similitudes between the different methods were found in the Bacchiglione case study. In this case, it was possible to identify two hot location for sensor deployment: One in the most upstream part of the catchment, and other in the inter-basin area at the south-west of the catchment. These similitudes occur as a consequence of the even distribution of the sensors within the study case, which lead the sensors to identify similar areas of interest.

In the Don River catchment, it was possible to observe KVP and MMD provide quite different solutions. KVP makes a consistent deployment of two sensors, in which one of them remains fairly static in the south end of the catchment, while other exhibits a more dynamic behaviour in the north. In contrast, in the Information-based methods, a hot spot is identified in the north

part of the catchment, and little attention is given to the south part of it. This discrepancy is triggered by the interpolation methods used in the generation of the observations in the south, and thus revealing, that the information-based dynamic networks may not necessarily be most adequate choice to identify areas with systematic lack of coverage.

Additionally, the experiments using the different perturbation scenarios reveal that the lack of knowledge about the precipitation processes will significantly alter the result of the deployment strategy. This lack of knowledge can be usually attributed to a static sensor network that is designed at a different spatial scale, and therefore, is not able to capture certain processes. In this sense, un-seen processes with a short scale may require that the DSN are deployed closer to the static sensor networks, to capture the variations between static sensors. Additionally, the assumptions of un-seen processes may be beneficial in the scheduling of DSN, as makes it possible to generate a set of more robust estimations of variance, which permit characterising

7. Conclusions and recommendations

7.1 Summary

This thesis explores the optimal design of static, and scheduling of dynamic sensors networks for precipitation monitoring. The design of conventional sensor networks is developed using various methodologies, exposing the interactions between different design objectives and solution methods. In addition, the scheduling of dynamic sensors is explored, and three deployment strategies are proposed and tested.

Chapter 1 describes the motivation, objectives and general scope of this work, highlighting the main objective: Develop and improve methods for optimal design of dynamic rainfall sensor networks with varying physical topology, in heterogeneous data environments for operational hydrological systems. To reach this general objective, the following steps were undertaken: 1) defining a framework for the design of sensor networks, 2) improve geostatistical methods for modelling of precipitation fields, 3) enhancing the current methods for the design of sensor networks for streamflow simulation, and 4) developing a methodological approach for the optimal scheduling of dynamic sensor networks which include data from static, dynamic gauges and citizen observatories.

Chapter 2 provided a literature review on the design of sensor networks, methods for design of static precipitation sensor networks. This review allowed to identify the current techniques in the design and evaluation of sensor networks, understand their limitations and potential advantages, and classify and identify knowledge gaps. As a result, we proposed a classification of methods and a framework for the design of sensor networks, achieving the first specific objective of this thesis. The results of this chapter have been presented as paper in a peer-reviewed journal (Chacon-Hurtado et al. 2017).

Chapter 3 presented the three case studies: Bacchiglione, Brue and, Don River catchment. The Bacchiglione River is located in Northern Italy, in the province of Veneto; the case study is of relevance due to the flooding hazard that the city of Vicenza. The Brue case study is located in Somerset (South-West England), and, since it is an experimental catchment, it is characterised for the availability of extremely detailed dataset (a large number of sensors in a relatively small catchment) collected during the HYREX experiment. The last case study corresponds to the Don River catchment, which presents flooding hazards to the communities in its lower end, in particular, the city of Doncaster (Yorkshire County), in East England. The Bacchiglione and Don River were also case studies of the WeSenseIt project which funded this PhD.

Chapter 4 explored the enhancement and testing of tools for the modelling of precipitation fields. These tools include an alternative formulation and algorithmic implementation of Kriging, which is able to use heterogeneous observations in non-stationary conditions, and a framework for the evaluation of measurement uncertainty estimation from partially observed data. The proposed Kriging approach relaxes some of the conventional assumptions such as: regionalised variable, equal observational uncertainty and spatial stationarity. As a consequence, the method provides more realistic approximations of the interpolation error than conventional (Ordinary) Kriging estimators. Additionally, the uncertainty in precipitation estimates due to the partial observations in time were assessed, thus yielding the theoretical basis for including observations from dynamic sensors into spatially distributed precipitation fields. Consequently, this chapter focused in achieving the second specific objective of this thesis.

Chapter 5 explored several aspects of designing static sensor networks. These aspects include: adequate formulation of the optimisation problem, selection of an optimisation algorithm, assessments of various optimality criteria in the final design, and its relationship with the performance of hydrological models, as well as an analysis of robustness of optimal solutions. The formulation of the problem, and the selection of the optimisation algorithm consisted in identifying the combination of such that ensure an efficient solution of the sensor network design problem. The different design criteria were compared using a large-scale Monte Carlo experiment that evaluated the relationship between model-based and model-free alternatives in the design of precipitation sensor networks. Following, the sensor networks problem is solved for each of the chosen objective functions, and the resulting sensor networks are presented. Finally, analysis of robustness of the optimal solutions for each resulting network was carried out. Accordingly, this chapter accounted for achieving the third specific objective of this thesis.

Chapter 6 presented the optimal scheduling of dynamic sensor networks, exploring the effect of different three different strategies for exploring precipitation fields. It introduced three strategies (KVP, NKVP and MMD) for the scheduling of dynamic sensors, and suggested the formulation of the optimal scheduling problem. Second, these strategies were tested in the case studies for three different time-windows (horizons). To further test these methods, a set of experiments including spatially correlated artificial noise were set. The results demonstrated the use of three different methodologies for scheduling of dynamic precipitation sensors, proving the theoretically usability of dynamic sensors. Subsequently, this chapter accounted for achieving of the fourth (and last) specific objective of this thesis.

7.2 Conclusions

The conclusions from this thesis are drawn as follows.

As result of the literature review, it was possible to establish that quite a considerable body of research done in this area, but also the fact that there is no agreement in the scientific community about a single method for the design of sensor networks. In this knowledge gap, we propose a

classification of methods and a generic framework for the design of sensor networks. This framework is able to encompass most of the approaches found in the literature, and can be seen as a first step towards the integration of design methodologies.

Additionally, it was found that the effect of different uncertainty sources in modelling of precipitation fields prompts for re-thinking some of the conventional assumptions. Among these are the assumptions regarding geostatistical interpolation methods, including heterogeneous observations, and stationarity assumptions. Also, it was found that one of the main challenges for the modelling of precipitation fields in the context of the citizen observatories, relates to the intra-hourly variability of the precipitation, and this means that instantaneous measurements of precipitation are hardly usable, as its uncertainty is greater than the precipitation autocorrelation at operational time scales (see Section 4.2 and 4.3).

This thesis also proposed a methodology for the use of heterogeneous data sources in modelling non-stationary precipitation fields. For this purpose, a variation (NSK) of the Ordinary Kriging is developed, such that it is possible to generalise the field variogram for locally built (centrosymmetric) variograms, which adapt to different precipitation conditions. NSK is considerably more data-intensive than Kriging, but relaxes the assumption of a regionalised variable, as there are not assumptions of spatial stationarity. NSK is flexible to adapt other exogenous variables that may trigger different statistical behaviour of the modelled processes, by incorporating this information in the definition of the variogram (CS variogram). These features do not necessarily lead to better deterministic results, but provided more reliable uncertainty bands, which are of utmost interest in the design of static, and deployment of dynamic sensor networks.

In this thesis we also established the lack of consensus in the definition of an optimal sensor network, considered the consequences of this, and explored the relationship among different objective functions. The results show that geostatistical objective functions (namely, Average and Maximum Kriging Variance) do offer insights which lead to the selection of networks that tend to yield better rainfall-runoff model results in operational settings at hourly scale. Also, it was found that Information Theory methods are able to discriminate sensor networks that yield poor performance of the hydrological model but were unsuccessful in determining whether or not the sensor network will yield optimal discharge results. It was also found out that model-based optimisation usually yield model-specific networks, which are not robust unless the used model is simple; therefore, these objective functions may not be reliable candidates for the design of sensor networks, as objectives (criteria used to assess a network) usually are wider, than just maximizing the hydrological model performance. In this sense, we have developed recommendations which may help to harmonise the selection of objective functions for the design of precipitation sensor networks.

The analysis of the error propagation in rainfall-runoff models, revealed that the precipitation errors tend to influence the results for long periods of time, and this influence largely depends on the conditions of the catchment when these errors occurred. Consequently, we advocate that methods where precipitation is estimated using inverse rainfall-runoff type model (Herrnegger

et al. 2015) under the assumption of a Markovian Process, have fundamental problems. The reason is in the explicit use of exact representation of the model states, which in practice is not possible for conceptual models, as processes are lumped at scales that do not match, and therefore, not measurable.

The results of applying the three different strategies (KVP, NKVP and MMD as presented in Chapter 6) for the scheduling of dynamic sensor networks, indicated that dynamic sensors can improve the network coverage. The experimental results indicate that the three strategies seem to be effective in the representation of precipitation fields, and can be used to reasonably schedule dynamic sensor networks. However, testing in field campaigns are required to verify and adjust the proposed models and methodology to realistic operational settings.

7.3 Limitations

There are several limitations found during the development of this thesis.

First, most of the proposed methods cannot be employed in data scarce regions. As a consequence, the dynamic sensors are only to be deployed in catchments where there is enough data from static networks to build acceptable spatial estimates of the precipitation field. Therefore, the dynamic sensors can provide data to help refine the first estimate of the precipitation field, but without sufficient data to understand the underlying phenomena, it is impossible to believe in an adequate deployment of dynamic sensors.

Second, the results of this thesis are based on a limited set of case studies, and therefore a much wider validation is required. In this respect, it is necessary to test the resulting methodologies in field applications, aiming to identify the weaknesses which may have been overlooked in the development of this thesis. The frameworks developed in this thesis should be also further incorporated into a wider decision making process, and tested, as sensor networks and monitoring programmes should consider many additional factors that the ones considered here.

Additionally, it is assumed that the dynamic sensors have a constant displacement capability. This distances that they need to travel are estimated from a Cartesian coordinate system, and therefore do not correspond to actual routes and traffic. In this study it is assumed that a sensor is always able to move freely in any direction, and this may be unrealistic in operational settings.

It is assumed also that the sensors are always available and ready to be deployed. In practice, obviously, volunteers may not follow the “instructions” on where and when to move. In the case that the sensors are deployed by operators (i.e. emergency response organisations), there are limits to the working hours, the places where should they be and the time to go before their turn is finished. Also, it will be possible that in critical events, their presence may be required for other tasks beyond providing precipitation data.

From the operational point of view, the deployment of these dynamic sensor networks is potentially a rather expensive task. For the events in this thesis, the total travel length of these sensors is considerable, implying that the costs associated with a vehicle, fuel, operator, sensor, among other expenses, may render unfeasible the use of the current "generation" of dynamic sensors. The mentioned issues were not considered in this work, but the developed framework can be updated to do so, and, e.g. be used in the programming of (cheaper) autonomous observation devices, such as drones in the near future.

7.4 Outlook and recommendations

Precipitation is not simple to measure. It is advised that the focus of citizen observatories regarding this variable be shifted towards a high engagement level (citizens having a sensor and maintaining it), in contrast with a larger participation of random, low engaged observers. The impact of this decision is that it will be possible to have more useful information, when it is derived from reliable data sources, in contrast with more observations at random places and times. Additionally, the results coming from highly engaged citizens (meaning that the observations are carried out during long continuous periods of time) are of a higher value than sporadic observations, as the intra-hour precipitation variability has a dominant role in the uncertainty of the measurements.

From the experience of the WeSenseIt project, and other related activities to this thesis, it has been found that engaging citizens is a very complex task. In this regard, the author suggests to shift the efforts in data collection of precipitation to automatic devices (rain gauges, radars, microwave links, etc.), and focus the participation of citizens in acquiring other variables such as water level in canals or soil moisture. The reason behind this reasoning rises from the usability of instantaneous data, as it was shown that this type of observations are almost unusable for precipitation analysis (this thesis), while they may of use in other types of water models (Mazzoleni et al. 2015). Ideally, measurement systems will not fail and data collection will be automatic, thus in the future, the focus should be directed towards ubiquity, robustness and automation of gauging systems.

In case of flood forecasting, the deployment of dynamic sensor networks for precipitation may not be practical. In many situations it could be more beneficial to obtain additional observations of discharge at upstream locations, and use that data to adjust the forecast using techniques such as data assimilation, as shown in Mazzoleni et al. (2015, 2016, 2017). The motive behind this reasoning lies in the time-window that is required for a flood to occur, which is usually in the order of hours for medium and small rivers. For this type of situations, hydrological forecasting is essential. In case of larger rivers, the rainfall-runoff processes are slower, and it has been demonstrated that indeed data assimilation techniques are highly effective to improve the discharge forecast in this type of systems.

It would be also beneficial to develop methods for the optimal deployment of dynamic precipitation sensors in data scarce regions. These methods can lead to more cost-efficient alternative than conventional monitoring. In terms of data analytics, it is envisioned that

Bayesian updating of the precipitation models with data from the dynamic sensors, may be a viable alternative.

Finally, the methodology for the deployment of dynamic precipitation sensor networks is quite general, and can be applied to other environmental or other spatially distributed variables or processes of interest, e.g. related to water quality of air pollution.

Bibliography

Abbott, M.B., Bathurst, J.C., Cunge, J.A., O'Connell, P.E. and Rasmussen, J. (1986) An introduction to the European Hydrological System — Systeme Hydrologique Europeen, SHE, 1: History and philosophy of a physically-based, distributed modelling system, Journal of Hydrology, vol. 87, Oct, pp. 45-59. 10.1016/0022-1694(86)90114-9.

Abo-Monasar, A. and Al-Zahrani, M. (2014) Estimation of rainfall distribution for the southwestern region of Saudi Arabia, Hydrological Sciences Journal, vol. 59, no. 2, pp. 420-431. 10.1080/02626667.2013.872788.

Aceves-Bueno, E., Adeleye, A., Feraud, M., Huang, Y., Tao, M., Yang, Y. and Anderson, S. (2017) The accuracy of citizen science data: A quantitative review, Bulletin of the Ecological Society of America, vol. 98, no. 4. 10.1002/bes2.1336.

Alfonso, L. (2010) Optimisation of monitoring networks for water systems: Information theory, value of information and public participation, UNESCO-IHE and Delft University of Technology.

Alfonso, L., Chacon-Hurtado, J.C. and Peña, G. (2015) Allowing citizens to effortlessly become rainfall sensors, 36th IAHR World Congress, The Hague, The Netherlands.

Alfonso, L., He, L., Lobbrecht, A. and Price, R. (2013) Information theory applied to evaluate the discharge monitoring network of the Magdalena River, Journal of Hydroinformatics, vol. 15, pp. 211-228. 10.2166/hydro.2012.066.

Alfonso, L., Lobbrecht, A. and Price, R. (2010) Optimization of water level monitoring network in polder systems using Information Theory, Water Resources Research, vol. 46, p. W12553. 10.1029/2009WR008953.

Alfonso, L., Mukolwe, M.M. and Baldassarre, G.D. (2016) Probabilistic flood maps to support decision-making: Mapping the Value of Information, Water Resources Research, vol. 52, Feb, pp. 1026-1043. 10.1002/2015wr017378.

Alfonso, L. and Price, R. (2012) Coupling hydrodynamic models and value of information for designing stage monitoring networks, Water Resources Research, vol. 48, p. W08530. 10.1029/2012WR012040.

Ali, Y. and Narasimhan, S. (1993) Sensor network design for maximizing reliability of linear processes, American Institute of Chemical Engineers, vol. 39, pp. 820-828. 10.1002/aic.690390510.

Amorocho, J. and Espildora, B. (1973) Entropy in the assessment of uncertainty in hydrologic systems and models, Water Resources Research, vol. 9, Dec, pp. 1511-1522. 10.1029/wr009i006p01511.

Anctil, F., Lauzon, N., Andréassian, V., Oudin, L. and Perrin, C. (2006) Improvement of rainfall-runoff forecasts through mean areal rainfall optimization, Journal of Hydrology, vol. 328, Sep, pp. 717-725. 10.1016/j.jhydrol.2006.01.016.

Arnold, J.G., Allen, P.M. and Bernhardt, G. (1993) A comprehensive surface-groundwater flow model, Journal of Hydrology, vol. 142, Feb, pp. 47-69. 10.1016/0022-1694(93)90004-s.

Ballari, D., Bruin, S. and Bregt, A.K. (2012) Value of information and mobility constraints for sampling with mobile sensors, Computers & Geosciences, vol. 49, pp. 102-111. 10.1016/j.cageo.2012.07.005.

Banik, B.K., Alfonso, L., Cristo, C.D., Leopardi, A. and Mynett, A. (2017) Evaluation of Different Formulations to Optimally Locate Sensors in Sewer Systems, Journal of Water Resources Planning and Management, vol. 143, Jul, p. 04017026. 10.1061/(asce)wr.1943-5452.0000778.

Barca, E., Passarella, G., Vurro, M. and Morea, A. (2015) MSANOS: Data-Driven, multi-approach software for optimal redesign of environmental monitoring networks, Water Resources Management, vol. 29, pp. 619-644. 10.1007/s11269-014-0859-9.

Bárdossy, A. (2006) Copula-based geostatistical models for groundwater quality parameters, Water Resources Research, vol. 42, p. W11416. 10.1029/2005WR004754.

Bárdossy, A. and Li, J. (2008) Geostatistical interpolation using copulas, Water Resources Research, vol. 44, p W07412. 10.1029/2007wr006115.

Bárdossy, A. and Pegram, G.G.S. (2009) Copula based multisite model for daily precipitation simulation, Hydrology and Earth System Sciences, vol. 13, Dec, pp. 2299-2314. 10.5194/hess-13-2299-2009.

Bárdossy, A. and Pegram, G. (2013) Interpolation of precipitation under topographic influence at different time scales, Water Resources Research, vol. 49, Aug, pp. 4545-4565. 10.1002/wrcr.20307.

Barredo, J.I. (2009) Normalised flood losses in Europe: 1970 - 2006, Natural Hazards and Earth System Sciences, vol. 9, pp. 97-104. 10.5194/nhess-9-97-2009.

Bastin, G. and Gevers, M. (1985) Identification and optimal estimation of random fields from scattered point-wise data, Automatica, vol. 2, pp. 139-155. 10.1016/0005-1098(85)90109-8.

Bastin, G., Lorent, B., Duque, C. and Gevers, M. (1984) Optimal estimation of the average areal rainfall and optimal selection of rain gauge locations, Water Resources Research, vol. 20, Apr, pp. 463-470. 10.1029/WR020i004p00463.

Bennett, N.D., Croke, B.F.W., Guariso, G., Guillaume, J.H.A., Hamilton, S.H., Jakeman, A.J., Marsili-Libelli, S., Newham, L.T.H., Norton, J.P., Perrin, C., Pierce, S.A., Robson, B., Seppelt, R., Voinov, A.A., Fath, B. and Andreassian, V. (2013) Characterising performance of environmental models, Environmental Modelling and Software, vol. 40, Feb, pp. 1-20. 10.1016/j.envsoft.2012.09.011.

Benson, M.A. and Matalas, N.C. (1967) Synthetic hydrology based on regional statistical parameters, Water Resources Research, vol. 3, Dec, pp. 931-935. 10.1029/wr003i004p00931.

Beven, K.J. (2012) Rainfall-Runoff Modelling, Wiley-Blackwell.

Beven, K. and Freer, J. (2001) Equifinality, data assimilation, and uncertainty estimation in mechanistic modelling of complex environmental systems using the GLUE methodology, Journal of Hydrology, vol. 249, Aug, pp. 11-29. 10.1016/s0022-1694(01)00421-8.

Beven, K.J. and Kirkby, M.J. (1979) A physically based, variable contributing area model of basin hydrology, Hydrological Sciences Bulletin, vol. 24, Mar, pp. 43-69. 10.1080/02626667909491834.

Black, A.R., Bennet, A.M., Hanley, N.D., Nevin, C.L. and Steel, M.E. (1999) Evaluating the benefits of hydrometric networks. Technical Report W146, UK Environmental Agency.

Bleasdale, A. (1965) Rain-gauge networks development and design with special reference to the United Kingdom, WMO/IAHS Symposium the design of hydrological networks. Quebec, Canada.

Blöschl, G. and Sivapalan, M. (1995) Scale issues in hydrological modelling: A review, Hydrological Processes, vol. 9, pp. 251-290. 10.1002/hyp.3360090305.

Bogárdi, I., Bárdossy, A. and Duckstein, L. (1985) Multicriterion network design using geostatistics, Water Resources Research, vol. 21, pp. 199-208. 10.1029/WR021i002p00199.

Bohling, G. (2005) Introduction to geostatistics and variogram analysis. Kansas Geological Survey, 1, 1-20.

Bonaccorso, B., Cancelliere, A. and Rossi, G. (2002) Network design for drought monitoring by geostatistical techniques, 5th EWRA conference "Water resources management in the era of transition".

Booij, M.J. and Krol, M.S. (2010) Balance between calibration objectives in a conceptual hydrological model, Hydrological Sciences Journal, vol. 55, Aug, pp. 1017-1032. 10.1080/02626667.2010.505892.

Bornn, L., Shaddick, G. and Zidek, J.V. (2012) Modelling non-stationary process through dimension expansion, Journal of the American statistical association, vol. 107, pp. 291-289. 10.1080/01621459.2011.646919.

Bose, S. and Steinhardt, A. (1996) Invariant tests for spatial stationarity using covariance structure, Acoustics, Speech, and Signal Processing, 1993. ICASSP-93., 1993 IEEE International Conference on.

Bostan, P.A., Heuvelink, G.B.M. and Akyurek, S.Z. (2012) Comparison of regression and kriging techniques for mapping the average annual precipitation of Turkey, International Journal of Applied Earth Observation and Geoinformation, vol. 19, Oct, pp. 115-126. 10.1016/j.jag.2012.04.010.

Box, G.E.P. (1982) Choice of response surface design and alphabetic optimality. Technical summary report #2333.

Brunsdon, C., Fotheringham, S. and Charlton, M. (1998) Geographically weighted regression - modelling spatial non-stationarity, The statistician, vol. 47, pp. 431-443. 10.1111/1467-9884.00145.

Burn, D.H. and Goulter, I.C. (1991) An approach to the rationalization of streamflow data collection networks, Journal of Hydrology, vol. 122, Jan, pp. 71-91. 10.1016/0022-1694(91)90173-f.

Buswell, A.M., Stout, G.E. and Neill, J.C. (1954) Quantitative measurement of rainfall by Radar, Journal - American Water Works Association, vol. 46, pp. 837-852.

Capecchi, V., Crisci, A., Melani, S., Morabito, M. and Politi, P. (2012) Fractal characterization of rain-gauge networks and precipitations: an application in central Italy, Theoretical and Applied Climatology, vol. 107, pp. 541-546. 10.1007/s00704-011-0503-z.

Carpenter, T.M. and Georgakakos, K.P. (2006) Intercomparison of lumped versus distributed hydrologic model ensemble simulations on operational forecast scales, Journal of Hydrology, vol. 329, no. 1-2, pp. 174-185. 10.1016/j.jhydrol.2006.02.013.

Caselton, W.F. and Zidek, J.V. (1984) Optimal monitoring network designs, Statistics and Probability Letters, vol. 2, Aug, pp. 223-227. 10.1016/0167-7152(84)90020-8.

Casman, E., Naiman, D. and Chamberlin, C. (1988) Confronting the ironies of optimal design: Non-optimal sampling design with desirable properties, Water resources research, vol. 24, pp. 409-415. 10.1029/WR024i003p00409.

Cerny, V. (1985) Thermodynamical approach to the traveling salesman problem: An efficient simulation algorithm, Journal of Optimization Theory and Applications, pp. 41-51. 10.1007/BF00940812.

Chacon-Hurtado, J.C., Alfonso, L. and Solomatine, D.P. (2014) Precipitation sensor network optimal design using time-space varying correlation structure, 11th International conference in Hydroinformatics, HIC 2014, New York, USA.

Chacon-Hurtado, J.C., Alfonso, L. and Solomatine, D. (2016) Comparison between passive and active social sensors of precipitation for flood forecasting, Citizen Observatories for Water Management, Venice, Italy.

Chacon-Hurtado, J.C., Alfonso, L. and Solomatine, D.P. (2017) Rainfall and streamflow sensor network design: a review of applications, classification and a proposed framework, Hydrology and Earth System Sciences. 10.5194/hess-21-3071-2017.

Chacón-Hurtado, J.C., Garzón-Contreras, F. and Montaña, D. (2009) Optmización de la red de pluviometros de Santiago de Cali, Colombia, por métodos geoestadísticos (In Spanish), Seminario estrategias para enfrentar el cambio climático.

Chakraborty, A. and Deglon, D. (2008) Development of a heuristic methodology for precise sensor network design, Computers and Chemical Engineering, vol. 32, pp. 382-395. 10.1016/j.compchemeng.2007.02.008.

Chaloner, K. and Verdinelli, I. (1995) Bayesian experimental design: a review, Statistical Science, vol. 10, Aug, pp. 273-304. 10.1214/ss/1177009939.

Cheng, K.S., Ling, Y.C. and Liou, J.J. (2007) Rain gauge network evaluation and augmentation using geostatistics, Hydrological Processes, vol. 22, pp. 2554-2564. 10.1002/hyp.6851.

Chen, C. and Li, y. (2012) An adaptive method of non-stationary variogram modelling for DEM error surface simulation, Transactions in GIS, pp. 885-899. 10.1111/j.1467-9671.2012.01326.x.

Chiles, J.-P. and Delfiner, P. (1999) Geostatistics: Modelling spatial uncertainty, Hoboken, NJ: Wiley.

Chow, V., Maidment, D. and Mays, L. (1988) Applied Hydrology, McGraw-Hill Science/Engineering/Math.

Christakos, G. (1984) On the problem of permissible covariance and variogram models, Water Resources Research, vol. 20, no. 2, pp. 251-265. 10.1029/WR020i002p00251.

Ciach, G.J. and Krajewski, W.F. (2006) Analysis and modeling of spatial correlation structure in small-scale rainfall in Central Oklahoma, Advances in Water Resources, vol. 29, Oct, pp. 1450-1463. 10.1016/j.advwatres.2005.11.003.

Cihlar, J., Grabs, W. and Landwehr, J. (2000) Establishment of a hydrological observation network for climate, Report of the GCOS/GTOS/HWRP expert meeting. Report GTOS 26.

Cooke, R.M. (1991) Experts in Uncertainty: Opinion and Subjective Probability in Science, Oxford University Press, USA.

Cooke, R.M. and Goosens, L.L.H.J. (2008) TU Delft expert judgement data base, Reliability Engineering and System Safety, vol. 93, pp. 657-674.

Coulibaly, P. and Samuel, J. (2014) Hybrid Model Approach To Water Monitoring Network Design, 11th International conference in Hydroinformatics, HIC 2014, New York, USA.

Coulibaly, P., Samuel, J., Pietroniro, A. and Harvey, D. (2013) Evaluation of Canadian National Hydrometric Network density based on WMO 2008 standards, Canadian Water Resources Journal, vol. 38, Jun, pp. 159-167. 10.1080/07011784.2013.787181.

Cover, T.M. and Thomas, J.A. (2006) Elements of Information Theory, Wiley John & Sons. New York, USA.

Cressie, N. (1993) Statistics for spatial data, Wiley. New York, USA.

Cressie, N. (2015) Statistics for Spatial Data, Revised Edition, John Wiley & Sons. New York, USA.

Crujeiras, R.M. and van Keilegom, I. (2010) Least squares estimation of nonlinear spatial trends, Computational Statistics and Data Analysis, vol. 54, no. 2, pp. 452-465. 10.1016/j.csda.2009.09.014.

Dahm, R., Jong, S., Talsma, J., Hut, R. and van de Giessen, N. (2014) The application of robust acoustic disdrometers in urban drainage modelling, 13th International Conference on Urban Drainage.

Daley, R. (1991) Atmospheric Data Analysis, Cambridge University Press. Cambridge, UK.

Dantu, K., Rahimi, M., Shah, H., Babel, S., Dhariwal, A. and Sukhatme, G. (2005) Robomote: Enabling mobility in sensor networks, 4th International Symposium on Information processing in sensor networks, 404-409.

DasGupta, A. (1996) Review of optimal Bayes Designs. Handbook of Statistics. Vol. 13, S0169-7161(96)13031-5. Elsevier.

de Haij, M. and Wauben, W. (2010) Investigations into the improvement of automated precipitation type observations at KNMI, De Bilt. Royal Netherlands Meteorological Institute – KNMI. De Bilt, The Netherlands.

de Vos, L., Leijnse, H., Overeem, A. and Uijlenhoet, R. (2017) The potential of urban rainfall monitoring with crowdsourced automatic weather stations in Amsterdam, Hydrology and Earth Systems Sciences, vol. 21, pp. 765-777. 10.5194/hess-21-765-2017.

Deb, K., Mohan, M. and Mishra, S. (2002) A Fast and Elitist Multi-objective Genetic Algorithm: NSGA-II, IEEE Transaction on evolutionary computation, pp. 182-197. 10.1109/4235.996017.

Deb, K., Mohan, M. and Mishra, s. (2005) A fast multi-objective evolutionary algorithm for finding well-spread Pareto-optimal solutions, Evolutionary Computation, pp. 501-526.

Delhomme, J. P. (1973) Kriging in the Hydrosciences. Advances in Water Resources, vol. 1, no. 5, pp. 251-266. 10.1016/0309-1708(78)90039-8.

Dent, J.E. (2012) Climate and meteorological information requirements for water management: A review of issues. World Meteorological Organization (WMO). Geneva, Switzerland.

Deutsch, C.V. and Journel, A.G. (1998) GSLIB: Geostatistical software library and user's guide, Oxford University Press. Oxford, UK.

Devia, G.K., Ganasri, B.P. and Dwarakish, G.S. (2015) A Review on Hydrological Models, Aquatic Procedia, vol. 4, pp. 1001-1007. 10.1016/j.aqpro.2015.02.126.

Di Baldassarre, G., Montanari, A., Lins, H., Koutsoyiannis, D., Brandimarte, L. and Blöschl, G. (2010) Flood fatalities in Africa: From diagnosis to mitigation, Geophysical Research Letters, vol. 37, p. L22402. 10.1029/2010GL045467.

Dickey, D.A. and Fuller, W.A. (1979) Distribution of the estimators for autoregressive time series with a unit root, Journal of the American statistical association, vol. 74, pp. 427-431. 10.2307/2286348.

Dogulu, N., López López, P., Solomatine, D.P., Weerts, A.H. and Shrestha, D.L. (2015) Estimation of predictive hydrologic uncertainty using the quantile regression and UNEEC methods and their comparison on contrasting catchments, Hydrology and Earth Sciences systems, pp. 3181-3201. 10.5194/hess-19-3181-2015

Dong, X., Dohmen-Janssen, C.M. and Booij, M.J. (2005) Appropriate spatial sampling of rainfall for flow simulation, Hydrological Sciences Journal, vol. 50, pp. 279-298. 10.1623/hysj.50.2.279.61801.

Dubois, D. and Prade, H. (1993) Belief revision and updates in numerical formalisms: an overview, with new results for the possibilistic framework, Proceedings of the 13th International Joint Conference on Artifical Intelligence - IJCAI, Vol 1, 620-625.

Environment Canada (2010) Audit of the national hydrometric program. Environment and Climate Change Canada.

EPA (2002) Guidance on choosing a sampling design for environmental data collection. United States Environmental Protection Agency. Washington, USA.

Ephraty, A., Tabrikian, J. and Messer, H. (2001) Underwater source detection using spatial stationarity test, Journal of the acoustic society of America, vol. 109, pp. 1053-1063. 10.1121/1.1349536.

Espinosa, B., Hromadka, T.V. and Perez, R. (2015) Comparison of radar data versus rainfall data, Methods X, vol. 2, pp. 423-431. 10.1016/j.mex.2015.10.007.

EU Commission (2000) EU Water Framework Directive. Directive 2000/60/EC, Brussels, Belgium.

EU Commission (2012) A new EU floods directive. Flood Action Programme.

Fahle, M., Hohenbrink, T.L., Dietrich, O. and Lischeid, G. (2015) Temporal variability of the optimal monitoring setup assessed using information theory, Water Resources Research, vol. 51, Sep, pp. 7723-7743. 10.1002/2015wr017137.

Fedorov, V.V. and Hackl, P. (1997) Model-Oriented Design of Experiments, Springer New York.

Ferri, M., Baruffi, F., Norbiato, D., Monego, M., Tomei, G., Solomatine, D., Alfonso, L., Mazzoleni, M., Chacon, J.C., Wehn, U. and Ciravegna, F. (2016) Citizen observatory of water as a data engine supporting the people-hydrology nexus: experience of the WeSenseIt project, EGU General assembly, Vienna.

Filho, C.J.A.B., Lima-Neto, F.B.d., Lins, A.J.C., Nascimento, A.I.S. and Lima, M.P. (2008) A novel search algorithm based on fish school behavior, Systems, Man and Cybernetics, SMC 2008. IEEE International Conference, 2646-2651.

Fisher, R.A. (1974) The design of experiments, Hafner Press. New York, USA.

Franz, K.J. and Hogue, T.S. (2011) Evaluating uncertainty estimates in hydrologic models: borrowing measures from the forecast verification community, Hydrology and Earth System Sciences, vol. 15, pp. 3367-3382. 10.5194/hess-15-3367-2011.

Fuentes, M. (2005) A formal test for nonstationarity of spatial stochastic processes, Journal of Multivariate Analysis, vol. 96, Sep, pp. 30-54. 10.1016/j.jmva.2004.09.003.

Fuentes, M., Chaudhuri, A. and Holland, D.H. (2007) Bayesian entropy for spatial sampling design of environmental data, Environmental and Ecological Statistics, vol. 14, pp. 323-340. 10.1007/s10651-007-0017-0.

Gallo, M.A. and Hancock, W.M. (2002) Networking Explained, Elsevier Science.

Garcia, M., Peters-Lidard, C.D. and Goodrich, D.C. (2008) Spatial interpolation of precipitation in a dense gauge network for monsoon storm events in the southwestern United States, Water Resources Research, vol. 44, Mar. 10.1029/2006wr005788.

Geem, Z., Kim, J. and Loganathan, G. (2001) A New Heuristic: Harmony Search, Simulation, pp. 60-68. 10.1177/003754970107600201.

Genton, M.G. and Kleiber, W. (2015) Cross-Covariance functions for multivariate geostatistics, Statistical Science, vol. 30, no. 2, pp. 147-163. 10.1214/14-STS487.

Gharesifard, M. and When, U. (2016) To share or not to share: Drivers and barriers for sharing data via online amateur weather networks, Journal of Hydrology, vol. 535, pp. 181-190. 10.1016/j.jhydrol.2016.01.036.

Gharesifard, M. and When, U. (2017) What drives citizens to engage in ICT-Enabled citizen science? Case study of amateur weather networks, IGI Global, 62-88. 10.4018/978-1-5225-0962-2.ch004

Giuli, D., Toccafondi, A., Biffi Gentili, G. and Freni, A. (1991) Tomographic Reconstruction of Rainfall Fields through Microwave Attenuation Measurements, Journal of Applied Meteorology, vol. 30, Sep, pp. 1323-1340. 10.1175/1520-0450(1991)0302.0.CO;2.

Goldberg, D. (1989) Genetic algorithms in search, optimization, and machine learning, Adison-Wesley Professional.

Grabs, W. and Thomas, A.R. (2001) Report of the GCOS/GTOS/HWRP expert meeting on the implementation of a global terrestrial network – hydrology (GTN-H). Report GCOS 71, GTOS 29.

Gray, R.M. and Neuhoff, D.L. (1998) Quantization, IEEE Transactions on Information Theory, vol. 44, Oct, pp. 2325-2380. 10.1109/18.720541.

Grimes, D.I.F., Pardo-Iguzquiza, E. and Bonifacio, R. (1999) Optimal areal rainfall estimation using raingauges and satellite data, Journal of Hydrology, vol. 222, pp. 93-108.

Guestrin, C., Krause, A. and Singh, A. (2005) Near-Optimal sensor placements in Gaussian processes. Proceedings of the 22 International Conference on Machine Learning, Bonn, Germany, 2005.

Gupta, H.V., Kling, H., Yilmaz, K.K. and Martinez, G.F. (2009) Decomposition of the mean squared error and NSE performance criteria: Implications for improving hydrological modelling, Journal of Hydrology, vol. 377, Oct, pp. 80-91. 10.1016/j.jhydrol.2009.08.003.

Guttorp, P., Le, N.D., Sampson, P.D. and Zidek, J.V. (1993) Using entropy in the redesign of an environmental monitoring network, Multivariate Environmental Statistics.

Haberlandt, U. and Sester, M. (2010) Areal rainfall estimation using moving cars as rain gauges - a modelling study, Hydrology and Earth System Sciences, vol. 14, pp. 1139-1151. 10.5194/hess-14-1139-2010.

Halverson, M. and Fleming, S. (2015) Complex network theory, streamflow and hydrometric monitoring system design, hydrology and Earth System Sciences, pp. 3301-3318. 10.5194/hess-19-3301-2015.

Hannachi, A., Jolliffe, L.T. and Stephenson, D.B. (2007) Empirical orthogonal functions and related techniques in atmospheric science: A review, International Journal of Climatology, vol. 27, pp. 1119-1152. 10.1002/joc.1499.

Harmancioglu, N. and Yevjevich, V. (1985) Transfer of hydrologic information along rivers partially fed by Karstified limestones, Karst Water Resources.

Harris, P., Charlton, M. and Fotheringham, A.S. (2010) Moving window kriging with geographically weighted variograms, Stochastic Environmental Research and Risk Assessment, vol. 24, no. 8, pp. 1193-1209. 10.1007/s00477-010-0391-2.

Hart, J.K. and Martinez, K. (2006) Environmental sensor networks: A revolution in the earth system science, Earth-Science reviews, vol. 78, pp. 177-191. 10.1016/j.earscirev.2006.05.001.

Hass, T. (1996) Multivariate spatial prediction in the presence of non-linear trend and covariance non-stationarity, Environmetrics, vol. 7, no. 2, pp. 145-165. 10.1002/(SICI)1099-095X(199603)7:23.0.CO;2-T.

Hassan, E.a.A.A., Sharif, H.O., Jackson, T. and Chintalapudi, S. (2013) Performance of a conceptual and physically based model in simulating the response of a semi-urbanized watershed in San Antonio, Texas, Hydrological Processes, vol. 27, pp. 3394-3408. 10.1002/hyp.9443.

Herrnegger, M., Nachtnebel, H.P. and Schulz, K. (2015) From runoff to rainfall: inverse rainfall runoff modelling in a high temporal resolution, Hydrology and Earth System Sciences, vol. 19, pp. 4619-4639. 10.5194/hess-19-4619-2015.

Herzberg, A.M., Wynn, H.P., Fedorov, V.V., Studden, W.J. and Klimko, E.M. (1972) Theory of Optimal Experiments., Biometrika, vol. 59, Dec, p. 697. 10.2307/2334826.

Higdon, D., Swall, J. and Kern, J. (1998) Non-stationary spatial modelling, Bayesian Statistics, vol. 6.

Hirshleifer, J. and Riley, J. (1979) The Analytics of Uncertainty and Information- An Expository Survey. UCLA Economics Working Papers, UCLA Department of Economics.

Holawe, F. and Dutter, R. (1999) Geostatistical study of precipitation series in Austria: time and space, Journal of Hydrology, vol. 219, pp. 70-82. 10.1016/S0022-1694(99)00046-3.

Howard, R. (1966) Information Value Theory, IEEE Transactions on Systems Science and Cybernetics, vol. 2, pp. 22-26. 10.1109/tssc.1966.300074.

Husain, T. (1987) Hydrologic network design formulation, Canadian Water Resources Journal, vol. 12, pp. 44-63. 10.4296/cwrj1201044.

Hutchinson, M.F. (1995) Interpolating mean rainfall using thin plate smoothing splines, International journal of geographical information systems, vol. 9, Jul, pp. 385-403. 10.1080/02693799508902045.

Huwald, H., Barrenetxea, G., de Jong, S., Ferri, M., Carvalho, R., Lanfranchi, V., McCarthy, S., Glorioso, G., Prior, S., Solà, E., Gil-Roldàn, E., Alfonso, L., Montalvo, U.W., Onencan, A., Solomatine, D. and Lobbrecht, A. (2013) D1.11 Sensor technology requirement analysis. FP7 WeSenseIt internal report.

Huwald, H., Brauchli, T.J. and Weijs, S. (2016) Sensing Technology for Citizen Observatories - The WeSenseIt Project, Intl. Conference on Citizen Observatories for Water Management, , Venice, Italy.

Izquierdo, J., Montalvo, I., Perez, R. and Fuentes, V. (2008) Design optimization of waste water collection networks by PSO, Applied Computational Mathematics, pp. 777-784. 10.1016/j.camwa.2008.02.007.

Jariboui, B., Cheikh, M., Siarry, P. and Rebai, A. (2007) Combinatorial particle swarm optimization (CPSO) for partitional clustering problem, Applied Mathematics and Computation, pp. 337-345. 10.1016/j.amc.2007.03.010.

Jaynes, E.T. (1957) Information theory and statistical mechanics, The Physical Review, vol. 106, pp. 620-630. 10.1103/PhysRev.106.620.

Jaynes, E.T. (1988) The relation of Bayesian and Maximum Entropy methods, Maximum-Entropy and Bayesian Methods in Science and Engineering, vol. 1, pp. 25-29. 10.1007/978-94-009-3049-0_2

Jonkman, S.N. (2005) Global perspectives on loss of human life caused by floods, Natural Hazards, vol. 34, pp. 151-175. 10.1007/s11069-004-8891-3.

Journel, A.G. and Alabert, F. (1989) Non-Gaussian data expansion in the Earth Sciences, Terra Nova, vol. 1, pp. 123-134. 10.1111/j.1365-3121.1989.tb00344.x.

Journel, A.G. and Huijbregts, C.J. (1978) Mining geostatistics, Academic Press, London.

Jun, M. and Genton, M.G. (2012) A test for stationarity of spatio-temporatl random fields on planar and spherical domains, Statistica Sinica, vol. 22, pp. 1737-1764. 10.5705/ss.2010.251.

Kamel Boulos, M., Resch, B., Crowley, D., Breslin, J., Sohn, G., Burtner, R., Pike, W., Jezierski, E. and Chuang, K.-Y. (2011) Crowdsourcing, citizen sensing and sensor web technologies for public and environmental health surveillance and crisis management: trends, OGC standards and application examples, International Journal of Health Geographics, vol. 10, p. 67. 10.1186/1476-072x-10-67.

Kanesvski, M., Pozdnoukhov, A. and Timonin, V. (2009) Machine learning for spatial environmental data, EPFL press. Lausanne, Switzerland.

Kanevski, M. (2008) Advanced Mapping Environmental Data, ISTE/Hermes Science Publishing.

Kanevski, M. (2010) Advanced Mapping of Environmental Data, 1st edition, John Wiley & Sons. Geneva, Switzerland.

Kang, J., Li, X., Jin, R., Ge, Y., Wang, J. and Wang, J. (2014) Hybrid Optimal Design of the Eco-Hydrological Wireless Sensor Network in the Middle Reach of the Heihe River Basin, China, Sensors, vol. 14, Oct, pp. 19095-19114. 10.3390/s141019095.

Karasseff, I.F. (1986) Principles of specifications of optimum networks of hydrologic observation sites, Integrated design of hydrological networks. Proceedings of the Budapest Symposium, July 1986. Budapest, Hungary.

Kennedy, J. and Eberhart, R. (1995) Particle Swarm Optimization, IEEE International conference on Neural Networks, Perth, WA, 1942-1948.

Khalleghi, B., Khamis, A., Karray, F. and Razavi, S. (2013) Multisensor data fusion: A review of the state-of-the-art, Information Fusion, vol. 14, no. 1, Oct, pp. 28-44. https://doi.org/10.1016/j.inffus.2011.08.001.

Kiefer, J. and Wolfowitz, J. (1985) Optimum Designs in Regression Problems, in Collected Papers III, Springer New York.

Kirk, R.E. (2009) The SAGE Handbook of Quantitative Methods in Psychology, SAGE PUBN.

Kirkpatrick, S., Gelatt, C. and Vecchi, M. (1983) Optimization by Simulated Annealing, Science, pp. 671-680.

Kitanidis, P.K. (1983) Orthonormal residuals in geostatistics: Model criticism and parameter estimation, Mathematical Geology, pp. 909-921. 10.1007/BF02082534.

Kitanidis, P.K. (1993) Generalized covariance functions in estimation, Mathematical Geology, vol. 25, no. 5, pp. 525-540. 10.1007/BF00890244.

Knapp, H. and Markus, M. (2003) Evaluation of the Illinois streamflow gaging network. Illinois department of natural resources.

Kollat, J. and Reed, P. (2006) Comparing state-of-the-art evolutionary multi-objective algorithms for long-term groundwater monitoring design, Advances in Water Resources, pp. 792-807. 10.1016/j.advwatres.2005.07.010.

Kollat, J.B., Reed, P.M. and Maxwell, R.M. (2011) Many-objective groundwater monitoring network design using bias-aware ensemble Kalman filtering, evolutionary optimization and visual analytics, Water Resources Research, vol. 47, p. W02529. 10.1029/2010WR009194.

Kolmogorov, A.N. (1965) Three approaches to the quantitative definition of information, Problemy Peredachi Informatsii, vol. 1, pp. 3-11.

Kotecha, P.R., Bushan, M., Gudi, R.D. and Keshari, M.K. (2008) A duality based framework for integrating reliability and precision for sensor network design, Journal of Process Control, vol. 18, pp. 189-201. j.jprocont.2007.06.005.

Krajewski, W.F. and Duffy, C.J. (1986) Estimation of the covariance and semivariogram for stationary, isotropic random fields. Proceedings of the Budapest Symposium, July 1986. Budapest, Hungary.

Krause, P., Boyle, D.P. and Bäse, F. (2005) Comparison of different efficiency criteria for hydrological model assessment, Advances in Geosciences, vol. 5, pp. 89-97. 10.5194/adgeo-5-89-2005.

Krstanovic, P.F. and Singh, V.P. (1992a) Evaluation of rainfall networks using Entropy: I. Theoretical development, Water Resources Management, vol. 6, pp. 279-293. 10.1007/BF00872281.

Krstanovic, P.F. and Singh, V.P. (1992b) Evaluation of rainfall networks using Entropy: II. Application, Water Resources Management, vol. 6, pp. 295-314. 10.1007/BF00872282.

Kunstmann, H., Krause, J. and Mayr, S. (2006) Inverse distributed hydrological modelling of Alpine catchments, Hydrology and Earth System Sciences, vol. 10, pp. 395-412. 10.5194/hess-10-395-2006.

Kwiatkowski, D., Phillips, P.C.B., Schimidt, P. and Shin, Y. (1992) Testing the null hypothesis of stationarity against the alternative of a unit root: How sure are we that economic time series have a unit root?, Journal of econometrics, vol. 54, pp. 159-178. 10.1016/0304-4076(92)90104-Y.

Lahoz, W.A. and Schneider, P. (2014) Data assimilation: making sense of Earth Observation, Frontiers in Environmental Science, vol. 2, May. 10.3389/fenvs.2014.00016.

Laize, C.L.R. (2004) Integration of spatial datasets to support the review of hydrometric networks and the identification of representative catchments, Hydrology and Earth System Sciences, vol. 8, pp. 1103-1117. 10.5194/hess-8-1103-2004.

Lanfranchi, V., Ireson, N., Wehn, U., Wrigley, S.N. and Ciravegna, F. (2014) Citizens' observatories for situation awareness in flooding, Proceeding of the 11th international ISCRAM conference.

Leach, J.M., Kornelsen, K.C., Samuel, J. and Coulibaly, P. (2015) Hydrometric network design using streamflow signatures and indicators of hydrologic alteration, Journal of Hydrology, vol. 529, Oct, pp. 1350-1359. 10.1016/j.jhydrol.2015.08.048.

Lee, S.-I. (1997) Geostatistical model validation using orthonormal residuals, Journal of Civil Engineering, vol. 1, no. 1, pp. 59-66. 10.1007/BF02830464.

Leijnse, H., Uijlenhoet, R. and Stricker, J. (2007) Rainfall measurement using radio links from cellular communication networks, Water Resources Research, vol. 43, p. W03201. 10.1029/2006WR005631.

Levene, H. (1960) Robust test for equality of variances. Contributions to Probability and Statistics: Essays in Honor of Harold Hotelling, 1st edition, Stanford: Stanford University.

Leybourne, S.J. and McCabe, B.P.M. (1994) A consistent test for a unit root, Journal of business and economic statistics, vol. 12, pp. 157-166. 10.1080/07350015.1994.10510004.

Leybourne, S.J. and McCabe, B.P.M. (1999) Modified stationarity t-test with data-dependent model selection rules, Journal of business and economic statistics, vol. 17, pp. 264-270. 10.1080/07350015.1999.10524816.

Liang, X., Lettenmaier, D.P., Wood, E.F. and Burges, S.J. (1994) A simple hydrologically based model of land surface water and energy fluxes for general circulation models, Journal of Geophysical Research, vol. 99, p. 14415. 10.1029/94jd00483.

Li, J. and Heap, A.D. (2011) A review of comparative studies of spatial interpolation methods in environmental sciences: Performance and impact factors, Ecological Informatics, vol. 6, Jul, pp. 228-241. 10.1016/j.ecoinf.2010.12.003.

Lindley, D.V. (1956) On a measure of the information provided by an experiment, The Annals of Mathematical Statistics, vol. 27, Dec, pp. 986-1005. 10.1214/aoms/1177728069. 10.1214/aoms/1177728069.

Lindström, G., Johansson, B., Persson, M., Gardelin, M. and Bergström, S. (1997) Development and test of the distributed HBV-96 hydrological model, J. Hydrol., vol. 201, pp. 272-288. 10.1016/S0022-1694(97)00041-3.

Li, C., Singh, V.P. and Mishra, A.K. (2012) Entropy theory-based criterion for hydrometric network evaluation and design: Maximum information minimum redundancy, Water Resources Research, vol. 48, p. W05521. 10.1029/2011WR011251.

Liu, B., Brass, P., Dousse, O., Nain, P. and Towsley, D. (2005) Mobility improves coverage of sensor networks, Proceedings of the 6th ACM international symposium on Mobile ad hoc networking and computing. Urbana-Champaign, IL, USA.

Liu, Y., Weerts, A.H., Clark, M., Franssen, H.-J.H., Kumar, S., Moradkhani, H., Seo, D.-J., Schwanenberg, D., Smith, P., Dijk, A.I.J.M., Velzen, N., He, M., Lee, H., Noh, S.J., Rakovec, O. and Restrepo, P. (2012) Advancing data assimilation in operational hydrologic forecasting: progresses, challenges, and emerging opportunities, Hydrology and Earth System Sciences, vol. 16, Oct, pp. 3863-3887. 10.5194/hess-16-3863-2012.

Lloyd, C.D. (2009) Nonstationary models for exploring and mapping monthly precipitation in the United Kingdom, International Journal of Climatology, vol. 30, no. 3, pp. 390-405. 10.1002/joc.1892.

Loquin, K. and Dubois, D. (2010) Kriging and epistemic uncertainty: a critical discussion, in Methods for Handling Imperfect Spatial Information, Studies in Fuzziness and Soft Computing, vol 256. Springer, Berlin, Heidelberg. 10.1007/978-3-642-14755-5_11.

Loucks, D.P. and van Beek, E. (2017) Water resources systems planning and management, Cham, Switzerland: Springer Nature.

Loucks, D.P., van Beek, E., Stedinger, J., Dijkman, J.P.M. and Villars, M.T. (2005) Water resources systems planning and management, UNESCO Publishing.

Lovejoy, S. and Mandelbrot, B.B. (1985) Fractal properties of rain, and a fractal model, Tellus, vol. 37A, pp. 209-232. 10.3402/tellusa.v37i3.11668.

Lovejoy, S. and Schertzer, D. (1985) Generalized scale invariance in the atmosphere and fractal models of rain, Water Resources Research, vol. 21, pp. 1233-1250. 10.1029/WR021i008p01233.

Lovejoy, S., Schertzer, D. and Ladoy, P. (1986) Fractal characterization of inhomogeneous geophysical measuring networks, Nature, vol. 319, pp. 43-44. 10.1038/319043a0.

Maddock, T. (1974) An optimum reduction of gauges to meet data program constraints, Hydrological Sciences Bulletin, vol. 19, Sep, pp. 337-345. 10.1080/02626667409493920.

Mades, D. and Oberg, K. (1986) Evaluation of the US Geological Survey Gaging Station Network in Illinois. US Geological Survey Water-Resources investigations Report 84-4123, Illinois District, Urbana, IL, USA.

Mandelbrot, B.B. (2001) Gaussian Self-Affinity and Fractals, Springer-Verlag New York.

Maniezzo, V. and Roffilli, M. (2008) Very Strongly Constrained Problems: An Ant Colony Optimization Approach, Cybernetics and Systems, pp. 295-424. 10.1080/01969720802039560.

Mardia, K.V., Goodall, C., Redfern, E.J. and Alonso, F.J. (1998) The Kriged Kalman filter, Sociedad de estadística e Investigación operativa Test, vol. 7, pp. 217-285. 10.1007/BF02565111.

Marsh, T. (2010) The UK Benchmark network – Designation, evolution and application, 10th symposium on stochastic hydraulics and 5th international conference on water resources and environment research, Quebec, Canada.

Mazzarella, A. and Tranfaglia, G. (2000) Fractal characterisation of geophysical measuring networks and its implication for an optimal location of additional stations: An application to a rain-gauge network, Theoretical and Applied Climatology, vol. 65, pp. 157-163.

Mazzetti, C. and Todini, E. (2009) Combining weather radar and raingauge data for hydrologic applications, in flood risk management: research and practice. CRC Press, Leiden, The Netherlands.

Mazzoleni, M., Alfonso, L., Chacon-Hurtado, J. and Solomatine, D. (2015) Assimilating uncertain, dynamic and intermittent streamflow observations in hydrological models, Advances in Water Resources, vol. 83, Sep, pp. 323-339. 10.1016/j.advwatres.2015.07.004.

Mazzoleni, M., Alfonso, L. and Solomatine, D. (2016) Influence of spatial distribution of sensors and observation accuracy on the assimilation of distributed streamflow data in

hydrological modelling, Hydrological Sciences Journal, Oct, pp. 1-19. 10.1080/02626667.2016.1247211.

Mazzoleni, M., Cortez-Arevalo, V., Wehn, U., Alfonso, L., Norbiato, D., Monego, M., Ferri, M. and Solomatine, D. (2018) Exploring the influence of citizen involvement on the assimilation of crowdsourced observations: A modelling study based on the 2013 flood event in the Bacchiglione catchment (Italy), Hydrology and Earth Systems Science, vol. 22, pp. 391-416. 10.5194/hess-22-391-2018

Mazzoleni, M., Verlaan, M., Alfonso, L., Monego, M., Norbiato, D., Ferri, M. and Solomatine, D.P. (2017) Can assimilation of crowdsourced data in hydrological modelling improve flood prediction?, Hydrology and Earth System Sciences, vol. 21, Feb, pp. 839-861. 10.5194/hess-21-839-2017.

McDougall, K. and Temple-Watts, P. (2012) The use of LIDAR and volunteered geographic information to map flood extents and inundation, XXII ISPRS Congress, Melbourne, Australia, 251-256.

McKay, M., Beckman, R. and Conover, W. (1979) A comparison of three methods for selecting values of input variables in the analysis of output form a computer code, Technometrics, pp. 239-245. 10.2307/1268522.

Melles, S.J., Heuvelink, G.B.M., Twenhöfel, C.J.W., van Dijk, A., Hiemstra, P., Baume, O. and Stöhlker, U. (2009) Optimization for the design of environmental monitoring networks in routine and emergency settings, StatGIS Conference Proceedings, Milos, 1-6.

Melles, S.J., Heuvelink, G.B.M., Twenhöfel, C.J.W., Dijk, A., Hiemstra, P.H., Baume, O. and Stöhlker, U. (2011) Optimizing the spatial pattern of networks for monitoring radioactive releases, Computers & Geosciences, vol. 37, pp. 280-288. 10.1016/j.cageo.2010.04.007.

Mernik, M., Liu, S.-H., Karaboga, D. and Črepinšek, M. (2015) On clarifying misconceptions when comparing variants of the Artificial Bee Colony Algorithm by offering a new implementation, Information Sciences, vol. 291, no. 1, Jan, pp. 115-127. 10.1016/j.ins.2014.08.040.

Merriam-Webster's (2013) Merriam Webster's Dictionary: Sensor, Feb. http://dictionary.reference.com/browse/sensor.

Messer, H., Zinevich, A. and Alpert, P. (2006) Environmental monitoring by wireless communication networks, Science, vol. 312. 10.1126/science.1120034.

Michaelides, S., Levizzani, V., Anagnostou, E., Bauer, P., Kasparis, T. and Lane, J.E. (2009) Precipitation: Measurement, remote sensing, climatology and modeling, Atmospheric Research, vol. 94, Dec, pp. 512-533. 10.1016/j.atmosres.2009.08.017.

Mishra, A.K. and Coulibaly, P. (2009) Developments in hydrometric network design: A review, Reviews of Geophysics, vol. 47, p. RG2001. 10.1029/2007RG000243.

Mogheir, Y. and Singh, V.P. (2002) Application of Information Theory to groundwater quality monitoring networks, Water Resources Management, vol. 16, pp. 37-49. 10.1023/a:1015511811686.

Montgomery, D.C. (2012) Design and Analysis of Experiments, John Wiley & Sons, Inc.

Moore, R., Jones, D., Cox, D. and Isham, V. (2000) Design of the HYREX raingauge network, Hydrology and Earth System Sciences, pp. 521-530. 10.5194/hess-4-521-2000.

Morrissey, M.L., Maliekal, J.A., Greene, J.S. and Wang, J. (1995) The uncertainty of simple spatial averages using rain gauge networks, Water Resources Research, vol. 31, pp. 2011-2017. 10.1029/95WR01232.

Moss, M., Gilroy, E., Tasker, G. and Karlinger, M. (1982) Design of surface water data networks for regional information. U.S. Dept. of the Interior, Geological Survey. 10.3133/wsp2178.

Moss, M.E. and Karlinger, M.R. (1974) Surface water network design by regression analysis simulation, Water Resources Research, vol. 10, Jun, pp. 427-433. 10.1029/wr010i003p00427.

Moss, M.E. and Tasker, G.D. (1991) An intercomparison of hydrological network-design technologies, Hydrological Sciences Journal, vol. 36, Jun, pp. 209-221. 10.1080/02626669109492504.

Moussa, R. and Chahinian, N. (2009) Comparison of different multi-objective calibration criteria using a conceptual rainfall-runoff model of flood events, Hydrology and Earth System Sciences, vol. 13, Apr, pp. 519-535. 10.5194/hess-13-519-2009.

Nash, J.E. and Sutcliffe, I.V. (1970) River flow forecasting through conceptual models part 1 - A discussion of principles, Journal of Hydrology, vol. 10, pp. 282-290. 10.1016/0022-1694(70)90255-6.

Neal, J.C., Atkinson, P.M. and Hutton, C.W. (2012) Adaptive space-time sampling with wireless sensor nodes for flood forecasting, Journal of Hydrology, vol. 414-415, pp. 136-147. 10.1016/j.jhydrol.2011.10.021.

Nelder, J. and Mead, R. (1965) A Simplex Method for Function Minimization, The Computer Journal, pp. 308-313. 10.1093/comjnl/7.4.308.

Nemec and Askew, A.J. (1986) Mean and variance in network design philosophies, Proceedings of the Budapest Symposium, July 1986. Budapest, Hungary.

New, M., Todd, M., Hulme, M. and Jones, P. (2001) Precipitation measurements and trends in the twentieth century, International Journal of Climatology, vol. 21, Dec, pp. 1889-1922. 10.1002/joc.680.

Nguyen, D. and Bagajewicz, M.J. (2010) New sensor network design and retrofit method based on value of information, American Institute of Chemical Engineers, vol. 57, Nov, pp. 2136-2148. 10.1002/aic.12440.

Nguyen, D.Q. and Bagajewicz, M.J. (2011) New sensor network design and retrofit method based on value of information, American Institute of Chemical Engineers, vol. 57, pp. 2136-2148.

NOAA (1998) Automated Surface Observing System (ASOS): User's Guide.

Nott, D.J. and Dunsmuir, W.T.M. (2002) Estimation of non-stationarity spatial covariance structure, Biometrika, vol. 89, pp. 819-829.

Nowak, W., Barros, F.P.J. and Rubin, Y. (2010) Bayesian geostatistical design: Task-driven optimal site investigation when the geostatistical model is uncertain, Water Resources Research, vol. 46, p. W03535. 10.1029/2009WR008312.

NRC (2004) Committee on Review of the USGS National Streamflow Information Program.

Ortiz, E. and Guna, V. (2009) Distributed hydrological models: comparison between TOPKAPI, a physically based model and TETIS, a conceptually based model, EGU General Assembly Conference Abstracts.

Overeem, A., Leijnse, H. and Uijlenhoet, R. (2011) Measuring urban rainfall using microwave links from commercial cellular communication networks, Water Resources Research, vol. 47, p. W12505. 10.1029/2010WR010350.

Overeem, A., Leijnse, H. and Uijlenhoet, R. (2012) Country-wide rainfall maps from a commercial cellular telephone network, EGU General Assembly 2012.

Pardo-Igúzquiza, E. (1998) Optimal selection of number and location of rainfall gauges for areal rainfall estimation using geostatistics and simulated annealing, Journal of Hydrology, vol. 210, pp. 206-220. 10.1016/S0022-1694(98)00188-7.

Pearson, C.P. (1998) Changes to the New Zealand's national hydrometric network in the 1990s, Journal of Hydrology, vol. 37, pp. 1-17.

Penfeld, P. (2003) Course notes on Information and Entropy: Principle of Maximum Entropy. http://www.mtl.mit.edu/Courses/6.050/2003/notes/chapter10.pdf.

Pham, H.V. and Tsai, F.T.-C. (2016) Optimal observation network design for conceptual model discrimination and uncertainty reduction, Water Resources Research, vol. 52, Feb, pp. 1245-1264. 10.1002/2015wr017474.

Pongchairerks, P. and Kachitvichyanukul, V. (2009) A particle swarm optimization algorithm on job-shop scheduling problems with multi-purpose machines, APJOR, pp. 161-184. 10.1142/S0217595909002158.

Popper, K. (1963) Science: Conjectures and Refutations, Routledge - Taylor and Francis group.

Priestley, M.B. and Subba-Rao, T. (1969) Non-stationarity of time series, Journal of the royal statistical society. Series B (Methodological), vol. 31, pp. 140-149. 10.1111/j.2517-6161.1969.tb00775.x.

Pryce, R.S. (2004) Review and Analysis of Stream Gauge Networks for the Ontario Stream Gauge Rehabilitation Project. Trent University, Watershed Science Centre. WSC Report No. 01-2004. Prepared for the Ontario Ministry of Natural Resources and Forestry.

Pukelsheim, F. (2006) Optimal design of experiments, Society for industrial and applied mathematics. Societyfor Industrial and Applied Mathematics –SIAM, 10.1137/1.9780898719109. John Wiley & Sons, New York, USA.

Putter, H. and Young, G.A. (2001) On the effect of covariance function estimation on the accuracy of Kriging predictors, Bernoulli, vol. 7, no. 3, pp. 421-438. 10.2307/3318494.

Rafiee, M., Barrau, A. and Bayen, A. (2012) State estimation in large-scale open channel networks using particle filters, IEEE 2012 American Control Conference (ACC). 10.1109/ACC.2012.6315186.

Rayitsfeld, A., Samuels, R., Zinevich, A., Hadar, U. and Alpert, P. (2012) Comparison of two methodologies for long term rainfall monitoring using a commercial microwave communication system, Atmospheric Research, vol. 104-105, pp. 119-127. 10.1016/j.atmosres.2011.08.011.

Rebonato, R. and Jaeckel, P. (2011) The most general methodology to create a valid correlation matrix for risk management and option pricing purposes, SSRN. 10.2139/ssrn.1969689.

Reed, P.M., Hadka, D., Hermana, J.D., Kasprzyka, J.R. and J.B.Kollat (2013) Evolutionary multiobjective optimization in water resources: The past, present, and future, Advances in Water Resources, vol. 51, no. 1, January, pp. 438-456. https://doi.org/10.1016/j.advwatres.2012.01.005.

Ridolfi, E., Alfonso, L., Baldassarre, G.D., Dottori, F., Russo, F. and Napolitano, F. (2013) An entropy approach for the optimization of cross-section spacing for river modelling, Hydrological Sciences Journal, vol. 59, Nov, pp. 126-137. 10.1080/02626667.2013.822640.

Ridolfi, E., Montesarchio, V., Russo, F. and Napolitano, F. (2011) An entropy approach for evaluating the maximum information content achievable by an urban rainfall network, Natural Hazards and Earth System Sciences, vol. 11, pp. 2075-2083. 10.5194/nhess-11-2075-2011.

Rodriguez-Iturbe, I. and Mejia, J.M. (1974) The design of rainfall networks in time and space, Water Resources Research., vol. 10, pp. 713-728. 10.1029/WR010i004p00713.

Said, S.E. and Dickey, D.A. (1984) Testing for unit root in autoregressive-moving average models of unknown order, Biometrika, vol. 71, pp. 599-607. 10.2307/2336570.

Samper, F.J. and Neuman, S.P. (1989) Estimation of spatial covariance structures by adjoint state maximum likelihood cross validation: 1 Theory, Water Resources Research, vol. 25, no. 3, pp. 351-362. 10.1029/WR025i003p00351.

Sampson, P.D. and Guttorp, P. (1992) Nonparametric estimation of nonstationary spatial covariance structure, Journal of the American Statistical Association, vol. 87, pp. 108-119. 10.2307/2290458.

Samuel, J., Coulibaly, P. and Kollat, J. (2013) CRDEMO: Combined regionalization and dual entropy-multiobjective optimization for hydrometric network design, Water Resources Research, vol. 49, Dec, pp. 8070-8089. 10.1002/2013wr014058.

Sauvageot, H. (1994) Rainfall measurement by radar: a review, Atmospheric Research, vol. 35, Oct, pp. 27-54. 10.1016/0169-8095(94)90071-x.

Schmidt, A.M. and O'Hagan, A. (2003) Bayesian inference for non-stationary spatial covariance structure via spatial deformations, Journal of statistical society: Series B (Statistical methodology), vol. 65, pp. 743-758.

Schubert, E.F. (2006) Light Emitting Diodes, Cambridge University Press. Cambridge, UK.

Schuurmans, J.M., Bierkens, M.F.P., Pebesma, E.J. and Uijlenhoet, R. (2007) Automatic prediction of the high-resolution daily rainfall fields for multiple extents: The potential of operational radar, Journal of Hydrometeorology, vol. 8, pp. 1204-1224. 10.1175/2007JHM792.1.

Seibert, J. (1999) Conceptual Runoff Models - Fiction or representation of reality (comprehensive summaries of Uppsala dissertations), Uppsala Universitet. Uppsala, Sweden.

Shafiei, M., Ghahraman, B., Saghafian, B., Pande, S., Gharari, S. and Davary, K. (2014) Assessment of rain-gauge networks using a probabilistic GIS based approach, Hydrology Research, vol. 45, no. 4-5, pp. 551-562. 10.2166/nh.2013.042.

Shannon, C.E. (1948) A mathematical theory of communication, The Bell System Technical Journal, vol. 27, pp. 379-429. 10.1002/j.1538-7305.1948.tb01338.x

Shrestha, D.L., Kayastha, N. and Solomatine, D.P. (2009) A novel approach to parameter uncertainty analysis of hydrological models using neural networks, Hydrology and Earth System Sciences, vol. 13, pp. 1235-1248. 10.5194/hess-13-1235-2009.

Shrestha, D.L. and Solomatine, D.P. (2006) Machine learning approaches for estimation of prediction interval for the model output, Neural Networks, vol. 19, Mar, pp. 225-235. 10.1016/j.neunet.2006.01.012.

Sieber, C. (1970) A proposed streamflow data program for Illinois. US Geological Survey Water-Resources investigations Report 70-303, Illinois District, Urbana, IL, USA. 10.3133/ofr70303.

Singh, V.P. (2000) The entropy theory as a tool for modelling and decision making in environmental and water resources, Water SA, vol. 26.

Singh, V.P. (2013) Entropy Theory and its Application in Environmental and Water Engineering, 10.1002/9781118428306. John Wiley & Sons, Ltd.

Singh, K.P., Ramamurthy, G.S. and Terstriep, M.L. (1986) Illinois streamgaging network program: Related studies and results, Illinois State Water Survey. Surface Water Section at the University of Illinois. Illinois Department of Energy and Natural Resources. Illinois, USA.

Sivakumar, B. and Woldemeskel, F. (2014) Complex Networks for streamflow dynamics, Hydrology and Earth System Sciences, pp. 7255-7289. 10.5194/hess-18-4565-2014.

Sluiter, R. (2009) Interpolation methods for climate data, Internal report IR 2009-04. Royal Netherlands Meteorological Institute (KNMI). De Bilt, The Netherlands.

Soenario, I. and Sluiter, R. (2010) Optimization of rainfall interpolation, Internal report IR 2010-01. Royal Netherlands Meteorological Institute (KNMI). De Bilt, The Netherlands.

Solomatine, D. (1999) Two Strategies of Adaptive Cluster Covering with Descent and Their Comparison to Other Algorithms, Journal of Global Optimisation, pp. 55-78. 10.1023/A:1008334632441.

Solomatine, D. (2012) AMODEU: Adaptive modelling in heterogeneous time-varying (dynamic) data environments under uncertainty: research directions. Internal report IHE Delft. Delft, The Netherlands.

Solomatine, D.P. and Ostfeld, A. (2008) Data-driven modelling: some past experiences and new approaches, Journal of Hydroinformatics, vol. 10, Jan, p. 3. 10.2166/hydro.2008.015.

Solomatine, D.P. and Wagener, T. (2011) Hydrological Modeling , in Wilderer, P. (ed.) Treatise on Water Science , 10.1016/B978-0-444-53199-5.00044-0, Oxford: Elsevier.

Solomatine, D.P. and Xue, Y. (2004) M5 Model Trees and Neural Networks: Application to Flood Forecasting in the Upper Reach of the Huai River in China, Journal of Hydrologic Engineering, vol. 9, Nov, pp. 491-501. 10.1061/(asce)1084-0699(2004)9:6(491).

Song, C., Gallos, L.K., Havlin, S. and Makse, H.A. (2007) How to calculate the fractal dimension of a complex network: the box covering algorithm, J. Stat. Mech: Theory Exp., vol. 2007, p. P03006. 10.1088/1742-5468/2007/03/p03006.

Sorooshian, S., AghaKouchak, A., Arkin, P., Eylander, J., Foufoula-Georgiou, E., Harmon, R., Hendrickx, J.M.H., Imam, B., Kuligowski, R., Skahill, B. and Skofronick-Jackson, G. (2011) Advanced concepts on remote sensing of precipitation at multiple scales, American Meteorological Society, pp. 1353-1357. 10.1175/2011BAMS3158.1.

Starks, T.H. and Fang, J.H. (1982) On the estimation of the generalized covariance function, Mathematical Geology, vol. 14, no. 1, pp. 57-64. 10.1007/BF01037447.

Stedinger, J.R. and Tasker, G.D. (1985) Regional Hydrologic Analysis: 1. Ordinary, Weighted, and Generalized Least Squares Compared, Water Resources Research, vol. 21, Sep, pp. 1421-1432. 10.1029/wr021i009p01421.

Steuer, R., Kurths, J., Daub, C.O., Weise, J. and Selbig, J. (2002) The mutual information: Detecting and evaluating dependencies between variables, Bioinformatics, vol. 18, Oct, pp. S231--S240. 10.1093/bioinformatics/18.suppl_2.s231.

Sugawara, M. (1961) On the analysis of runoff structure about several Japanese River, Japanese journal of Geophysics.

Sun, L., Seidou, O., Nistor, I. and Liu, K. (2016) Review of the Kalman-type hydrological data assimilation, Hydrological Sciences Journal, vol. 61, Jul, pp. 2348-2366. 10.1080/02626667.2015.1127376.

Su, H.-T. and You, G.J.-Y. (2014) Developing an entropy-based model of spatial information estimation and its application in the design of precipitation gauge networks, Journal of Hydrology, vol. 519, Nov, pp. 3316-3327. 10.1016/j.jhydrol.2014.10.022.

Tait, A., Henderson, R., Turner, R. and Zheng, X. (2006) Thin plate smoothing spline interpolation of daily rainfall for New Zealand using a climatological rainfall surface, International Journal of Climatology, vol. 26, pp. 2097-2115. 10.1002/joc.1350.

Tarboton, D.G., Bras, R.L. and Puente, C.E. (1987) Combined hydrologic sampling criteria for rainfall and streamflow, Journal of Hydrology., vol. 95, pp. 323-339. 10.1016/0022-1694(87)90009-6.

Tasker, G. (1986) Generating efficient gauging plans for regional information, Integrated Design of hydrological Networks, Proceedings of the Budapest Symposium, July 1986. Budapest, Hungary.

Tayfur, G. (2017) Modern Optimization Methods in Water Resources Planning, Engineering and Management, Water Resources Management, vol. 31, no. 10, pp. 3205-3233. 10.1007/s11269-017-1694-6.

Terakawa, A. (2003) Hydrological Data Management: Present state and Trends. WMO- No. 964; Operational hydrology report (OHR)- No. 48, WMO. Geneva, Switzerland.

Thenkabail, P.S. (2015) Remote Sensing of Water Resources, Disasters, and Urban Studies: Volume 2 (Remote Sensing Handbook), CRC Press.

Thorndahl, S., Einfalt, T., Willems, P., Nielsen, J.E., Veldhuis, M.-C., Arnbjerg-Nielsen, K., Rasmussen, M.R. and Molnar, P. (2017) Weather radar rainfall data in urban hydrology, Hydrology and Earth System Sciences, vol. 21, Mar, pp. 1359-1380. 10.5194/hess-21-1359-2017.

TNO (1986) Design aspects of hydrological networks, TNO Committee on hydrological research. Netherlands Organisation for Applied Research.

Tserstou, A., Jonoski, A., Popescu, I., Herman-Assumpcao, T., Athanasiou, G., Kallioras, A. and Nichersu, I. (2017) SCENT: Citizen Sourced Data in Support of Environmental Modelling, 21st International Conference on Control Systems and Computer Science (CSCS), Bucharest, Romania, 612-616.

van de Beek, R., Lijnse, H., Torfs, P. and Uijlenhoet, R. (2009) Seasonal variation of rainfall variogram parameters in The Netherlands, EGU General Assembly, Vienna, Austria.

van Overloop, P.J., Kuijten, R., Klerk, W.J. and Vierstra, M. (2013) Mobile canal control, an automatic administration system for manual canal operations using smart-phone technology.

Veas, E., Grasset, R., Ferencik, I. and Grünewald, T. (2012) Mobile augmented reality for environmental monitoring, Personal and ubiquitous computing. Vol. 17-7, pp 1515-1531, 10.1007/s00779-012-0597-z.

Velasco-Forero, C.A., Sempere-Torres, D., Cassiraga, E.F. and Gomez-Hernández, J.J. (2009) A non-parametric automatic blending methodology to estimate rainfall fields from rain gauge and radar data, Advances in Water Resources, vol. 32, pp. 986-1002. 10.1016/j.advwatres.2008.10.004

Vivekanandan and Jagtap, R. (2012) Optimization of Hydrometric Network using Spatial Regression Approach, Bonfring International Journal of Industrial Engineering and Management Science, vol. 2, p. 56-61.

Volkmann, T. (2011) Inverse hydrological modelling of headwater basins with sensor network data. MSc Thesis. Hydrology institute of the Albert-Ludwig university of Freiburg.

Volkmann, T., Lyon, S., Gupta, H. and Troch, P. (2010) Multicriteria design of rain gauge networks for flash flood prediction in semiarid catchments with complex terrain, Water Resources Research, vol. 46, p. w11554. 10.1029/2010WR009145

Wackernagel, H. (1998) Multivariate Geostatistics, Springer, Berlin, Heidelberg.

Wagner, W., Verhoest, N. E. C., Ludwig, R., and Tedesco, M. (2009) Editorial "Remote sensing in hydrological sciences", Hydrology and Earth Systems Sciences, 13, 813-817, 10.5194/hess-13-813-2009.

Wahl and Crippen, J. (1984) A pragmatic Approach to evaluating a multipurpose stream-gaging network. USGS - Water Resources Investigations Report 84-4228. 10.3133/wri844228.

Walker, S. (2000) The value of hydrometric information in water resources management and flood control, Meteorological Applications, vol. 7, Dec, pp. 387-397. 10.1017/s1350482700001626.

Wehn, U. and Evers, J. (2015) The social innovation potential of ICT-enabled citizen observatories to increase e-Participation in local flood risk management, Technology in Society, pp. 187-198. https://doi.org/10.1016/j.techsoc.2015.05.002.

Wehn, U., Rusca, M., Evers, J. and Lanfranchi, V. (2015) Participation in flood risk management and the potential of citizen observatories: A governance analysis, Environmental Science and Policy, vol. 48, no. 1, April, pp. 225-236. 10.1016/j.envsci.2014.12.017.

Weyland, D. (2010) A rigorous analysis of the harmony search algorithm - how the research community can be misled by a "novel" methodology, International Journal of Metaheuristic Computing, pp. 50-60. 10.4018/jamc.2010040104.

Whitfield, P.H., Burn, D.H., Hannaford, J., Higgins, H., Hodgkins, G.A., Marsh, T. and Looser, U. (2012) Reference hydrologic networks I. The status and potential future directions of national reference hydrologic networks for detecting trends, Hydrological Sciences Journal, vol. 57, Nov, pp. 1562-1579. 10.1080/02626667.2012.728706.

Witayangkurn, A., Nagai, M., Honda, K., Dailey, M. and Shibasaki, R. (2011) Real time monitoring system using unmanned aerial vehicle integrated with sensor observation service, International archives of the photogrammetry, remote sensing and spatial information sciences, Conference on unmanned aerial vehicle in geomatics, 1-6.

WMO (2008) Guide to hydrological practices, Volume I: Hydrology - From measurements to hydrological information, World Meteorological Organization. Geneva, Switzerland.

WMO (2008a) Guide to Meteorological Instruments and Methods of Observation, World Meteorological Organization. Geneva, Switzerland.

WMO (2009) Guide to hydrological practices. Volume II: Management of water resources and application of hydrological practices, World Meteorological Organization. Geneva, Switzerland.

Wood, S.J., Jones, D.A. and Moore, R.J. (2000) Accuracy of rainfall measurement for scales of hydrological interest, Hydrology and Earth Sciences Systems, vol. 4, pp. 531-543. 10.5194/hess-4-531-2000.

Woolhiser, D.A. and Roldan, J. (1986) Seasonal and regional variability of parameters for stochastic daily precipitation models: South Dakota, U.S.A., Water Resources Research, vol. 22, pp. 965-978. 10.1029/WR022i006p00965.

Xiong, L. and OConnor, K.M. (2002) Comparison of four updating models for real-time river flow forecasting, Hydrological Sciences Journal, vol. 47, Aug, pp. 621-639. 10.1080/02626660209492964.

Xu, H., Xu, C.-Y., Chen, H., Zhang, Z. and Li, L. (2013) Assessing the influence of rain gauge density and distribution on hydrological model performance in a humid region of China , J. Hydrol., vol. 505, pp. 1-12. http://dx.doi.org/10.1016/j.jhydrol.2013.09.004.

Yang, Y. and Burn, D.H. (1994) An entropy approach to data collection network design, Journal of Hydrology, vol. 157, pp. 307-324. 10.1016/0022-1694(94)90111-2.

Yeh, H.-C., Chen, Y.-C., Wei, C. and Chen, R.-H. (2011) Entropy and kriging approach to rainfall network design, Paddy and Water Environment, vol. 9, pp. 343-355. 10.1007/s10333-010-0247-x.

Yilmaz, K.K., Hogue, T.S., Hsu, K.-l., Sorooshian, S., Gupta, H.V. and Wagener, T. (2005) Intercomparison of Rain Gauge, Radar, and Satellite-Based Precipitation Estimates with Emphasis on Hydrologic Forecasting, Journal of Hydrometeorology, vol. 6, Aug, pp. 497-517. 10.1175/jhm431.1.

Zeeuw, J.W. (1973) Hydrograph analysis for areas with mainly groundwater runoff, 1st edition, International Institute for Land Reclamation and Improvement (ILRI).

Zhang, G., Yang, L. and Qu, M. (2015) Assessing the local uncertainty of precipitation by using moving window geostatistical models, Ecological Informatics, vol. 30, pp. 133-141. 10.1016/j.ecoinf.2015.10.004.

Zidek, J.V., Sun, W. and Le, N.D. (2000) Designing and integrating composite networks for monitoring multivariate Gaussian pollution fields, Journal of the Royal Statistical Society: Series C (Applied Statistics), vol. 49, Feb, pp. 63-79. 10.1111/1467-9876.00179.

Zinevich, A., Alpert, P. and Messer, H. (2008) Estimation of rainfall fields using commercial microwave communication networks of variable density, Advances in Water Resources, vol. 312, pp. 1470-1480. 10.1016/j.advwatres.2008.03.003.

Zitzler E., Künzli S. (2004) Indicator-Based Selection in Multiobjective Search. In: Yao X. et al. (eds) Parallel Problem Solving from Nature - PPSN VIII. PPSN 2004. Lecture Notes in Computer Science, vol 3242. Springer, Berlin, Heidelberg

Zitzler, E., Laumanns, M. and Thiele, L. (2001) SPEA2: Improving the Strength Pareto Evolutionary Algorithm, Evolutionary Methods for Design, Optimization and Control with Applications to Industrial Problems. Proceedings of the EUROGEN 2001. Athens. Greece.

ANNEX 1. Overview of candidate algorithms for sensor network optimisation

An optimisation problem can be defined as the problem of finding a vector of decision variables that satisfies a set of constraints and minimises (or maximises) the value of a certain objective function. Depending on the number of objectives, optimisation problem can be categorised into single-objective (SOO), or multi-objective (MOO) optimisation. It has to be noted that the objective functions in MOO have to conflict, meaning that the optimality of one function affects the optimality of other, otherwise, the problem can be simplified to a SOO.

From this point of view, the design of a sensor network can be seen as an optimisation problem where the decision variables are the location of the sensors, and the objective functions are the optimality criteria. Applications of this type of tools are wide-spread into water resources, as they help to tackle large combinatorial problems (Mishra and Coulibaly 2009, Reed et al. 2013, Mishra and Coulibaly 2009, Tayfur 2017). In the particular case of precipitation sensor network design, SOO applications have been carried out (Pardo-Igúzquiza 1998, Chacón-Hurtado et al. 2009), or as a MOO problem (Samuel et al. 2013, Barca et al. 2015).

1.1 Random Search

Random search is one of the oldest methods for global optimization, as it does not require assumptions of any type in its implementation. The main drawback of this algorithm is inefficiency, and thus, its large demand on the number of function calls. This method is also known as the Monte Carlo optimisation. This method can be slightly boosted by using smart sampling strategies such as Latin Hypercube, which explores the decision space in a more efficient manner (McKay et al. 1979).

1.2 Evolutionary computation

Evolutionary computation aims to solve large optimization problems using artificial intelligence concepts (Goldberg 1989). These methods attempt to analytically determine the optimal solution of an optimisation problem by exploring the solution space in an iterative processes, which is usually rooted in concepts of biological evolution. These methods are also commonly known as metaheuristics. Among the most popular evolutionary computation algorithms are NSGAII (Deb et al. 2002), SPEAII (Zitzler et al. 2001, Zitzler and Kunzli 2004), and the ϵ-MOEA variants (Deb et al. 2005).

1.2.1 Non Sorting Genetic Algorithms (NSGA) II

This algorithm was introduced by Deb et al. (2002), and it is based on the crossover and mutation of the set of dominant solutions. The offspring population *Q (t)* is created from the parent population *P (t)*, by means of crossover between the dominant solutions. Later, these population is perturbed by a mutation operator, which introduces randomness in the selection of the optimal locations, preventing the solutions of reaching only local minima, and thus, exploring the solution space more completely. This processes continues until a convergence stopping criteria is reached.

1.2.2 Harmony search

The concept behind this algorithm (Geem et al. 2001) is based on how musicians aim to maximise the aesthetics (objective) of a tune in an improvisation session. This is achieved by the selection of the proper pitch (decision variables) to play in a limited memory of the system. The model will randomly initialise the memory of the system, and from this point the generation of new harmonies is randomised, excluding the worst solution every time. This algorithm has been reported as a specific case of evolutionary strategies (Weyland 2010).

1.3 Particle Swarm Optimisation

This method is based in the strategy of the movement of several groups of animals such as birds (Kennedy and Eberhart 1995), fish schools (Filho et al. 2008), ants (Maniezzo and Roffilli 2008) or bees (Mernik et al. 2015). It is part of heuristic methods based on a population that converge to the optimal in each generation. Particle Swarm Optimisation (PSO) is similar to GA but without crossover operators. Each individual in the swarm move towards the best solution with specific velocity and acceleration. PSO has been applied in several engineering (Jariboui et al. 2007, Pongchairerks and Kachitvichyanukul 2009, Izquierdo et al. 2008).

1.4 Simulated Annealing Optimisation

This method is inspired in the tempering process of metals, in which a better configuration of the molecules will result in a lower energy state (Kirkpatrick et al. 1983, Cerny 1985). In this idea, in each generation, the temperature threshold is reduced by a certain amount, forcing the generation of new random solutions which are below the threshold. As consequence, this method is pseudo-random, and considerably inefficient, as it only draws a rejection limit for the solutions which cannot be hold, while it forces a number of solutions to be within such bounds.

1.5 Clustering optimization algorithms

Clustering algorithms belong to the family of multistart methods. In this type of algorithms, a local search is applied, using different initial solutions. In order to improve the convergence of this type of methods, clustering techniques can be included to restrain the search space of the initial solutions, as shown by Solomatine (1999). Among these methods, exist the Adaptive Cluster COvering (ACCO), in which the local search is replaced by a global randomized search (Solomatine 1999), or by using local downhill simplex methods (Nelder and Mead 1965) to improve the convergence rate and solution efficiency.

ANNEX 2. Hydrological models used for the Brue catchment

In this Annex we present the hydrological models that were used in the development of this thesis for the Brue catchment. Here, we present the results for the HBV96, Sugawara and Linear Reservoir models, as described in Section 2.4.1.

HBV-96

The results in terms of error of the model are adequate as it can be seen that the major processes in the catchment were described by the model. The results indicate the lack of important systematic error along both calibration and validation periods, supporting the hypothesis that the model calibration was successful. Additionally, the time to the peak was adequately achieved. However, the model mostly underestimates the peak discharge. The reason for this can be attributed to the calibration metric (maximisation of NSE), which leads to a good overall performance of the model, however, limit the efficiency of the model to simulate extreme conditions.

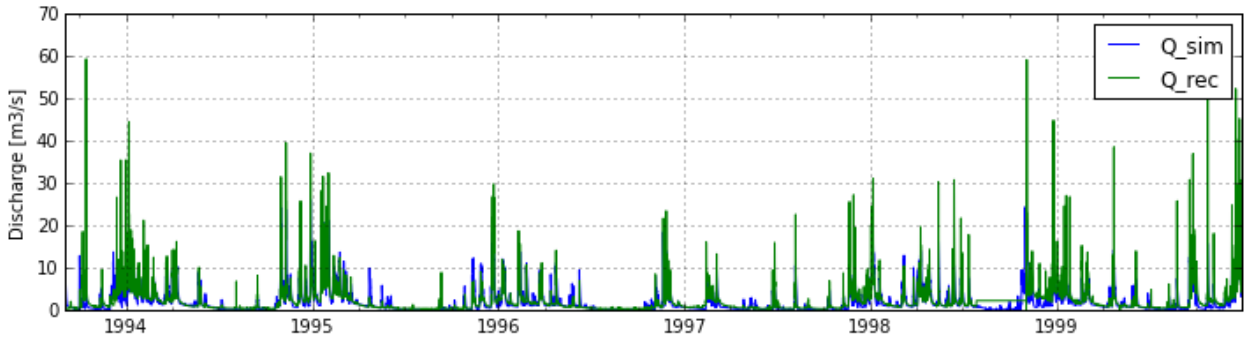

Figure 1 Calibration and validation periods in Brue catchment using HBV-96

The results for the states reflects a fast response from the catchment, as processes are mostly driven by the soil moisture (Figure 2) and the fast response components (Figure 3), due to the relatively high gradients and discharge values at the peaks. This behaviour is expected from small catchments, relatively impermeable soils or high topographic gradients.

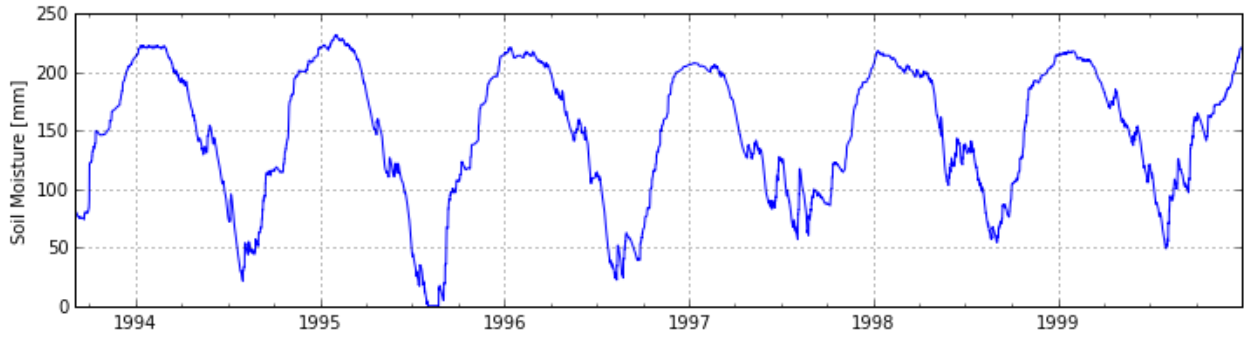

Figure 2 Soil moisture for calibration and validation

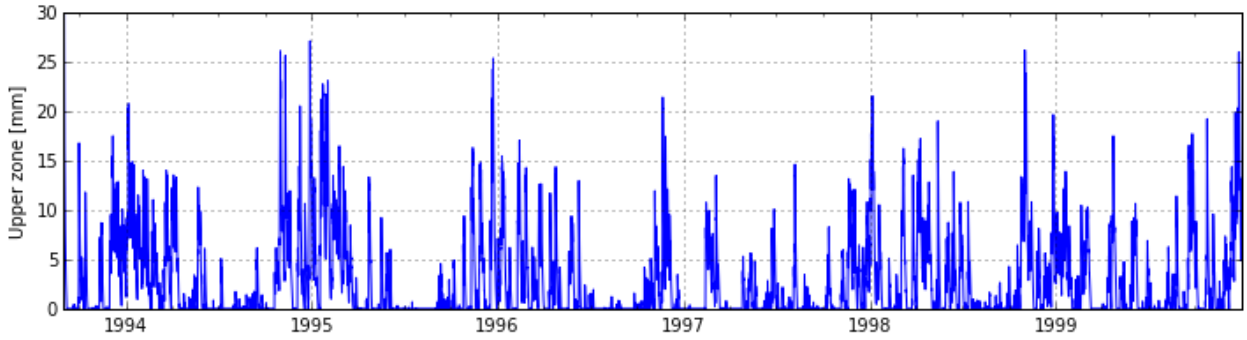

Figure 3 Upper zone for calibration and validation

To support the hypothesis of adequate model calibration, it can be observed that the contribution of the lower zone (Figure 4) has variations that are almost annual, indicating that the base flow in the catchment is regulated in such a way. However, some unusual behaviour seems to appear in 1997, which the recharge of the aquifer is limited. This can be explained by the fact that temporal precipitation patterns change due to an exceptionally dry winter and spring which lead to the precipitation to be kept as moisture, instead of reaching the aquifer, replicating in lower, discharge peaks, and quite low discharge levels around the season.

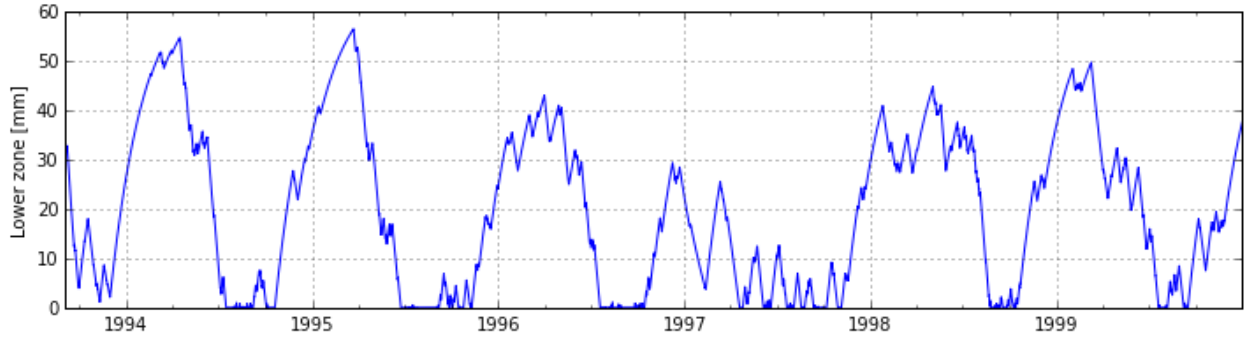

Figure 4 Lower zone for calibration and validation

The results regarding the snow component are relatively small, and has little effect on the results, as the variations in the winter periods are minimal. This occurs due to relatively high temperatures during the winter for long periods, as the snow melts in frequent intervals along the winter.

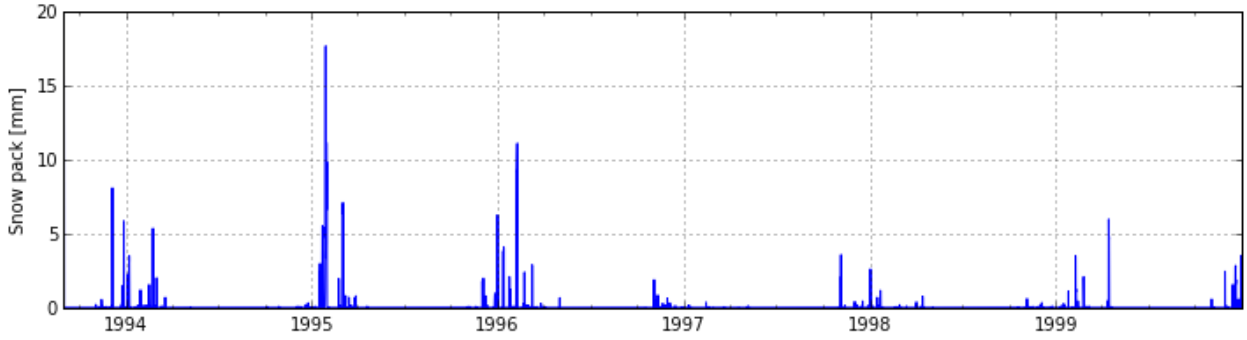

Figure 5 Snowpack for calibration and validation

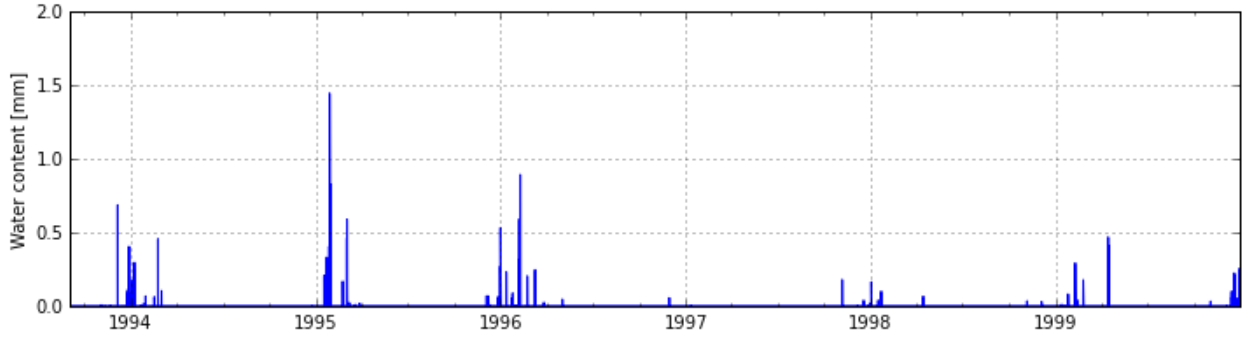

Figure 6 Water content in snow pack for calibration and validation

Linear reservoir

The calibration of this model consisted in the identification of 2 values: k and a systematic correction for the precipitation. The first represents the coefficient of the response of the catchment while the latter performs a systematic correction of the precipitation. The latter is introduced to compensate for systematic errors in the measurement.

The results of the calibration show that the model may represent the dynamics of the problem, however due to the lack of a separation of the base and excess flow, the model tend to overshoot precipitation peaks at dry periods, while underestimating high peaks in constantly wet conditions.

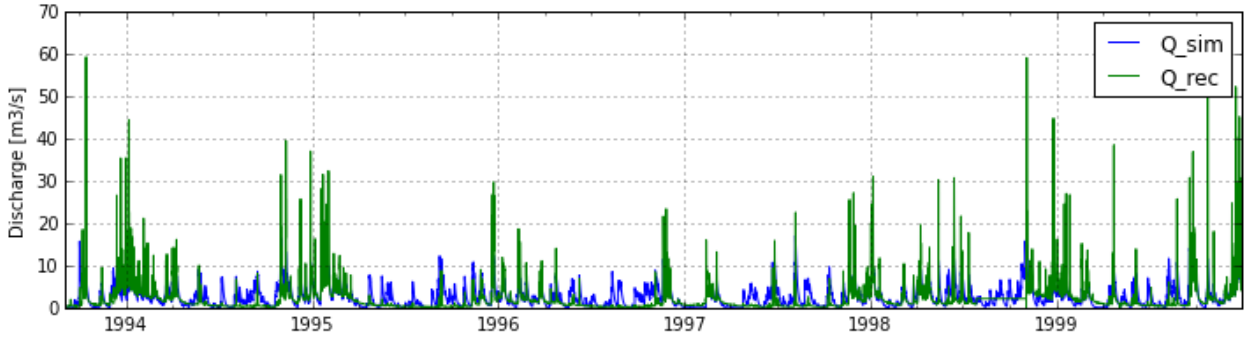

Figure 7 Linear reservoir calibration results

Sugawara

In the Sugawara (1961) tank model, there were 7 parameters to be identified. The 6 Sugawara parameters correspond to the location of the fast response box, 3 parameters for the linear response of the fast and slow response box while the last controls the flow from the top to the bottom box. Similarly as in the other models, a systematic correction of the precipitation was introduced in the calibration of the model, as an additional calibration parameter.

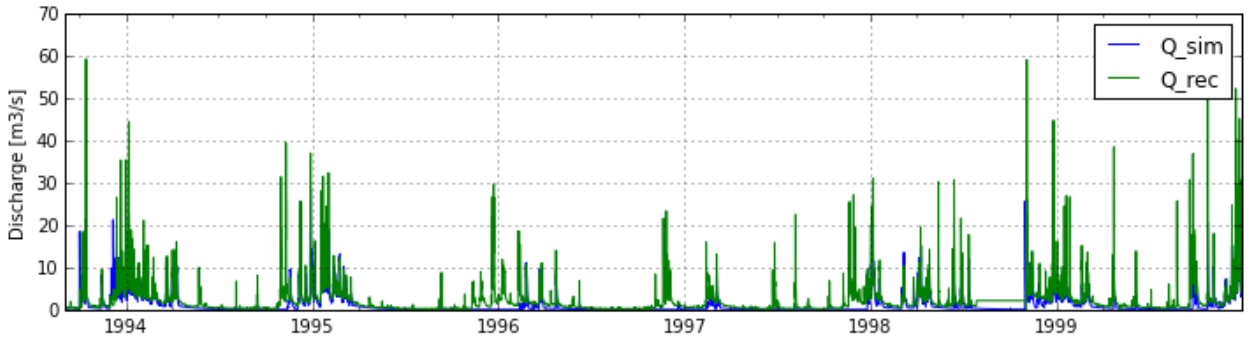

Figure 8 Sugawara tank calibration results

Model states are represented by S1 and S2, corresponding to the conceptual level in the fast and slow response boxes. As can be seen from Figure 9 and Figure 10, the calibration results show a much slower contribution of the slow response box, while the fast response box coincides with the discharge peaks, leading to the hypothesis that the model is adequately calibrated, as base and excess flow seem to be adequately characterised.

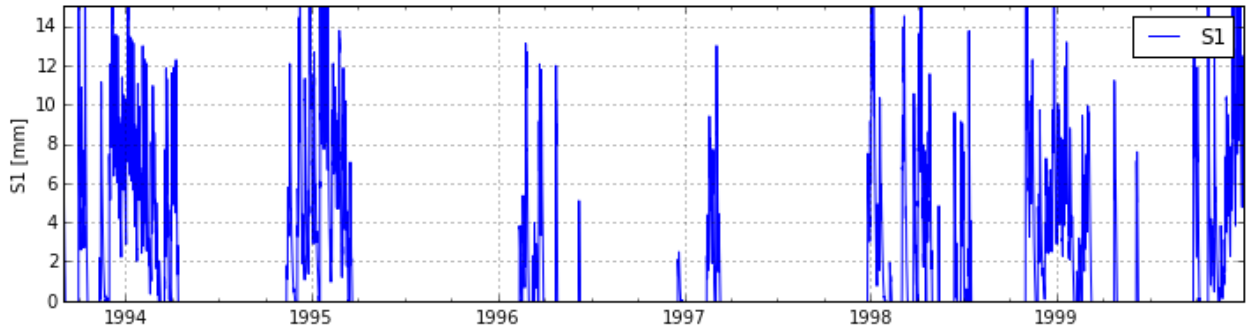

Figure 9 Fast response box behaviour

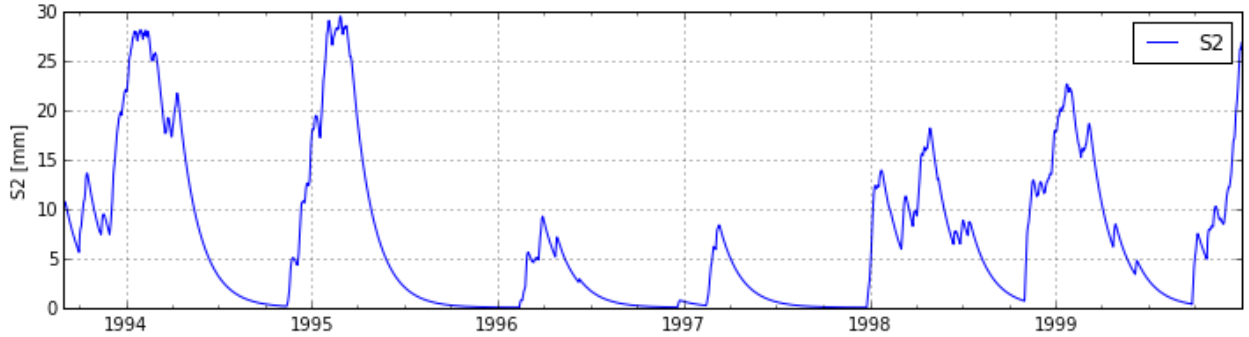

Figure 10 Slow response box behaviour

ANNEX 3. Perturbation specification for simulating incomplete precipitation data

To test the strategies for the scheduling of sensor networks, it envisioned to test the results under different perturbation scenarios, which can be controlled in the design of the experiments. On this regard, it is necessary to establish a methodology to produce controlled perturbations in the precipitation fields which are spatially correlated.

The proposed spatial perturbation has three main components, namely: the generator function (*G*; also known as kernel), the field fluctuation scale (*f*), and the noise level (*a*, also known as amplitude). The generator corresponds of a kernel function which specifies the type of noise which is generated, defining if the noise is either temporally uncorrelated (white), or with a temporal frequency structure (pink, red), and coming from a given probability distribution (Gaussian, uniform, etc.). The fluctuation scale defines the distance in which the correlation between samples become independent. The noise level (or amplitude) corresponds to a measure of the interval in which the noise is applied, as different compositions of the noise are defined, the amplitude is specifically defined for each type of generator function.

On the implementation side, the noise generator is built by generating samples at locations which are statistically independent. The spatially independent locations are selected by using a hexagonal lattice, which distance corresponds to the fluctuation scale (*f*) of the perturbation field. At each of these locations, a unit noise sample is generated, using the noise kernel. Finally, results are scaled (and truncated to ensure physically-possible values), according to the noise level. The workflow of this is approach is as.

1. Define: Kernel (*G*), Fluctuation Scale (*fs*) and amplitude (*a*)
2. Create a randomised seed point for the hexagonal lattice within the domain of the perturbation field
3. Create a hexagonal lattice with separation fs, starting from the seed point
4. Sample random values from the generator function (*G*) at each lattice node
5. Interpolate to the domain of the perturbation field using a Kriging approximation, with sill = *a*, range = *fs*
6. Go to 2 for next time step

A sample of the perturbation generator using a white Gaussian noise for a unit amplitude at different fluctuation scales is presented in Figure 1.

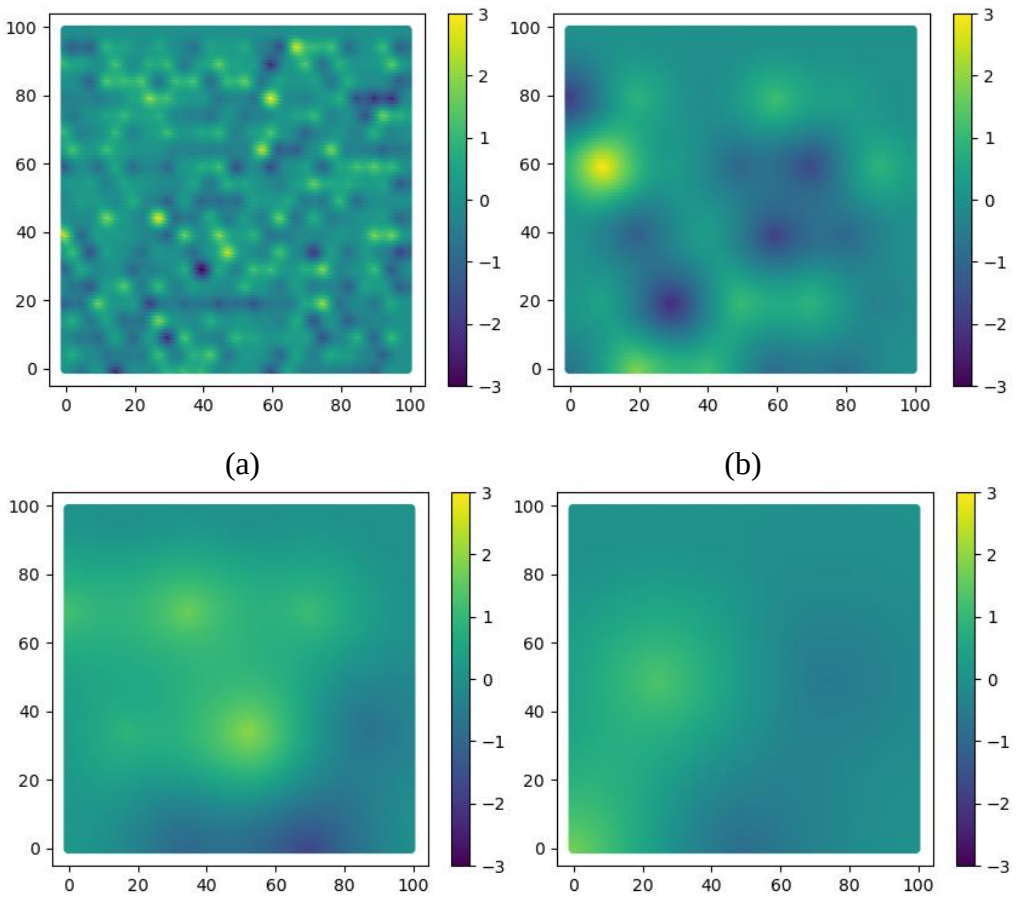

Figure 1 Sample of white Gaussian spatially distributed noise using different correlation lenghts 5 Km (a), 20 Km (b), 35 Km (c) and 50 Km (d)

Netherlands Research School for the
Socio-Economic and Natural Sciences of the Environment

D I P L O M A

For specialised PhD training

The Netherlands Research School for the
Socio-Economic and Natural Sciences of the Environment
(SENSE) declares that

Juan Carlos Chacon-Hurtado

born on 7 March 1986 in Cali, Columbia

has successfully fulfilled all requirements of the
Educational Programme of SENSE.

Delft, 24 September 2019

The Chairman of the SENSE board

Prof. dr. Martin Wassen

the SENSE Director of Education

Dr. Ad van Dommelen

The SENSE Research School has been accredited by the Royal Netherlands Academy of Arts and Sciences (KNAW)

KONINKLIJKE NEDERLANDSE
AKADEMIE VAN WETENSCHAPPEN

The SENSE Research School declares that **Juan Carlos Chacon-Hurtado** has successfully fulfilled all requirements of the Educational PhD Programme of SENSE with a work load of 33.3 EC, including the following activities:

SENSE PhD Courses

- Uncertainty propagation in spatial and environmental modelling (2014)
- Environmental research in context (2015)
- Research in context activity: 'Taking initiative and developing of an open-source hydrological modelling tool, to be used in different contexts of education, research and application for rational water management' (2017)

Other PhD and Advanced MSc Courses

- Data assimilation, FIVA – University of Copenhagen (2011)
- Analytic storytelling, TU delft (2014)

Management and Didactic Skills Training

- Supervising MSc student with thesis entitled 'Arch dam deformation prediction using computational intelligence techniques, International commission in large dams' (2017)
- Supervising MSc student with thesis entitled 'Optimization of run-of-river hydropower', Water Power Magazine' (2018)
- Teaching in the MSc course 'Introduction to software engineering' (2019)

Communication skills

- Co-author on 'Optimization of run-of-river hydropower', published in Water Power Magazine' (2018)

Oral Presentations

- *Precipitation sensor network optimal design using time-space varying correlation structure*. Hydroinformatics Conference, 17-21 August 2014, New York, United States of America
- *Testing of a conceptually distributed-lumped hydrological model for streamflow simulation.* IWA Hydroinformatics Conference, 1-6 July 2018, Palermo, Italy.
- *On the use of surrogate inverse models for hydrological data assimilation*. Hydroinformatics Conference, 21-26 August 2016, Incheon, South Korea
- *Dimensioning of precipitation citizen observatories in an uncertainty-aware context.* EGU general assembly, 23-28 April 2017, Vienna, Austria

SENSE Coordinator PhD Education

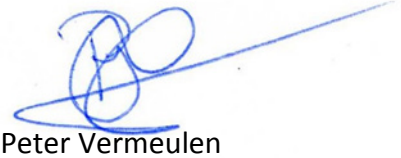

Dr. Peter Vermeulen